UNDERSTANDING AND PREDICTING FOREST HARVESTING EFFECTS ON PEAK FLOWS IN SNOW ENVIRONMENTS WITH NONSTATIONARY FREQUENCY MODELLING

by

JOE YU

B.S.F., University of British Columbia, 2011

A DISSERTATION SUBMITTED IN PARTIAL FULFILLMENT OF
THE REQUIREMENTS FOR THE DEGREE OF

DOCTOR OF PHILOSOPHY

in

THE FACULTY OF GRADUATE AND POSTDOCTORAL STUDIES

(Forestry)

THE UNIVERSITY OF BRITISH COLUMBIA

(Vancouver)

March 2020

The following individuals certify that they have read, and recommend to the Faculty of Graduate and Postdoctoral Studies for acceptance, the dissertation entitled:

Understanding and predicting forest harvesting effects on peak flows in snow environments with nonstationary frequency modelling

Submitted by Joe Yu in partial fulfillment of the requirement for

the degree of Doctor of Philosophy

in Forestry

Examining Committee:

Younes Alila, Forestry
Supervisor

Peter Marshall, Forestry
Supervisory Committee Member

Bruce Larson, Forestry
Supervisory Committee Member

Guangyu Wang, Forestry
University Examiner

Roger Beckie, Earth, Ocean and Atmospheric Sciences
University Examiner

Abstract

A century of paired watershed studies evaluated the effects of forest harvesting on peak flows by pairing events by equal chronology. This method has recently come under repeated criticism and calls have been made to abandon the practice and pair by equal frequency instead. However, the stationarity assumption imposed by conventional frequency analyses complicates the use of frequency pairing because peak flows contain change-point and trend-shifting nonstationarities caused by continuous harvesting and forest regrowth. Here, a new nonstationary frequency pairing method was introduced to evaluate harvesting effects by allowing the parameters of peak flow frequency distributions to change in time using physically-based covariates. This research falls within the emerging field of "attribution science", which uses observations and models to identify separately the factors contributing to extremes.

The outcomes of applying this new method at five treatment-control, snow-dominated watersheds (37 km^2 to 3550 km^2) revealed how harvesting increased the magnitude and frequency of not only small (< 10-yr return period) but also large (>10-yr return period) peak flows. This was a consequence of changes to both the means (+28% to +113%) and standard deviations (no effects to +110%) of the peak flow frequency distributions. Large peak flows became 3-4 (10-20) times more frequent in the least (most) sensitive watershed. The different treatment effects reveal contrasting watershed sensitivities to harvesting, owing to different physiographic characteristics and logging histories. Based on the collective outcomes, a physical model encapsulating harvesting effects at the stand- and watershed-levels was developed to advance the probabilistic understanding of the forests and floods relation.

Advantages of the new method include: (i) relaxing the watershed size and proximity constraints between control and treatment watersheds; (ii) detecting small levels of change in the

peak flow time series with moderate harvesting levels; (iii) bypassing the need for a calibration equation, hence eliminating associated sources of uncertainty; (iv) making use of larger sample sizes to conduct frequency analysis, which make better inferences about the effects on extreme events; and (v) allowing for the estimation of harvesting effects at different historic snapshots of a watershed, thus providing an evaluation of hydrologic recovery.

Lay summary

The regression-based, century-old method of evaluating forest harvesting effects on peak flows has been challenged recently. A new method of evaluation calls for the use of frequency analysis instead. However, forest regrowth and continuous forest harvesting can produce peak flows that violate the fundamental stationarity assumption when conducting frequency analysis. This thesis introduces a new method in forest hydrology, nonstationary frequency analysis, for evaluating continuous forest harvesting effects on peak flows. The method was originally developed in the wider hydrology literature to overcome the challenges associated with nonstationarity. The application of this new method is illustrated in five pairs of treatment-control watersheds (37 km^2 to 3550 km^2), located in snow environments, in British Columbia, Canada. The collective outcomes reveal different levels of peak flow sensitivity to harvesting due to different physiographic features and logging regimes. The outcomes from the emerging method run counter to the prevailing wisdom in forest hydrology.

Preface

I have been the principal investigator for all components of the research presented in this thesis. I developed the research questions and the associated experimental design under the guidance of Dr. Younes Alila and the support of my supervisory committee. I conducted all tasks related to the research including data collection, data analyses, results interpretation, and drafting the thesis and manuscripts. The research in this thesis will be compartmentalized into five publications, the first of which was published in 2019:

i. The new nonstationary frequency pairing method is introduced to evaluate harvesting effects by allowing the parameters of peak flow frequency distributions to change in time using physically-based covariates. This paper using data from the **Camp Creek-Greata Creek pair** is a proof of concept featuring the feasibility of the method to transform the science on this topic when guided by the new way of pairing peak flows by equal frequency. The outcomes were published: Yu, X. J., & Alila, Y. (2019). Nonstationary frequency pairing reveals a highly sensitive peak flow regime to harvesting across a wide range of return periods. *Forest Ecology and Management*, *444*(April), 187–206. https://doi.org/10.1016/j.foreco.2019.04.008. I was the lead investigator, responsible for designing the experiment, data collection, data analyses, results interpretation, and manuscript preparation. Younes Alila was the supervisory author on this publication involved in designing the experiment and manuscript preparation.

ii. Under the old experimental framework, the weather and physiography should be as similar as possible between the paired watersheds, but these limiting

constraints are relaxed under the nonstationary FP framework due to the changing role of the control watershed. The new role of the control is to rule out a changing frequency distribution over time allowing for the attribution of any temporal changes in the treatment watershed to disturbance. This attribution process does not require the paired watersheds to be neighbouring, which is featured by the outcomes of **Baker Creek-McKale River, Mather Creek-Fry Creek pairs.** The research outcomes from these two pairs will be published in a journal paper illustrating the contrasting watershed sensitivities to harvesting as a result of different watershed physiographies and forest disturbance regimes.

iii. Besides the constraint of proximity, the watershed size constraint between the control and treatment watersheds is also relaxed under the new framework featured by the outcomes of **Bowron River-McGregor River and Willow River-McGregor River pairs**. The results of these two pairs will be published in a journal paper revealing high sensitivities to harvesting of the large-sized Bowron River and Willow River treatment watersheds. Such high sensitivity is unexpected, and the outcomes are contradicting the conventional wisdom in the forest hydrology literature. The predictions from the two pairs are corroborated using an independent hydro-geomorphology evaluation.

iv. The **meta-analysis,** which led to a physical model, will be published as a journal paper. The collective outcomes are compiled and organized into a physical model that provides readers and practitioners an up-to-date understanding of the forests and floods relation at the stand- and watershed-levels in the newly emerging probabilistic framework. The physical model can offer a holistic understanding of

how forest harvesting may be affecting the flood regime across scales and locations, by identifying the overall differences in hydrologic effects driven by different physiographies and disturbance regimes based on the collective outcomes of the five pairs in the thesis.

v. The **literature review** from the Introduction Chapter will be organized and published as a journal paper. The introduction identifies a knowledge gap in the existing forest hydrology literature using the frequency-based framework to evaluate the forests and floods relation, especially in large watersheds. The continuous historic forest harvesting and regrowth in the cut-blocks can inherently violate the stationarity assumption of conventional frequency analysis. Newly emerging studies and research methodologies in the wider hydrology literature can be brought to bear on the topic of forest harvesting effects on peak flows.

Table of contents

List of tables

List of figures

List of abbreviations

AIC Akaike information criterion……..……..51

asl above sea level……...20

BACI Before-after, control-impact……..……..……2

BC British Columbia……...……..……19

BEC Biogeoclimatic ecosystem classification……..……30

CDF Cumulative density function…….……53

CI Confidence interval……...66

CM Control model……58

CP Chronological pairing.……...……9

CV Coefficient of variation……...6

DHSVM Distributed hydrology soil vegetation model…….....……..……13

DMC Double mass curve……..6

ECA Equivalent clear cut area…….……..23

ESSF Engelman spruce-subalpine fir……..……..…….29

FDC Flow duration curve……..……6

FFC Flood frequency curve……..66

FP Frequency pairing……10

GEV Generalized extreme value distribution……..……..53

GPD Generalized pareto distribution…….……60

ICH Interior cedar hemlock…….……....29

LR Likelihood ratio test……..57

MLE Maximum likelihood estimation……..54

MPB Mountain pine beetle……..…..…….……...…22

MS Montane spruce…….…….29

PDF Probability density function……..…….53

POT Peaks-over-threshold……..……61

SBS Sub-boreal spruce……...……..30

SWE Snow water equivalent……..……22

TM Treatment model……..……..58

VRI Vegetation resource inventory…….……...……24

WSC Water Survey of Canada……..…….20

List of symbols

Q2 Discharge equaled or exceeded once in 2 years on average (m^3/s).....……...……...78

Q20 Discharge equaled or exceeded once in 20 years on average (m^3/s)……...……78

Q100 Discharge equaled or exceeded once in 100 years on average (m^3/s) ……...…….78

Qp Peak discharge (m^3/s)...……...…….……58

Qn Peak flows (m^3/s) for the new location…….……..……41

Qo Peak flows (m^3/s) for the previous location……...…….41

An New catchment area (km^2)……..…….……41

Ao Previous catchment area (km^2)…..……..……41

Acknowledgments

Above all, I am grateful for the limitless patience and support of my supervisor Dr. Younes Alila. Younes is a dedicated, enthusiastic, and caring mentor who helped me with research, career, and life in many ways above and beyond his role as an academic supervisor. I could not have made it to the end of this journey without Younes. I embrace our friendship and will remember fondly our many nights and weekends of working together side-by-side.

I am also grateful to my advisory committee members Dr. Peter Marshall and Dr. Bruce Larson for their mentorship at the undergraduate and graduate levels. I am thankful for Bruce and Peter for their input on the technical aspects of the thesis and the feedbacks provided at various stages of the research program.

I feel extremely lucky to have met my friend Nick Rong during this journey. Ever since I met Nick, there has been nothing but fond memories of being a friend of Nick. We spent countless hours studying and working together, and I still learn something new and interesting from Nick every day. Nick is a brutally honest and extremely supportive friend. His constant encouragement helped me through major challenges throughout the journey, especially towards the end.

I thank Michael Andres, Robbie Johnson, Eric Nance, Noa Mayer, and Dan Kovacek for their editorial assistance. I would like to thank Jangar Tsembel for his assistance and especially his companionship for the stress-relieving short walks.

I am forever thankful for the unconditional love and support from my family, especially my mother. It would be impossible to complete this journey without their financial support but more so their emotional support. I would like to thank my beautiful wife and her family for

always believing and supporting me. I am especially thankful for my wife's understanding, tolerance, and endless encouragement.

I acknowledge Water Survey of Canada, Meteorological Survey of Canada, and BC Ministry of Forests, Lands, Natural Resource Operations & Rural Development for the hydrometric, climate, and vegetation inventory data sets used in this thesis. This thesis was partially funded by the Natural Sciences and Engineering Research Council of Canada Discovery Grant RGPIN 194388-11 to Dr. Younes Alila, and Mitacs Accelerate Project (IT number: IT04112) to Dr. Younes Alila.

This dissertation is dedicated to my mom,

Amy. Her support and constant love have

sustained me throughout the journey.

Chapter 1: Introduction

Forests' effects on peak flows is of interest to scientists from a wide range of disciplines and is the subject of frequent public policy related discussions by the popular press, environmentalists, and non-governmental and government organizations. The importance of this topic is derived from how modifications of the peak flow regime could potentially trickle down to affect virtually all aspects of the fluvial ecosystem, from sediment transport (Macdonald et al., 2003) to fish populations (Valdal and Quinn, 2011). For engineers, infrastructural designs such as culverts and bridges depend on a reliable quantification of such peak flow regimes. Forest hydrologists have been devotedly debating and disagreeing for decades on how forests, and forest harvesting practices, affect the peak flow regime of a stream (e.g., Alila et al., 2009, 2010; Alila and Green, 2014a, 2014b; Anderson, 1949, 1950; Bathurst, 2014; Birkinshaw, 2014; Bradshaw et al., 2009; Burton, 1997, 1999; Harr et al., 1979; Harr, 1986; Ives, 2006; Jones and Grant, 1996; Lewis et al., 2010; Rothatcher, 1973; Thomas and Megahan, 2001; Troendle and Stednick, 1999; van Dijk et al., 2009). Eisenbies et al. (2007, p. 81) described the state of science on this topic as "enigmatic." How will ecologists and engineers adaptively plan for the future, if hydrologists are not able to provide sufficient and credible evidence on how the peak flow regime is affected by forests and the associated changes in the forest cover caused by human activities or natural disturbances?

1.1 Limitations and challenges of the paired watershed experimental design

1.1.1 Conventional paired watershed experiment

The paired watershed experiment is perhaps one of the most widely used tools to evaluate the effects of forest harvesting on hydrologic responses (Bren and Lane, 2014). Paired watershed studies conventionally involve the before-after, control-impact (BACI) computation technique to evaluate treatment effects on peak flows. The term before-after, control-impact implies that both control and treatment watersheds are monitored before and after the impact (which occurs only in treatment watershed) in order to evaluate the effects of the impact by controlling for external factors. In brief, both control and treatment watersheds are monitored prior to the implementation of forest harvesting, then empirical relationships are developed, usually in the form of simple linear regressions referred to as calibration equations, using pre-treatment measured peak flows of the control and treatment watersheds. The calibration equation is used to estimate the expected peak flows of the treatment watershed had the treatment not occurred, based on peak flows from the control watershed as predictors. The forest harvesting effects are then quantified through a comparison between the observed (i.e., measured) and expected (i.e., estimated from the calibration equation) peak flows of the treatment watershed during the post-harvesting period. These paired watershed studies are associated with small (usually less than several square kilometers) catchments in close proximity in an attempt to minimize the effects of confounding factors, such as differences in physiographic and weather conditions, when evaluating treatment effects on hydrologic responses.

1.1.2 The uncertainty associated with the calibration process

The development and use of the calibration equation constitutes one of several sources of uncertainty associated with predicted treatment effects because the calibration process directly dictates the peak flow response associated with forested conditions. First, the calibration period, where both control and treatment watersheds are subject to monitoring prior to treatment, is time-consuming and costly (Slivitzsky and Hendler, 1964). For instance, it can take 12 years of calibration and another 12 years of treatment in order to detect a 5% change in the water yield significant at $\alpha = 0.05$ (Kovner and Evans, 1954; Wilm, 1949), but in practice, a 12-year calibration period (or longer) is rare (Bren and Lane, 2014). In addition to the length of the calibration period, there can be other external factors affecting the calibration relationship over time during the treatment period, such as silvicultural activities (Ssegane et al., 2017) and climate variability (Vogel and Lopes, 2010). Most importantly, the calibration period often does not capture the large range of flows in the long-term record when the calibration is used after treatment (Hornbeck, 1973). Therefore, the use of a calibration equation post-treatment often results in extrapolating outside the range of the regression model developed within the calibration period. In short, the overall calibration process is a well-recognized major source of uncertainty, directly associated with the quantification of treatment effects, which is inherent in all published paired watershed studies.

1.1.3 Limitations brought by watershed size and proximity

There are two fundamental limitations associated with the conventional paired watershed design that ultimately inhibit the transferability of results from experiments to management, namely: watershed size and proximity of the paired watersheds. Such limitations of watershed size and proximity were imposed by the need for homogeneity in physiography and weather input factors between control and treatment watersheds when evaluating the effects of forest harvesting on hydrologic responses. Hence, the paired watershed experiment often involves small-sized watersheds in close proximity (e.g., Ganatsios et al., 2010; Le Tellier et al., 2009; Negley and Eshleman, 2006; Serengil et al., 2007; Stephan et al., 2012; Swindel and Douglass, 1984). This explains why existing paired watershed studies are usually less than 10 km^2 in size (e.g., Brown et al., 2005) and situated in close proximity often less than several kilometers apart (e.g., Swank et al., 1988), so "*any climate impacts should be buffered"* (King et al. 2008, p. 385).

The homogeneity assumptions become increasingly difficult to maintain as the watersheds increase in size and their proximity is compromised. For instance, as Slivitzsky and Hendler (1964) pointed out, the homogeneity assumption is difficult to maintain in larger basins where the weather conditions may vary within the watershed (McDonnell et al., 2007). In addition, large watersheds can have fundamentally different physical mechanisms driving their hydrologic responses (Brooks et al., 2012). The timing of streamflow from small watersheds can also be different from that produced by large watersheds (Lundquist et al., 2005; Reynolds and Leyton, 1967). As a result, the different physical processes between small and large watersheds make it difficult and misleading to transfer results from small paired watershed studies to larger watersheds, a well-recognized challenge referred to as the *unrepresentativeness* (Hewlett et al., 1969; Reynolds and Leyton, 1967; Slivitzsky and Hendler, 1964). Pilgrim (1983, p. 71) stated:

"Attempts to generalize are dangerous, and counter-productive to the wider understanding of processes and the development of valid relationships. Recognition of this fact seems to be a major step in the right direction."

However, and despite the lack of research on larger watersheds, this has not stopped forest hydrologists from making sweeping and perhaps unsubstantiated generalizations such as:

"In general, the largest or least frequent peaks observed in all of the studies cited, regardless of watershed size, were not significantly affected." (Troendle et al., 2001, p. 186)

and

"Now forest hydrologists generally agree that, although forests mitigate floods at the local scale and for small to medium-sized flood events, there is no evidence of significant benefit at larger scales and for larger events." (Calder et al., 2007, p. 945)

In summary, the size and proximity of paired watersheds are limitations imposed by the homogeneity assumption (weather input and physiography) of the conventional paired watershed design. These two limitations have created a major knowledge gap by applying results from small paired watersheds to large watersheds, which have greater practical importance (Pilgrim, 1983). More research is needed to understand and quantify the effect of forest land-use and land cover changes in large watersheds (Brown et al., 2005).

1.2 Other research methods used to evaluate forest disturbance effects on hydrologic responses

Even though the paired watershed study approach is rarely employed with large watersheds, there are other techniques that have been used as attempts to relate and quantify forest disturbance effects in large catchments, namely: flow duration curve analysis (FDC), trend analysis, double mass curve analysis (DMC), and linear regression.

1.2.1 Flow duration curve analysis

FDC is an illustration of the percentage of time that streamflow of a certain magnitude is likely to equal or exceed some specified magnitude. However, FDC analysis is not suitable for the analysis of extreme events. FDC analysis is a nonparametric technique, which inadequately describes the often skewed and heavy-tailed peak flow frequency distributions derived from extreme events (Vogel and Fennessey, 1994). The FDC analysis in the context of forest disturbance is sometimes applied to daily flows (Zhang et al., 2016). However, daily flows can also be skewed as the moments describing the frequency distributions, such as the coefficient of variations (CV), can be highly biased even with large sample sizes (Vogel and Fennessey, 1993). In addition, FDC analysis is sensitive to extreme events that occurred in particular time periods (Vogel and Fennessey, 1994). Therefore, some uncertainties can arise when FDC analysis is conducted using data derived from subdividing the entire time series (e.g., Rosburg et al., 2017).

1.2.2 Trend analysis

Another technique commonly used to detect changes in hydrologic response is trend analysis (e.g., Kahya and Kalayci, 2004; Villarini et al., 2009). Trend analysis has been used to detect changes in the hydrologic response of large watersheds in association with forest disturbance (e.g., Déry et al., 2012; Dung et al., 2011; Zegre et al., 2014). However, trend

analyses fall short of fully evaluating forest disturbance effects on peak flows for several reasons. The majority of trend tests only detect the time trends without providing an estimation of changes in magnitude. The Man-Kendall and Sen's slope are examples of these tests in the trend analysis literature (Gocic and Trajkovic, 2013; Yue et al., 2002; Zhang and Lu, 2009). In addition, such estimation cannot detect a change in the variability of extreme events, which is commonly associated with forest disturbance (Green and Alila, 2012). Changes in the variability of peak flows over time caused by forest disturbance can have implications on peak flow frequency, yet this dimension of changing frequency is rarely invoked under conventional trend analyses (Bjorndal et al., 1999). Therefore, it can be misleading to use conventional trend analysis for evaluating forest disturbance effects on the magnitude and frequency of peak flows.

1.2.3 Double mass curve

Double mass curve (DMC) analysis is another technique used to detect time trends in watershed responses. DMC was a popular tool used in the early literature to test for homogeneity in time of precipitation records (Buishand, 1982; Searcy and Hardison, 1960) that was also used in watershed analyses (Buttle and Metcalfe, 2000). DMC analysis is often applied to cumulative runoffs in watersheds. To conduct an analysis using DMC, the cumulative runoff from the treatment watershed is plotted against the cumulative runoff from the control watershed chronologically. The plot should produce a straight line prior to disturbance, while a deviation from this straight line is expected to occur post-disturbance. A deviation from the predictable straight line is commonly attributed to the land-use changes in the treatment watershed. However, DMC analysis only detects a time trend without quantification of treatment effects, and it doesn't reveal changes in the frequency of peak flows. DMC also cannot detect changes in variability in the time series, as recognized in the early literature (e.g., Wigbout, 1973).

1.2.4 Linear regression

Linear regression is another technique used in paired watersheds to evaluate forest disturbance effects on peak flows. Linear regression equations are developed based on the matching of peak flows paired between the control and treatment watersheds by the same storm inputs. The respective linear regressions, developed in the pre- and post-disturbance periods, are compared to draw conclusions on forest disturbance effects on peak flows (e.g., Beschta et al., 2000; Jones and Grant, 2001, 1996; Thomas and Megahan, 2001, 1998). However, linear regression is not suitable to evaluate forest disturbance effects on peak flows. First, the post-disturbance peak flows are often nonstationary as a result of forest regrowth, therefore inhibiting the use of the entire record to evaluate disturbance induced hydrologic effects. In an attempt to maintain the stationarity assumption, Jones and Grant (1996) and Thomas and Megahan (1998) subdivided the post-disturbance period into 5-year periods; however, the number of large peak flows within any 5-year period is limited. Moreover, the development and comparison of two regression lines, on which the conclusions are based, only detect and evaluate the changes in the mean of the pre- and post-disturbance peak flows. The comparison of the two regression lines also cannot account for changes in variability around the mean (of the peak flows) as a result of forest disturbance. The linear regression technique also ignores the critical effects on the frequency and magnitude of larger peak flows brought by changes in peak flow variability. As a result, it is not suitable to use a linear regression type of analysis to evaluate forest harvesting effects on peak flows, especially large peak flows (Alila et al., 2009; Green and Alila, 2012).

1.3 Old way of pairing: from uncertainty to irrelevancy?

The existing research methods for large catchments may not be useful in evaluating forest harvesting effects on peak flows. Some of them may also be associated with a more fundamental issue related to the experimental design applicable to both small-scale paired watershed experiments and large-scale watershed methods. The conventional way of predicting forest harvesting effects on peak flows within experimental design has recently come under serious and largely unchallenged criticism (Alila et al., 2009; Alila et al., 2010; Alila and Green, 2014a, 2014b). In the paired watershed study literature, the difference in the magnitude of peak flow response between the control and treatment watersheds when paired by the equal time of occurrence, referred to as Chronological Pairing (CP), has been interpreted to be a measure of the effects of harvesting on such peak flow events. In rain environments, the two peak flows are paired by equal storm input, while in snow environments they are paired by equal snowmelt season. The first limitation of CP is related to the fact that matching peak flows chronologically in snow environments, for instance, is an impossible task because the control and treatment watersheds, even when small and in close proximity, often peak days or weeks apart (Moore and Scott, 2005; Troendle et al., 2001; Troendle and King, 1985, 1987; Troendle and Olsen, 1994; Troendle and Stednick, 1999; Van Haveren, 1988). Link and Marks (1999a, 1999b) demonstrated through distributed modelling how canopy structure can delay snowmelt in forested areas by up to three weeks relative to open areas. In addition, subsurface runoff travel time from soil moisture reservoirs to the channel network can create lagged effects in streamflow response on the order of months in some forested watersheds (Jones and Post, 2004; Nippgen et al., 2016; Swank et al., 1988).

The second limitation of CP, and perhaps the most critical, is the fact that it does not invoke, nor does it account for potential changes in the frequency of peak flows caused by forest harvesting (Alila et al., 2009, 2010). Since some have continued to extend the life of CP (e.g., Bathurst et al., 2018; Bathurst, 2014; Birkinshaw, 2014), it is reiterated briefly in the next paragraph why it is necessary to invoke simultaneously the dimensions of magnitude and frequency in any evaluation of the effects of harvesting on peak flows.

Using the case of snow environments for illustration, the magnitude of a peak flow event of the same watershed, in either forested or harvested conditions, is controlled by several hydro-meteorological factors: snow accumulating on the ground, energy creating the melt, occasional rain falling on melting snow, and the antecedent moisture condition in the soil. Many different combinations of these four factors, which all occur randomly, could generate the same peak flow event magnitude. Hence, every peak flow event occurs with a certain frequency, and disproving such a peak flow event has not changed in magnitude as a result of harvesting ought to be conducted simultaneously for every one of the possible combinations. Therein lies the need for invoking the dimension of frequency in any research question or hypothesis when investigating the effects of harvesting on the peak flow regime. Therefore, the question that should guide research work on this topic should be: What is the change in magnitude (frequency) caused by harvesting for a peak flow event of a certain frequency (magnitude)? In the context of a paired watershed study design, this translates into the following question: What is the difference in magnitude (frequency) between control and treatment peak flows when both are of the same frequency (magnitude)? Therefore, pairing between control and treatment watershed peak flows, which is vital for the design of the controlled experiment intended to isolate the effects of forest harvesting, must be by equal frequency (FP) and not equal chronology (CP). If the pairing is

conducted in any way other than by FP, the experimental design neither fully nor appropriately isolates the effects of harvesting on the peak flows. Hence, the CP- and FP-based changes in magnitude are not equivalent and they should not be used interchangeably (Alila et al., 2009). Alila and Green (2014a, 2014b) asserted that because CP leads to an uncontrolled experiment, CP-based changes in the magnitude of peak flows are incorrect and misleading. CP-based study outcomes, be it from small-scale paired watershed experiments, or large-scale experiments involving DMC or linear regression methods, are irrelevant to how forest harvesting affects peak flows of all sizes, and especially so for the larger peak flows (Alila et al., 2009).

1.4 A new way of pairing: challenges or opportunities?

FP necessitates that the investigation of forest harvesting effects on the peak flow regime is conducted within the framework of the peak flow frequency distribution. The understanding and quantification of the effects of forest harvesting on a peak flow of a certain frequency must therefore pass through an evaluation of how forest harvesting may have changed the characteristics of the peak flow frequency distribution (e.g., its location, scale, and shape parameters). The frequency distribution framework is commonly used by the wider hydrology (e.g., Katz et al., 2002 and references therein) and climatology (e.g., Salas et al., 2012 and references therein) communities for evaluating the effects of land-use and climate change effects on hydro-climatological extremes. However, until recently it has rarely been used for investigating the effects of forest harvesting on peak flows using paired watersheds in the forest hydrology literature (Alila et al., 2009 and references therein), because of the dominance of the CP framework for over close to a century.

Alila et al. (2009) called for a new era of research on the topic of forest harvesting effects on peak flows, guided by the new paradigm of pairing events by equal frequency. Published FP-

based studies since have revealed how forest harvesting can affect not only small and medium (<10-yr return periods), but also larger (>10-yr return periods) peak flow events. Further, there are cases where the larger the peak flow event, the larger the effects of forest harvesting on that event (Alila et al., 2009; Green and Alila, 2012; Kuraś et al., 2012; Schnorbus and Alila, 2004a, 2013). These outcomes run counter to the century-old prevailing wisdom in forest hydrological science (Schultz, 2012; Treacy, 2012).

Current FP-based experiments conducted to evaluate forest harvesting effects on peak flows have taken place primarily in small-scale watersheds. This holds whether conventional frequency analysis using measured data from existing paired watersheds (e.g., Alila et al., 2009, Green and Alila, 2012), or modelling studies driven by deterministic hydrologic models (e.g., Kuraś et al., 2012; Schnorbus and Alila, 2004a, 2013) were employed. However, there are inherent challenges and uncertainties associated with these two FP-based research methods.

A source of complication in using the FP framework in forest hydrology stems from the stationarity assumption normally imposed by the use of conventional frequency analyses. Forest harvesting, either on the whole or part of the watershed, could result in "jumps" or change-point nonstationarity in the long-term record of peak flows. In addition, forest regrowth, either planted or by natural succession, introduces nonstationarity in the peak flows due to a resulting shift of the changing peak flow frequency distribution. Contemporary logging practices often harvest only some of the watershed (cut blocks) and rotate between cut blocks while allowing recently harvested cut blocks to regrow. This complicates the isolation of the harvesting effect as multiple change-point and trend-shifting non-stationarities are confounded to produce the observed peak flows. Further, the treatment (logging and/or construction of roads) is usually only applied once in the paired-watershed experimental design. By only analyzing the post-treatment period of

peak flows, only the trend-shifting nonstationarity caused by forest regrowth is present and can be correlated with a "time-since-treatment" variable (Green and Alila, 2012).

Such effects of forest regrowth can be statistically detected and removed from the post-treatment peak flows to produce a set of stationary peak flow observations to fulfill the assumption of stationarity under the FP framework. This method was used in recent FP-based studies, but constrained the studies to quantify only the hydrologic effects immediately after harvesting (Alila et al., 2009; Green and Alila, 2012). However, the need for evaluating the hydrologic effects at different stages of forest re-establishment post initial forest harvesting has long been recognized (Thomas, 1990). The quantification of the immediate harvesting effects hinders the practicality of the analysis when, in fact, most harvested watersheds are nonstationary in nature (Bonell and Bruijnzeel, 2005; Dolidon et al., 2009; Wheater and Evans, 2009). It is also difficult to define a stationary treatment period with continuous levels of disturbance (Grant et al., 2008). When the nonstationarity of peak flows is caused by a continuously increasing level of harvesting, distinguishing nonstationarities caused by harvesting from those by forest regrowth becomes difficult, if not impossible, hence the challenges forest hydrologists face in this new FP era.

The nonstationary effects of forest regrowth can be accommodated in modelling exercises using a deterministic model to simulate flows. Current research methods on conducting frequency analysis to evaluate forest harvesting effects on hydrologic responses often draw upon deterministic modelling. The spatially distributed, physically based hydrology models, such as the Distributed Hydrology Soil Vegetation Model (DHSVM) has been developed (Wigmosta et al., 1994), calibrated (e.g., Alila and Beckers, 2001; Thyer et al., 2004; Whitaker et al., 2003), and used as a tool to understand and quantify hydrologic effects caused by forest harvesting

scenarios (e.g., Kuraś et al., 2012; Schnorbus and Alila, 2004a, 2013). The stationary assumption can be maintained by statistically removing the effects of forest regrowth on hydrologic responses (e.g., Green and Alila, 2012), or simply maintained by "turning off" the forest regrowth in the deterministic model to represent a stationary condition (e.g., Kuraś et al., 2012; Schnorbus and Alila, 2013, 2004a). However, calibrating a deterministic hydrologic model such as DHSVM is operationally exhaustive even for small scale experimental watersheds (e.g., Kuraś et al., 2008; Thyer et al., 2004). The calibration process requires long-term and comprehensive data sets, which is an issue as such detailed monitoring of meteorological inputs and hydrologic outputs are rare even for small watersheds. The financial and logistic burden of calibrating a model on a large watershed thousands of square kilometers in size becomes yet another challenge. The lack of research on large scale watersheds for the past century is a good testimony of the outlined challenges.

Despite the challenges associated with conducting FP-based experiments, in other science communities outside forest hydrology, methods for quantifying the relationship between magnitude and frequency of extremes under nonstationary conditions have been widely explored in recent years; such as in climatology (e.g., Hundecha et al., 2008; Lee and Ouarda, 2010; Villarini et al., 2010), hydrology (e.g., Chebana et al., 2013; Leclerc and Ouarda, 2007; Ouarda and El Adlouni, 2011; Villarini et al., 2009a, 2009b), engineering (e.g., Salas and Obeysekera, 2014), ecology (e.g., Katz et al., 2005), and oceanography (e.g., Bernier et al., 2007). Allowing the frequency distribution to be nonstationary or to change with time and/or time-related variables, the nonstationary frequency analysis has been used for different purposes in the wider hydrology literature, primarily evolving around the research objectives of detection, attribution, and quantification. There are studies that used the nonstationary frequency analysis to detect

trends associated with historically changing frequency distributions of peak flows (e.g., Delgado et al., 2010; Katz et al., 2002; Villarini et al., 2009a, 2012). Based on such identified trends in the peak flow time series, some studies quantified the effects on peak flow magnitudes and frequency using nonstationary frequency distributions for planning and engineering purposes (e.g., Gado and Nguyen, 2016; Obeysekera and Salas, 2016; Read and Vogel, 2015; Salas and Obeysekera, 2014; Villarini et al., 2009a; Zhang et al., 2015). When investigating trends employing nonstationary frequency analysis, it is a fairly new practice to use peak flow controlling factors to explain the temporal variability of peak flows, and to achieve better estimation of time-varying peak flow magnitude and frequency (e.g., Condon et al., 2015; Prosdocimi et al., 2015; Sun et al., 2014). Prosdocimi et al. (2015) pioneered the use of nonstationary frequency analysis to attribute changes in the peak flow time series to historic urban development, using a pair of control (29 km^2) and treatment (55 km^2) watersheds about 30 km apart, where the attribution was successful only after introducing peak flow controlling factors in the form of covariates to account for the natural background variability in the peak flow time series.

In summary, while there have been significant advancements in nonstationary frequency analyses in the wider science literature, such advancements have not found their development and application in forest hydrology. In this dissertation, I use these recent developments and bring them to bear on the topic of forest harvesting effects on peak flows.

1.5 Thesis objective and overview

1.5.1 Thesis objective

The research presented in this dissertation was undertaken with the primary objective to understand and quantify forest harvesting effects on the peak flow regime in snow environments, by introducing and applying frequency pairing (FP) under nonstationary conditions in five pairs of watersheds with varying watershed sizes and proximities in British Columbia, Canada.

To the best of my knowledge, this is the first nonstationary frequency analysis (FP) ever conducted to evaluate forest harvesting effects on peak flows by first introducing the method in a well-established existing small paired watershed study site, then applying the method at four other large watershed pairs. The application of the nonstationary frequency analysis constitutes the second scientific contribution of this research, as the nonstationary frequency analysis can relax some of the most constraining challenges associated with conventional paired watershed studies in regards to watershed size and proximity. Based on the outcomes of the five pairs of watersheds, the third scientific contribution of this research is the development of a general physical model governing the relation between forest harvesting and peak flow regime in snow environments, which can guide future researchers and practitioners under the new FP framework.

The following research questions form the basis of the dissertation:

1. Is it possible to use nonstationary frequency analysis to understand and quantify forest harvesting effects on peak flows using data from existing paired watersheds?
2. Can nonstationary frequency analysis be used to resolve the constraints of catchment size and proximity imposed by conventional paired watershed design?
3. What are the first-order physical controls of the relation between forest harvesting and the peak flow regime in snow environments?

1.5.2 Thesis overview

The remainder of Chapter 1 reviews the challenges and limitations of the current paired watershed experimental design. The existing methods for evaluating forest harvesting effects in large watersheds are highlighted and questioned. A new research method from outside of forest hydrology is introduced to potentially resolve the fundamental constraints associated with the paired watershed design.

Chapter 2 provides a detailed description of the paired watershed study sites and data involved in the nonstationary frequency analysis of this dissertation. A detailed description of the physical characteristics and forest disturbance history of each watershed are provided. The hydrologic and climatic data used in the nonstationary frequency analysis are described in terms of the station location, record length, and proximity to the corresponding watersheds.

Chapter 3 reviews the extreme value theories with an emphasis on stationary and nonstationary frequency modelling. Different nonstationary models are developed and shown for the corresponding paired watersheds. Two methods used for evaluating forest harvesting effects of peak flows are described in detail.

Chapter 4 outlines the results associated with the detection and attribution of time trends in the peak flow time series to historic forest harvesting. Forest harvesting effects on peak flows at various historic time steps are quantified and presented.

Chapter 5 provides a discussion of the results with a specific focus on physical processes governing snowmelt peak flows under harvested conditions. The frequency-based meta-analysis of the five paired watersheds is then used to develop a physical model to guide future research and practitioners in the understanding and prediction of forest harvesting effects on peak flows with varying watershed physiographic features and logging regimes. The advantages of the

nonstationary FP method, in comparison to its CP and stationary FP counterparts, are highlighted.

Chapter 6 presents an overarching philosophical discussion of the old CP versus new FP paradigms guiding research work in forest hydrology. A summary of research findings and future research directions addressing the uncertainties and limitations associated with this dissertation are provided.

Chapter 2: Study sites and data

The thesis used five pairs of treatment-control watersheds located in the continental snow environment of British Columbia (BC), Canada (Figure 1). The Camp Creek (treatment)-Greata Creek (control) paired watersheds are located in the southern interior of BC. The Mather Creek-Fry Creek and Baker Creek-McKale River pairs are located in the eastern interior of BC. McGregor River is the control watershed for both Bowron River and Willow River, all of which are located in the central interior of BC.

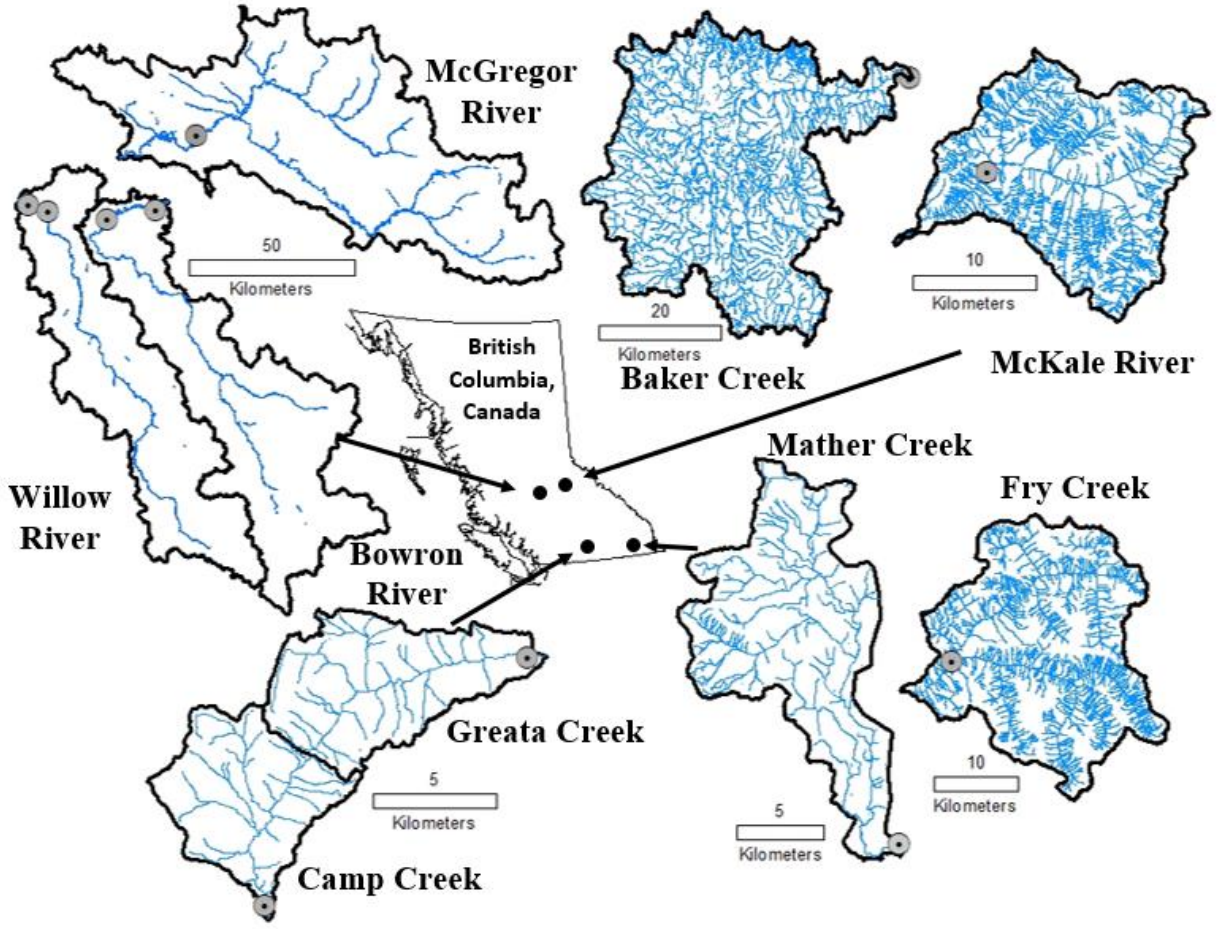

Figure 1: Location of the paired watersheds.

2.1 Camp Creek-Greata Creek pair

In order to first showcase the new method, it was necessary to use a harvested watershed with temporally increasing levels of harvesting and a control watershed that had experienced little or no land-use changes. The demo pair of control-treatment watersheds should belong to the same hydro-climate regime, in this case the interior continental snow environment. The hydrologic record should be available in both watersheds at the time when forest disturbance affected the peak flow regime in the treatment watershed. In addition, the paired watersheds should not be affected by features such as reservoirs or dams that may attenuate the natural response from climate inputs. Contrary to the old perception that the paired watersheds have to be small and neighboring, I used five pairs of control-treatment watersheds with varying sizes, proximities, and physiographies. The difference between the old and the new methods in terms of size and proximity constraints between the control and treatment watersheds are discussed in Section 5.4.

The Greata and Camp Creeks watersheds have long-term streamflow monitored by Water Survey of Canada (WSC). These watersheds have been the subject of several CP (Cheng, 1989; Moore and Scott, 2005) and stationary FP-based (Green and Alila, 2012) studies on the effects of harvesting on the peak flow regime. The two watersheds are located on the western slopes of the Okanagan Valley, about 20 km west of Peachland, BC (Figure 2). The sizes of Camp Creek and Greata Creek are 37 km^2 and 41 km^2, and the corresponding elevations range from 1079 to 1920 m and 880 to 1620 m above sea level (asl), respectively. The average slopes are 20% and 23%, while the predominant aspects are south- and north-exposed for Camp Creek and Greata Creek, respectively. There are 23 km and 27 km of stream channels in Camp Creek and Greata Creek, which correspond to stream densities of 0.62 km/km^2 and 0.66 km/km^2. Mixed

stands of lodgepole pine (*Pinus contorta Dougl*) and Douglas-fir (*Pseudotsuga menziesii*) cover the majority of both watersheds, with a higher abundance of lodgepole pine in the lower and more Douglas-fir in the intermediate elevations. White spruce (*Picea Engelmanii Parry*) and subalpine fir (*Abies lasiocarpa*) mixed stands are present at higher elevations. The physiographic properties of the watersheds are summarized in Table 1.

The Water Survey of Canada stream gauges IDs for Camp Creek and Greata Creek are 08NM134 and 08NM173, with hydrometric data being used from 1968 to 2012 and 1971 to 2011, shown in Figure 3a and Figure 4a, respectively. For the Camp Creek-Greata Creek pair, peak flows were defined as the annual maximum daily discharges. Peak flow outliers occurred in 1972 and 1997. They were identified for both watersheds based on a statistical test outlined in Pilon and Harvey (1994). The nonstationary frequency analysis was carried out with and without outliers. Weather data from 1968 to 1993 were obtained from "Summerland CS" station (ID: 112G8L1), located about 49 km southeast of the Camp Creek stream gauge. Weather data from 1994 to 2012 were obtained from "Peachland Brenda Mines" station (ID: 1126077) located about 21 km northwest of the Greata Creek stream gauge. Even though two weather stations were used, the distance between the two weather stations is close enough to be considered in a group where there is little difference in the long-term characteristics of climate measurements (Degaetano, 2001). The mean annual temperature is 10°C. January has the lowest monthly mean temperature (-1°C) and July is the warmest month (22°C), based on weather data from "Summerland CS". The mean annual precipitation is about 600 mm, 60% of which falls as snow in winter between November and March. Snow data were based on the average of the two nearby snow pillow stations: "Trout Lake" (ID: 2F01) and "Summerland Reservoir" (ID: 2F02). These are located about 19 km west of the Camp Creek stream gauge and 18 km west of the Greata

Creek stream gauge, respectively. Both stations are surveyed by the BC Provincial Government. The peak of the snowpack water equivalent (SWE) was selected on an annual basis to represent the general snowfall condition partially responsible for peak flows.

As mentioned in Chapter 1, peak flows in snow-dominated regimes are governed by several factors such as: (i) the amount of moisture in the form of snow accumulation; (ii) moisture in the soil; (iii) energy causing the melt; and (iv) occasional rain falling on melting snow. During the peak of the freshet, the soil in both watersheds (control and treatment) should be highly saturated from the snowmelt induced moisture in the days preceding the peak flow of the freshet hydrograph (Williams et al., 2009). Antecedent soil moisture plays less of a role in controlling the peak flow of the annual snowmelt hydrograph in small (Schnorbus and Alila, 2013) and large watersheds (Curry and Zwiers, 2018). Therefore, antecedent soil moisture was not considered for further analysis. In addition, precipitation events were also not considered in the analysis of Camp Creek and Greata Creek, because significant rain on spring melting snow is rare for small watersheds in the BC's interior (Loukas et al., 2000; Schnorbus and Alila, 2004a, 2013; Troendle et al., 2001). The relatively small sizes of Camp Creek and Greata Creek reduce the chance of them receiving localized precipitation events. Following Green and Alila (2012) and Curry and Zwiers (2018), two primary climate inputs controlling the magnitude of the annual peak flows were used for Greata Creek and Camp Creek: (i) peak snow accumulation and (ii) average 3-day temperature preceding peak flows (Figure 3b, 3c and Figure 4b, 4c for Camp Creek and Greata Creek, respectively).

Continuous forest harvesting and changes in forest cover conditions took place at Camp Creek over 30 years. Logging commenced in 1976, and over 29% of the watershed was harvested by the end of 1977 in response to a widespread Mountain Pine Beetle (MPB) outbreak.

An additional 12% was harvested since then resulting in 41% of Camp Creek being disturbed. In Greata Creek, approximately 9% of the total catchment area was harvested. Some of the logging occurred prior to 1980, while the remaining occurred between 1980 and 1991. More than half of the total disturbance occurred in the lower half of Greata Creek (Figure 2). Harvesting at low elevations is not expected to affect the peak flow of the annual snowmelt hydrograph (Schnorbus and Alila, 2004a, Figure 8 and related discussion). Therefore, the forest harvesting that occurred at Greata Creek was ignored, as in previous CP- and stationary FP-based studies of the same paired watershed site (Cheng, 1989; Green and Alila, 2012; Moore and Scott, 2005).

The overall land-use conditions resulting from historic forest harvesting, which occurred at Camp Creek from 1968 to 2012, were quantified and used in the nonstationary modelling as a covariate. Since forest harvesting is temporally and spatially cumulative, equivalent clearcut area (ECA) was used as a metric to describe the combined effects of forest harvesting over space and time. The Camp Creek time series of ECA is shown in Figure 5. ECA can: (i) describe individual forest harvesting areas or cut blocks into a quantifiable metric; (ii) account for cut blocks that occurred at different locations of the watershed; and (iii) account for cut blocks that occurred at different times in the disturbance history of the watershed with vegetative re-establishment. The use of ECA is common in the literature on the effects of forest management on hydrology (e.g., King, 1989; Macdonald, 2000; Price et al., 2009; Talbot and Plamondon, 2002; Valdal and Quinn, 2011; Varhola et al., 2010a).

The initial hydrologic effects of the individual harvest areas can reduce over time as a result of vegetative regrowth, be it natural regeneration and/or planting. For instance, the ECA of a new cut block is 100%, where there is little to no forest-related hydrologic functions served by the new cut block. However, the new cut block ECA can reduce to zero over time as vegetation

re-establishes, leading to the recovery of hydrologic response to pre-harvest conditions (hence the concept of recovery). At the watershed level, ECA can increase and decrease over time, depending on the evolution of forest harvesting and forest regrowth. To form the ECA time series, the ECA values of individual cut blocks were obtained from the sum of harvested areas in the catchment to form the ECA value at the catchment level. The combined ECA was adjusted on an annual basis to accommodate the increase of ECA due to additional forest harvesting and the decrease of ECA due to forest regrowth in the harvested areas. Despite 41% of Camp Creek being logged historically (Figure 2), the peak ECA value was approximately 26% due to the partial hydrologic recovery of previous cut blocks (Figure 5).

Therefore, the calculation of ECA at the catchment level hinges on two factors: (i) the history of forest harvesting and (ii) the empirical relationship between ECA and forest stand conditions used to calculate the reduction of ECA as a result of the hydrologic recovery. This relationship is assumed to be a nonlinear function between forest stand height (dominant trees) and ECA. The generalized relation between ECA and forest stand conditions, representative of Camp Creek watershed, was taken from Winkler and Boon (2015). The history of forest harvesting at Camp Creek, in terms of the size of individual harvesting areas and their respective date, was obtained from a digital forest cover information database derived from the Vegetation Resource Inventory (VRI) provided by the BC Provincial Government (http://geobc.gov.bc.ca). The associated spatial data were processed using ArcGIS®.

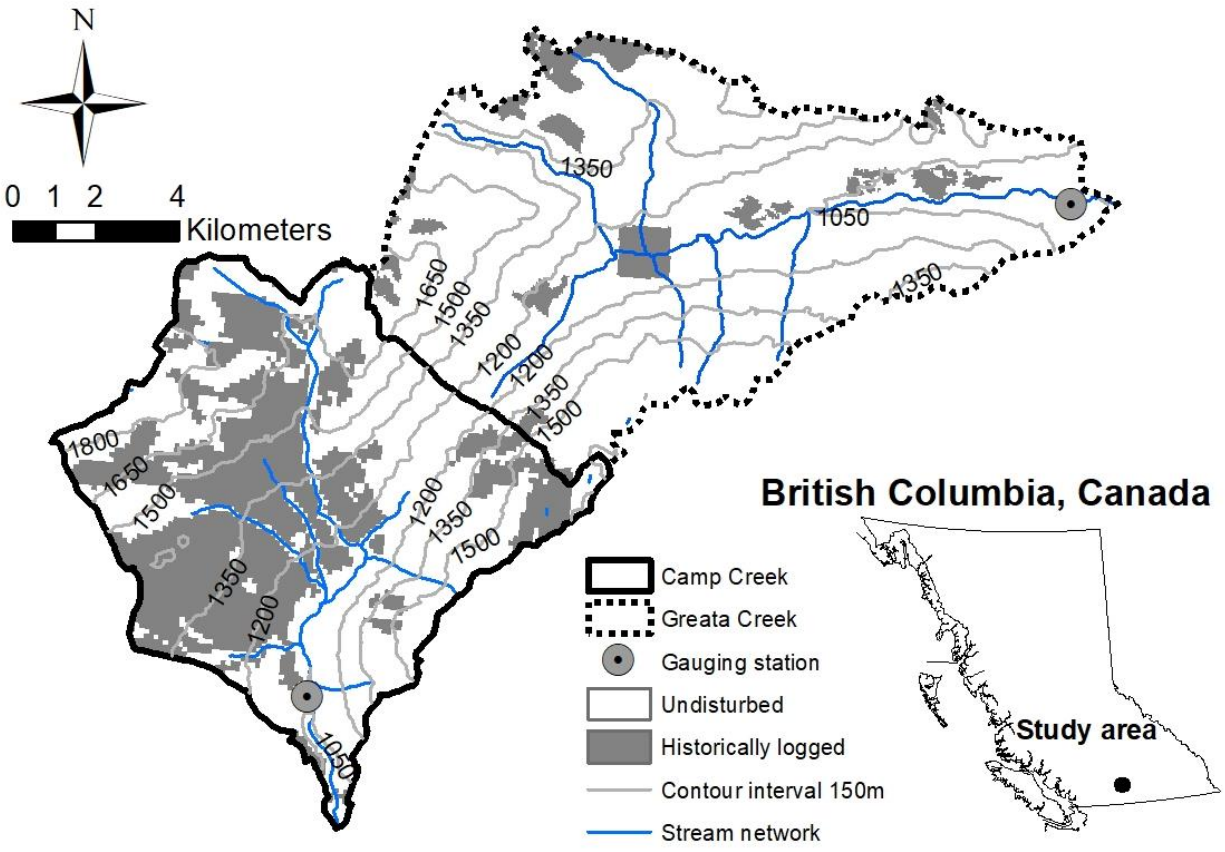

Figure 2: Location and topography of the Camp Creek and Greata Creek.

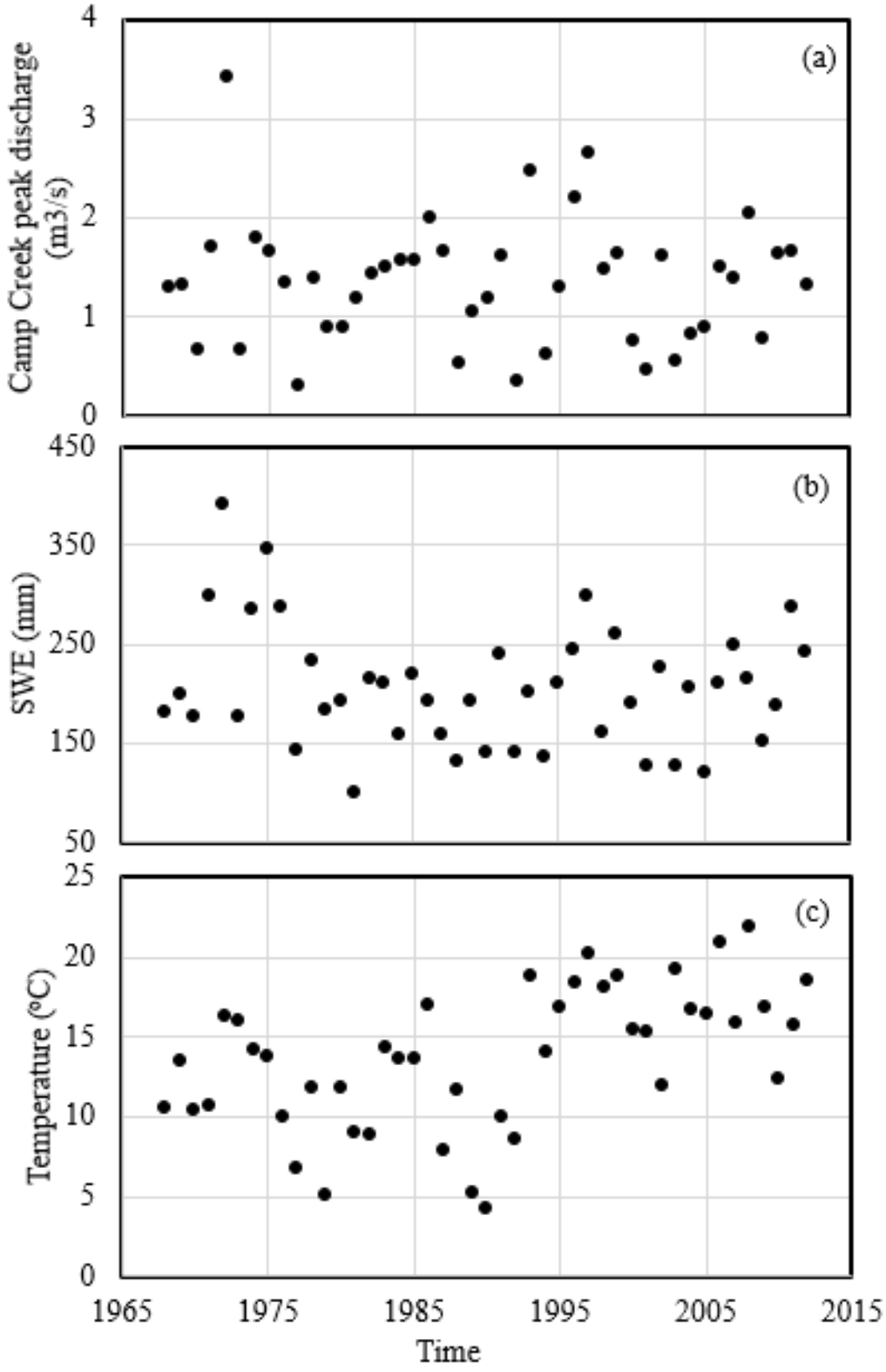

Figure 3: The time series of (a) Camp Creek peak discharge, (b) peak snow accumulation at the time of peak discharge and, (c) average 3-day temperature preceding peak discharge of Camp Creek.

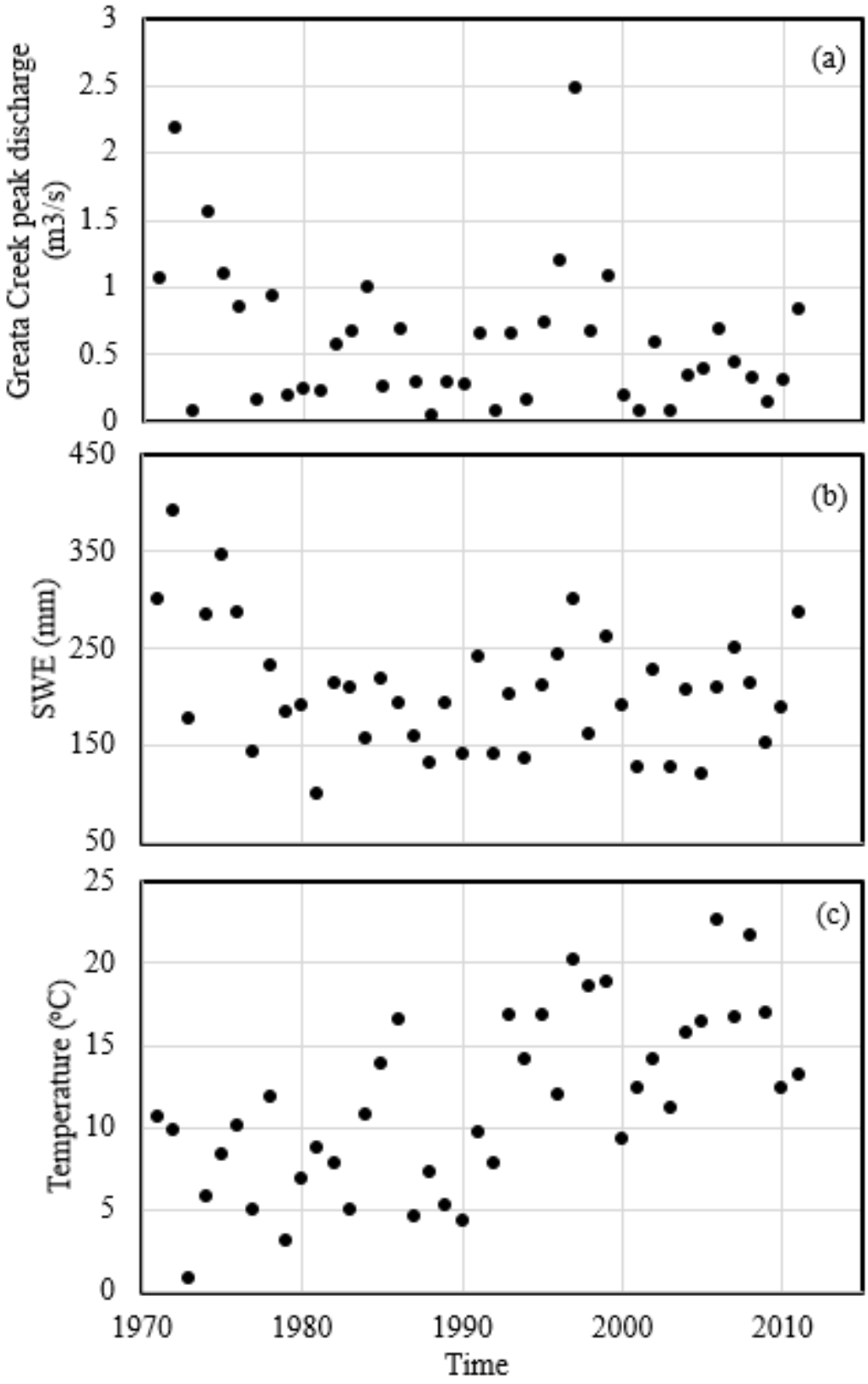

Figure 4: The time series of (a) Greata Creek peak discharge, (b) peak snow accumulation, and (c) average 3-day temperature preceding peak discharge of Greata Creek.

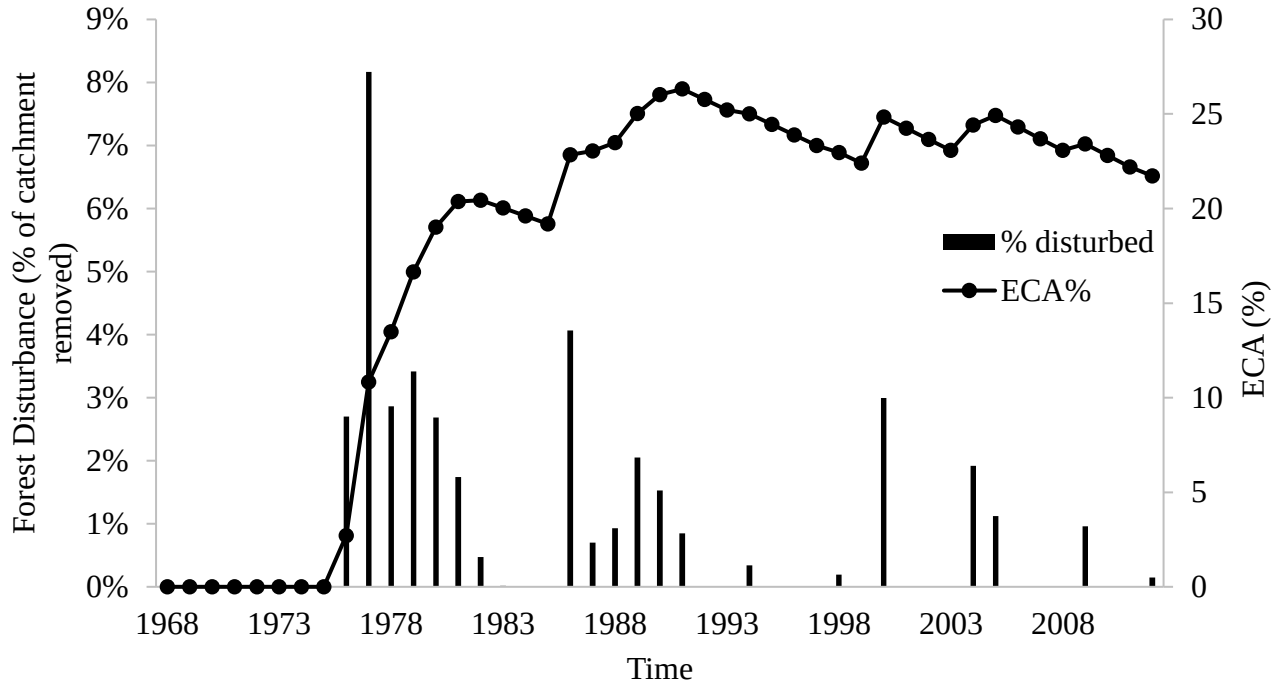

Figure 5: ECA time series and annual forest harvesting of Camp Creek from 1968 to 2012.

Table 1: Physiography of treatment Camp Creek and control Greata Creek watersheds.

	Camp Creek	Greata Creek
Catchment area (km^2)	37	41
Elevation range (m)	1079-1920	880-1620
Aspect distribution	S/SE/E/W	N/NW/SE/S
Peak ECA	26%	-
Dominant vegetation	Lp/Df/Sp/Bf	Lp/Df/Sp/Bf
Average slope	20%	23%
Stream length (km)	23.0	27.0
Stream density (km/km^2)	0.62	0.66
Stream gauge	08NM134	08NM173
Snow pillow	2F01, 2F02	
Weather station	112G8L1, 1126077	
Record length	45 (1968-2012)	41 (1971-2011)
Outliers	1972, 1997	

2.2 Mather Creek-Fry Creek and Baker Creek-McKale River pairs

To illustrate how the nonstationary frequency pairing can potentially relax the proximity constraint under the framework of the conventional paired watershed study design, two pairs (two treatments and two controls) of watersheds were used in this research. Mather Creek and Baker Creek are treatment watersheds, while the respective control watersheds are Fry Creek and McKale River. The two control watersheds have experienced little or no historic land-use changes. The selection of additional pairs of control-treatment watersheds used in this thesis follows the same criteria outlined in Section 2.1, which guided the selection of the Camp Creek-Greata Creek pair.

Mather Creek (treatment watershed) and Fry Creek (control watershed) are located in southeastern BC (Figure 6), with respective sizes of 133 km^2 and 585 km^2. The elevation ranges from 1100 to 2600 m and 550 to 3200 masl, giving rise to an average slope of 22% and 53% for Mather Creek and Fry Creek, respectively. The predominant slope is east- and west-facing for Mather Creek, while it is west- and north-facing for Fry Creek. There are 104 km and 542 km of stream channels in Mather Creek and Fry Creek, which correspond to 0.79 km/km^2 and 0.93 km/km^2 of stream densities. For Mather Creek, the Engelmann Spruce-Subalpine Fir (ESSF) zone is situated in the higher elevations, while the Montane Spruce (MS) zone is located in the lower elevations. The dominant tree species include lodgepole pine, western larch (*Larix occidentalis*), Engelmann spruce (*Picea engelmannii*), and subalpine fir. For Fry Creek, the ESSF zone predominates, with a small proportion of the Interior Cedar-Hemlock (ICH) at the lower elevations. The dominant tree species include subalpine fir and Engelmann spruce. The catchment characteristics for both pairs of watersheds are summarized in Table 2.

Baker Creek (treatment watershed) and McKale River (its control watershed) are located in central BC (Figure 6). The size of Baker Creek and McKale River watersheds are 1564 km^2 and 353 km^2, respectively. The elevations range from 469 to 1524 m and 700 to 3450 masl, respectively. There are approximately 1407 km and 249 km of stream channels in Baker Creek and McKale River, giving rise to stream densities of 0.90 km/km^2 and 0.99 km/km^2. The topography in Baker Creek is plateau-like, with an average slope of 9%. The terrain at McKale River is more mountainous, with an average slope of 48%. The slopes of McKale River are predominantly east- and west-facing. The Biogeoclimatic Ecosystem Classification (BEC) zones in the Baker Creek watershed are primarily Sub-Boreal Pine Spruce (SBPS) and Sub-Boreal Spruce (SBS), with dominant tree species including lodgepole pine, interior spruce (*Picea glauca* x *englemannii*), and a smaller portion of trembling aspen (*Populus tremuloides*). The BEC zones in the McKale River watershed are primarily ESSF in the mid-high elevations, with small portions of SBS and ICH in low elevation areas. The dominant tree species are subalpine fir and Engelmann Spruce.

The WSC stream-gauge IDs for Mather Creek and Fry Creek are 08NG076 and 08NH130, with annual peak flows being used from 1973 to 2014 and 1973 to 2015, respectively. Based on the statistical test outlined in Pilon and Harvey (1994), the peak flows that occurred in 2013, 2005 and 2013, were identified as outliers for Mather Creek and Fry Creek, respectively. Weather data for Mather Creek were obtained from two weather stations: “Marysville” (ID: 1154909) and “Kimberley PCC” (ID: 1154203), for data from 1973 to 2004 and 2005 to 2014, respectively. The weather stations are located about 10 km south of the Mather Creek stream gauge. According to “Marysville” weather station, the mean annual precipitation at Mather Creek is 433 mm, while the mean annual temperature is 5.41°C. January has the lowest monthly

mean temperature (-7.23°C), while July is the warmest month (17.76°C). Weather data for Fry Creek were obtained from the "Kaslo" weather station (ID: 1143900), located about 16 km south of the stream gauge. Peak snow accumulation for both Mather Creek and Fry Creek were obtained from the "Sullivan Mine" snow pillow station (ID: 2C04).

The WSC stream-gauge IDs for Baker Creek and McKale River are 08KE016 and 08KA009, with annual peak flows being used from 1964 to 2012 and 1971 to 2014, respectively. Based on the statistical test outlined in Pilon and Harvey (1994), the peak flows that occurred in 1991, 1995 and 2001, were identified as outliers for Baker Creek and McKale River, respectively. The nonstationary frequency analysis was carried out with and without outliers. Weather data for Baker Creek were obtained from three weather stations less than 10 km away from the Baker Creek stream gauge. These were "Quesnel A" station (ID: 1096630), "Quesnel AWOS" station (ID: 1096625), and "Quesnel Airport" station (ID: 1096631), for data from 1964 to 2006, 2007 to 2010, and 2011 to 2013, respectively. Weather data for McKale River were obtained from two weather stations: "McBride North" station (ID: 1094955) and "Red Lake" station (ID: 1166658), for data from 1973 to 1985 and 1986 to 2014, respectively. The two weather stations are located about 20 km southeast of the stream gauge. Missing data in 1972 were obtained from "McBride 4SE" station (ID: 1094950), while missing data in 1997, 1998, and 2001 were obtained from "McBride Elder Creek" station (ID: 1094948). According to the "Quesnel A" weather station, the mean annual precipitation at Baker Creek is about 530 mm, while the mean annual temperature is about 5°C. January has the lowest monthly mean temperature (-9°C) and July is the warmest month (17°C). Snow data were collected from the nearby "Nazko" snow pillow station (ID: 1C08), surveyed by the BC Provincial Government.

The peak of the snowpack water equivalent (SWE) was selected on an annual basis to represent the general snowfall conditions partially responsible for peak flows.

Convective storms in the BC's interior become important in the summer (May to August) as they are high intensity and short duration events that cover small areas in space (Eaton and Moore, 2010). As watershed size increases, the influence of convective storms in producing peak flows is reduced since the relative rain-cell size becomes increasingly smaller in comparison to the catchment size. However, increasing watershed size increases the likelihood of the watershed catching these localized convective storms. Therefore, in addition to peak snow accumulation and average 3-day temperature preceding peak flows, the total 7-day precipitation preceding peak flows was used as another climate input controlling the magnitude of the annual peak flows at the Baker Creek-McKale River and Mather Creek-Fry Creek pairs. The time series of peak flows, SWE, temperature, and precipitation used in the analyses are shown in Figure 7a-7d, Figure 8a-8d, Figure 9a-9d, and Figure 10a-10d, for Mather Creek, Fry Creek, Baker Creek, and McKale River, respectively.

Continuous forest harvesting and changes in forest cover conditions occurred at both Mather Creek and Baker Creek. Forest harvesting at Mather Creek took place from the mid-1990s to 2010, resulting in cumulative logging of 24.22%, concentrated in the lower 50% of the watershed. No forest harvesting occurred at Fry Creek. Historic harvesting at Baker Creek began in the 1970s, with major harvesting events starting in the 2000s as a response to a widespread MPB outbreak. The cumulative area logged from 1964 to 2012 was 48.25%. The distribution of the historic logging was such that there were no specific concentrations at certain elevations or aspects (Figure 6). Approximately 4% of McKale River was harvested in the lowest elevation bands in the 2000s (Figure 6). Since this level of harvesting at low elevation is not expected to

affect the peak flow of the snowmelt season hydrograph, logging at McKale River was ignored. The total logging that occurred at the treatment watersheds Mather Creek and Baker Creek were quantified into ECA time series, as it was done for Camp Creek. The ECA time series of Mather Creek and Baker Creek are shown in Figure 11 and Figure 12, respectively.

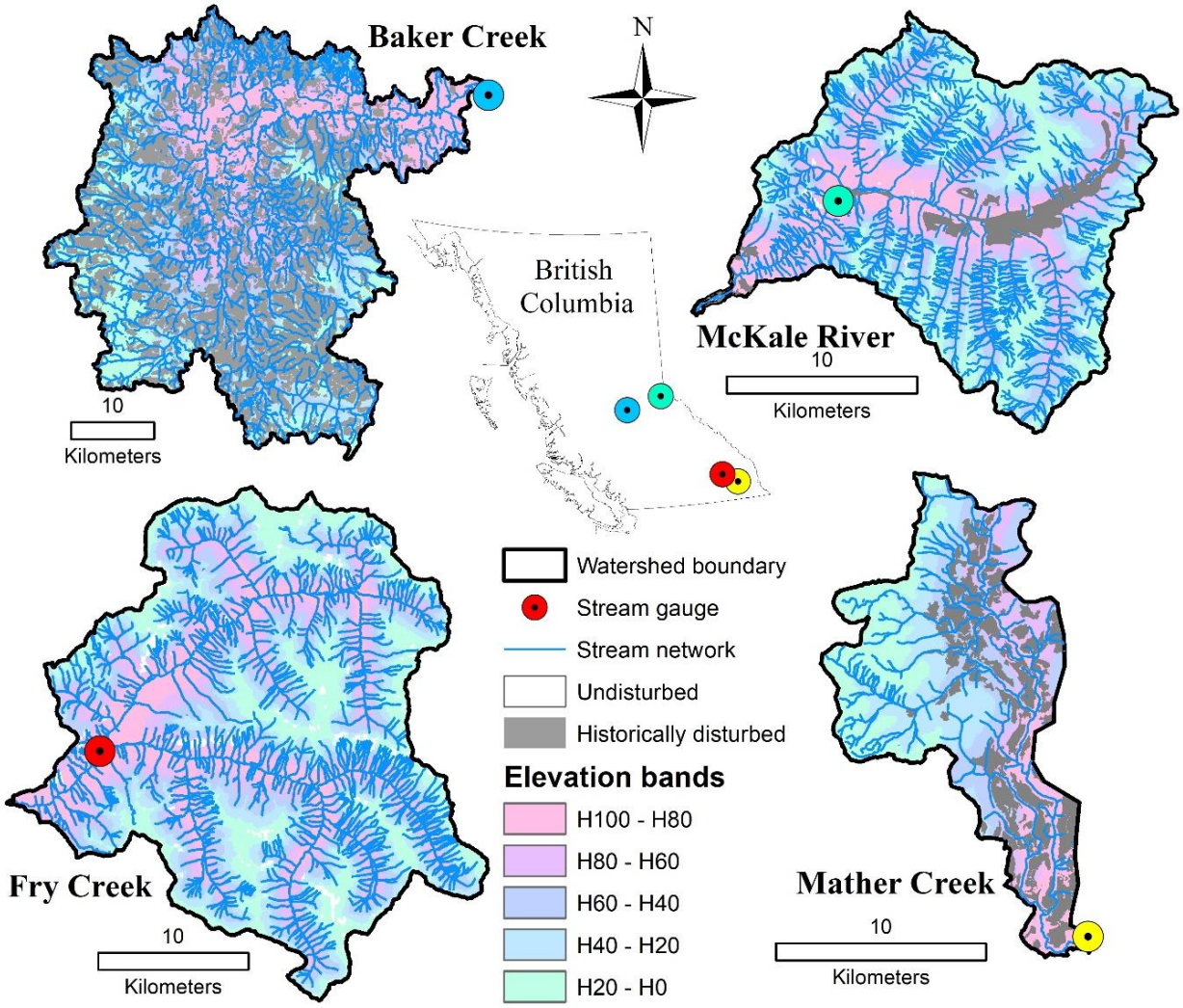

Figure 6: Location and topography of Baker Creek, McKale River, Mather Creek, and Fry Creek.

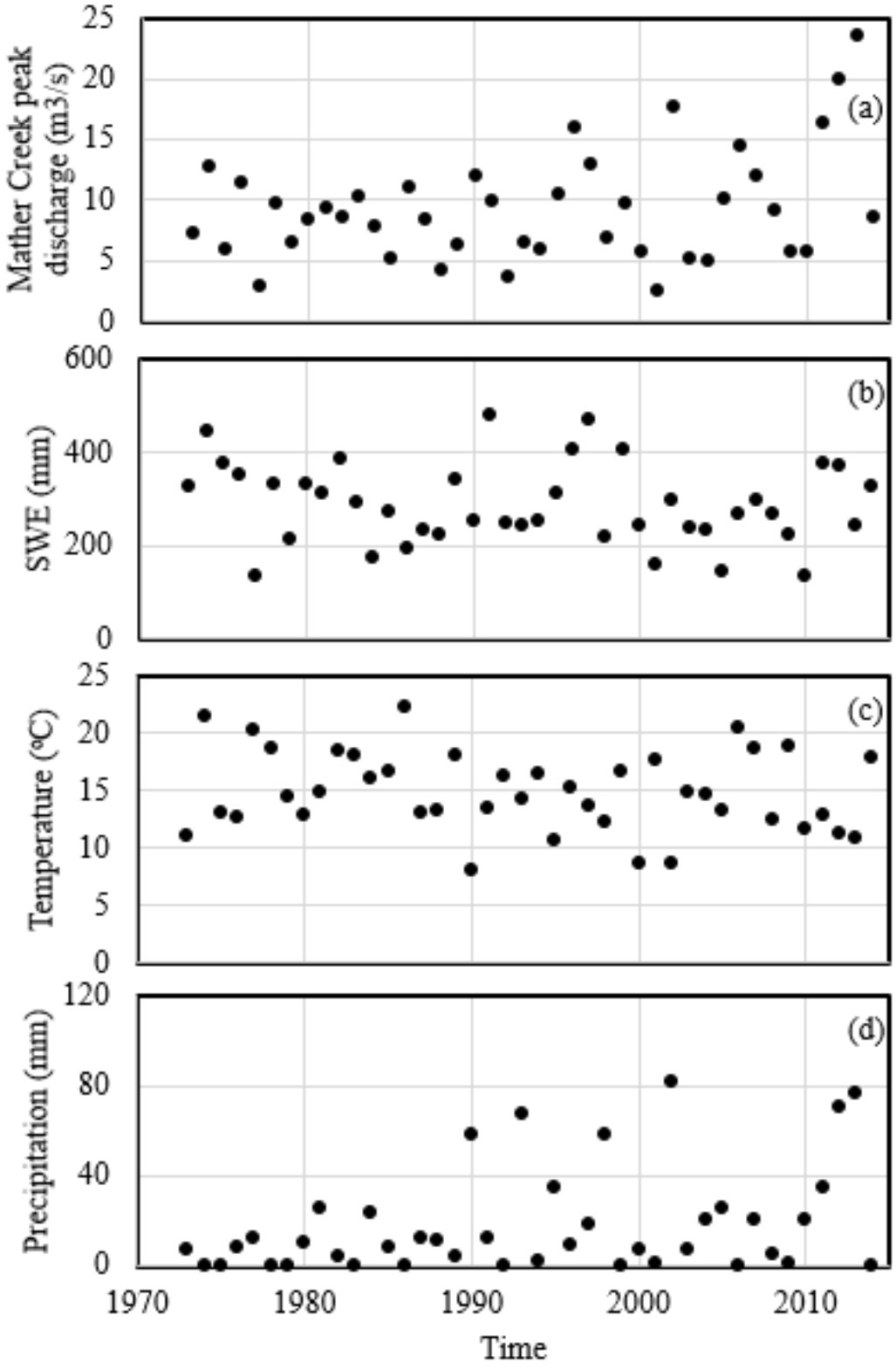

Figure 7: The time series of (a) Mather Creek peak discharge, (b) peak snow accumulation at the time of peak discharge, (c) average 3-day temperature preceding peak discharge and, (d) total 7-day precipitation preceding peak discharge of Mather Creek.

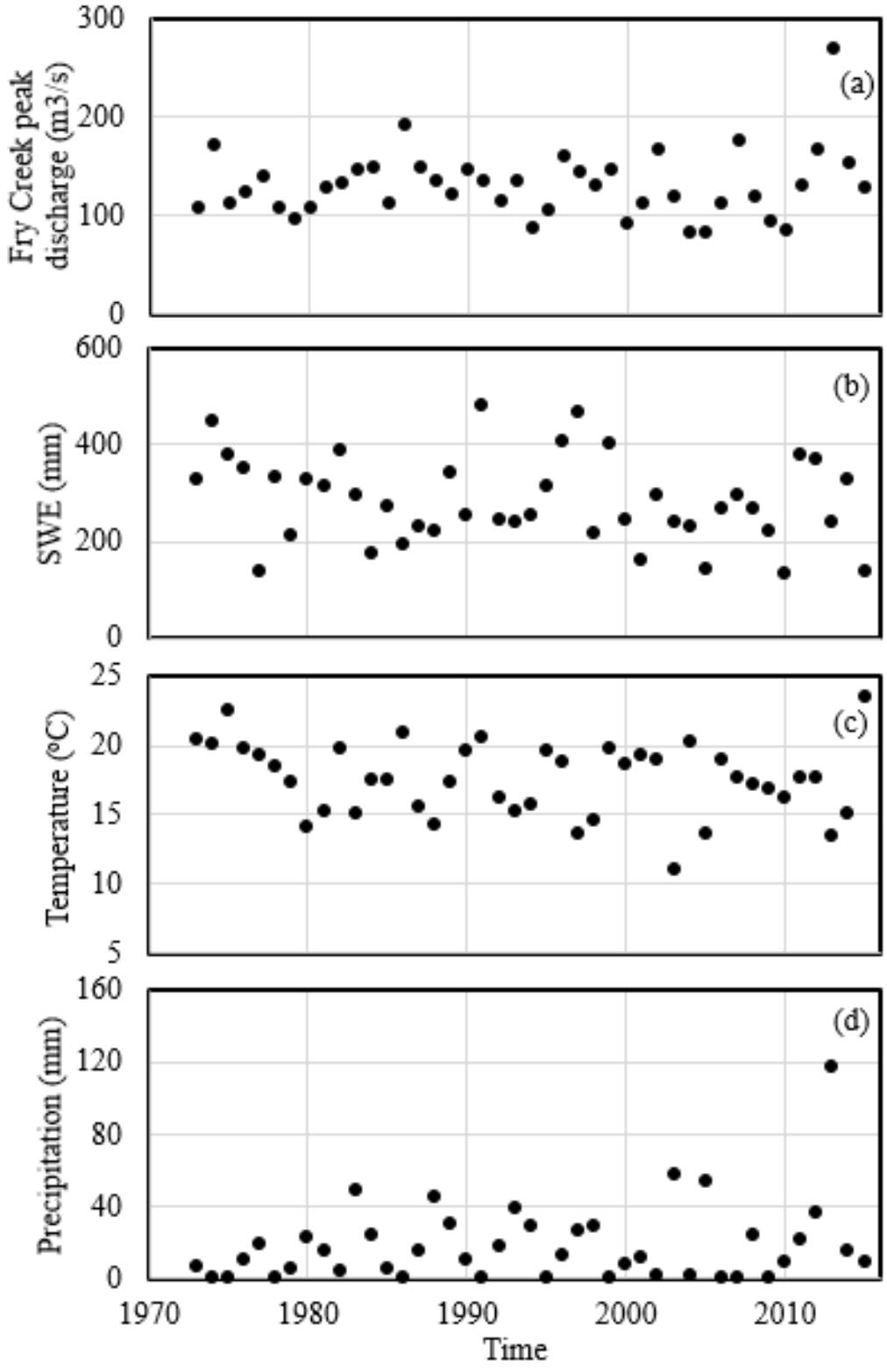

Figure 8: The time series of (a) Fry Creek peak discharge, (b) peak snow accumulation at the time of peak discharge, (c) average 3-day temperature preceding peak discharge and, (d) total 7-day precipitation preceding peak discharge of Fry Creek.

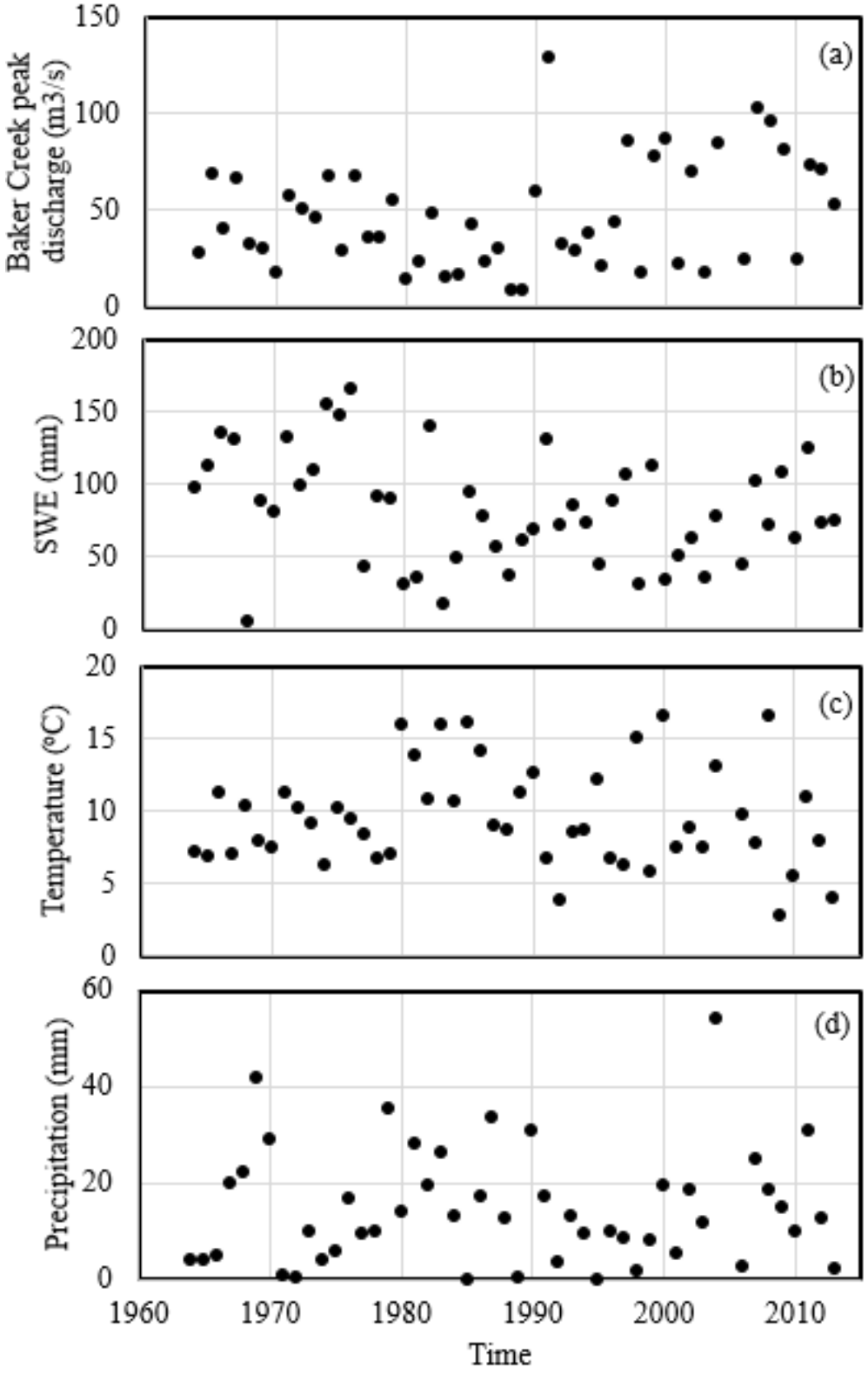

Figure 9: The time series of (a) Baker Creek peak discharge, (b) peak snow accumulation at the time of peak discharge, (c) average 3-day temperature preceding peak discharge and, (d) total 7-day precipitation preceding peak discharge of Baker Creek.

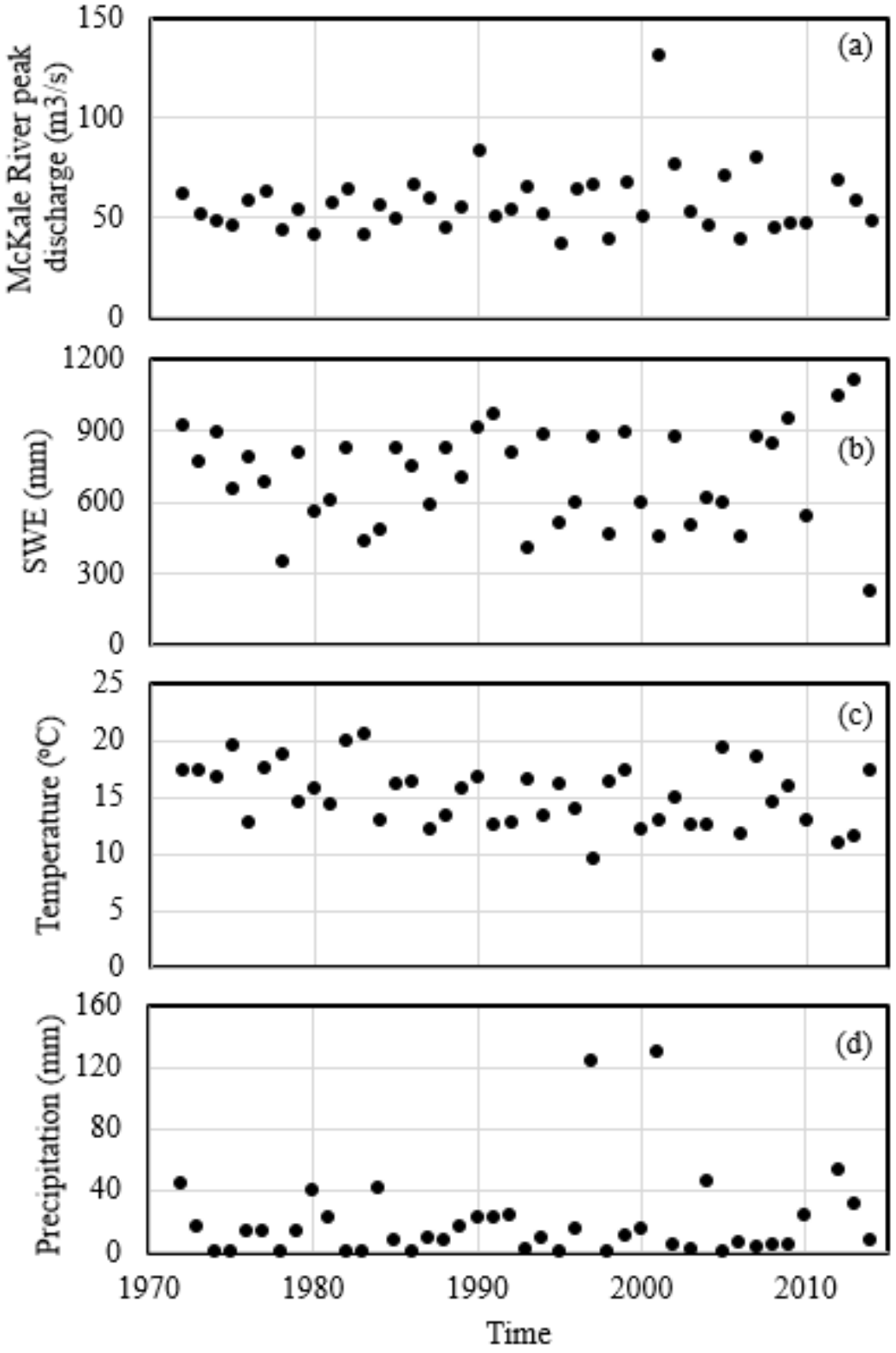

Figure 10: The time series of (a) McKale River peak discharge, (b) peak snow accumulation at the time of peak discharge, (c) average 3-day temperature preceding peak discharge and, (d) total 7-day precipitation preceding peak discharge of McKale River.

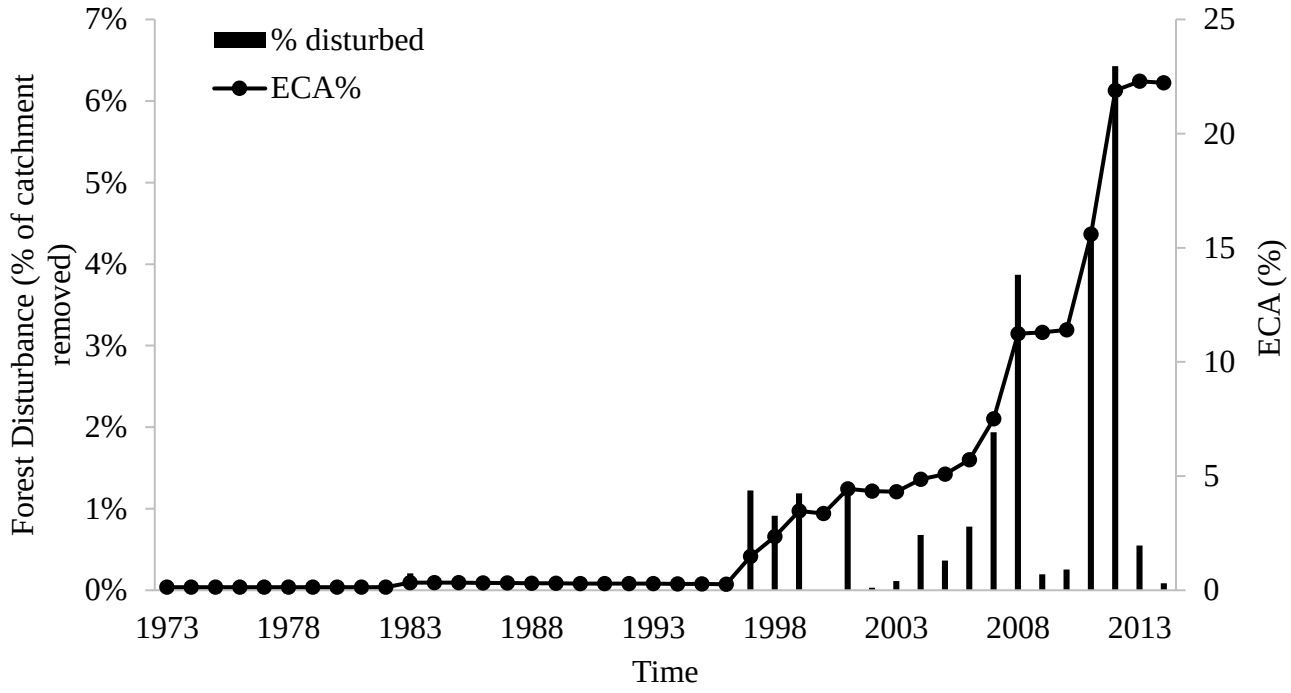

Figure 11: ECA time series and annual forest harvesting of Mather Creek from 1973 to 2014.

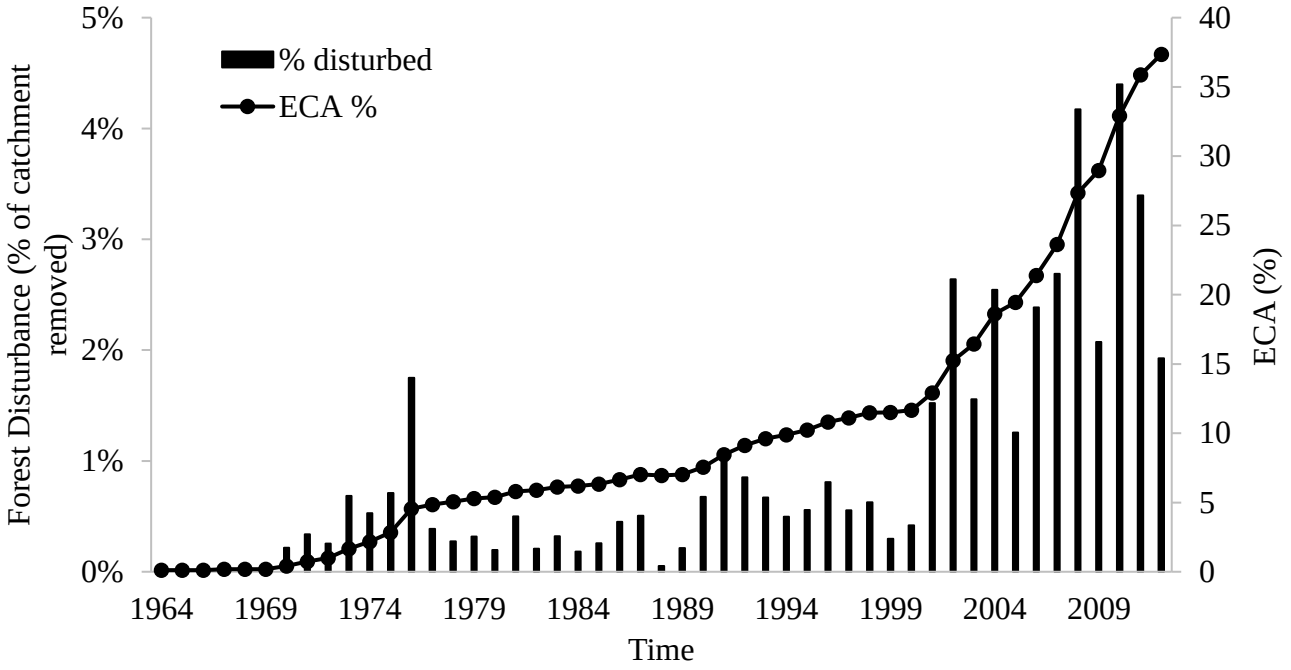

Figure 12: ECA time series and annual forest harvesting of Baker Creek from 1964 to 2012.

Table 2: Physiography of treatment (Mather Creek and Baker Creek) and control (Fry Creek and McKale River) watersheds.

	Mather Creek	Fry Creek	Baker Creek	McKale River
Catchment area (km^2)	133.16	585	1563.90	353
Elevation range (m)	1100 – 2600	550 - 3200	469 - 1524	700 - 2450
Aspect distribution	E/W/S=N	W/N/SW/E	NW/W/S=N	E=W/S=N
Peak ECA	22%	-	52%	4%
Dominant vegetation	PL, LW, SE, BL	BL, SE, FDI, LA	PL, PLI, S, AT	BL, S, CW, HW
Average slope (%)	22	53	9	48
Stream length (km)	104.02	542.70	1406.69	248.75
Stream density (km/km2)	0.78	0.93	0.90	0.99
Stream gauge	08NG076	08NH130	08KE016	08KA009
Snow pillow	2C04	2C04	1C08	1A14
Weather stations	Marysville (1154909) Kimberley PCC (1154203)	Kaslo (1143900)	Quesnel A (1096630) Quesnel AWOS (1096625) Quesnel Airport Auto (1096631)	McBride Elder Creek (1094948) McBride 4SE (1094950) McBride north (1094955) McBride S & W ranch (1094962) Red Lake (1166658)
Record length	42 (1973 – 2014)	43 (1973 – 2015)	48 (1964 – 2012)	42 (1971-2014)
Outliers	2013	2005, 2013	1991	1995, 2001

2.3 Bowron River- and Willow River-McGregor River pairs

Bowron River, Willow River, and McGregor River make up the fourth and fifth control-treatment pairs of watersheds used in this thesis (Figure 1). These large watersheds are located in the BC's interior with long-term records of streamflow. The sizes of the neighbouring treatment watersheds, Bowron River and Willow River are 3550 km^2 and 3110 km^2, respectively. The size of their common control watershed, McGregor, is 4780 km^2. The elevations of Bowron River and Willow River watersheds range from 600 to 2350 m and 570 to 2080 masl. There are 2747 km and 2730 km of stream channels in the Bowron River and Willow River watersheds, giving rise to stream densities of 0.82 km/km^2 and 0.95 km/km^2. The Bowron River watershed has a higher relief than the Willow River watershed, characterized by average slopes of 22% and 15%, respectively. The distributions of the landscapes by aspect within the Bowron River and Willow River watersheds are similar, with predominantly northeast- followed by southwest-facing slopes (Table 3). The landforms are glaciofluvial and fluvial terraces along the Bowron and Willow Rivers. The soils for both watersheds are loamy glaciological material along the broad valley bottoms, while the valley sides are covered by a variable layer of till and colluvium (Dawson, 1989). The BEC zones in the Willow River watershed are SBS in the lower elevations and ESSF in the higher elevations. In the Bowron River watershed, the BEC zones are ICH and SBS in the lower elevations and ESSF in the higher elevations. The split in BEC zones occurs at about 1100 m for both watersheds, which is H40 for Willow River and H50 for Bowron River (e.g., H40 and H50 are hypsometric elevation contour lines above which lies 40% and 50% of the total watershed area). Coniferous species such as lodgepole pine and Douglas-fir are found in the dryer areas, while interior spruce and subalpine fir are found in moister areas. Deciduous species such as trembling aspen (*Populus tremuloides*) and paper birch (*Betula papyrifera*) are found in

seral stands. Alders (*Alnus sp*.) and willow (Salix sp.) are present in some riparian areas (Beaudry and Nassey, 1994).

Streamflows have been monitored by WSC at Bowron River, Willow River, and McGregor River. The WSC stream-gauge ID for McGregor River is 08KB003, with hydrometric data being used from 1963 to 2009. For Bowron River, flow data were obtained from two stations, 08KD004 and 08KD007, with collective hydrometric data being used from 1955 to 2009. Station 08KD007 was installed at the outlet of the watershed in 1954, and it was relocated upstream to 08KD004 in 1977, resulting in a reduction of drainage area from 3550 km^2 to 3330 km^2. For Willow River, flow data were also obtained from two stations, 08KD006 and 08KD003. The hydrometric data from 1953 to 2009 were used. Station 08KD003 was discontinued and relocated to station 08KD006 in 1976. The relocation resulted in a reduction of drainage area from 3110 km^2 to 2860 km^2. Relocation of stream gauges is not uncommon in practice (e.g., Frazier and Page, 2006; Siriwardena et al., 2006; Yihdego and Webb, 2013). The streamflow data for both Bowron River and Willow River were adjusted using a nonlinear equation to accommodate for the nonlinear features between peak flows and catchment area, following Coulson and Neill (2004), Obedkoff (1998), and Watt (1989):

$$Q_n = Q_o * (A_n / A_o)^{0.785} \quad (1)$$

where Q_n and Q_o are peak flows (m^3/s) for the new and old locations, while A_n and A_o are the new and old catchment areas (km^2), respectively. This form of the equation is commonly used for adjusting measured flow to account for gauge relocation in science and professional practice alike. It was used in the analysis of the effects of harvesting on streamflows in Bowron River and Willow River by Zhang and Wei (2014). Weather station “Prince George A”, about 40 km west of the outlet of Willow River, was used to obtain the general climate conditions for the Bowron

River and Willow River watersheds. According to data obtained from "Prince George A", the mean annual precipitation and mean annual temperature are 603.48 mm and 3.81°C. January is the coldest month in terms of monthly mean temperature (-10.15°C) while July is the warmest month (15.32°C).

Following Curry and Zwiers (2018), the warming rate, defined by the slope of the trend line fitted to the daily mean temperature between April 1st and peak snow accumulation (SWE), appears to be a dominant climate control of peak flows generated in large scale, snow-dominated catchments in British Columbia. Hence, the warming rates for each of the successive peak flows were computed using data from weather station "Prince George A". Data with warming rates greater than zero were retained for further analysis. Peak snow accumulation data were obtained from nearby snow pillow stations. For the McGregor River watershed, snow data were obtained from the "Pacific Lake" station (ID: 1A11). For both Bowron River and Willow River watersheds, snow data were mostly obtained from the "Barkerville" station (ID: 1A03P). However, there are some missing data at this station. Therefore, linear regression models were developed, as shown in Equations (2) and (3), to estimate the snow accumulation at the 1A03P station using data from nearby snow pillow stations as predictors. These stations are "Longworth (upper)" (ID: 1A05) for the Bowron River watershed and "Prince George Airport" (ID: 1A10) for the Willow River watershed.

$$\text{1A03P SWE} = 0.20 * \text{1A05 SWE} + 210.41 \ (r^2 = 0.21, p < 0.01) \qquad (2)$$

$$\text{1A03P SWE} = 0.90 * \text{1A10 SWE} + 256.62 \ (r^2 = 0.37, p < 0.01) \qquad (3)$$

The time series of peak flows, SWE, and warming rates used in the analyses are shown in Figure 14a-14c, Figure 15a-15c, and Figure 16a-16c, for Bowron River, Willow River, and McGregor River watersheds, respectively. Unlike Camp Creek, where annual peak flows were used, peaks-

over-threshold (POT) events were used for Bowron River and Willow River paired watersheds resulting in longer sample sizes. The longer sample size increased the likelihood of relating peak flows with their corresponding climate inputs to account for the natural background variability, which can lead to better detection of land-use change effects on peak flows (Prosdocimi et al., 2015). The enhancement brought by an increased sample size in the POT time series, in comparison to the annual peak flow time series, is particularly useful for these three largest watersheds. The climatic variability can sometimes offset the hydrologic response as a result of land-use changes, increasing the difficulty to detect changes in the peak flow time series (Schulze, 2000).

Forest harvesting and changes in forest cover conditions began in the 1960s and continued throughout the next several decades for both the Bowron River and Willow River watersheds. In the Bowron River watershed, an epidemic of spruce bark beetle infestation occurred in 1975 and it triggered a landscape-level salvage logging to control and reduce fire hazards. Logging was concentrated in the mid and low elevations, although some harvesting occurred at higher elevations. The historic rate of annual logging in the Bowron River watershed is shown in Figure 17. In the Willow River watershed, as Figure 18 shows, continuous, small-scale logging occurred over the entire 60 years of record. Several major harvesting events happened in the mid-80s, most of which were concentrated at the mid and high elevations. The total logged area of the Bowron River and Willow River watersheds was 28.7% and 34.7%, respectively. The overall logging in both watersheds was quantified into ECA time series, as it was done for Camp Creek.

In the McGregor River watershed, about 8% of the total watershed was harvested mostly in the 1980s, all at the lower elevation band (Figure 13). This low level of harvesting in the lower

elevation band is not expected to affect the peak flow of the snowmelt season. Therefore, the forest harvesting that occurred in the McGregor River watershed was ignored.

The effects of forest roads on watershed hydrology have been a focus of concern in watershed management (Luce, 2002; Luce and Wemple, 2001). Forest roads can increase the watershed's drainage efficiency via (i) increasing the impervious area in the watershed through soil compaction; (ii) altering the natural flow pathways by intercepting surface and sub-surface runoff; (iii) re-routing runoff through roadside ditches to existing streams and/or other road networks (e.g., Harr et al., 1975; Jones, 2000; Luce, 2002; Tague and Band, 2001; Wemple and Jones, 2003). However, in comparison to the rain and rain-on-snow environments, watersheds in the snow environment, especially with subdued topographies, are inherently less conducive to road effects on peak flows. Snow deposited on forest roads often melts earlier due to a lack of shade (Bowling and Lettenmaier, 1997), hence not contributing to moisture recharge and peak flows to a large extent. In some cases, part of the earlier snowmelt can be lost to the atmosphere via evapotranspiration creating a water deficit after the construction of roads (Kuraś et al., 2012). In addition, subdued terrains can limit the movement of subsurface flows when the land is not sloping (Whipkey, 1965). There are also fewer road cuts and ditch surfaces in the forest roads of subdued terrains, which further reduce the effects of subsurface flows and limit the effects of runoff re-routing via forest roads. Therefore, the roadside ditches are not always "activated" during the freshet in the snow environment (Kuraś et al., 2012; Megahan, 1972). Forest road construction did not appear to affect the peak flows in the snow environments (King and Tennyson, 1984; Kuraś et al., 2012). In addition, logging in BC's interior often occurs in winter months when soils are frozen and covered with snow accumulation (Conlin et al., 2004). Logging in winter, as opposed to other seasons, can mitigate soil disturbance associated with

ground-based harvesting systems (Johnson et al., 2007; Miller et al., 2004). In this thesis, therefore, the potential effects of forest roads on peak flows associated with the five pairs of watersheds were assumed negligible, in comparison to the effects of changes in the vegetation cover.

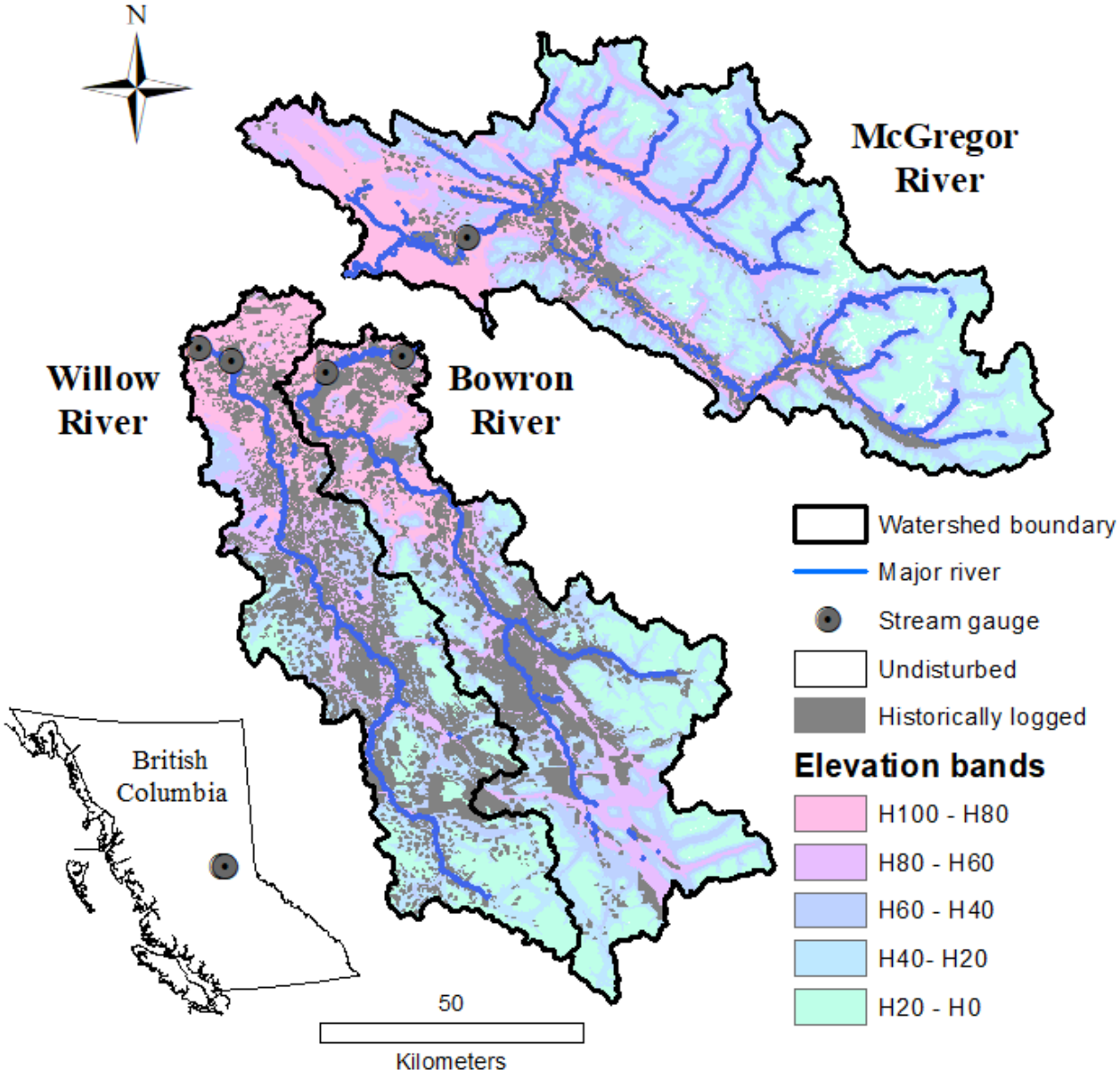

Figure 13: Location and topography of McGregor River, Willow River, and Bowron River.

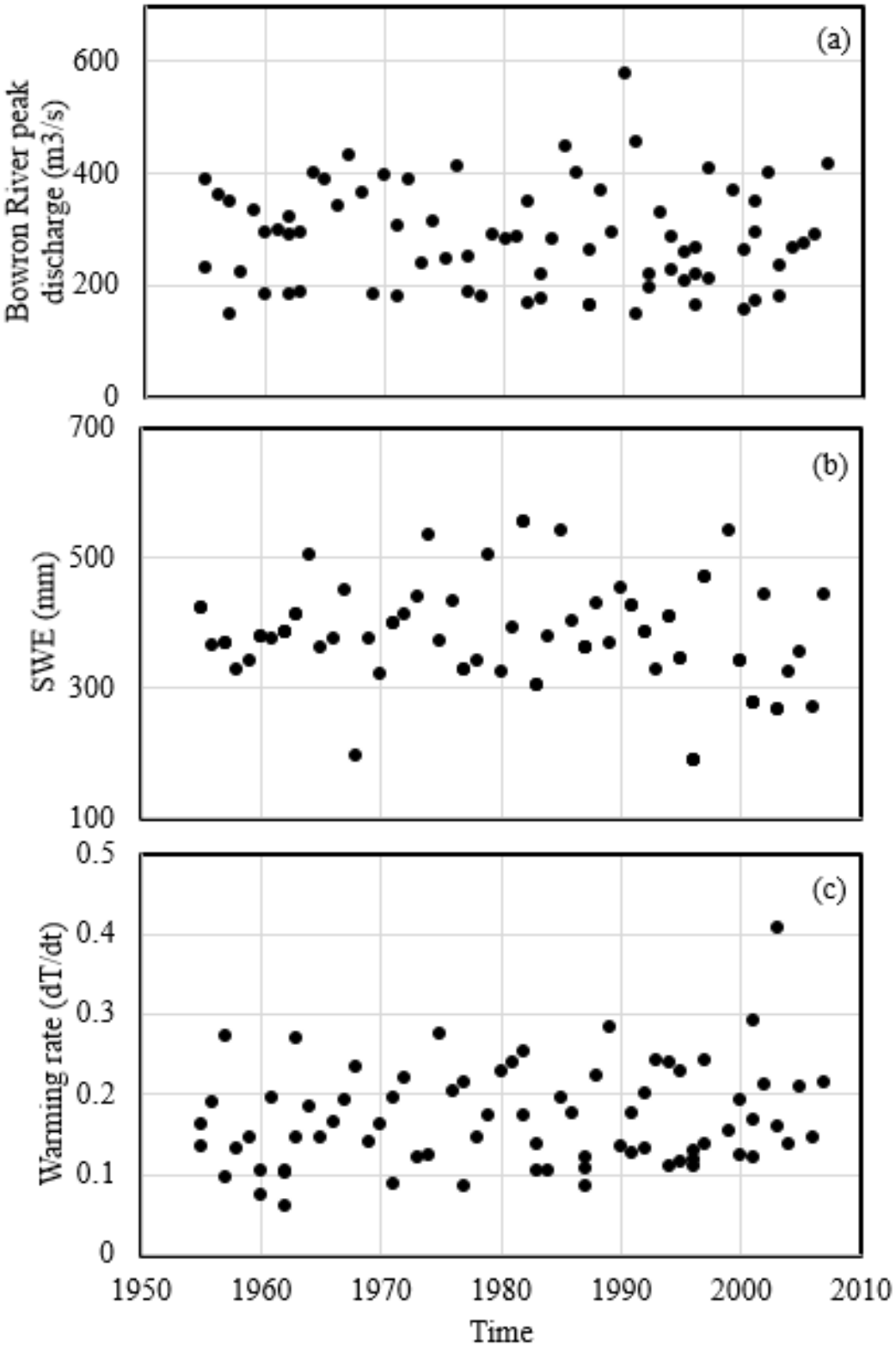

Figure 14: The time series of (a) peaks-over-threshold (POT) of Bowron River with separation *r* = 13, (b) peak snow accumulation at the time of peak discharge and, (c) warming rate preceding peak discharge of Bowron River.

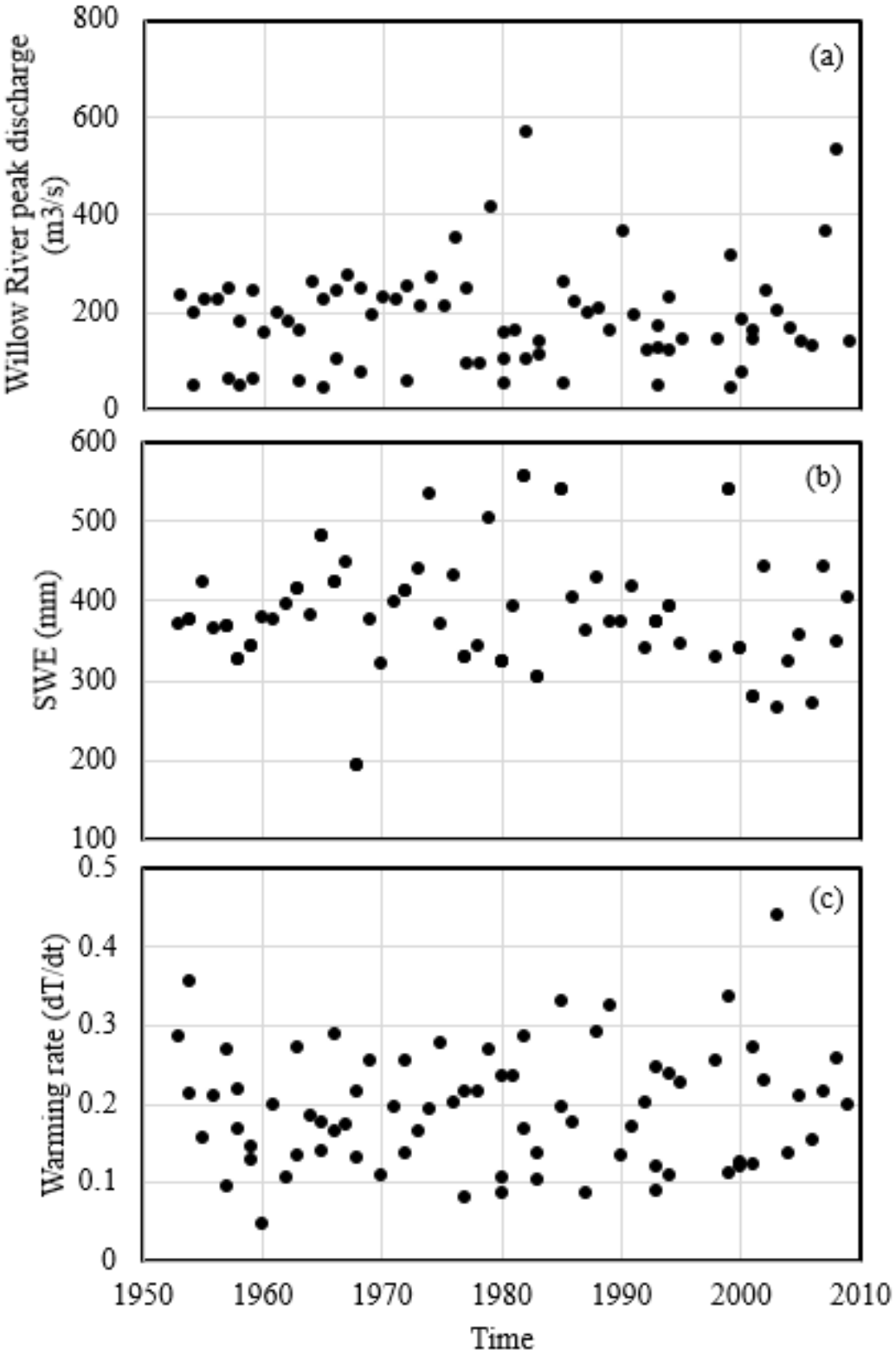

Figure 15: The time series of (a) peaks-over-threshold (POT) of Willow River with separation *r* = 9, (b) peak snow accumulation at the time of peak discharge and, (c) warming rate preceding peak discharge of Willow River.

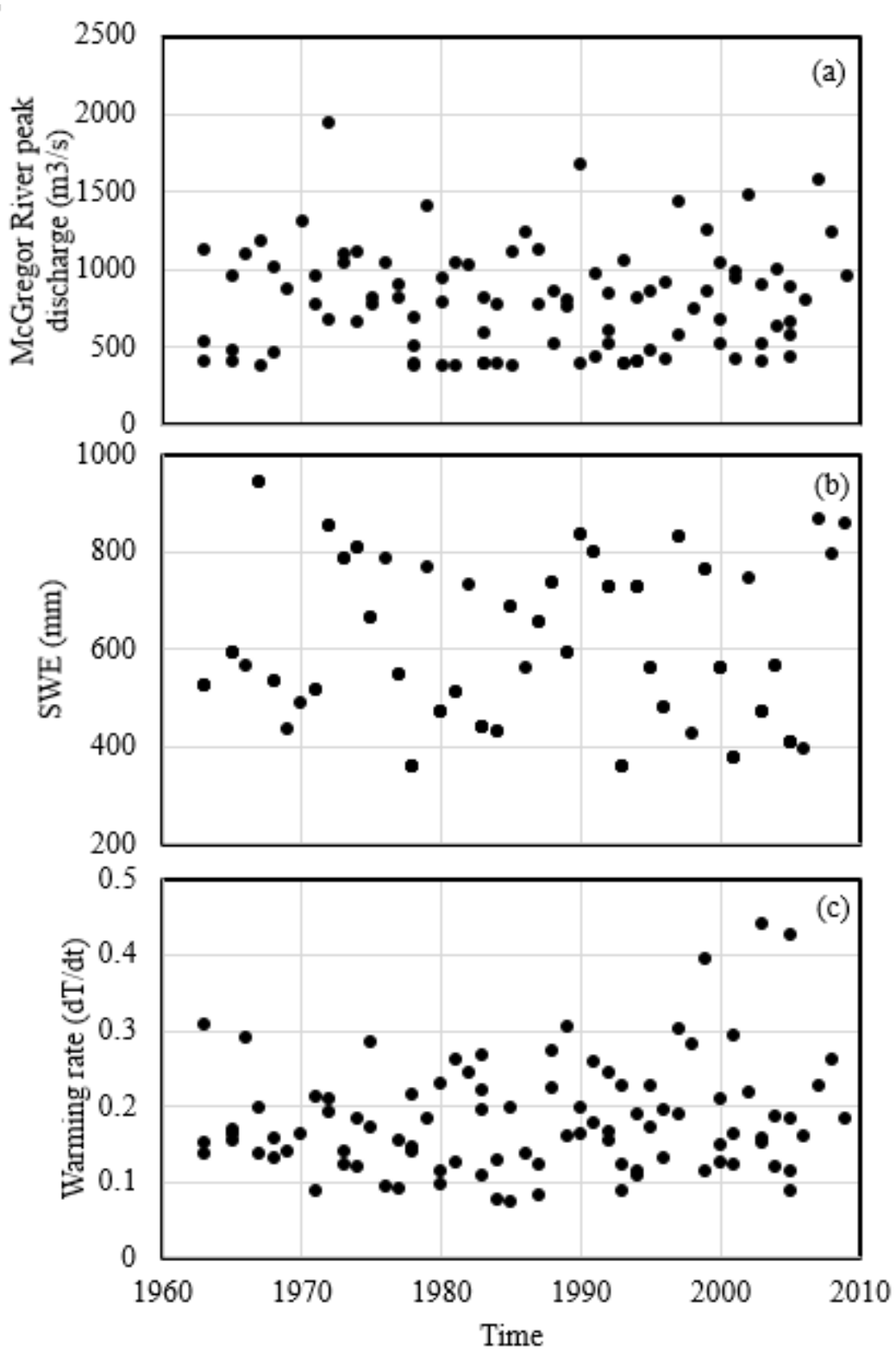

Figure 16: The time series of (a) peaks-over-threshold (POT) of McGregor River with separation $r = 7$, (b) peak snow accumulation at the time of peak discharge and, (c) warming rate preceding peak discharge of McGregor River.

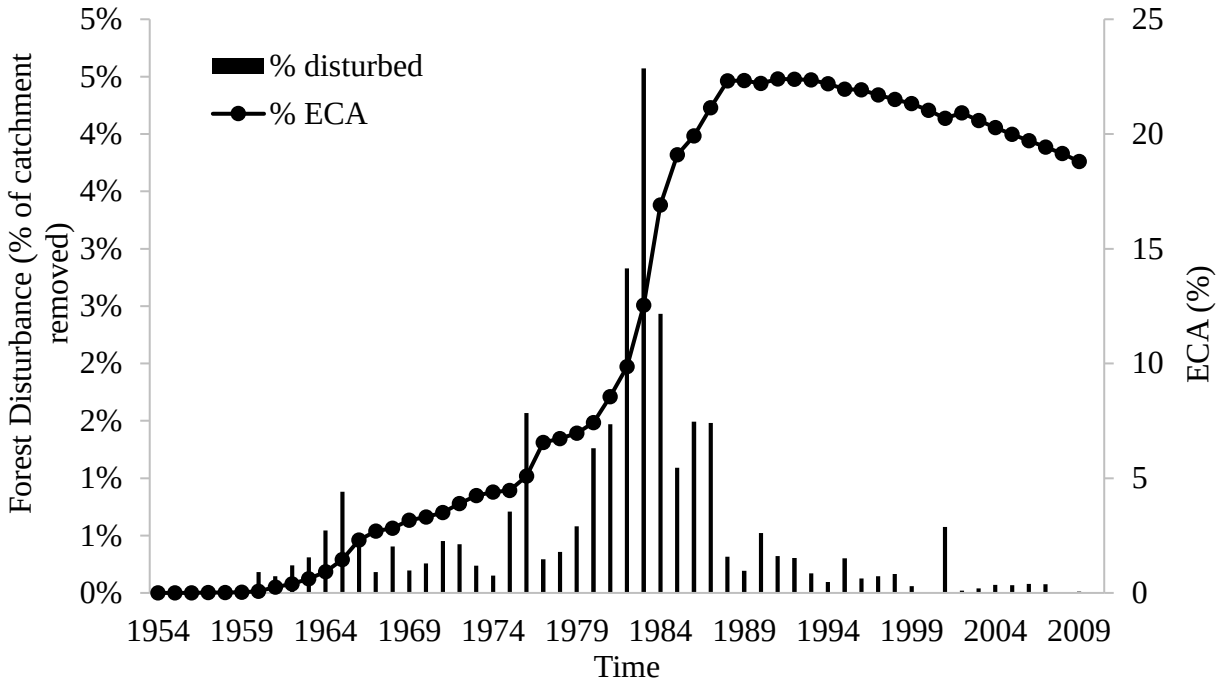

Figure 17: ECA time series and annual forest harvesting of Bowron River from 1954-2009.

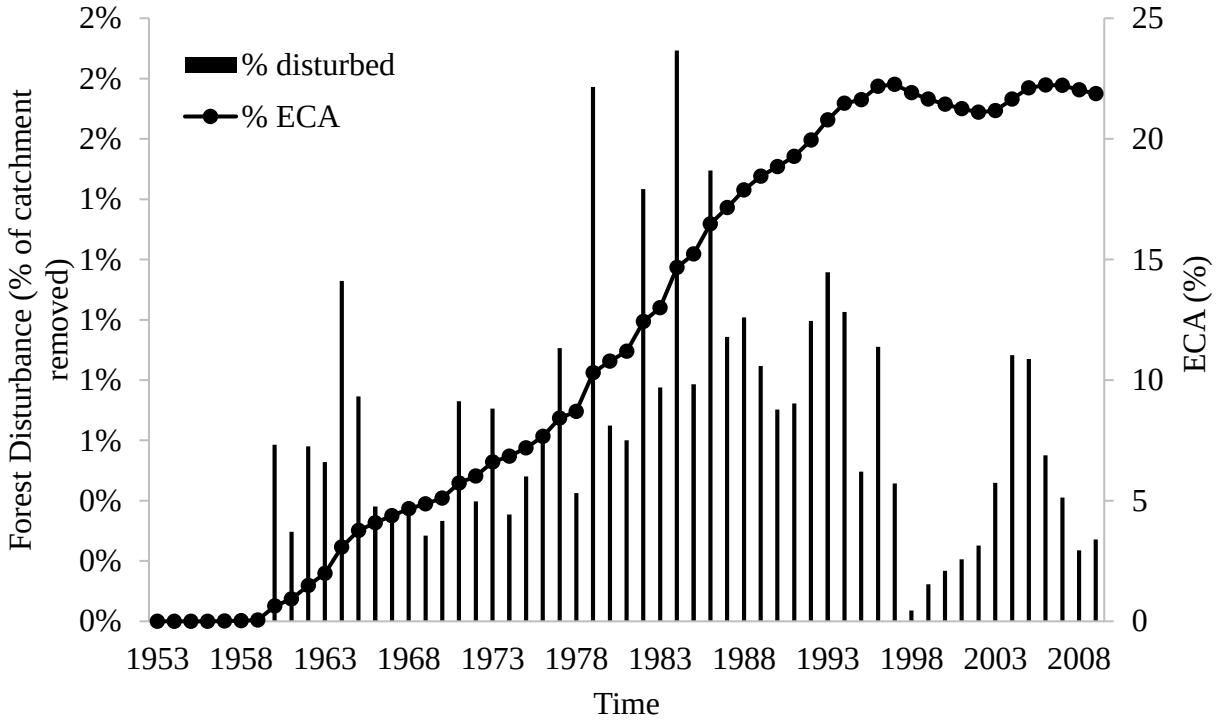

Figure 18: ECA time series and annual forest harvesting of Willow River from 1953-2009.

Table 3: Physiography of treatment Bowron River, Willow River, and control McGregor River watersheds.

	Bowron River	Willow River	McGregor River
Catchment area (km^2)	3550 3330	3110 2860	4780
Elevation range (m)	600 -2350	570 - 2080	600 - 3221
Aspect distribution	NE/SW/NW=S	NE=W/S=SW	S/SW/N/S
Peak ECA	22%	22%	-
Dominant vegetation	BL, SW, SX	SW, BL, PLI, SX	BL, SX, S
Average slope (%)	22	15	31
Stream length (km)	2747	2730	5315
Stream density (km/km2)	0.82	0.95	1.11
Stream gauge	08KD004 08KD007	08KD006 08KD003	08KB003
Snow pillow	1A03P, 1A05	1A03P, 1A10	1A11
Record length	1954 - 2009	1953 - 2009	1963 - 2009
Separation	11/13/15	1/5/9	7/8/9
Arrival rate	1.5/1.43/1.35	1.6/1.50/1.39	2.04/1.93/1.83
Sample size	81/77/73	77/76/75	94/89/84

Chapter 3: Method

3.1 Overview

The effect of forest harvesting on the peak flow time series is detected and attributed using nonstationary frequency models by incorporating covariates in the modelling procedures. Historic forest harvesting that occurred at the treatment watersheds was quantified into a time series of ECA, and subsequently used as a covariate in the modelling procedures. However, forest harvesting effects alone may or may not be able to explain any variability in the time series of peak flows due to the typical natural background variability of peak flows. Therefore, climate-controlling factors (e.g., snow, temperature) were first used as covariates to explain such variability in the peak flows, prior to the introduction of ECA in the modelling procedure. Such a procedure is conceptually similar to a stepwise method in developing deterministic regression models, with manual selection and introduction of independent variables (Bendel and Afifi, 1977). The summary statistics (of models) were used to compare various nonstationary models via the Likelihood Ratio (LR) test and Akaike Information Criterion (AIC).

The theoretical frequency distribution describing the peak flows is characterized by several distribution parameters such as the location, scale, and shape parameters for the Generalized Extreme Value (GEV) distribution, and scale and shape parameters for the Generalized Pareto distribution (GPD). The GEV distribution, describing the annual peak flows, was used for the Camp Creek, Baker Creek, and Mather Creek watershed pairs. The GPD distribution, describing the peaks-over-threshold (POT) events, was used for the Bowron River, Willow River, and McGregor River watersheds. Each of these distribution parameters can be related to different climate-controlling factors of peak flows for physically meaningful reasons. Since it is possible to have different combinations of climate covariates associated with different

distribution parameters that best explain the variability of peak flows, a list of models for each watershed was developed (e.g., Table 4). The same model development procedures were applied for each pair of control and treatment watersheds. However, forest harvesting was only introduced as a covariate to the nonstationary treatment watershed models. The quantification of forest harvesting effects on peak flows proceeded after (i) no temporal trends were found in the control watershed, and (ii) when changes in the peak flow time series were attributed to forest harvesting in the treatment watershed.

The effects of forest harvesting on peak flows were quantified via two methods. The first method allowed the climate covariates and forest harvesting to change historically to evaluate how the magnitude of a peak flow event (of a fixed frequency) has consequently changed in time during the disturbance history. The second method fixed the climate covariates using their long-term average values to evaluate the effects on the magnitude (frequency) of a peak flow event on a fixed frequency (magnitude). It allows for the quantification of treatment effects at specific forest harvesting levels (i.e., a snapshot in time at various stages of forest re-establishment, and/or continued forest harvesting activities).

3.2 Nonstationary analysis of annual extreme events

3.2.1 Generalized Extreme Value (GEV) distribution

Annual peak flows and the GEV distribution were used for the analysis of the Camp Creek-Greata Creek, Baker Creek-McKale River, and Mather Creek-Fry Creek watershed pairs. The peak flow time series, composed of the annual maximum discharge of each snowmelt season, is often assumed to be generated from heavy-tailed distributions such as the GEV (El Adlouni et al., 2008; Katz et al., 2002). The GEV distribution is one of the most applicable regional parent distributions of BC's interior (Wang, 2000 p. 74; Yue and Wang, 2004), and it has been used previously to analyze peak flows generated in the snow environments in this region (e.g., Kuraś et al., 2012; Schnorbus and Alila, 2004a, 2013; Shrestha et al., 2017). Denoting Q as the random variable describing annual peak flows and q as the sample of peak flows (from the parent GEV), the probability density function (pdf), and cumulative density function (cdf) of the sample GEV distribution are defined by (Hosking and Wallis, 1997) as:

$$f_q(q) = \sigma^{-1} e^{-(1-\xi)t - e^{-t}}, \; t = \begin{cases} -\xi^{-1} \ln\left(1 - \frac{\xi(q-\mu)}{\sigma}\right), when\ \xi \neq 0, \\ \frac{(q-\mu)}{\sigma}, when\ \xi = 0 \end{cases} \quad (4)$$

$$F_q(q) = \exp\{-e^{-t}\} \quad (5)$$

where μ, σ, and ξ are the location, scale, and shape parameters of the GEV distribution, respectively. The set of flow values (q) that defines the function is determined by the shape parameter as: $\mu + \sigma/\xi < q < \infty$ if $\xi < 0$; $-\infty < q < \infty$ if $\xi = 0$; $-\infty < q \leq \mu + \sigma/\xi$ if $\xi > 0$. See Hosking and Wallis (1997) for more details on the GEV distribution.

3.2.2 Stationary vs. nonstationary GEV modelling

In the case of stationary modelling, peak flows were fitted to a GEV distribution $Q \sim GEV(\mu, \sigma, \xi)$, where all three parameters were kept constant (i.e., not changing in time). In the

nonstationary case, one or more GEV distribution parameters were modelled to change as a function of one or more covariates. For instance, a simple linear function can be used to model the location parameter in association with a vector of a covariate ($X_1,\ldots, X_p$), so that $\mu(X_1,\ldots, X_p) = \beta_0 + \sum_{j=1}^{\rho} \beta_j X_j$, where β_0 and β_j are parameters. The estimation process would then be optimized for β_0 and β_j, as opposed to one single value for the location parameter (under the stationary scenario). As a result, the location parameter of the distribution takes a different value for each observation of the covariate *j*. Preliminary analysis showed no nonlinear features of the relationships between peak flows of either watersheds and the covariates. Therefore, only linear models were considered for this research. While the location and scale parameters of the GEV distribution were allowed to change as a function of covariates, the shape parameter was kept constant due to computational uncertainties related to modelling the shape parameter (Coles, 2001; Prosdocimi et al., 2015).

Both stationary and nonstationary models developed for the Camp Creek, Baker Creek, and Mather Creek watershed pairs were fitted using Maximum Likelihood Estimation (MLE). MLE is widely accepted in the hydrology literature (Strupczewski et al., 2001). However, the difficulty of reaching convergence under MLE increases rapidly when multiple covariates are used to model peak flows. Therefore, it is possible to have a lack of convergence ending with a non-optimum point under MLE (Restrepo and Bras, 1985).

3.2.3 Model development to meet the research objective

The goal of the modelling procedures was to search for signals in the peak flow time series of the treatment watersheds (e.g., Camp Creek) in relation to forest harvesting. However, it is inherently difficult to detect any changes in peak flows caused by continuous forest harvesting because climate variability and forest harvesting affect the time series simultaneously. As a

result, the development of nonstationary models involves several primary factors controlling the magnitude of peak flows following Green and Alila (2012) and Curry and Zwiers (2018): (i) the peak snow accumulation measured at nearby snow pillow stations; (ii) average 3-day temperature preceding peak flows for the Camp Creek-Greata Creek, Mather Creek-Fry Creek, and Baker Creek-McKale River watershed pairs; (iii) warming rates preceding peak flows for the Bowron River- and Willow River-McGregor River watershed pairs; and (iv) total 7-day precipitation preceding peak flows for the Baker Creek-McKale River and Mather Creek-Fry Creek pairs. These climate-controlling factors were used to explain the natural background variability of peak flows and, subsequently, to isolate any signal caused by forest harvesting. Therefore, the introduction of ECA only took place when a nonstationary model with climate-controlling factors was judged as explaining the natural background variability of the peak flows. This judgment was conducted using the LR test and AIC as detailed in the next sub-section. The time series of ECA, representative of historic forest harvesting conditions, was developed and applied to the harvested watersheds only.

Time was introduced in a nonstationary model either by itself (e.g., Villarini et al., 2009a, 2009b) or in addition to climate-controlling factors (Prosdocimi et al., 2015), for all treatment and control pairs. The introduction of time in the nonstationary models can illustrate: (i) the potential detection (or lack thereof) using time as a surrogate for the forest harvesting (ECA) time series and/or (ii) the potential detection (or lack thereof) without considering the climate-controlling factors of peak flow. The list of nonstationary models is shown in Table 4 for the Camp Creek-Greata Creek watershed pair, Table 5 for the Mather Creek-Fry Creek and Baker Creek-McKale River watershed pairs, and Table 6 for the Bowron River- and Willow River-McGregor River watershed pairs. The abbreviation CM1 refers to Control watershed Model 1,

while TM1 refers to Treatment watershed Model 1. To limit the number of acronyms introduced in this thesis, these same abbreviations were used consistently for each of the five pairs of watersheds. In the attribution process, the data used to fit all the models were rescaled to (0, 1) (Prosdocimi et al., 2015) via the equation $x_{new} = \frac{x - x_{min}}{x_{max} - x_{min}}$ (Jain et al., 2005); where x, x_{new}, x_{min}, and x_{max} are the original, rescaled, minimum, and maximum value in the time series, respectively.

3.2.4 Evaluating the GEV models

When covariates are used to develop different nonstationary models, it is critical to evaluate if the addition of a certain covariate can help further explain the variability of the peak flows. There are two ways of comparing the performance of various GEV models: (i) a formal hypothesis testing procedure using the LR test and (ii) the comparison of AIC scores between models, all of which are based on the log-likelihood function of the models. Formal hypothesis testing was carried out using the LR test that involves a statistical comparison of the respective log-likelihood functions of the nested models (Coles, 2001). Based on the MLE estimates for the location (μ), scale (σ), and shape (ξ) parameters of a GEV distribution (when $\xi \neq 0$), the log-likelihood of the stationary GEV model can be derived as (Prosdocimi et al., 2015):

$$l(\mu, \sigma, \xi; q) = \sum_{i=1}^{M} \ln\left(f(\mu, \sigma, \xi;\ q_i)\right) = -M \ln \sigma - \sum_{i=1}^{n} \{t_i(1 - \xi) + e^{-t_i}\} \quad (6)$$

$$t_i = -\xi^{-1} \ln(1 - \xi(q_i - \mu)/\sigma) \quad (7)$$

where $q = (q_1, \ldots q_M)$ is the time series of M peak flows.

For the nonstationary case, where the location parameter (μ) is changing linearly as a function of a covariate X, i.e., $\mu_i = \beta_0 + \beta_1 X_i$, the estimation procedure for the model leads to four parameters ($\beta_0, \beta_1, \sigma, \xi$), as opposed to three parameters (μ, σ, ξ) as in the case under stationary

conditions. The log-likelihood function then becomes a modified version of the above equations (Prosdocimi et al., 2015):

$$l(\beta_0, \beta_1, \sigma, \xi; \text{q}) = \text{-Mln } \sigma - \sum_{i=1}^{n}\{t_i(1-\xi) + e^{-t_i}\} \quad (8)$$

$$t_i = \text{- } \xi^{-1}\ln(1\text{- } \xi(q_i \text{ - } \beta_0 - \beta_1 x_i)/\sigma) \quad (9)$$

The LR test involves comparing the difference of the double log-likelihood functions of two nested models, to the (1 – α) quantile of the Chi-square statistic, χ_k^2, where α is the level of significance and *k* is the difference in the number of parameters between the two nested models. The advantage of the LR test is that it provides formal hypothesis testing, but the procedure is limited to nested models. For instance, model A is nested in model B if the parameters of model A are a subset of the parameters of model B. The LR test is commonly used in the nonstationary frequency analysis literature for the purpose of detecting trends (e.g., Coles, 2001; Prosdocimi et al., 2015, 2014; Sun et al., 2014).

One way to overcome the challenge of comparing only nested models using the LR test is through the use of the AIC. However, model evaluation using AIC does not allow formal statistical hypothesis testing. The AIC is a metric derived from the log-likelihood functions ($\widehat{M}$) of the fitted models: AIC = -2(log-lik ($\widehat{M}$) – *p*) where *p* is the number of parameters in the fitted model, as a penalty term in the AIC formulation. The penalty term is used because higher likelihood values (or smaller negative log-likelihood values) can always be obtained when more parameters are added into a model, regardless of the contribution of the covariate. Hence, the use of AIC to evaluate models can also alleviate the challenges of overfitting when the use of extra covariates does not explain additional variability of peak flows (López and Francés, 2013; Yan et al., 2017). Both AIC and LR tests are considered in this research to allow for a more objective discrimination between models.

Table 4: Nonstationary GEV models developed for Camp Creek-Greata Creek pair.

	Treatment watershed		Control watershed	
Model	Camp Creek		Greata Creek	
1, Qp(μ, σ, ξ)	TM1*	✓	CM1*	✓
2, Qp(μ(time), σ, ξ)	TM2	✓	CM2	✓
3, Qp(μ, σ(time), ξ)	TM3	✓	CM3	✓
4, Qp(μ(time), σ(time), ξ)	TM4	✓	CM4	✓
5, Qp(μ(snow), σ, ξ)	TM5	✓	CM5	✓
6, Qp(μ, σ(snow), ξ)	TM6	✓	CM6	✓
7, Qp(μ(snow), σ(snow), ξ)	TM7	✓	CM7	✓
8, Qp(μ(temp), σ, ξ)	TM8	✓	CM8	✓
9, Qp(μ, σ(temp), ξ)	TM9	✓	CM9	✓
10, Qp(μ(temp), σ(temp), ξ)	TM10	✓	CM10	✓
11, Qp(μ(ECA), σ, ξ)	TM11	✓	-	-
12, Qp(μ, σ(ECA), ξ)	TM12	✓	-	-
13, Qp(μ(ECA), σ(ECA), ξ)	TM13	✓	-	-

* TM and CM stand for Treatment and Control Watershed Models, respectively.

Table 5: Nonstationary GEV models developed for the Mather Creek-Fry Creek and Baker Creek-McKale River pairs.

	Treatment watershed		Control watershed	
Model	Mather Creek Baker Creek		Fry Creek McKale River	
1, Qp(μ, σ, ξ)	TM1*	✓	CM1*	✓
2, Qp(μ(time), σ, ξ)	TM2	✓	CM2	✓
3, Qp(μ, σ(time), ξ)	TM3	✓	CM3	✓
4, Qp(μ(time), σ(time), ξ)	TM4	✓	CM4	✓
5, Qp(μ(ECA), σ, ξ)	TM5	✓	-	-
6, Qp(μ, σ(ECA), ξ)	TM6	✓	-	-
7, Qp(μ(ECA), σ(ECA), ξ)	TM7	✓	-	-
8, Qp(μ(snow), σ, ξ)	TM8	✓	CM5	✓
9, Qp(μ, σ(snow), ξ)	TM9	✓	CM6	✓
10, Qp(μ(snow), σ(snow), ξ)	TM10	✓	CM7	✓
11, Qp(μ(temp), σ, ξ)	TM11	✓	CM8	✓
12, Qp(μ, σ(temp), ξ)	TM12	✓	CM9	✓
13, Qp(μ(temp), *σ*(temp), *ξ*)	TM13	✓	CM10	✓
14, Qp(μ(precip), σ, ξ)	TM14	✓	CM11	✓
15, Qp(μ, σ(precip), ξ)	TM15	✓	CM12	✓
16, Qp(μ(precip), σ(precip), ξ)	TM16	✓	CM13	✓

* TM and CM stand for Treatment and Control Watershed Models, respectively.

3.3 Nonstationary analysis of peaks-over-threshold events

3.3.1 Generalized Pareto distribution (GPD)

Peaks-over-threshold (POT) events were used for the Bowron River, Willow River treatment watersheds and their common control watershed, McGregor River. The POT approach is described as follows (Khaliq et al., 2006). Consider a sequence of M independent and identically distributed (iid) random variables X_1, X_2, … X_m conditioned on $X > \mu$, where μ is a sufficiently high threshold. It can be shown that given sufficiently high threshold μ, the distribution function of the excess values $Y = X - \mu$ can converge to the generalized Pareto distribution (GPD) (Khaliq et al., 2006; Sugahara et al., 2009):

$$F(y,\sigma,\xi) = Pr(X \leq \mu + y | X \geq \mu) \tag{10}$$

$$= \begin{cases} 1 - \left(1 + \frac{\xi}{\sigma} y\right)^{-1/\xi}, \sigma > 0, 1 + \xi\left(\frac{y}{\sigma}\right) > 0 \\ 1 - \exp\left(\frac{-y}{\sigma}\right), \sigma > 0, \xi = 0 \end{cases}$$

The GPD is described by σ and ξ, which are the scale and shape parameters, respectively. The scale parameter describes the spread of distribution (analogous to variability in standard terms), while the shape parameter describes the tail behavior of the distribution, often termed the tail index. When $\xi < 0$, the GPD is thin-tailed, and if $\xi > 0$ the distribution is heavy-tailed or Pareto. When $\xi = 0$, the distribution is light-tailed or exponential. The inverse of F, F^{-1}, is the quantile function such that the (1- p) quantile, y_{1-p}, is given by:

$$y_{1-p} = F^{-1}(1-p,\sigma,\xi) = \begin{cases} \left(\frac{\sigma}{\xi}\right)\left(p^{-\xi} - 1\right), \xi \neq 0 \\ \sigma log\left(\frac{1}{p}\right), \xi = 0 \end{cases} \tag{11}$$

where *log* indicates natural logarithm.

Under the POT framework, it is a common practice to express the quantile function in terms of the return period, *T*, and the rate of occurrence, λ, (e.g., the long-term average number of events per year) as: $y_T = \sigma((T\,\lambda)^{\xi} - 1)/\,\xi$ (e.g., Khaliq et al., 2006) where y_T is the *T*-year return level (the magnitude exceeded once in *T* years), or the magnitude exceeded in any one year with probability 1/*T*. See Khaliq et al. (2006) and Sugahara et al. (2009) for more details on the GPD.

3.3.2 Condition of independence and de-clustering

When conducting extreme value analysis, peak flow observations have to be statistically independent when selected from a daily discharge time series. De-clustering is perhaps the most widely-adopted method to do so. It was used to filter dependent observations to obtain a set of threshold excess observations, which make up the POT time series and are approximately independent (e.g., Acero et al., 2011; Beguería and Vicente-Serrano, 2006; Caires et al., 2006).

The selection of POT events depends on two criteria: (i) the threshold magnitude above which an observation is considered as a peak and (ii) the separation criterion. The threshold should remain low enough to include extra peak flows, yet high enough so the peak flows remain independent. A commonly used threshold in the hydrologic analysis of extreme events is the minimum of the annual maxima time series (e.g., Hosking and Wallis, 1987; Langbein, 1949). Hence, at least one event per year is selected in the entire time series of daily flows. Threshold stability plots and mean residual life plots (plots not shown), adopted from Coles (2001), were used to evaluate the suitability of such threshold for the three large watersheds. Once the threshold was determined, the method of runs de-clustering was employed in the separation process to compose the POT time series. In brief, runs de-clustering first involves choosing a run length or separation, denoted by *r*. A cluster is identified when there are *r* consecutive

exceedances of events above the selected threshold. The maxima of the clusters are preserved and used for subsequent analysis. However, the selection of *r* is an arbitrary process similar to selecting the threshold. Hence, the metric of the extremal index was employed to identify a suitable *r* (Coles, 2001; Ferro and Segers, 2003). The nonstationary analysis was carried out using multiple independent POT time series de-clustered using different *r* values. See Coles (2001) for more details on the de-clustering process.

3.3.3 Stationary vs. nonstationary GPD modelling

In the case of stationary modelling, the samples of peak flow maxima, Q, were fitted into a GPD, denoted by Q ~ GPD (σ, ξ) where the GPD parameters were kept constant. Under nonstationary modelling, the GPD parameters were modelled as a function of one or more covariates. For example, to model the scale parameter in association with covariates (X_1,…, X_p), a simple linear function can be used so that $\sigma(X_1,\ldots, X_p) = \beta_0 + \sum_{j=1}^{\rho} \beta_j X_j$. The two parameters, β_0 and β_j, are optimized in the estimation process, as opposed to optimizing for only one single value for the scale parameter (as under the stationary condition). As a result, the scale parameter of the distribution can change at each time step according to the covariate, and it would have a different value for each observation of the covariate *j*. Only linear models were used in the model development as it was the case for the GEV analysis. While the scale parameter of the GPD was allowed to change as a function of covariates (e.g., Khaliq et al., 2006; Tramblay et al., 2013), the shape parameter was kept constant due to computational uncertainties associated with the estimation for the shape parameter under nonstationary conditions (e.g., Pujol et al., 2007; Renard et al., 2006). See Coles (2001) for more details on the use of GPD under nonstationary conditions or other applications of nonstationary analysis using GPD (e.g., Beguería et al., 2011; Coles, 2001; Eastoe and Tawn, 2009; Kyselý et al., 2010; Roth et al., 2012; Silva et al., 2016;

Thiombiano et al., 2017; Tramblay et al., 2013). Both stationary and nonstationary models developed for treatment and control watersheds were fitted using MLE.

3.3.4 Model development to meet the research objective

The ultimate goal of the modelling processes is to explore the signals in the peak flow time series of the treatment watersheds in relation to historic forest harvesting. However, it is challenging to detect any changes in a time series of extreme events caused by previous disturbance because the peak flow time series are simultaneously affected by climate variability and forest harvesting. Following Curry and Zwiers (2018), peak snow accumulation (SWE) and warming rates, defined by the slope of trend line fitted to the daily mean temperature between April 1st and the date of peak flow, appear to be the dominant climate control on the peak flows generated in large scale, snow-dominated catchments in British Columbia. These climate-controlling factors were used as predictors to explain the natural background variability, and subsequently, to isolate any leftover signal caused by forest harvesting. The ECA time series was developed and introduced as a covariate for the Bowron River and Willow River treatment watersheds only. It was introduced when a nonstationary model with climate-controlling factors can explain the natural background variability of peak flows. The list of nonstationary models developed for the Bowron River, Willow River, and McGregor River watersheds are shown in Table 6.

3.3.5 Evaluating the GPD models

When covariates are used to develop nonstationary models, it is important to evaluate if the addition of a certain covariate can further explain the variability of the peak flows. To this effect, the performance of the GPD models is evaluated in two ways: (i) a formal hypothesis test using the LR test and (ii) the comparison of AIC scores among models. Both the LR test and AIC

comparison of the models are based on the log-likelihood function, which can be shown as (Del Castillo and Daoudi 2009):

$$l(\sigma, \xi; q) = -\log(s\xi\sigma) - \frac{1+\xi}{\xi n}\sum_{i=1}^{M} \log\,(1 + sq_i/\sigma), \text{ where s = sign } (\xi) \qquad (12)$$

where $q = (q_1,\ldots q_M)$ is the time series of M peak flows. For the nonstationary case, the scale parameter is changing linearly as a function of covariates, for instance, $\xi(x) = \beta_0 + \beta_1 x_i$. The estimation procedure for this nonstationary model leads to three parameters (β_0, β_1, ξ), as opposed to only two parameters (σ, ξ) under stationary conditions. The log-likelihood function estimation under nonstationary conditions would replace the scale parameter, ξ, with a linear equation, $\beta_0 + \beta_1 x_i$, in the estimation procedures. Both the LR test and AIC were used to evaluate GPD models. The evaluations of GPD models are similar to those of the GEV models described in Section 3.2.4.

3.4 Quantifying forest harvesting effects on peak flows

Two conditional quantification techniques were used to evaluate forest harvesting effects for data fitted to both GEV and GPD. The quantification was conducted based on the final fitted nonstationary models incorporating ECA in addition to the chosen climate covariates, which best explain the peak flow data. The first technique is illustrated as return level plots, which consist of time series of estimated peak flow magnitudes of fixed frequencies, one at a time, from the final fitted model. Return level plots allow for all climate covariates and ECA to change in time. Because the final fitted model incorporates the climate covariates and ECA time series, the natural background variability in the peak flow time series from the climate inputs can be accounted for. Therefore, any change or trend in the return level plots can be attributed to historic forest harvesting. Based on the final fitted model with climate and ECA covariates, peak flow magnitudes (of fixed frequency) can be derived from historically changing peak flow frequency distributions. The frequency distribution parameters can be estimated using coefficients of the covariates and the covariates themselves. Conditional quantification in the form of return level plots derived from nonstationary models involving peak flow controlling covariates, such as climate inputs, is common in the nonstationary frequency analysis literature (e.g., Du et al., 2015; Sugahara et al., 2009; Sun et al., 2014).

While the first conditional quantification method allows both climate covariates and ECA to change, the second method fixes both climate and ECA conditions. This quantification technique can reveal the treatment effects on the magnitude (frequency) for a peak flow of a certain frequency (magnitude) as a snapshot at any specific time of interest during the disturbance history of the harvested watershed. Although the return level plots explained above can reveal the evolution of peak flow magnitude as a result of forest harvesting, it is necessary to

develop flood frequency curves (FFC), representative of forested and harvested conditions, in order to quantify how specific peak flow events (e.g., 100-yr, 50-yr, 20-yr) were affected. Such treatment effect quantification involves the development of GEV- and GPD-based FFCs representative of fixed ECA levels of interest. The estimation of the GEV or GPD parameters were based on (i) the coefficients of the covariates of the final fitted model that incorporate climate-controlling factors and ECA; (ii) the level of ECA of interest; (iii) and the long-term average value of the climate covariates. The nonstationary model was driven with the long-term climate average to control for the temporal variability of the climate (e.g., Lane et al., 2005). The nonstationary model adjusted for climate produces an estimation of hydrologic responses over time as a result of only the logging. For instance, the GEV distribution is described by three parameters (location, scale, and shape). The quantification of the location and scale parameters of a nonstationary model would be a simple linear regression, making use of the estimated coefficients of the associated covariates and the covariates themselves. Once the FFCs were developed, sample statistics were derived from these FFCs to evaluate forest disturbance effects on the mean and standard deviation of peak flows. Sample statistics were calculated based on samples of peak flows (n = 10,000) randomly generated using the corresponding GEV distributions. These are the same GEV distributions used to develop FFCs at different ECA levels.

3.5 Uncertainty analysis of GEV- and GPD-based Quantiles

The confidence interval (CI), for the FFC representative of forested conditions, was developed based on a re-sampling exercise for data fitted to the GEV distributions. This technique is similar to the ones used by Alila et al. (2009), Green and Alila (2012), and Sugahara et al. (2009). The traditional resampling process involves several steps. First, the observed peak

flows were fitted to a frequency distribution, the so-called parent distribution (GEV). Sample peak flows of the same record length were then randomly generated based on the parent distribution. The sample peak flows were fitted to a GEV frequency distribution that gave rise to the sample distribution. Peak flows at the return period of interest (e.g., 100-yr, 50-yr, 20-yr) were estimated based on this sample distribution. The above re-sampling process was repeated for 10,000 iterations, providing samples with which to calculate confidence limits of the peak flows of the FFC.

For data fitted to the GPD, the CI of the forested FFC was based on the estimation of standard errors via the Delta method. A benefit of using MLE to approximate the distribution parameters is that standard and widely used approximations are available for a number of useful sampling distributions, which lead to approximations for standard errors (Coles, 2001). The standard errors and the variances of the estimated peak flow magnitude for a specific return period are often used to compute the confidence interval of the peak flows. The confidence interval of the FFCs representative of forested conditions was developed based on the Delta method (Casella and Berger, 2002), which relies on the asymptotic normality of maximum-likelihood estimators, and produces a symmetric confidence interval (Cooley, 2013). The Delta method is based on the Taylor series approximation. It allows for an approximation of the mean and variance of a function of a random variable, based on the variance-covariance matrix computed using the expected information matrix. See Casella and Berger (2002), Coles (2001), and Cooley (2013) for more details on the Delta method. The calculations were carried out in R (R Core Team, 2016), using the package “extReme” (Gilleland and Katz, 2016).

It is inherently difficult to detect any signal caused by climate or land-use changes in a hydrologic time series (Delgado et al., 2010), given the background variability in the time series

from natural climate variability (Burt, 1994; Burt et al., 2015). Therefore, we do not report or discuss the results as important only if they are statistically significant. This is an attempt to avoid dismissing true treatment effects based on the conventional null hypothesis testing and its subjective choice of the level of significance (Amrhein et al., 2019; Johnson, 1999; Yoccoz, 1991). This is especially the case when such effects are physically plausible (Klemeš, 1974) and practically significant (Kirk, 1996). This becomes even more important when small changes in the peak flow magnitude, as a result of forest harvesting, can invoke surprisingly large changes in the peak flow frequency (Alila et al., 2010, 2009; Wigley, 1985).

Table 6: Nonstationary GPD models developed for Bowron River-McGregor River and Willow River pair-McGregor River pairs.

	Treatment watershed		Control watershed	
Model	Bowron River Willow River		McGregor River	
$Qp(\sigma, \xi)$	TM1	✓	CM1	✓
$Qp(\sigma(snow), \xi)$	TM2	✓	CM2	✓
$Qp(\sigma(dT/dt), \xi)$	TM3	✓	CM3	✓
$Qp(\sigma(time), \xi)$	TM4	✓	CM4	✓
$Qp(\sigma(ECA), \xi)$	TM5	✓	-	-
$Qp(\sigma(snow, dT/dt), \xi)$	TM6	✓	CM5	✓
$Qp(\sigma(snow, dT/dt, ECA), \xi)$	TM7	✓	-	-
$Qp(\sigma(snow, dT/dt, time), \xi)$	TM8	✓	CM6	✓

* TM and CM stand for Treatment and Control Watershed Models, respectively.

Chapter 4: Results

4.1 Camp Creek-Greata Creek pair

4.1.1 Are peak flows at the control watershed stationary after accounting for climate variability via covariates?

Prior to conducting the detection and attribution processes for the Camp Creek watershed, it was necessary to rule out any trend in Greata Creek to ensure stationarity, therefore allowing the attribution of any potential trends found in Camp Creek to forest harvesting. The associated negative log-likelihood, AIC value, and LR test results for nonstationary models developed for Greata Creek are shown in Table 7.

No trends in relation to time were detected in the location and scale parameters of the peak flow distribution of Greata Creek, when time alone was used as a covariate to model the distribution parameters (CM2, CM3, and CM4 vs. stationary model or CM1). For instance, when the peak flows were modelled to change as a function of time for the location (CM2), scale (CM3) and, both location and scale (CM4) parameters of the frequency distribution, there was no evidence that the addition of time (CM2, CM3, and CM4) led to a significant increase in likelihood over the stationary model (CM1), when evaluated by either LR test or the AIC outcomes. For example, the associated negative log-likelihood values for CM1 and CM3 are: 173.08 and 172.40, and the double of the difference in negative log-likelihood values between CM1 and CM3 is 1.36. Since 1.36 is less than the critical values of 2.71 and 3.84, which are the approximate 90^{th} and 95^{th} quantiles of χ_1^2, there was no evidence that the scale parameter of the peak flow frequency distribution is changing in time (CM3).

Peak snow accumulation was a significant covariate for both the location and scale parameters of the peak flow frequency distribution. Both location (CM5) and scale (CM6)

parameters changed as a function of peak snow accumulation. The addition of snow in CM5 and CM6 yielded a significant increase in likelihood over the stationary model. Although convergence issues were encountered for CM6 using the full record, the same conclusions, with regards to the significance between snow and the location parameter, and between snow and the scale parameter, were reached using the reduced record. A different route to evaluate the role of snow in relation to the scale parameter is via a comparison between CM5 and CM7. The component where the scale parameter changes as a function of snow is the difference between CM5 and CM7, and such a component is shown in CM6. Therefore, the comparison between CM5 and CM7 is similar to the comparison between CM6 and the stationary model CM1. According to the negative likelihood values and AIC scores, there is evidence that the addition of snow from CM5 to CM7 led to a significant increase in likelihood. Therefore, the same conclusion with regards to the relation between snow and the scale parameter can also be reached. Whether a nonstationary model with one covariate (e.g., CM5) or two covariates (e.g., CM7) is used, both models led to the conclusion, i.e., that both the location and scale parameters of the peak flow frequency distribution of Greata Creek were related to peak snow accumulation.

Another feature that is worth noting is the potential dominance of one climate covariate over another. For instance, the significant relation between snow and the scale parameter of the frequency distribution can be shown by comparing CM6 and the stationary model CM1. The same evaluation of the significance of the relation between snow and the scale parameter can take place by comparing the combined model with both parameters changing as a function of snow (CM7) and its reduced model with only the location parameter changing as a function of snow (CM5). It is interesting to note that the addition of snow to model the scale parameter yielded a significant increase of likelihood only between CM6 and the stationary model CM1,

not between CM5 and CM7. The effects of snow in relation to the scale parameter was dominated by the other component in the model when comparing CM5 and CM7. The significance between snow and the scale parameter cannot be ignored, given the fact that both CM6 and CM7 are statistically better than the stationary model CM1. As a result, the convergence issues associated with CM6 using the full record and the dominating effects further emphasize the importance of using both reduced and full records and the need to develop models allowing only one (e.g., CM5) and both distribution parameters (e.g., CM7) to vary as a function of covariates.

Temperature, on the other hand, appeared to be a significant climate covariate for only the location parameter of the peak flow frequency distribution of Greata Creek. The nonstationary models, CM8, CM9, and CM10 for instance, were developed to allow the distribution parameters to change as a function of temperature. The addition of temperature to only the location parameter (CM8) caused a significant increase in the likelihood over the stationary model CM1. As a result of the non-significant relation between temperature and the scale parameter, the combined model (CM10), with both location and scale parameters changing as a function of temperature, was not an improvement over the stationary model CM1. There were some dominating effects shown here as well between CM10 and the stationary model. Even though the location parameter was shown to be strongly related to temperature (CM8 vs. stationary model CM1), the lack of relationship between temperature and the scale parameter (CM9 vs. stationary model CM1) demonstrates that the combined model (CM10) did not provide an improvement over the stationary model CM1.

Given the strong relation between snow and both distribution parameters, and temperature with the location parameter, CM11 was developed. Even though prior results

showed that temperature had only a weak relationship with the scale parameter, CM12 was developed to further scrutinize the lack of relationship between the scale parameter and temperature. However, comparing CM11 and CM12 showed no significant relationship between temperature and the scale parameter, in line with previous results. Therefore, CM11 was considered to be the best model given the available climate covariates and was used to further evaluate the potential time trends in the peak flow time series.

Time was introduced as a covariate in addition to CM11 for both the location and scale parameters, giving rise to CM13. However, CM13 was not significantly improved over CM11. Therefore, the time series of peak flows of Greata Creek appeared to be stationary given the climate covariates used in this research. A similar conclusion was reached by comparing CM2 to CM4, without accounting for the temporal variability caused by the climate inputs. However, the comparison between CM11 and CM13 lends more confidence to this conclusion by taking into account the natural background variability of peak flows.

Table 7: Negative log-likelihood functions and AIC values for the GEV models of Greata Creek (control watershed).

Control Model	Model Description	Greata Creek (full record)		Greata Creek (reduced record)	
		Negative log-likelihood	AIC	Negative log-likelihood	AIC
CM1	Qp(μ, σ, ξ)	173.08	352.15	176.43	358.87
CM2	Qp(μ(time), σ, ξ)	173.07	354.14	176.43	360.87
CM3	Qp(μ, σ(time), ξ)	172.40	352.80	175.58	359.16
CM4	Qp(μ(time), σ(time), ξ)	172.04	354.08	175.35	360.71
CM5	Qp(μ(snow), σ, ξ)	156.29*	320.58	160.37*	328.74
CM6	Qp(μ, σ(snow), ξ)	135.02~	278.04	172.34*	352.69
CM7	Qp(μ(snow), σ(snow), ξ)	154.07*	318.14	159.82*	329.63
CM8	Qp(μ(temp), σ, ξ)	171.17#	350.35	174.49*	356.98
CM9	Qp(μ, σ(temp), ξ)	173.04	354.07	176.31	360.63
CM10	Qp(μ(temp), σ(temp), ξ)	151.88~	313.76	174.15	358.29
CM11	Qp(μ(snow, temp), σ(snow), ξ)	152.63*	317.26	158.58*	329.17
CM12	Qp(μ(snow, temp), σ(snow, temp), ξ)	151.91*	317.82	158.03*	330.06
CM13	Qp(μ(snow, temp, time), σ(snow, time), ξ)	150.68*	317.36	156.47*	328.95
* significant over the stationary model at 95% significance levels when LR test is applied					
# significant over the stationary model at 90% significance levels when LR test is applied					
~ the estimation of model parameter did not converge					

4.1.2 Is there a remaining signal in the peak flows of the treatment watershed attributable to forest harvesting, after accounting for climate variability via covariates?

Procedures to detect any signal caused by forest harvesting in the peak flow time series of the Camp Creek (treatment watershed) are similar to those of the Greata Creek (control watershed). Snow and temperature were used as covariates to account for the natural background variability of peak flows. Instead of searching for a trend in relation to time as a surrogate variable for forest harvesting activities in the peak flow time series, the objective was to attribute any changes in the peak flow time series of Camp Creek directly to the historic time series of ECA. The detection and attribution of forest harvesting effects on peak flows at Camp Creek consisted of several steps: (i) identify the best combination of climate covariates that explains the natural background variability of peak flows of Camp Creek; (ii) identify nonstationary signals in the peak flow time series in relation to forest harvesting using ECA as an add-on predictor to the best-fitted climate model; and (iii) verify the nonstationary signals by comparing results from the control watershed. The modelling results for Camp Creek are summarized in Table 8.

The peak flow time series for Camp Creek did not change as a function of time, when time was used as a covariate. TM2, TM3, and TM4 correspond to nonstationary models allowing for the location, scale, and both location and scale parameters to change as a function of time, respectively. Since there was no significant increase in likelihood between the nonstationary models (TM2, TM3, and TM4) and the stationary model (TM1), the location and scale parameters of the peak flow frequency distribution were considered to not change as a function of time. The lack of a statistically significant improvement can also be found when ECA was used to model the location (TM5) and scale (TM6) parameters individually, or simultaneously

(TM7). Without the use of climate covariates, the time series of peak flows of Camp Creek did not appear to be changing as a function of time or ECA.

If the peak flows of Camp Creek are changing as a result of ECA or time, and given a high natural background variability, the detection of such a signal may not be possible without introducing climate covariates in the attribution process. Snow and temperature, were introduced as climate covariates in the modelling process to account for the natural background variability of the peak flow time series. Snow appeared to be a significant covariate for the location (TM8) and the scale (TM9) parameters of the peak flow frequency distribution. When both the location and scale parameters were modelled to change as a function of snow (TM10), the combined model was an improvement over the stationary model (TM1), but not over TM8. Given the strong signal between snow and the location parameter (TM8), the significance of snow in relation to the scale parameter in the combined model (TM10) was relatively weak, resulting in some dominating effects similar to Greata Creek. A convergence issue was encountered for TM10 using the reduced record, therefore most of the inferences made between snow and the distribution parameters were based on modelling results of the full record.

In addition to snow, temperature appeared to be strongly related to both location and scale parameters. When both location and scale parameters were modelled to change as a function of temperature (TM13), the model was significantly improved over the stationary model (TM1). Similar conclusions can be reached when individual distribution parameters were modelled to change as a function of temperature (e.g., TM11 vs. TM1, TM12 vs. TM1). The only model that did not show a significant relationship between temperature and the scale parameter was TM12 (full record), where the addition of temperature did not yield a significant increase in likelihood over the stationary model. However, considering the overall pattern of

results with regards to temperature and the frequency distribution parameters, the role of temperature in relation to the scale parameter cannot be ignored. This is especially so when TM13 (both distribution parameters changing as a function of temperature) constituted a statistical improvement over the stationary model (TM1).

As a result of the significant relations between the climate covariates and the distribution parameters, TM14 was created, where both distribution parameters were changing as a function of both climate covariates. However, although there was a significant increase in the likelihood of TM14 over the stationary model, given the four climate covariates in TM14, and the potential of adding ECA on both distribution parameters resulting in six covariates in total, potential convergence issues existed. Therefore, only one climate covariate was kept for each distribution parameter. Snow was determined to be a stronger covariate than temperature for the location parameter by comparing AIC scores between TM8 and TM11. On the other hand, temperature appeared to be a stronger covariate than snow in relation to the scale parameter by comparing AIC scores between TM9 and TM12. Thus, temperature and snow were removed as covariates for the location and scale parameters, respectively, giving rise to TM15. TM15 was a better model than TM14 based on AIC scores and the LR test. Therefore, ECA was introduced in addition to TM15 giving rise to TM16.

The addition of ECA led to a significant increase in likelihood according to the LR test results (reduced record). The same conclusion was reached using the AIC scores (full record). To further confirm that the signal in the peak flow time series was caused by forest harvesting and not time, time was introduced as a covariate in addition to TM15. However, there was no evidence that the signal in the peak flow time series of Camp Creek was changing as a function of time (TM17 vs. TM15). In summary, after accounting for the natural background variability

of peak flows using both snow and temperature, ECA as a surrogate of forest harvesting continued to improve the modelling results for Camp Creek, while no further time trends were found for Greata Creek.

Table 8: Negative log-likelihood functions and AIC values for the GEV models of Camp Creek (treatment watershed).

Treatment Model	Model Description	Camp Creek (full record)		Camp Creek (reduced record)	
		Negative log-likelihood	AIC	Negative log-likelihood	AIC
TM1	Qp(μ, σ, ξ)	196.63	399.25	196.52	399.04
TM2	Qp(μ(time), σ, ξ)	196.63	401.25	196.45	400.90
TM3	Qp(μ, σ(time), ξ)	196.43	400.86	196.29	400.59
TM4	Qp(μ(time), σ(time), ξ)	196.43	402.85	196.26	402.52
TM5	Qp(μ(ECA), σ, ξ)	196.48	400.97	196.51	401.01
TM6	Qp(μ, σ(ECA), ξ)	196.43	400.86	195.96	399.92
TM7	Qp(μ(ECA), σ(ECA), ξ)	196.25	402.51	195.96	401.92
TM8	Qp(μ(snow), σ, ξ)	179.91*	367.81	184.79*	377.58
TM9	Qp(μ, σ(snow), ξ)	193.78*	395.57	196.24	400.48
TM10	Qp(μ(snow), σ(snow), ξ)	179.70*	369.40	155.87~	321.75
TM11	Qp(μ(temp), σ, ξ)	194.76#	397.52	193.42*	394.84
TM12	Qp(μ, σ(temp), ξ)	195.64	399.27	193.15*	394.29
TM13	Qp(*μ*(temp), *σ*(temp), *ξ*)	193.41*	396.82	191.60*	393.19
TM14	Qp(μ(snow, temp), σ(snow, temp), ξ)	178.29*	370.58	152.91~	319.83
TM15	Qp(μ(snow), σ(temp), ξ)	179.73*	369.45	184.78*	379.55
TM16	Qp(μ(snow, ECA), σ(temp, ECA), ξ)	177.38*	368.76	182.03*	378.07
TM17	Qp(μ(snow, time), σ(temp, time), ξ)	178.58*	371.17	183.90*	381.80
* significant over the stationary model at 95% significance levels when LR test is applied					
# significant over the stationary model at 90% significance levels when LR test is applied					
~ the estimation of model parameter did not converge					

4.1.3 Conditional predictions of forest harvesting effects on peak flows at Camp Creek

The return level plots for the time series of estimated peak flow magnitudes for Camp Creek are illustrated in Figure 19a for the 100-yr (Q100) and 25-yr (Q25), Figure 19b for the 50-yr (Q50) and 15-yr (Q15), and Figure 19c for the 20-yr (Q20) and 7-yr (Q7) events. These time series were derived from the final model (TM16), with both location and scale parameters changing in time as functions of climate and forest harvesting covariates. Despite the fluctuations in the peak flow time series associated with the natural background variability of snow and temperature, there was an obvious temporal upward trend associated with the time series of each quantile (Q100 to Q7) because of forest harvesting. Based on a simple linear regression analysis using time as a predictor, the slope of the trend line fitted to the Q100, Q50, Q25, Q20, Q15, and Q7 ranged from 0.01 m^3/s to 0.005 m^3/s per year, with slope increasing with the return period. Over the course of 40 years, forest harvesting appeared to cause about a 10% increase in peak flow magnitude for events of all return periods, which hints to a change in frequency. For instance, Figure 19a shows how the magnitude of Q25, which is 2.4 m^3/s at the end of the return level plot, is the same as the magnitude of Q100 at the beginning of the same return level plot. Therefore, the flow magnitude that was originally defined to be a 100-yr event became about four times more frequent 40 years after the start of forest harvesting in the Camp Creek watershed. Similarly, Figure 19b (19c) illustrates how the 50-year (20-year) event changed into a 15-year (7-year) event, 40 years after the start of forest harvesting in the Camp Creek watershed.

Another way of quantifying the effects of forest harvesting on peak flow frequency (and magnitude) is based on a snapshot comparison of pre- and post-harvest flood frequency curves (FFC) at any one time in the disturbance history of the Camp Creek watershed. Each FFC in Figure 20 represents a specific harvested condition shown in Figure 21 (i.e., state of disturbance).

These harvested conditions represent historic snapshots at various stages of forest harvesting and regrowth. The estimated peak flow magnitudes and frequencies were derived from GEV distributions with fixed snow and temperature conditions (long-term averages), allowing only ECA to vary. Therefore, the difference between FFCs was a result of varying forest disturbance conditions. The effects of forest harvesting are summarized in Table 9 for a range of peak flow quantiles from Q2 to Q100. These were derived from the TM16 frequency model for the 11%, 17%, and 24% ECA levels, which were arbitrarily selected for illustrative purposes. At 24% ECA, the magnitude had increased from 31% to 19% for the 2-yr to 100-yr peak flow events. At 24% ECA where 41% of the area of the Camp Creek watershed had historically been disturbed (Figure 21), forest harvesting also made peak flow events 3 to 4 times more frequent, where a 100-yr event becomes a 25-yr event, a 50-yr becomes a 15-yr, and a 20-yr becomes a 7-yr (Figure 20). The ECA level of 11%, which resulted in only a 14% (9%) increase in the peak flow magnitude of the 2-yr (100-yr) event, doubled the frequency of all peak flows between the 2-yr and 100-yr return periods. ECA levels of 17% and 24% resulted in an effect on the frequency that increased with peak flow event size, where a 20-yr event became 2 to 3 times more frequent, while a 100-yr event became 3 to 4 times more frequent (Figure 20). The confidence interval of forested FFC (representative of no disturbance conditions) intersected the 24% ECA FFC at a return period of 40-yr approximately. Hence, the detection limit, as per the null hypothesis testing at the subjectively selected significance level, would be up to the approximate 40-yr event, given 24% ECA and 45 years of data. The tilt at the upper end of the confidence band is associated with the increasing uncertainty in estimating large peak flows (>50-yr) for the given record length. Here, I report and recognize the role of confidence intervals, but without touting

the predictions of the nonstationary FP model as important only if they are statistically significant. This issue will be discussed further in the next section.

Table 9: Magnitude of peak flows of various return periods predicted by TM16 frequency model for control (ECA=0) and treatment (ECA=11%, 17%, and 24%) scenarios, with % change in comparison to control provided in parenthesis.

Return period (years)	Magnitude (m^3/s)			
	Control	11% ECA	17% ECA	24% ECA
2	1.04	1.19 (14%)	1.27 (22%)	1.36 (31%)
5	1.39	1.55 (12%)	1.64 (18%)	1.74 (25%)
10	1.62	1.79 (10%)	1.88 (16%)	2.00 (23%)
20	1.83	2.02 (10%)	2.12 (16%)	2.24 (22%)
50	2.12	2.32 (9%)	2.42 (14%)	2.55 (20%)
100	2.33	2.54 (9%)	2.65 (14%)	2.78 (19%)

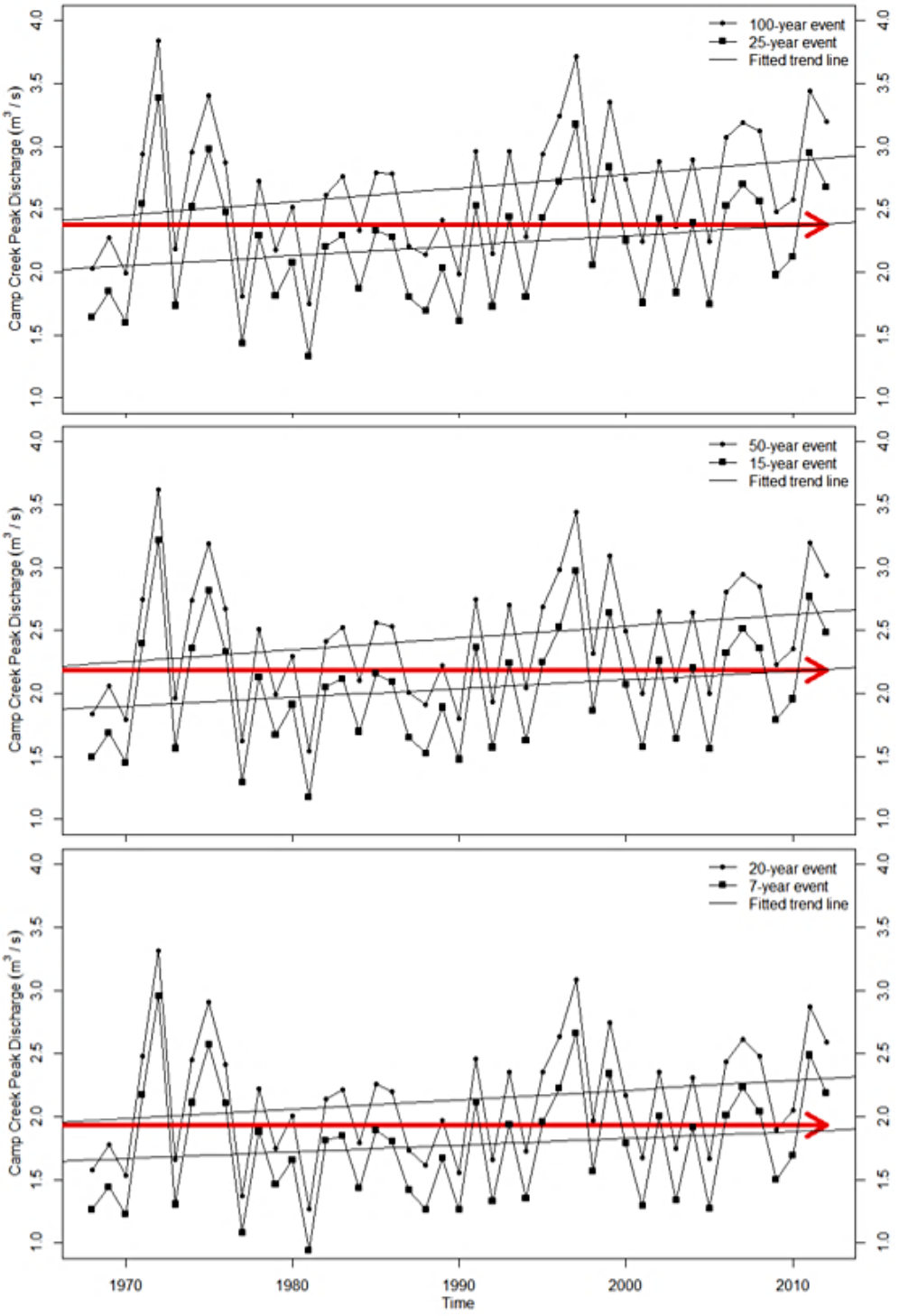

Figure 19: The estimated peak flow magnitudes of (a) 100-yr (Q100) and 25-yr (Q25) events, (b) 50-yr (Q50) and 15-yr (Q15) events, and (c) 20-yr (Q20) and 7-yr (Q7) events, and their respective trend lines fitted to the time series. The red line arrows within the respective panels are showing an increase in the frequency of peak flows (e.g., the magnitude of the 100-yr event at the beginning of the time series has become the magnitude of the 25-yr event over 40 years historic disturbance in the Camp Creek watershed).

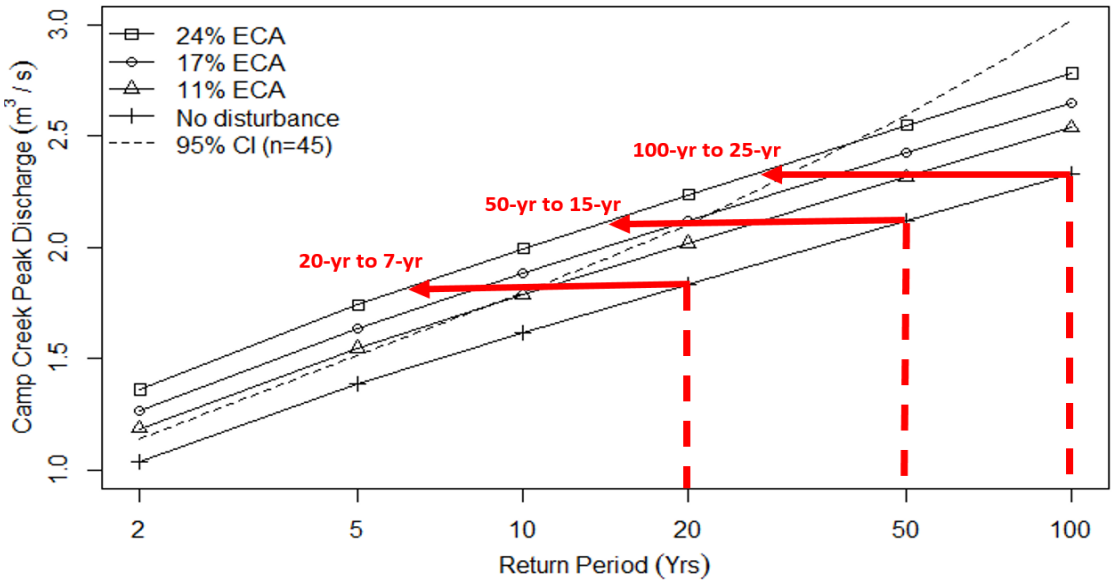

Figure 20: Flood frequency curves representative of 24%, 17%, 11% ECA levels, and no disturbance conditions in the Camp Creek watershed. The vertical dashed lines indicate the magnitudes of large peak flows (i.e., Q20, Q50, and Q100) under no disturbance condition. The red line arrows demonstrate the effects on the return periods of these large events as a result of harvesting at 24% ECA.

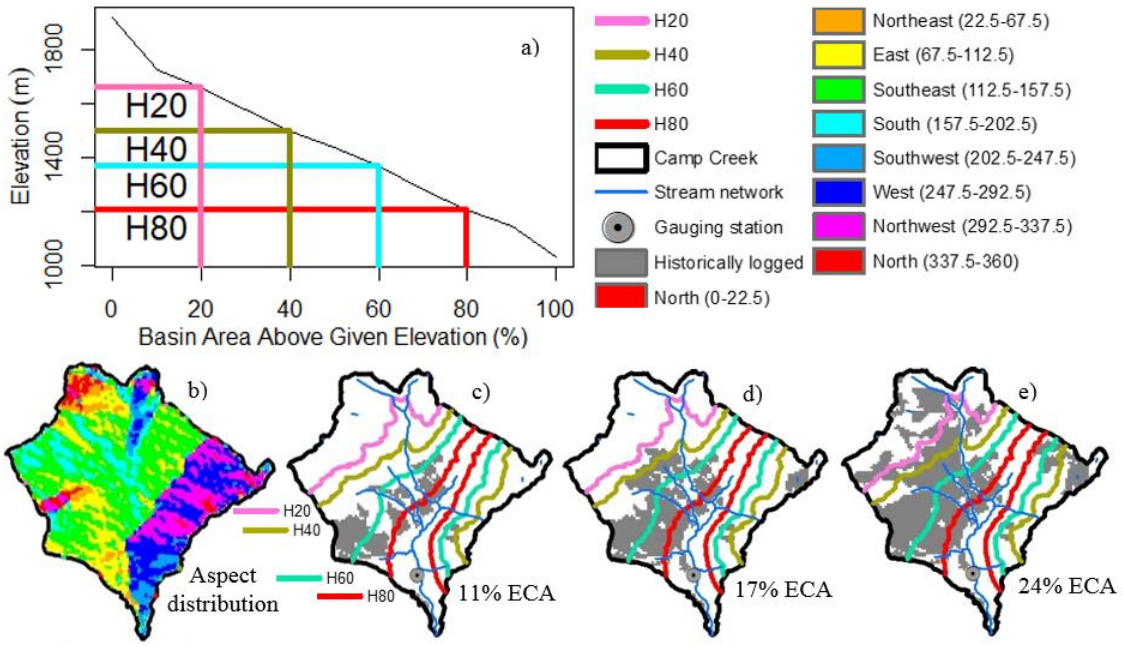

Figure 21: Hypsometric elevation contour lines of the Camp Creek watershed (panel a) (e.g., H40 and H60 are hypsometric elevation contour lines above which lies 40% and 60% of the total watershed area) in relation to (b) aspect distribution, and cut block locations at: (c) 11% ECA, (d) 17% ECA, and (e) 24% ECA.

4.2 Mather Creek-Fry Creek and Baker Creek-McKale River watershed pairs

4.2.1 Are peak flows at the control watersheds stationary after accounting for climate variability via covariates?

Both the location and scale parameters of the McKale River (control watershed) did not change as a function of time (Table 10), when time alone was used as a covariate (CM2, CM3, and CM4 vs. stationary model or CM1). For Fry Creek (control watershed), the distribution parameters did change with time, based on the same model comparisons (Table 11). Both CM3 and CM4 were significantly improved over CM1 at a $\alpha = 0.05$ when the full record of peak flows was used. However, the same conclusion could not be made with the reduced record. Therefore, the time trends found in CM3 and CM4 for Fry Creek could have been an artifact of outliers. Hence, the time trends needed to be scrutinized further using climate covariates to account for some temporal variability of peak flows.

Peak snow accumulation (SWE) was a significant covariate for the location parameter of the peak flow frequency distribution for McKale River. There are two ways to evaluate the increase of likelihood brought by an additional covariate (SWE) in a nonstationary model, by comparing CM5 and CM1, as well as comparing CM7 and CM6. The difference between the two is the addition of SWE to model the location parameter. Based on the results in Table 10, there is evidence that the location parameter (CM5) changed as a function of SWE. The addition of SWE in CM5 led to a significant increase in likelihood over the stationary model (CM1). The improvement brought by SWE, in relation to the location parameter, is consistent with the comparison between CM7 and CM6. In addition, SWE was also a significant covariate for the scale parameter when the full record was used via a comparison between CM1 and CM6. However, the signal was lost when the reduced record was used. The non-significance of SWE in

relation to the scale parameter was also consistent with the comparison between CM5 and CM7. Therefore, SWE was a significant and stronger covariate for the location than the scale parameter for peak flows at McKale River.

SWE was a significant covariate for both the location and scale parameters of the peak flow frequency distribution for Fry Creek. For the location parameter, the significance of SWE was shown by comparisons between CM5 and CM1, and CM6 and CM7. The significance of SWE for the scale parameter was shown by a comparison of CM5 and CM7. Despite the fact that SWE was not a significant covariate for the scale parameter via a comparison between CM1 and CM6, a comparison of the two-covariate model (CM7) and CM5 showed that SWE was indeed a significant covariate for the scale parameter.

Temperature was not a significant climate covariate for both the location and scale parameters for both McKale River and Fry Creek. Although some convergence issues were encountered for Fry Creek using the reduced record (e.g., CM9 and CM10 in Table 11), the conclusion remained the same when the analysis was conducted using the full record. Hence, temperature was not considered in further model development and evaluation.

Precipitation was a significant covariate for the location parameter of the McKale River peak flows, based on the comparison between CM11 and CM1 (full record). However, the significance was lost when the reduced record was used. Despite the fact that the combined model (CM13) was significantly improved over the stationary model, CM13 was not improved over its reduced counterpart CM11. Hence, precipitation may be related to the location parameter only, instead of both distribution parameters. On the other hand, only the scale parameter changed as a function of precipitation for Fry Creek. Amongst the three models (CM11, CM12,

and CM13) that used precipitation as a covariate, only CM12 was statistically improved over the nonstationary model, albeit at a 0.10 significance level.

The distribution parameters for McKale River and Fry Creek appear to be related to different combinations of snow and precipitation. Additional climate models were developed for the two watersheds for further evaluation (CM14, CM15, CM16, and CM17 for McKale River; CM14 and CM15 for Fry Creek). CM16 was the best-fitting model amongst the newly developed combined models for McKale River, based on the corresponding log-likelihood and AIC scores. CM16 was also significantly improved over its reduced model CM7 counterpart indicating that SWE was a significant covariate for both distribution parameters, while precipitation was a significant covariate for only the location parameter. This is consistent with previous findings in CM5 and CM11. For Fry Creek, when precipitation was incorporated to model the scale parameter in CM14 and CM15, both models were not statistically improved over their reduced model counterpart (CM7). Hence, the use of precipitation did not yield any additional improvement. Therefore, SWE was the only significant covariate for both the location and scale parameters for Fry Creek. Consequently, CM16 and CM7 were considered to be the best climate models for McKale River and Fry Creek, respectively.

To further evaluate the stationarity (or lack thereof) of the control watershed peak flow time series, CM18 and CM16 were developed for McKale River and Fry Creek, respectively, by introducing time as a covariate on top of the best climate models. Both CM18 and CM16 were not improved over their respective reduced climate models (i.e., CM16 for McKale River and CM7 for Fry Creek). Therefore, the time series of peak flows of McKale River and Fry Creek were stationary given the climate covariates used in this thesis. It is interesting to note that the same conclusions were reached for McKale River using models CM2, CM3, and CM4. This was

not the case for Fry Creek without accounting for the temporal variability. Comparisons using the combined model with climate inputs and time can lend more confidence to the stationarity conclusion by taking into account the natural background variability of the peak flow time series.

Table 10: Negative log-likelihood functions and AIC values for the GEV models of McKale River (control watershed).

Control Model	Model Description	McKale River (full record)		McKale River (reduced record)	
		Negative log-likelihood	AIC	Negative log-likelihood	AIC
CM1	Qp(μ, σ, ξ)	168.12	342.24	183.40	372.79
CM2	Qp(μ(time), σ, ξ)	168.07	344.14	183.40	374.79
CM3	Qp(μ, σ(time), ξ)	166.96	341.92	182.59	373.18
CM4	Qp(μ(time), σ(time), ξ)	166.90	343.80	182.51	375.02
CM5	Qp(μ(snow), σ, ξ)	163.19*	334.38	179.53*	367.06
CM6	Qp(μ, σ(snow), ξ)	166.63#	341.26	183.37	374.74
CM7	Qp(μ(snow), σ(snow), ξ)	163.16*	336.33	179.31*	368.63
CM8	Qp(μ(temp), σ, ξ)	167.85	343.71	183.33	374.67
CM9	Qp(μ, σ(temp), ξ)	167.96	343.93	182.76	373.53
CM10	Qp(μ(temp), σ(temp), ξ)	167.81	345.62	182.75	375.51
CM11	Qp(μ(precip), σ, ξ)	165.25*	338.49	182.20	372.40
CM12	Qp(μ, σ(precip), ξ)	167.23	342.46	183.38	374.76
CM13	Qp(μ(precip), σ(precip), ξ)	164.39*	338.78	148.19~	306.39
CM14	Qp(μ(snow), σ(precip), ξ)	162.89*	335.78	179.41*	368.82
CM15	Qp(μ(snow), σ(snow, precip), ξ)	162.88*	337.75	179.08*	370.16
CM16	Qp(μ(snow, precip), σ(snow), ξ)	160.12*	332.23	178.37*	368.74
CM17	Qp(μ(snow, precip), σ(snow, precip), ξ)	159.95*	333.90	145.75~	305.51
CM18	Qp(μ(snow, precip, time), σ(snow, time),	159.68*	335.36	177.79#	371.59
* significant over the stationary model at 95% significance levels when LR test is applied					
# significant over the stationary model at 90% significance levels when LR test is applied					
~ the estimation of model parameter did not converge					

Table 11: Negative log-likelihood functions and AIC values for the GEV models of Fry Creek (control watershed).

Control Model	Model Description	Fry Creek (full record)		Fry Creek (reduced record)	
		Negative log-likelihood	AIC	Negative log-likelihood	AIC
CM1	Qp(μ, σ, ξ)	180.33	366.65	187.26	380.53
CM2	Qp(μ(time), σ, ξ)	179.70	367.41	187.15	382.30
CM3	Qp(μ, σ(time), ξ)	177.55*	363.10	186.68	381.37
CM4	Qp(μ(time), σ(time), ξ)	177.52#	365.04	186.59	383.17
CM5	Qp(μ(snow), σ, ξ)	174.81*	357.62	184.52*	377.05
CM6	Qp(μ, σ(snow), ξ)	179.07	366.14	187.06	382.12
CM7	Qp(μ(snow), σ(snow), ξ)	172.94*	355.87	182.89*	375.77
CM8	Qp(μ(temp), σ, ξ)	180.20	368.40	187.20	382.40
CM9	Qp(μ, σ(temp), ξ)	179.88	367.76	153.37~	314.74
CM10	Qp(μ(temp), σ(temp), ξ)	179.84	369.68	165.62~	341.24
CM11	Qp(μ(precip), σ, ξ)	179.96	367.92	186.87	381.74
CM12	Qp(μ, σ(precip), ξ)	178.77#	365.53	185.70#	379.40
CM13	Qp(μ(precip), σ(precip), ξ)	178.21	366.42	185.20	380.41
CM14	Qp(μ(snow), σ(snow, precip), ξ)	172.72*	357.45	182.37*	376.74
CM15	Qp(μ(snow), σ(precip), ξ)	174.20*	358.40	183.90*	377.80
CM16	Qp(μ(snow, time), σ(snow, time), ξ)	171.92*	357.84	182.20#	378.41
* significant over the stationary model at 95% significance levels when LR test is applied					
# significant over the stationary model at 90% significance levels when LR test is applied					
~ the estimation of model parameter did not converge					

4.2.2 Is there a remaining signal in the peak flows of the treatment watersheds attributable to forest harvesting, after accounting for climate variability via covariates?

The modelling results are summarized in Table 12 for Mather Creek and Table 13 for Baker Creek. The peak flow time series of Mather Creek and Baker Creek changed as a function of time, when time alone was used as a covariate. When TM3 and TM4 were compared to TM1, there was evidence that both the location and scale parameters were changing as a function of time for both treatment watersheds, albeit at a 0.10 significance level. Similar time trends were concluded using ECA as a covariate (TM5, TM6, and TM7). However, the ECA signals were inconclusive between the full and reduced records. For instance, it can be concluded that forest harvesting was not affecting the peak flow time series for Baker Creek when both distribution parameters were not changing as a function of ECA (TM7) using the full record. The opposite can be concluded with the same TM7 for Baker Creek using the reduced record. Therefore, such inconclusive outcomes based on time and ECA as standalone covariates can be misleading.

SWE is a significant covariate for both Mather Creek and Baker Creek. Amongst the three nonstationary models incorporating SWE as a covariate (TM8, TM9, and TM10), both TM8 and TM10 were improved over the stationary model. Hence, the scale parameter (TM9) may not be changing as a function of SWE for both Mather Creek and Baker Creek. Interestingly, when both location and scale parameters were modelled to change as a function of SWE (TM10), the combined model was improved over the stationary model (TM1) for both treatment watersheds. SWE was a significant covariate for both distribution parameters for Baker Creek, since TM10 was improved over the reduced models TM8 and TM9. However, TM10 was not improved over its reduced counterpart TM8 for the Mather Creek. This indicated a non-

significant relation between SWE and the scale parameter. Therefore, SWE was a significant covariate for the location parameter only for Mather Creek.

When temperature was used as a covariate in nonstationary models TM11, TM12, and TM13, the models mostly showed no improvement over TM1 for both treatment watersheds. The addition of temperature showed an improvement over the stationary model at a 0.10 significance level (TM11), and only when the full record was used for Mather Creek. The significance of temperature as a covariate in further model development was likely to be overshadowed by the use of other climate covariates (e.g., SWE), as indicated previously. Hence, temperature was not considered in further model development.

Precipitation was a significant covariate for both the location and scale parameters for Mather Creek based on the outcomes of nonstationary models TM14, TM15, and TM16. Therefore, both SWE and precipitation were considered for further model development, giving rise to models TM17, TM18, and TM19. Amongst these newly developed models incorporating SWE and precipitation for Mather Creek, TM18 was the best climate model based on the associated AIC scores. TM18 is also an improvement over its reduced model counterpart (TM16). Therefore, the location parameter was changing as a function of SWE and precipitation (consistent with TM8 and TM14). The scale parameter was changing as a function of precipitation alone (consistent with TM15). For Baker Creek, there was no evidence that the nonstationary models, incorporating precipitation as a covariate (TM14, TM15, and TM16), were improved over the stationary model. Since SWE was the only significant climate covariate for Baker Creek, TM10 was the best climate model to use for further evaluation.

To evaluate potential time trends caused by forest harvesting, ECA was introduced as a covariate to the corresponding final climate models. Nonstationary models TM20, TM21, and

TM22 for Mather Creek, and TM17, TM18, and TM19 for Baker Creek were developed. For Mather Creek, the comparison between TM20 and its reduced counterpart, TM18, suggested that only the location parameter was changing as a function of ECA, rather than both distribution parameters. Although convergence issues were encountered for TM22, where both distribution parameters were modelled as a function of ECA, it was apparent that ECA was related to the location parameter (i.e., TM20 vs. TM18), but not the scale parameter (i.e., TM21 vs. TM18). For Baker Creek, both location and scale parameters were changing as a function of ECA based on comparisons between TM19 and its reduced model counterparts TM10, TM17, and TM18. Unlike the inconclusive outcomes from TM5, TM6, and TM7, where ECA alone was used as a covariate, consistent outcomes in relation to ECA were obtained between the full and reduced records when climate covariates were used in the nonstationary models. Therefore, TM20 and TM19 were considered to be the final models to quantify forest harvesting effects on peak flows for Mather Creek and Baker Creek, respectively.

To further evaluate the time trend signal in the peak flow time series, time as a covariate was introduced to TM18 and TM10, for Mather Creek and Baker Creek, respectively. These nonstationary models incorporating climate covariates and time (TM23, TM24, and TM25 for Mather Creek; TM20, TM21, and TM22 for Baker Creek) showed no improvement over their respective reduced models. Hence, there was no evidence that the peak flow time series was changing as a function of time, after accounting for the temporal variability of peak flows using climate covariates for both treatment watersheds. ECA, as a surrogate of forest harvesting, continued to improve modelling results at both Mather Creek and Baker Creek. No further time trends were found in their respective control watersheds, Fry Creek and McKale River.

Table 12: Negative log-likelihood functions and AIC values for the GEV models of Mather Creek (treatment watershed).

Treatment Model	Model Description	Mather Creek (full record)		Mather Creek (reduced record)	
		Negative log-likelihood	AIC	Negative log-likelihood	AIC
TM1	Qp(μ, σ, ξ)	183.91	373.83	183.77	373.54
TM2	Qp(μ(time), σ, ξ)	183.69	375.39	183.61	375.22
TM3	Qp(μ, σ(time), ξ)	182.02#	372.04	182.33#	372.67
TM4	Qp(μ(time), σ(time), ξ)	181.46#	372.91	182.04	374.08
TM5	Qp(μ(ECA), σ, ξ)	182.47#	372.94	182.97	373.94
TM6	Qp(μ, σ(ECA), ξ)	180.63*	369.27	182.15#	372.29
TM7	Qp(μ(ECA), σ(ECA), ξ)	179.87*	369.74	181.76	373.53
TM8	Qp(μ(snow), σ, ξ)	175.13*	358.26	174.71*	357.42
TM9	Qp(μ, σ(snow), ξ)	183.65	375.29	183.76	375.51
TM10	Qp(μ(snow), σ(snow), ξ)	174.98*	359.95	174.43*	358.87
TM11	Qp(μ(temp), σ, ξ)	182.38#	372.75	182.95	373.90
TM12	Qp(μ, σ(temp), ξ)	183.89	375.78	183.73	375.46
TM13	Qp(μ(temp), σ(temp), ξ)	182.37	374.75	182.88	375.76
TM14	Qp(μ(precip), σ, ξ)	179.83*	367.65	181.41*	370.82
TM15	Qp(μ, σ(precip), ξ)	181.00*	369.99	182.03#	372.07
TM16	Qp(μ(precip), σ(precip), ξ)	178.84*	367.67	180.40*	370.80
TM17	Qp(μ(snow, precip), σ(snow), ξ)	170.52	353.03	170.34	352.69
TM18	Qp(μ(snow, precip), σ(precip), ξ)	167.64	347.28	169.06	350.11
TM19	Qp(μ(snow), σ(snow, precip), ξ)	172.76	357.51	173.30	358.60
TM20	Qp(μ(snow, precip, ECA), σ(precip), ξ)	164.72*	343.45	166.60*	347.20
TM21	Qp(μ(snow, precip), σ(precip, ECA), ξ)	167.62	349.25	169.01	352.02
TM22	Qp(μ(snow, precip, ECA), σ(precip, ECA), ξ)	136.35~	288.70	131.39~	278.77
TM23	Qp(μ(snow, precip, time), σ(precip), ξ)	166.34	346.68	167.89	349.77
TM24	Qp(μ(snow, precip), σ(precip, time), ξ)	167.63	349.26	169.06	352.11
TM25	Qp(μ(snow, precip, time), σ(precip, time), ξ)	166.21	348.41	167.84	351.67
* significant over the stationary model at 95% significance levels when LR test is applied					
# significant over the stationary model at 90% significance levels when LR test is applied					
~ the estimation of model parameter did not converge					

Table 13: Negative log-likelihood functions and AIC values for the GEV models of Baker Creek (treatment watershed).

Treatment Model	Model Description	Baker Creek (full record)		Baker Creek (reduced record)	
		Negative log-likelihood	AIC	Negative log-likelihood	AIC
TM1	Qp(μ, σ, ξ)	214.54	435.08	218.79	443.58
TM2	Qp(μ(time), σ, ξ)	214.50	437.00	218.65	445.31
TM3	Qp(μ, σ(time), ξ)	212.22*	432.44	216.22*	440.45
TM4	Qp(μ(time), σ(time), ξ)	212.19#	434.37	216.20#	442.39
TM5	Qp(μ(ECA), σ, ξ)	213.73	435.45	217.18#	442.36
TM6	Qp(μ, σ(ECA), ξ)	212.67#	433.34	216.07*	440.15
TM7	Qp(μ(ECA), σ(ECA), ξ)	212.24	434.48	215.60*	441.20
TM8	Qp(μ(snow), σ, ξ)	205.48*	418.96	209.93*	427.87
TM9	Qp(μ, σ(snow), ξ)	214.42	436.84	218.78	445.56
TM10	Qp(μ(snow), σ(snow), ξ)	203.69*	417.37	208.77*	427.55
TM11	Qp(μ(temp), σ, ξ)	213.40	434.81	217.78	443.56
TM12	Qp(μ, σ(temp), ξ)	214.48	436.96	218.65	445.29
TM13	Qp(μ(temp), σ(temp), ξ)	213.38	436.75	217.78	445.55
TM14	Qp(μ(precip), σ, ξ)	213.98	435.97	218.17	444.33
TM15	Qp(μ, σ(precip), ξ)	214.23	436.47	218.33	444.67
TM16	Qp(μ(precip), σ(precip), ξ)	213.26	436.51	217.45	444.90
TM17	Qp(μ(snow, ECA), σ(snow), ξ)	201.36*	414.72	206.17*	424.35
TM18	Qp(μ(snow), σ(snow, ECA), ξ)	202.87*	417.75	207.28*	426.55
TM19	Qp(μ(snow, ECA), σ(snow, ECA), ξ)	199.87*	413.74	204.26*	422.52
TM20	Qp(μ(snow, time), σ(snow), ξ)	201.54*	415.07	206.49*	424.98
TM21	Qp(μ(snow), σ(snow, time), ξ)	202.84*	417.67	207.53*	427.06
TM22	Qp(μ(snow, time), σ(snow, time), ξ)	200.57*	415.14	205.34*	424.68
* significant over the stationary model at 95% significance levels when LR test is applied					
# significant over the stationary model at 90% significance levels when LR test is applied					
~ the estimation of model parameter did not converge					

4.2.3 Conditional predictions of forest harvesting effects on peak flows at Mather Creek and Baker Creek

The return level plots for the time series of estimated peak flow magnitudes are illustrated in Figure 22a-22c and Figure 23a-23c for Mather Creek and Baker Creek, respectively. These time series, ranging from Q100 to Q2, were estimated based on the corresponding final quantification models, TM20 for Mather Creek and TM19 for Baker Creek. This quantification technique allowed the distribution parameters to change as functions of climate and ECA covariates. There are visually identifiable upward trends associated with all estimated peak flow time series as a result of forest harvesting for both treatment watersheds. Based on a simple linear regression analysis using time as a predictor, the slopes of the trend line fitted to the estimated Q100, Q50, Q30, Q20, and Q7 time series of Mather Creek ranged from 0.19 m^3/s to 0.12 m^3/s per year (Figure 22). The same slopes ranged from 1.29 m^3/s to 0.35 m^3/s per year for the estimated Q100, Q50, Q20, Q4, Q3, and Q2 time series of Baker Creek (Figure 23). The slopes are increasing with return periods for both watersheds. According to the fitted trend lines, the 100-yr event had increased from approximately 17 m^3/s to 25 m^3/s (Figure 22a) and 91 m^3/s to 151 m^3/s (Figure 23a), for Mather Creek and Baker Creek, a 47% and 66% increase, respectively.

Over four to five decades, forest harvesting caused as much as a 38% and 114% increase in peak flow magnitude at 22% and 37% ECA levels at Mather Creek and Baker Creek, respectively. Such changes in the peak flow magnitude are hinting to a change of peak flow frequency as a result of forest harvesting. For instance, Figure 23a shows how the magnitude of the 100-yr event, which is about 150 m^3/s at the end of the return level plot according to the fitted trend line, is similar to the magnitude of 4-yr events at the beginning of the same return

level plot. Therefore, the flow magnitude that was originally defined to be the 100-yr event has become 25 times more frequent 43 years after the start of forest harvesting in the Baker Creek watershed. For Mather Creek, forest harvesting appeared to cause an increase in peak flow magnitude, hence a shift in peak flow frequency as well. Such effects on the peak flow frequency are similar to those of Camp Creek, yet the effects are lower than those predicted for Baker Creek.

Despite the fact that the red arrows are not perfectly horizontal in Figure 22, these arrows still provide an illustrative example of forest harvesting effects on the frequency from the perspective of a return level plot. The effects of forest harvesting on peak flow frequency (and magnitude) is based on a snapshot comparison of pre- and post-harvest flood frequency curves (FFC), at any one time in the disturbance history of the Mather Creek and Baker Creek watersheds, shown in Figure 24 and Figure 25, respectively. Again, these harvested conditions, represent historic snapshots at various stages of forest harvesting and regrowth. The estimated peak flow magnitudes and frequencies were derived from GEV distributions with fixed climate conditions (long-term averages), allowing only ECA to vary. Therefore, the difference between FFCs is a result of varying forest disturbance conditions. The forest harvesting effects are summarized in Table 14 and Table 15 for Mather Creek and Baker Creek, respectively. The peak flow quantiles, ranging from 2-yr to 100-yr events at various ECA levels, were selected arbitrarily for illustrative purposes.

At a 22% ECA level, the magnitude had increased from 38% to 15% for the 2-yr to 100-yr peak flow events (Table 14) at Mather Creek, where about 25% of the watershed had been disturbed (Figure 26). Large peak flows still became approximately three times as frequent, so that a 50-yr event became a 15-yr event, and a 100-yr event became a 30-yr event. At a 10%

ECA for the Mather Creek watershed, an increase in the magnitude of only 17% to 7% resulted in doubling the frequency of all peak flows between the 2-yr and 100-yr return periods. At a 37% ECA for Baker Creek watershed, where 46% of the area had been historically disturbed (Figure 27), the treatment effects are higher than those predicted for Mather Creek. The magnitude increased by 114% to 112% for the 2-yr to 100-yr peak flow events (Table 15). Forest harvesting caused the peak flows to be 10 to 25 times more frequent, where a 20-yr event became a 2-yr event, a 50-yr event became a 3-yr event, and a 100-yr event became a 4-yr event. The effect on frequency tends to increase with peak flow event size. At Baker Creek, an ECA level of 10% resulted in about a 30% increase in peak flow magnitude (Table 15). This level of increase tripled the frequency of all peak flows between the 2-yr and 100-yr return periods.

The 95% confidence intervals (CI) of the forested FFC followed a similar trajectory for both treatment watersheds. The CIs were lower than the corresponding 10% ECA FFCs at the lower end. The CIs intersect their FFCs at approximately Q7 for Mather Creek and Q50 for Baker Creek. As a result of a larger uncertainty in the estimation of the large peak flows, the upper tails of the CIs were tilted upwards. The CIs illustrate how the detection limit would be up to approximately the Q7 event, given 22% ECA and 42 years of data for Mather Creek. The detection limit for Baker Creek would be up to approximately the Q50 event, given 37% ECA and 48 years of data.

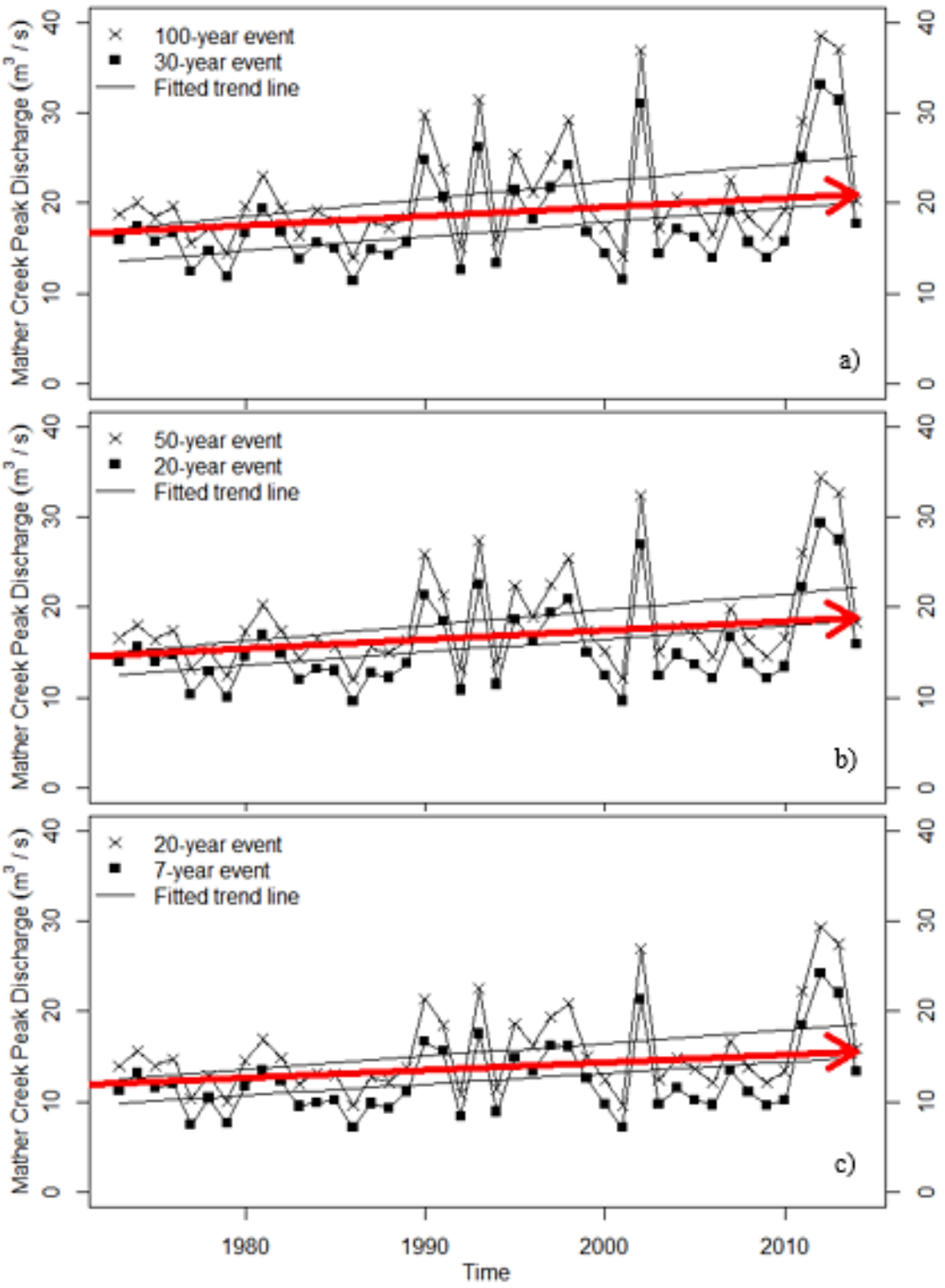

Figure 22: The estimated peak flow magnitudes of (a) 100-yr (Q100) and 30-yr (Q30) events, (b) 50-yr (Q50) and 20-yr (Q15) events, and (c) 20-yr (Q20) and 7-yr (Q7) events, and their respective trend lines fitted to the time series. The red line arrows within the respective panels are showing an increase in the frequency of peak flows (e.g., the magnitude of the 100-yr event at the beginning of the time series has become the magnitude of the 30-yr event over 40 years historic disturbance for Mather Creek).

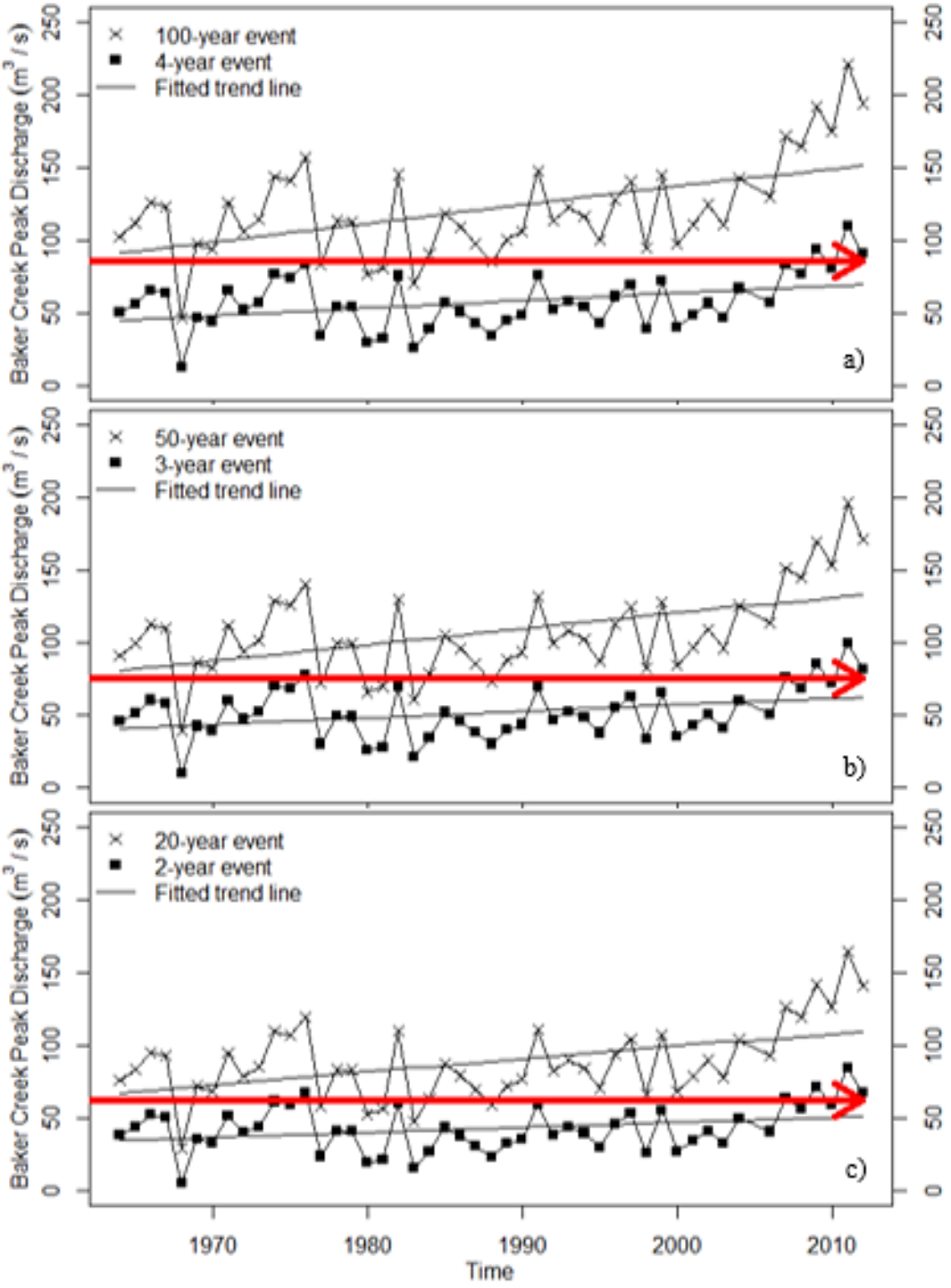

Figure 23: The estimated peak flow magnitudes of (a) 100-yr (Q100) and 4-yr (Q4) events, (b) 50-yr (Q50) and 3-yr (Q3) events, and (c) 20-yr (Q20) and 2-yr (Q2) events, and their respective trend lines fitted to the time series. The red line arrows within the respective panels are showing an increase in the frequency of peak flows (e.g., the magnitude of the 100-yr event at the beginning of the time series has become the magnitude of the 4-yr event over 50 years historic disturbance for Baker Creek).

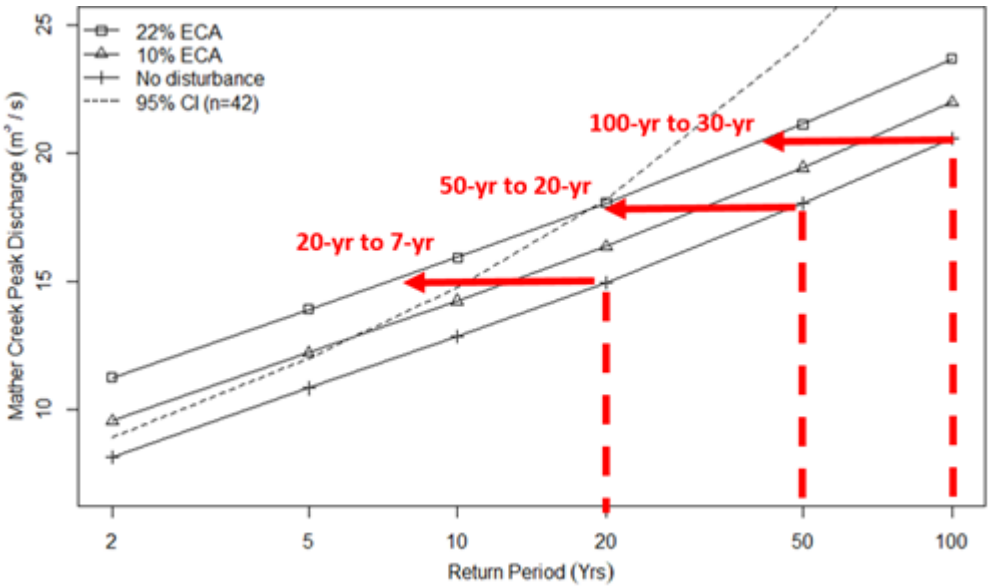

Figure 24: Flood frequency curves representative of 22%, 10% ECA levels, and no harvesting conditions for Mather Creek. The vertical dashed lines indicate the magnitudes of large peak flows (i.e., Q20, Q50, and Q100) under no disturbance condition. The red line arrows demonstrate the effects on return periods of these large events as a result of harvesting at 22% ECA.

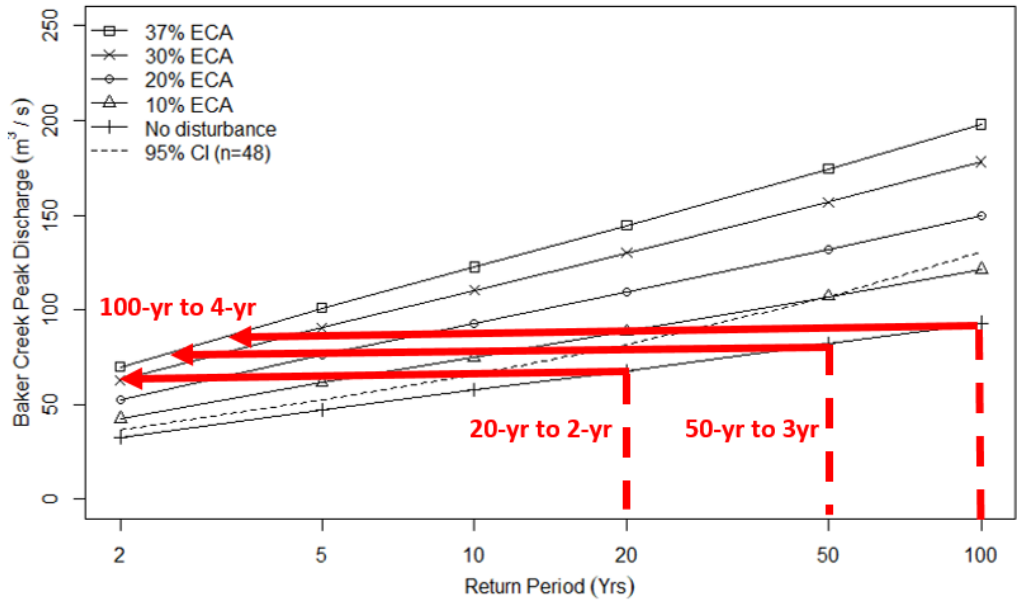

Figure 25: Flood frequency curves representative of 37%, 30%, 20%, 10% ECA levels, and no harvesting conditions for Baker Creek. The vertical dashed lines indicate the magnitudes of large peak flows (i.e., Q20, Q50, and Q100) under no disturbance condition. The red line arrows demonstrate the effects on return periods of these large events as a result of harvesting at 37% ECA.

Table 14: Magnitude of peak flows of various return periods predicted by TM20 frequency model for control (ECA=0) and treatment (ECA=10%, and 22%) scenarios for Mather Creek, with % change in comparison to control provided in parenthesis.

Return period (years)	Magnitude (m^3/s)		
	Control	10% ECA	22% ECA
2	8.17	9.57 (17%)	11.26 (38%)
5	10.85	12.25 (13%)	13.95 (29%)
10	12.86	14.26 (11%)	15.96 (24%)
20	14.99	16.38 (9%)	18.08 (21%)
50	18.05	19.45 (8%)	21.14 (17%)
100	20.6	22.00 (7%)	23.69 (15%)

Table 15: Magnitude of peak flows of various return periods predicted by TM19 frequency model for control (ECA=0) and treatment (ECA=10%, 20%, 30%, and 37%) scenarios for Baker Creek, with % change in comparison to control provided in parenthesis.

Return period (years)	Magnitude (m^3/s)				
	Control	10% ECA	20% ECA	30% ECA	37% ECA
2	32.71	42.77 (31%)	52.85 (62%)	62.92 (92%)	69.97 (114%)
5	47.33	61.79 (31%)	76.28 (61%)	90.76 (92%)	100.90 (113%)
10	57.61	75.17 (30%)	92.76 (61%)	110.34 (92%)	122.65 (113%)
20	67.94	88.62 (30%)	109.33 (61%)	130.03 (91%)	144.52 (113%)
50	82.05	106.99 (30%)	131.95 (61%)	156.91 (91%)	174.38 (113%)
100	93.19	121.49 (30%)	149.81 (61%)	178.13 (91%)	197.96 (112%)

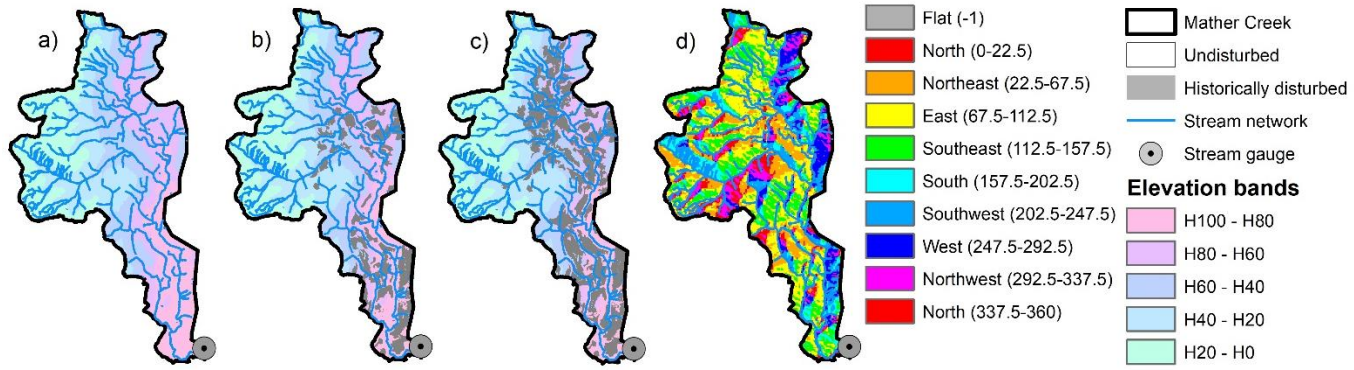

Figure 26: Hypsometric elevation contour for the Mather Creek watershed with (a) no logging, (b) 10% ECA, (c) 22% ECA, in relation to aspect distribution (panel d).

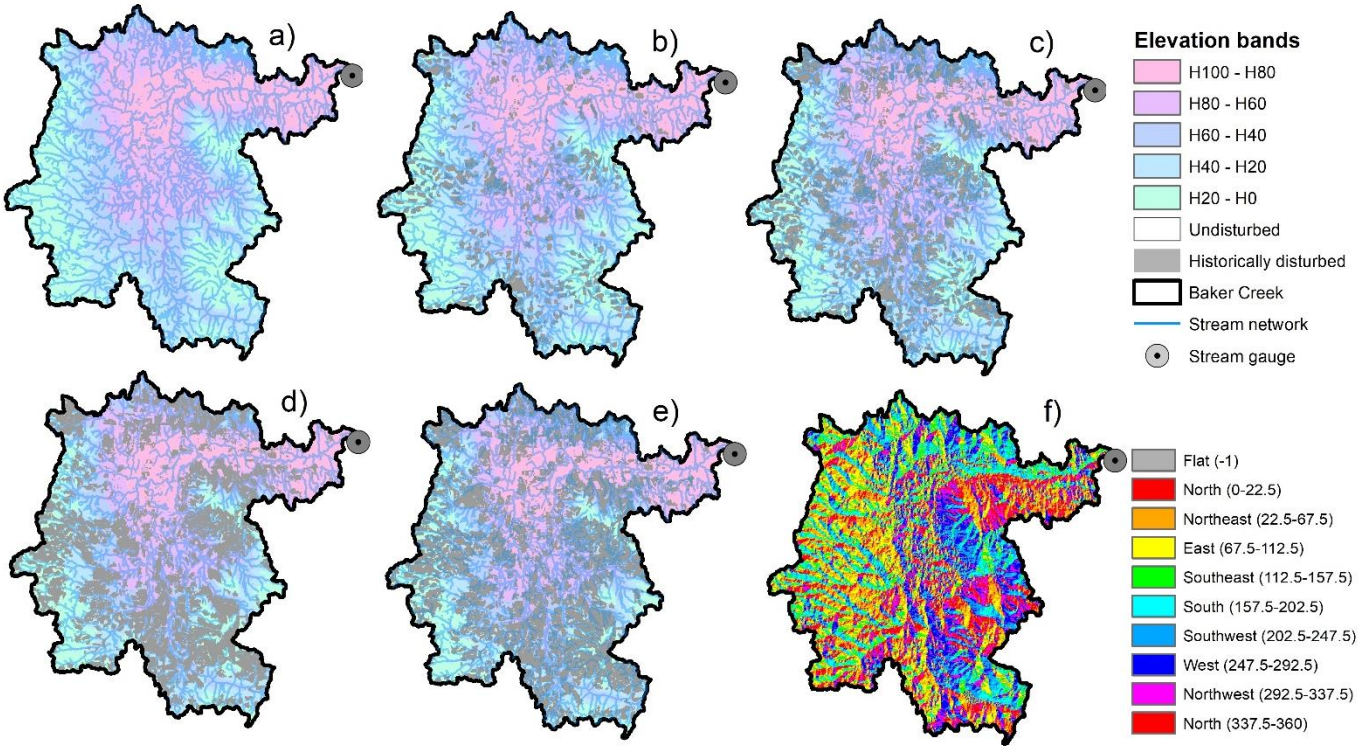

Figure 27: Hypsometric elevation contour for the Baker Creek watershed with (a) no logging, (b) 10% ECA, (c) 20% ECA, (d) 30% ECA, (e) 37% ECA, in relation to aspect distribution (panel f).

4.3 Bowron River- and Willow River-McGregor River watershed pairs

4.3.1 Are peak flows at the control watershed stationary after accounting for climate variability via covariates?

It is necessary to rule out any potential time trends for McGregor River (control watershed) prior to conducting attribution processes in the treatment watersheds. This allows for the attribution of any potential time trends found for the Bowron River and the Willow River watersheds to forest harvesting. The modelling procedures were carried out with POT peak flows that were identified using separations, *r*, equal to 7, 8, and 9. The resulting arrival rates, defined by the number of peak flow events per year, ranged from 1.83 to 2.04. The negative log-likelihood, AIC scores, and the LR test results of the models associated with the McGregor River are shown in Table 16.

No time trends were detected in the scale parameter of the peak flow distribution for the McGregor River watershed when time alone was used as a covariate (CM2). The non-significance is consistent amongst the three POT time series with different arrival rates. However, such stationary conclusions can be misleading given the large temporal variability of the peak flow time series, as shown previously. The time trends need to be scrutinized by climate covariates, as illustrated below.

SWE was a significant covariate for the scale parameter of the peak flow frequency distribution for McGregor River, demonstrated by the comparison between CM3 and the stationary model (CM1). The significance is consistent amongst the three POT time series. However, the same cannot be concluded for the other climate covariate, warming rates. The introduction of warming rates in CM4 yielded significant improvement only when the POT time series with the lowest arrival rate was used. No improvement was made for the other two time

series. Despite the lack of consistency, warming rates was retained for further model development to evaluate the contribution of warming rates in a two-covariate model. Therefore, both SWE and warming rates were used to develop the nonstationary model, CM5. This combined model seemed to be an improvement over the stationary model. However, the improvement brought by warming rates was lost when it was compared to its reduced model counterpart (CM3). The lack of improvement brought by warming rates is in line with the outcomes of CM4. As a result, SWE was the only significant covariate for modelling the peak flows of McGregor River and CM3 was the best climate model.

Time as a covariate was introduced to CM3, giving rise to CM6, to evaluate if there was any leftover signal in the peak flows. As the results of CM6 suggest, there was no evidence that the addition of time led to a significant increase in likelihood. Both the nonstationary model with time alone (i.e., CM2) or with one climate covariate (i.e., CM6), led to the same conclusion: the peak flow time series of McGregor River was stationary given the climate covariates used in this thesis.

Table 16: Negative log-likelihood functions and AIC values for the GPD models for McGregor River control watershed.

Model	McGregor River	*r* =7, m =2.04		*r* =8, m =1.93		*r* =9, m =1.83	
		Negative log-likelihood	AIC	Negative log-likelihood	AIC	Negative log-likelihood	AIC
CM1	Qp(σ, ξ)	396.70	797.41	377.36	758.73	358.62	721.24
CM2	Qp(σ(time), ξ)	396.58	799.16	377.26	760.51	358.54	723.07
CM3	Qp(σ(snow), ξ)	386.53*	779.05	366.54*	739.08	346.37*	698.73
CM4	Qp(σ(dT/dt), ξ)	396.24	798.48	376.44	758.88	357.20#	720.39
CM5	Qp(σ(snow, dT/dt), ξ)	386.44*	780.88	366.32*	740.65	346.14*	700.28
CM6	Qp(σ(snow, time), ξ)	385.99*	779.99	366.05*	740.10	345.89*	699.78
* significant over the stationary model at 95% significance levels when LR test is applied							
# significant over the stationary model at 90% significance levels when LR test is applied							

4.3.2 Is there a remaining signal in the peak flows of the treatment watershed attributable to forest harvesting, after accounting for climate variability via covariates?

To detect the signals caused by forest harvesting in the peak flow time series for the Bowron River and Willow River watersheds, it is important to follow similar procedures as for the McGregor River watershed. The modelling results are shown in Table 17 and Table 18, for the Bowron River and Willow River, respectively. No time trends were detected in the scale parameter of the peak flow distribution of Bowron River, when time alone was used as a covariate (TM2). However, the addition of ECA has led to a significant increase in the likelihood of TM3 from the stationary model for Bowron River. The outcomes in regards to ECA are consistent for the three POT time series. On the other hand, the peak flow time series was changing as a function of both time (TM2) and ECA (TM3), albeit only at a 0.10 significance level for Willow River. The improvement brought by ECA was applicable to two of the three POT time series. Hence, the ECA signal at Willow River remained inconclusive, and it needs further evaluation using climate covariates.

SWE and warming rates were both statistically significant covariates for the peak flow frequency distributions of Bowron River and Willow River. There was strong evidence that the addition of SWE led to a significant increase in the likelihood of TM4 over TM1. However, a similar comparison between TM5 and TM1 revealed that warming rates can be a significant covariate for the peak flows of Willow River, but not Bowron River. Further evaluation, using TM6 and TM4 for Bowron River, revealed significant improvement brought by warming rates. This comparison indicated that the scale parameter was changing as a function of warming rates at Bowron River, similar to Willow River. Therefore, warming rates was a significant covariate for the peak flow frequency distribution for both treatment watersheds via different comparisons.

It is interesting to note that SWE appeared to be a significant covariate in similar ways for both Bowron River and Willow River. This was determined by the difference in AIC values between TM1 and TM4. Warming rates, on the other hand, was a stronger covariate for the peak flows of Willow River than Bowron River. For instance, warming rates alone was not a significant covariate for Bowron River (i.e., TM5 vs. TM1) and the difference in AIC values between the nested models (i.e., TM5 vs. TM1, TM6 vs. TM4) were greater for Willow River than Bowron River.

Both SWE and warming rates were significant covariates for Bowron River and Willow River. Hence, TM6 was the best climate model for both treatment watersheds. ECA was introduced to TM6 giving rise to TM7, which was used to evaluate forest harvesting signals in the peak flow time series. The addition of ECA led to a significant increase in the likelihood of TM7 over TM6 for both treatment watersheds. The improvement was consistent for all three POT time series. After accounting for the natural background variability of peak flows using SWE and warming rates, ECA, as a surrogate of forest harvesting, continued to improve the nonstationary modelling results at Bowron River and Willow River. No further time trends were concluded in their nearby control watershed McGregor River.

To further evaluate the time trend signal in the peak flow time series for Bowron River and Willow River, time as a covariate was introduced to TM6, giving rise to TM8 for both treatment watersheds. There is no evidence that the peak flow time series of Bowron River was changing as a function of time after accounting for some temporal variability using SWE and warming rates. For Willow River, on the other hand, time as a covariate made similar improvements in the nonstationary model as ECA (i.e., TM7 vs. TM6, TM8 vs. TM6). As a matter of fact, the historic forest harvesting that occurred in Willow River watershed resulted in a

gradual and monotonic increase in ECA levels (Figure 18), which was similar to the pattern of time as a covariate. Hence, time as a surrogate of ECA could explain the leftover signal in the peak flow time series in relation to forest harvesting.

Table 17: Negative log-likelihood functions and AIC values for the GPD models for Bowron River.

Model	Bowron River	*r* =11, m = 1.5		*r* =13, m = 1.43		*r* =15, m =1.35	
		Negative log-likelihood	AIC	Negative log-likelihood	AIC	Negative log-likelihood	AIC
TM1	Qp(σ, ξ)	350.33	704.66	334.91	673.81	318.99	641.97
TM2	Qp(σ(time), ξ)	349.65	705.29	334.25	674.49	318.38	642.76
TM3	Qp(σ(ECA), ξ)	348.16*	702.31	332.37*	670.74	315.81*	637.62
TM4	Qp(σ(snow), ξ)	347.79*	701.59	332.44*	670.88	316.88*	639.76
TM5	Qp(σ(dT/dt), ξ)	349.47	704.94	334.19	674.39	318.88	643.75
TM6	Qp(σ(snow, dT/dt), ξ)	345.08*	698.15	329.42*	666.84	314.58*	637.16
TM7	Qp(σ(snow, dT/dt, ECA), ξ)	343.63*	697.27	327.92*	665.85	313.22*	636.44
TM8	Qp(σ(snow, dT/dt, time), ξ)	344.46*	698.93	328.85*	667.70	314.26*	638.53
* significant over the stationary model at 95% significance levels when LR test is applied							
# significant over the stationary model at 90% significance levels when LR test is applied							

Table 18: Negative log-likelihood functions and AIC values for the GPD models for Willow River.

Model	Willow River	*r* =1, m =1.76		*r* =5, m =1.50		*r* =9, m =1.39	
		Negative log-likelihood	AIC	Negative log-likelihood	AIC	Negative log-likelihood	AIC
TM1	Qp(σ, ξ)	384.97	773.93	337.10	678.21	315.00	634.00
TM2	Qp(σ(time), ξ)	383.30#	772.61	335.21#	676.43	313.90	633.80
TM3	Qp(σ(ECA), ξ)	383.32#	772.65	335.44#	676.89	314.12	634.24
TM4	Qp(σ(snow), ξ)	383.11#	772.22	334.53*	675.07	312.49*	630.97
TM5	Qp(σ(dT/dt), ξ)	372.70*	751.39	329.10*	664.20	308.30*	622.60
TM6	Qp(σ(snow, dT/dt), ξ)	372.22*	752.44	328.05*	664.10	307.13*	622.26
TM7	Qp(σ(snow, dT/dt, ECA), ξ)	374.66*	759.32	325.60*	661.20	305.05*	620.10
TM8	Qp(σ(snow, dT/dt, time), ξ)	374.50*	759.01	325.05*	660.09	304.29*	618.58
* significant over the stationary model at 95% significance levels when LR test is applied							
# significant over the stationary model at 90% significance levels when LR test is applied							

4.3.3 Conditional predictions of hydrologic effects from forest harvesting at Bowron River and Willow River

The nonstationary frequency models were used in this research for two purposes. The first purpose was to detect and attribute the effects of forest harvesting on the frequency distribution parameters and, hence, on the magnitude and frequency of peak flows. The second purpose was to quantify the potential effects of forest harvesting on the magnitude and frequency of peak flows. In the previous sections, I have shown that the peak flow time series of McGregor River (control watershed) appeared to be stationary. The peak flow time series of the treatment watersheds were found to be related to forest harvesting, using the nonstationary frequency models driven by climate covariates and ECA. In this section, I further illustrate the forest harvesting effects on peak flow using two quantification techniques. Both methods were based on the final fitted model for the treatment watersheds (TM7). The quantification of treatment effects was carried out using r = 13 and 9, for Bowron River and Willow River, respectively.

The return level plots for the time series of estimated peak flow magnitudes are illustrated in Figure 28a, 28b and Figure 29a, 29b, for Bowron River and Willow River, respectively. These time series of peak flows, ranging from Q100 to Q3, were estimated based on their final quantification model (TM7). This quantification technique allowed distribution parameters to change as functions of climate and ECA covariates. Despite the fluctuations in the peak flow time series, as a result of the natural background variability, there are obvious upward trends associated with the estimated time series for both treatment watersheds, brought about by forest harvesting. Based on simple linear regression analyses using time as a predictor, the slopes of the trend line fitted to the estimated Q100, Q20, Q4, and Q3 time series ranged from 2.61 m^3/s to 1.78 m^3/s per year for Bowron River. The same slopes ranged from 3.14 m^3/s to 1.92 m^3/s per

year for the estimated Q100, Q20, Q5, and Q4 time series for Willow River, with the slope increasing with return period. According to the fitted trend line, the 100-yr event increased from approximately 392 m^3/s to 590 m^3/s (Figure 28a) and 330 m^3/s to 562 m^3/s (Figure 29a) for Bowron River and Willow River (51% and 61% increase), respectively, over the course of approximately five to six decades. For Bowron River (Willow River), forest harvesting elevated the magnitude of 4-yr (5-yr) events at the end of the return level plot similar to those of 100-yr events. Despite both 100-yr and 10-yr events being subject to a similar upward trend for Bowron River and Willow River, it is interesting to note that the difference between the magnitude of 100-yr and 10-yr events got increasingly larger with time. This implies that the bigger event, the bigger are treatment effects, as was implied in the increasing slopes (of fitted trend lines) with increasing return period.

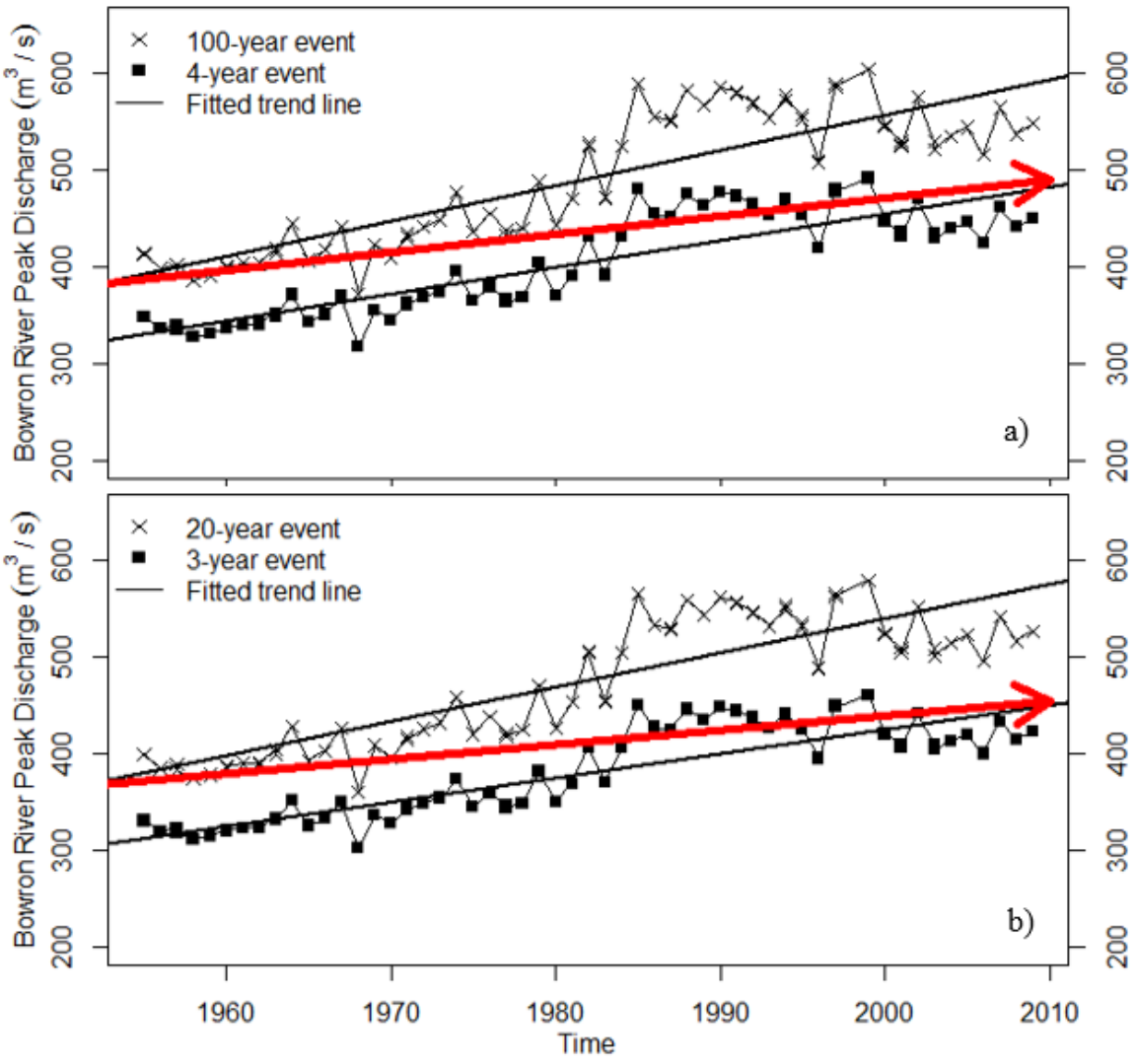

Figure 28: The estimated peak flow magnitudes of (a) 100-yr (Q100) and 4-yr (Q4) events and (b) 20-yr (Q20) and 3-yr (Q3) events, and their respective trend lines fitted to the time series. The red line arrows within the respective panels are showing an increase in the frequency of peak flows (e.g., the magnitude of the 100-yr event at the beginning of the time series has become the magnitude of the 4-yr event over 50 years historic disturbance for the Bowron River).

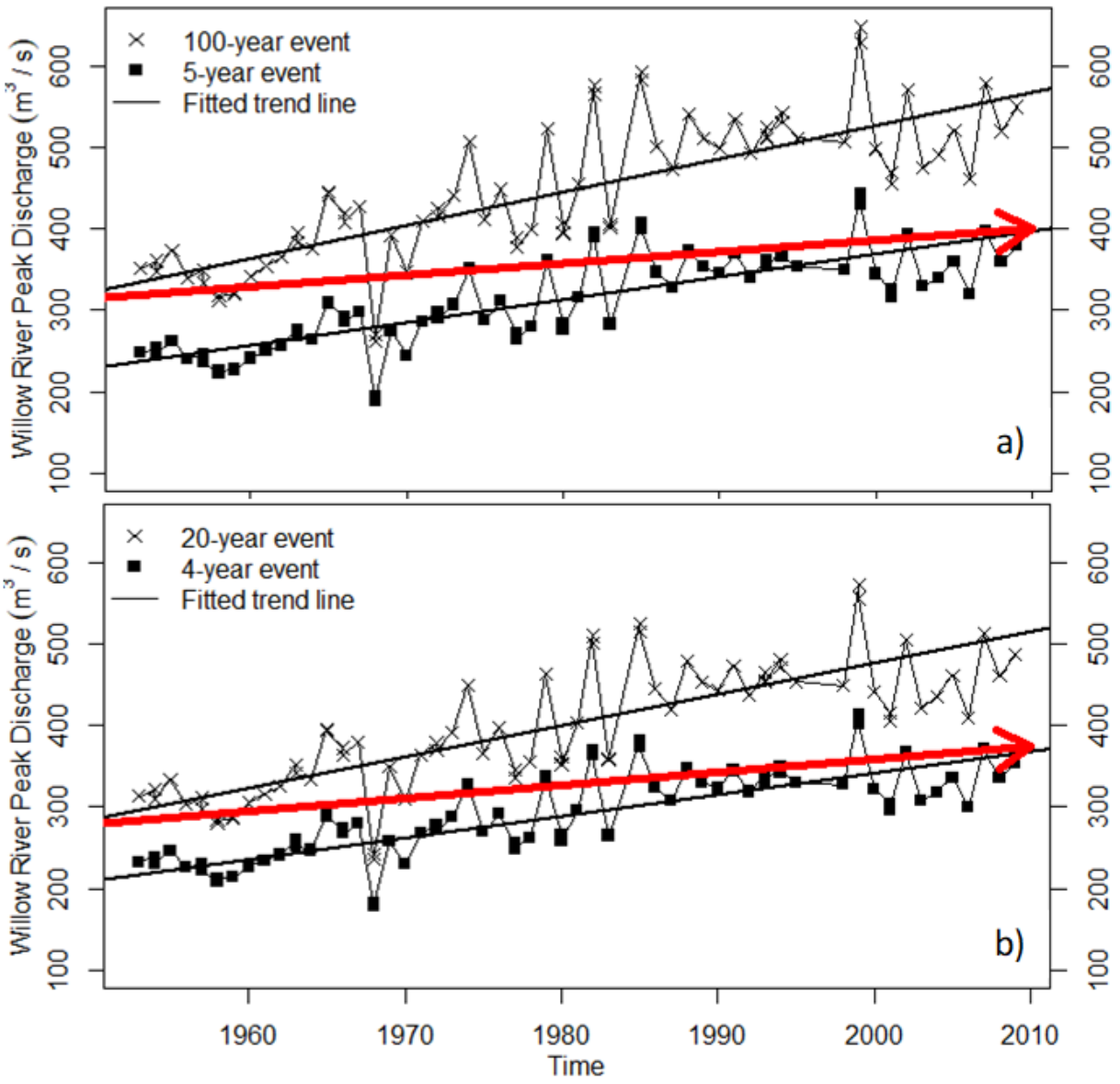

Figure 29: The estimated peak flow magnitudes of (a) 100-yr (Q100) and 5-yr (Q5) events and (b) 20-yr (Q20) and 4-yr (Q4) events, and their respective trend lines fitted to the time series. The red line arrows within the respective panels are showing an increase in the frequency of peak flows (e.g., the magnitude of the 100-yr event at the beginning of the time series has become the magnitude of the 5-yr event over 50 years historic disturbance for the Willow River).

A snapshot comparison of pre- and post-harvest FFC, at any one time in the disturbance history, can be used to quantify the effects of forest harvesting on peak flow frequency (and magnitude). The FFCs for Bowron River and Willow River are shown in Figure 30 and Figure 31, respectively. The corresponding cut block distributions are shown in Figure 32. The estimated peak flow magnitudes and frequencies were derived from GPD, with fixed SWE and warming rates (long-term averages), allowing only ECA to vary. Therefore, the difference between FFCs was a result of varying forest disturbance conditions. The effects of forest harvesting are summarized in Table 19 and Table 20, for Bowron River and Willow River, respectively. The peak flow quantiles, ranging from 2-yr to 100-yr, were predicted by the TM7 frequency model. The 10% and 22% ECA levels were arbitrarily selected for illustrative purposes. At 22% ECA, large peak flows such as 20-yr, 50-yr, and 100-yr events under forested conditions became events with less than a 5-yr return period. The magnitude had increased by 27% to 40% for Bowron River (Table 19), and 42% to 55% for Willow River (Table 20), for peak flow events ranging from 2-yr to 100-yr. At 10% ECA, large events (20-yr, 50-yr, and 100-yr) become events with less than a 10-yr return period for both watersheds, as a result of an increase in magnitude ranging from 12% to 18% (19% to 25%) at Bowron River (Willow River). The percentage increase in peak flow magnitude was higher at Willow River than Bowron River (Table 19 and Table 20), which is consistent with the effects predicted by the return plots above.

The 95% CI of the forested FFC intersected the 22% ECA FFC at about a 30-yr return period for Bowron River. This illustrates the detection limit, as per the null hypothesis testing at the subjectively selected significance level (0.05), would be at about the 30-yr event, given 22% ECA and sample size of 75 POT events. The upper tail of the Bowron River FFC (>20-yr) was steepened as a result of a larger uncertainty in estimating the larger peak flows of given record

length. For Willow River, the 95% CI of the forested FFC resembles the 10% ECA FFC. Therefore, forest harvesting effects beyond 10% ECA can be statistically detected, as per the null hypothesis testing, based on a sample size of 77 POT events.

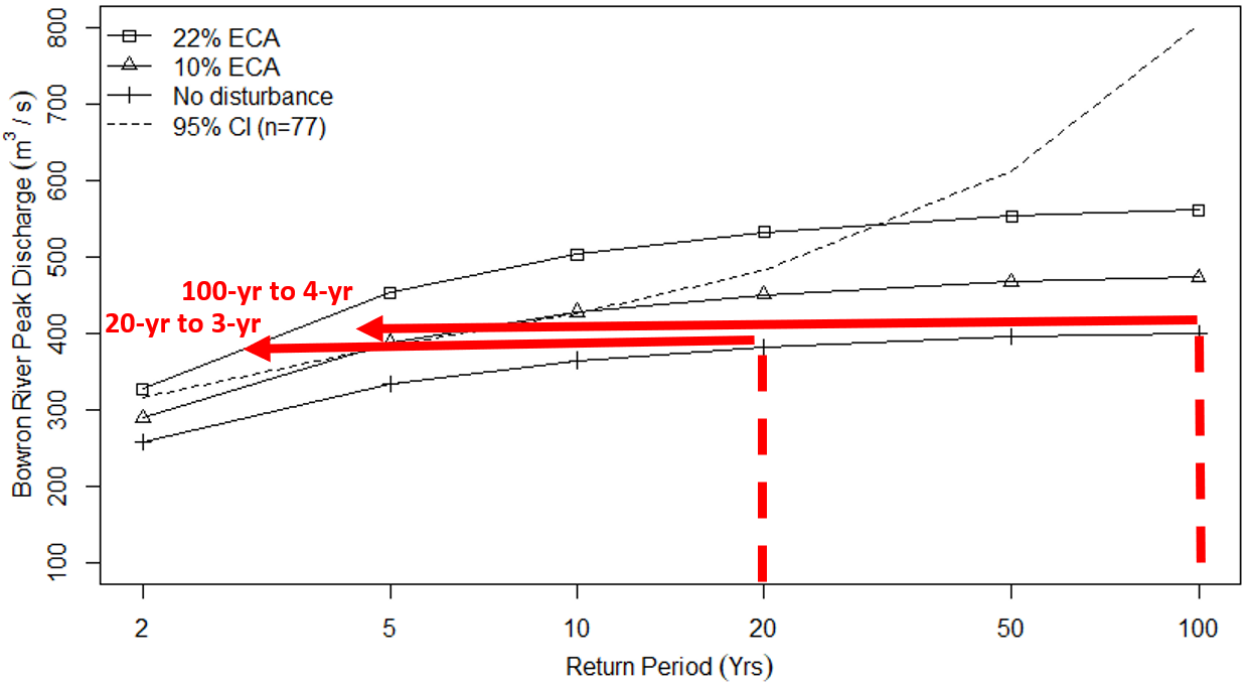

Figure 30: Flood frequency curves representative of 22%, 10% ECA levels, and no harvesting conditions for the Bowron River. The vertical dashed lines indicate the magnitudes of large peak flows (i.e., Q20 and Q100) under the no disturbance condition. The red line arrows demonstrate the effects on return periods of these large events as a result of harvesting at a 22% ECA.

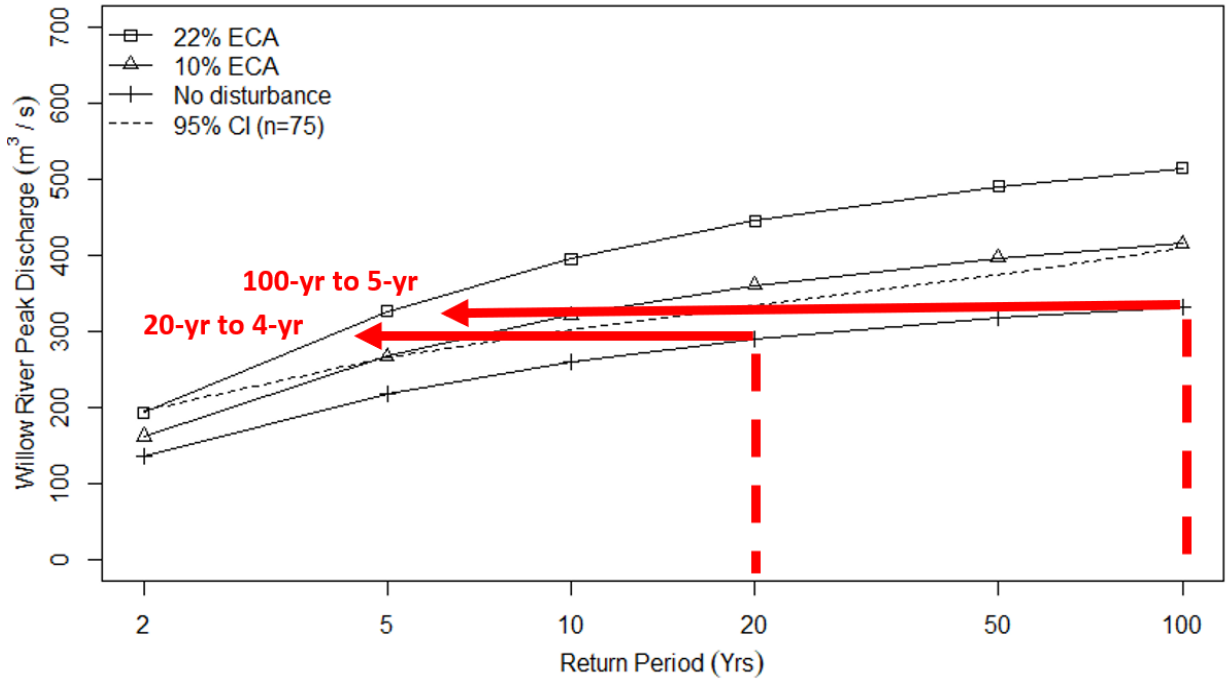

Figure 31: Flood frequency curves representative of 22%, 10% ECA levels, and no harvesting conditions for the Willow River. The vertical dashed lines indicate the magnitudes of large peak flows (i.e., Q20 and Q100) under the no disturbance condition. The red line arrows demonstrate the effects on return periods of these large events as a result of harvesting at a 22% ECA.

Table 19: Magnitude of peak flows of various return periods predicted by TM7 frequency model for control (ECA=0) and treatment (ECA=10% and 22%) scenarios for the Bowron River, with % change in comparison to control provided in parenthesis.

Return period (years)	Magnitude (m^3/s)		
	Control	10% ECA	22% ECA
2	257.32	288.88 (12%)	326.80 (27%)
5	334.03	388.01 (16%)	452.86 (36%)
10	364.64	427.57 (17%)	503.17 (38%)
20	382.43	450.56 (18%)	532.40 (39%)
50	395.06	466.88 (18%)	553.16 (40%)
100	400.10	473.40 (18%)	561.44 (40%)

Table 20: Magnitude of peak flows of various return periods predicted by TM7 frequency model for control (ECA=0) and treatment (ECA=10% and 22%) scenarios for the Willow River, with % change in comparison to control provided in parenthesis.

Return period (years)	Magnitude (m^3/s)		
	Control	10% ECA	22% ECA
2	135.67	161.64 (19%)	192.74 (42%)
5	217.32	266.92 (23%)	326.50 (50%)
10	259.55	321.37 (24%)	395.63 (52%)
20	290.07	360.72 (24%)	445.58 (54%)
50	317.83	396.51 (25%)	491.02 (54%)
100	332.18	415.02 (25%)	514.52 (55%)

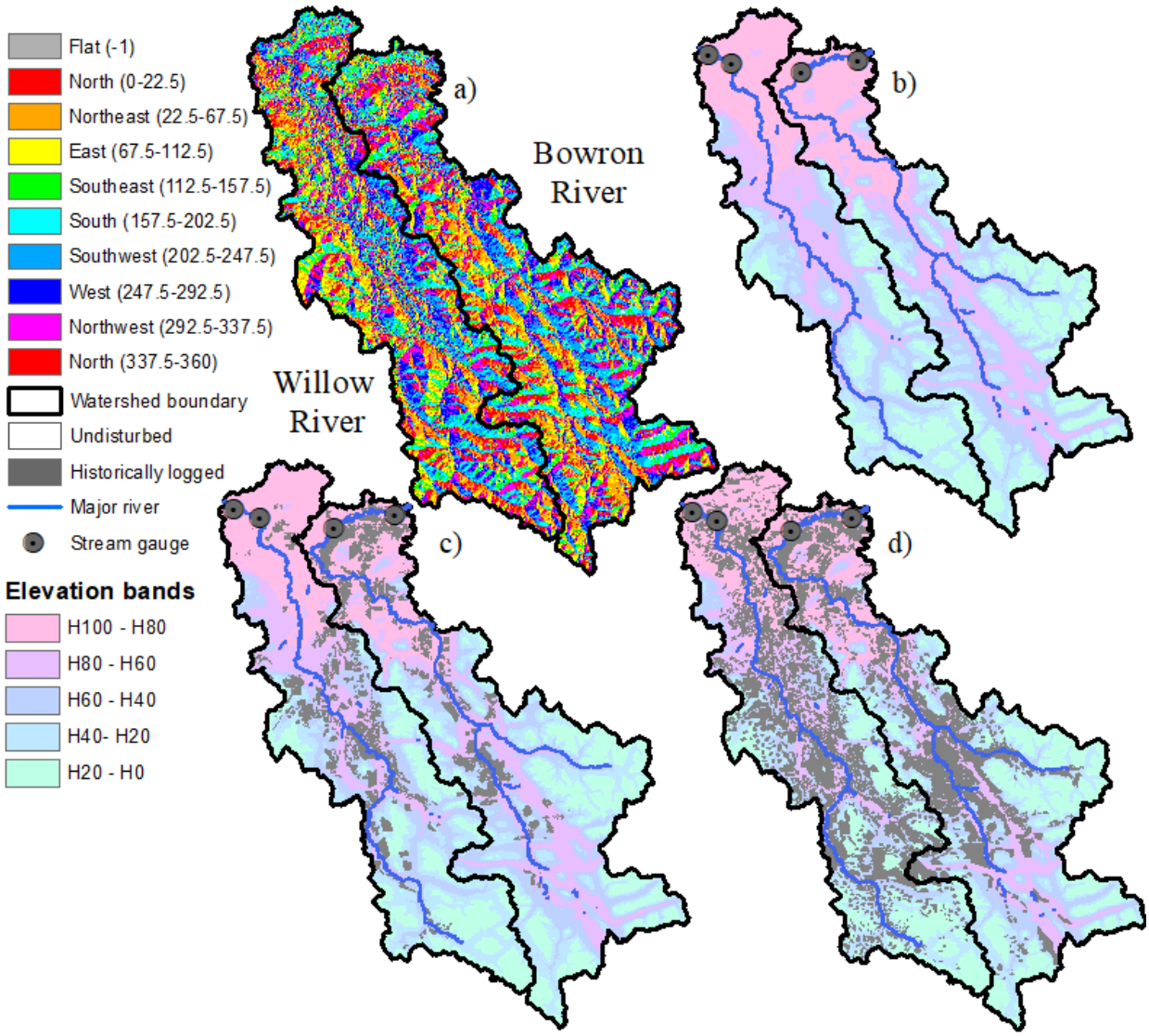

Figure 32: Hypsometric elevation contours of the Bowron River and Willow River watersheds in relation to (a) aspect distribution, at (b) no logging, (c) 10% ECA, and (d) 22% ECA conditions.

Chapter 5: Discussion

5.1 Understanding the physics of peak flows in a nonstationary stochastic framework

5.1.1 Forest harvesting effects on stand-level processes

Under both forested and harvested conditions, peak snow accumulation (SWE) appears to be the dominant climate covariate for the location parameter of the GEV distribution of Camp Creek, Mather Creek, and Baker Creek. The location parameter is a function of the mean of the peak flow frequency distribution, which can be interpreted as the peak flow event with an approximate 2-yr return period (Q2). The relationship between Q2 and snow accumulation has been implied in the regional flood frequency analysis literature. This type of analysis is often used to estimate the magnitude and frequency of peak flows in ungauged watersheds, using regression analysis to relate watershed and climate characteristics to peak flows. For example, drainage area is highly correlated to the volume and rate of precipitation falling on the watershed (Benson, 1964). Drainage area is the dominant predictor for all 50 states in the United States (US) and in some cases the only predictor in the regression equations (Jennings et al., 1994). In addition, mean annual snowfall is the dominant predictor of peak flows for snow-dominated states such as Vermont and Wisconsin (Jennings et al., 1994). Mean watershed elevation, a surrogate of soil moisture input from rain or snow, depending on climate (Gupta and Dawdy, 1995), is the dominant predictor for snow-dominated states, such as New Mexico (Waltemeyer, 1986) and Utah (Thomas and Lindskov, 1983). A recent study revealed the strong relationship between peak snow accumulation and annual peak flows in snow-dominated watersheds across a range of spatial scales in British Columbia (Curry and Zwiers, 2018). Whether it be drainage area, annual precipitation, annual snowfall, or mean watershed elevation, these predictors

represent the direct (e.g., precipitation) and indirect (e.g., drainage area) soil moisture input that is potentially contributing to peak flows.

Temperature and warming rates were significant predictors of peak flows in the nonstationary modelling results of Camp Creek, Bowron River, Willow River, and McGregor River. The outcomes were in line with the findings of Green and Alila (2012) and Curry and Zwiers (2018). The modelling results showed that peak flows under harvested conditions are more related to temperature and warming rates, than those generated under forested conditions. For Greata Creek, this was shown in the improvement made by using temperature as a covariate for only the location parameter. For Camp Creek, temperature appeared to be a significant covariate for both distribution parameters. Warming rates were significant climate covariates for Bowron River and Willow River, but not their control watershed McGregor River (Table 16-18). Based on the well-established understanding of energy balance in relation to harvesting, it is reasonable to expect peak flows generated under harvested conditions to be more sensitive to temperature. In continental snow environments, peak flows are primarily generated as a result of snowmelt, which is largely driven by radiative energy (US Army Corps of Engineers, 1956). Even though both forested and harvested watersheds receive the same source of radiation from the atmosphere, the presence of forest cover can alter the form of energy. The accumulated snow receives different total amounts of energy for snowmelt under forested and harvested conditions. For instance, under harvested conditions, the dominant energy source generating snowmelt is shortwave irradiance, whereas under forested conditions canopy extinction reduces shortwave irradiance by reflection and absorption (Ellis and Pomeroy, 2007; Link and Marks, 1999a). While shortwave irradiance is reduced by the canopy, the effects of heating increase as a result of increasing longwave irradiance from thermal emission off the branches, foliage, and tree

trunks (Black et al., 1991). As a result, longwave radiation becomes the dominant source of energy for snowmelt under forested conditions. Hence, the significant relationship found between warming rates and the peak flows of the large treatment watersheds. The total amount of energy acting on the snowpack contributed primarily by shortwave irradiance is generally higher under harvested conditions than forested conditions, especially on south-exposed slopes (Ellis et al., 2011). At Camp Creek, for instance, since harvesting occurred mostly on south-exposed slopes (Figure 21), the peak flows generated under harvested conditions are expected to be more sensitive to temperature input than those generated under forested conditions.

Precipitation, in the form of rain during the days leading to the peak of the melt season hydrograph, was found to be a significant climate covariate for the peak flows of McKale River, Mather Creek, and Fry Creek. There are several interesting patterns between precipitation and peak flows, in relation to watershed location and size.

Firstly, it is interesting how the nonstationary frequency modelling was able to detect some relation between precipitation and peak flows, because the majority of peak flow events are primarily generated as a result of snowmelt, largely driven by net shortwave radiation (US Army Corps of Engineers, 1956). However, some peak flows can be affected by precipitation events in the form of rain via their contributions to snowmelt energy and moisture input. These precipitation events in BC's interior are mostly convective, where the moisture availability and amount of surface heating determine the duration and intensity of the precipitation event (Eaton and Moore, 2010). Convective precipitation events are usually of short duration (less than a day), high volume, high intensity, and localized (less than 30 km^2) (Borga et al., 2008). When temperatures are above freezing, these precipitation events can occur in late spring through early fall.

Secondly, a relationship between precipitation and peak flows was found in three watersheds, which are all located on the windward side of the Rocky Mountain Range (Figure 6), where annual precipitation is higher than the watersheds located in BC's interior. (e.g., Schnorbus et al., 2010 Figure 6 p. 7). The air mass derived from the Pacific Ocean ascends and releases moisture on the western slopes of the Coastal Mountains (of BC), so the leeside (BC's interior) receives little moisture from the air mass and has some of the driest climates within the entire province. As the air masses move farther eastward in the province, they reach the Rocky Mountain Range and release some additional moisture on the windward side of the Rocky Mountains (Eaton and Moore, 2010), where the Mather Creek-Fry Creek pair is located. Therefore, extra moisture arriving in the form of convective events in the area, in addition to the existing snow accumulation and melt, can increase the likelihood of precipitation affecting the peak flow events.

Lastly, the signal between precipitation and peak flows in the three watersheds is reduced with increasing watershed size. For instance, the relationship between precipitation and peak flows is: (i) significant via both distribution parameters of the peak flow frequency distribution at 0.05 significance levels at Mather Creek (133 km^2); (ii) significant via only one parameter at McKale River (353 km^2); and (iii) only weakly significant via one parameter at Fry Creek (585 km^2). As watershed size increases, it is more likely to catch the localized convective precipitation events affecting the peak flows. However, the signal between precipitation and peak flows can be reduced and eventually lost in larger watersheds (Baker Creek, 1564 km^2). Given the relatively small size of the convective rain cells, the moisture contribution from the precipitation event is reduced relatively, as watershed size increases. The amount of moisture brought by precipitation can be relatively small in comparison to the amount of snowmelt (Macdonald and Hoffman,

1995). This rational remains speculative as precipitation measured by nearby weather stations may not accurately represent the contribution to the peak flows with increasing watershed size. There is often a shortage of weather stations in large watersheds to provide adequate spatial coverage of the localized precipitation events (Macdonald and Hoffman, 1995).

Forest harvesting can affect the mass and energy balance in snowmelt events affected by precipitation, causing peak flows to be more sensitive to energy inputs in the open conditions. In a typical liquid precipitation event occurring during snowmelt, due to conditions brought by overcast and often considerable wind speeds, shortwave radiation becomes less important while turbulent heat exchange becomes the dominant form of the snowmelt energy balance (Berris and Harr, 1987; Harr, 1981; Marks et al., 1998; Pomeroy et al., 2016). Marks et al. (1998, 2001) and Mazurkiewicz et al. (2008) have repeatedly found that 54% to 90% of the snowmelt energy came from turbulent heat exchanges[1] associated with saturated air conditions and dew point temperatures above 0°C. Forest cover can have counteracting effects on both mass and energy by intercepting precipitation in the canopy and by reducing the amount of turbulent heat exchange by reducing wind speed via canopy extinction (Ellis and Pomeroy, 2007; Link and Marks, 1999a). Increased wind speeds in open areas during precipitation events can increase the amount of turbulent heat exchange at the snow surface. The snowmelt in open areas can be significantly greater than in forested areas (Marks et al., 1998). Turbulent energy accounts for 67% to 72% of the total energy for snowmelt in open areas, while only accounting for 32% to 47% under forested conditions (Garvelmann et al., 2014). Similar patterns were found by Berris and Harr

[1] The components of turbulent heat exchange are: (i) sensible heat which is the amount of convective heat transfer at the snow-air interface, and (ii) latent energy flux which is a result of evaporation, condensation, or sublimation driving more rapid snowmelt during precipitation events (Mazurkiewicz et al., 2008).

(1987), where the total energy available in open areas was 40% greater than in forested areas. Their measured water outflow, which included both precipitation and snowmelt generated flows, was 21% greater in the open area than in the forested area. Marks et al. (1998) also found that high temperature, humidity, and relatively high wind speeds in open areas, accounted for 60% to 90% of the energy for snowmelt derived from the turbulent heat exchange. Therefore, when liquid precipitation falls on a melting snowpack peak flows generated in treatment watersheds can be more sensitive to changes in energy inputs than those generated under forested conditions.

Two features should be highlighted while interpreting the relationship between climate covariates and the frequency distribution parameters. Different combinations of climate covariates were found to be related to different distribution parameters (location vs. scale), with the patterns changing between open and forested conditions. The climate covariates can be related to both distribution parameters. However, parsimony and computational difficulty limited the number of covariates used in the nonstationary analysis. As a result, only one or two climate covariates were included in the final fitted model. Despite the fact that SWE was found to affect the location parameter, as a surrogate of the moisture contribution to the peak flows, SWE was also related to the scale parameter. However, in some cases, SWE was excluded from the final GEV fitted model because temperature was a better covariate than SWE for the scale parameter for physically meaningful reasons.

In addition, SWE appears to be the dominant climate covariate for the location parameter of the GEV, while also being the dominant covariate for the scale parameter of the GPD. There are three parameters associated with the GEV distribution (location, scale, and shape), while the GPD distribution is associated with only two parameters (scale and shape). Direct evaluation between the location parameter of GPD and climate covariates is limited. The threshold of the

GPD is perhaps analogous to the location parameter of the GEV in defining the frequency distribution. However, such an evaluation between the threshold and climate covariates is beyond the scope of the current research.

5.1.2 Linking stand-level processes to watershed level responses to forest harvesting

5.1.2.1 Camp Creek

Despite the complexity of the hydro-meteorology and related space-time heterogeneity revealed by decades of reductionist and deterministic mass and energy balance studies at the smaller plot and hillslope scales (Sivapalan, 2003), the effect of removing trees appears to have a recognizable and rather predictable signal in the statistical characteristics of peak flows for all watersheds. ECA levels of (i) 11%, (ii) 17%, and (iii) 24% at Camp Creek resulted in (i) 14% and 5%, (ii) 21% and 7%, and (iii) 31% and 10% increases in the means and standard deviations of sample peak flows, respectively. The combination of forest stand hydrologic processes and watershed spatial integration of such processes can explain these effects on peak flows at Camp Creek. The higher effects on the mean than the standard deviation of the frequency distribution are consistent with the outcomes of the stationary FP analysis of the same post-harvest peak flow data, conducted at the same paired watershed study site by Green and Alila (2012).

To explain the treatment effects on the peak flow frequency distribution, Green and Alila (2012) hypothesized that an increase in the mean of the peak flows was a result of an increase in soil moisture input, while an increase in peak flow variability around their mean (measured by the standard deviation) was caused by an enhancement of snowmelt synchronization at the watershed level. The findings of Camp Creek further support the concept that the mean and variability around the mean of peak flows are dominantly related to the soil moisture input and snowmelt synchronization, respectively. Forest harvesting can indeed increase the overall moisture input contributing to peak flows by increasing the snowmelt energy due to a transition from longwave- to shortwave-dominated snowmelt (see Subsection 5.1), and increasing the amount of snow accumulation via the reduction of canopy interception and sublimation

processes. Seasonal loss of the total annual snowfall from interception and sublimation measured at the stand level can be as high as 31% for mature pine stands and 40% for mature spruce stands (Pomeroy et al., 1998). Therefore, an increase in snow accumulation associated with forest harvesting is not uncommon in snow environments (Varhola et al., 2010b). It is reasonable to expect an increase in the mean of peak flow frequency, in association with an increase in overall moisture input contributing to peak flows caused by forest harvesting in snow environments.

The inherent catchment physiography of Camp Creek, in addition to the locations of forest harvesting, can further explain the physical processes of an increase in peak flow variability. The dominant aspect of Camp Creek is largely south-exposed; this makes the snowmelt of Camp Creek dominated by shortwave irradiance and sensitive to energy input (e.g., Ellis et al., 2011; Musselman et al., 2015; Pomeroy et al., 2008; Sicart et al., 2004), as previously explained. The relation between an increase in shortwave irradiance and forest removal locations is more pronounced on south-facing slopes than on north-facing slopes. This is because there is a larger amount of shortwave irradiance acting on the south-facing slopes (Ellis et al., 2011). Therefore, forest harvesting in the Camp Creek watershed resulted in an increase in snowmelt synchronization that translated into an increase in the variability of peak flows. However, the locations of forest harvesting may have mitigated some of the synchronization of snowmelt at the spatial scale, leading to a smaller increase in the peak flow variability than the mean in the post-harvesting period. There was a concentration of harvesting occurring in the mid-elevations of Camp Creek between 1200 m and 1500 m, or the middle third of the catchment between H40 and H60 elevation contours (Table 21). There was a further concentration of harvesting occurring on the southeast-facing portion of the watershed, while the southwest aspect is mostly unlogged. Such logging patterns can create a difference in the timing of snowmelt along elevation gradient

and within elevation band (Ellis et al., 2013; Schnorbus and Alila, 2013), or in vertical and horizontal orientations (Figure 21). It is expected that the concentration of forest harvesting occurring in mid-elevation, south-exposed landscapes, could break down the spatial synchronization of snowmelt at Camp Creek. As a result, the snowmelt de-synchronization can mitigate some of the effects associated with peak flow variability. This could explain the lower effects associated with the variability than with the mean in relation to forest harvesting at Camp Creek (Green and Alila, 2012).

Table 21: Percentage of Camp Creek watershed harvested historically at different elevations.

Time / Elevation	1968-1977	1978-1979	1980-2012	Total	
	<11% ECA	11%-17 % ECA	17%-22% ECA		
H0 - H20	0%	0%	6.7%	6.7%	27.2%
H20 - H40	0.2%	0.4%	8.3%	8.9%	
H40 - H60	4.2%	2.5%	4.9%	11.6%	
H60 - H80	5.4%	1.9%	2.3%	9.6%	13.9%
H80 - H100	2.4%	1.5%	0.4%	4.3%	
Total	12.2%	6.3%	22.6%	41.1%	

5.1.2.2 Mather Creek and Baker Creek

ECA levels of 10% and 22% at the Mather Creek watershed resulted in a 16% and 35% increase in the means, respectively, and no effects on the standard deviations of sample peak flows. There are several features of the Mather Creek watershed that reduced spatial synchronization of snowmelt at the watershed level, which limited forest harvesting effects on peak flow variability. The lower 50% of Mather Creek drains southward, with an average slope of less than 20%. The upper 50% of the watershed is more mountainous, drains eastward, and has a higher average slope of more than 30% (Figure 33). There is also a diverse aspect distribution at Mather Creek (Figure 33) that further limits snowmelt synchronization. Snowmelt can occur at different times, due to different amounts of energy acting on slopes facing different aspects (Ellis et al., 2011; López-Moreno et al., 2013; Seyednasrollah and Kumar, 2013). There was no concentration of logging on specific aspects because of the diverse aspect distribution of the watershed. The concentration of logging located primarily below the H50 elevation can also limit snowmelt synchronization throughout the elevation ranges, suppressing peak flow variability (Table 22). Therefore, the topographic features of the watershed and logging patterns are both leading to a de-synchronization of snowmelt, making it reasonable to expect little to no effect associated with peak flow variability at Mather Creek.

It is interesting to compare results from Camp Creek (the mean and variability have increased by 31% and 10%) and Mather Creek (35% increase in the mean with no change in variability), when both watersheds have similar ECA levels and similar patterns of effects on the mean and variability. Both Camp Creek and Mather Creek have logging patterns that can limit snowmelt synchronization. The difference between the two watersheds is that Camp Creek is a sensitive watershed (primarily south-exposed) while Mather Creek is inherently less sensitive

from its unique topographic features (upper and lower halves drain to different directions and have different slopes). Camp Creek produced a 10% increase in variability with harvesting patterns that limit snowmelt synchronization. It is reasonable to expect little or no effect on the peak flow variability associated with Mather Creek, especially when both the topography and logging locations are expected to limit snowmelt synchronization. Lastly, the effects on the peak flow variability brought by forest harvesting appear to be the lowest for Mather Creek and Camp Creek amongst the five pairs of watersheds. Interestingly, these two watersheds happen to have the lowest stream densities, which can limit the delivery efficiency of snowmelt runoff, and hence the effects on peak flow variability. The Camp Creek and Mather Creek outcomes derived from nonstationary frequency modelling are consistent with previous stationary FP research, based on the same line of reasoning concerning physical processes (Green and Alila, 2012).

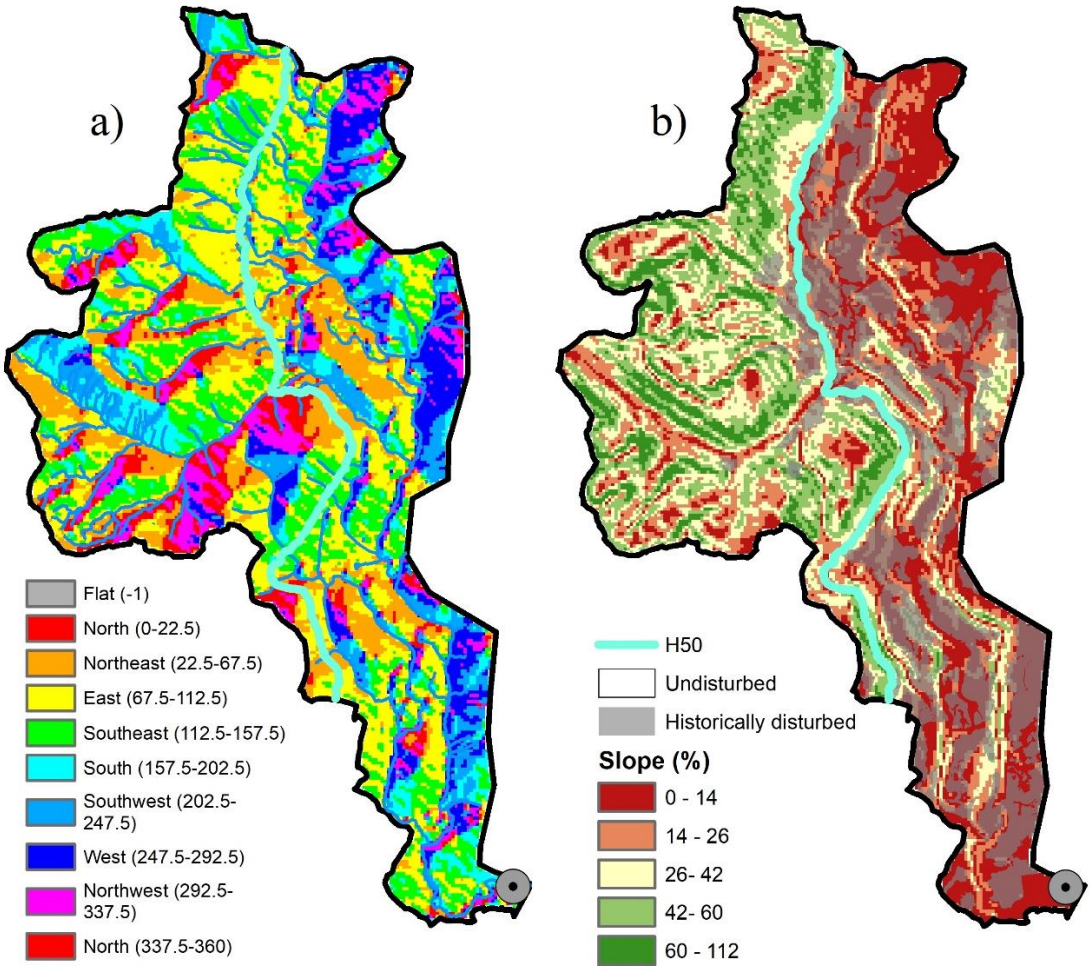

Figure 33: The aspect distribution (panel a) and average slope (panel b) of Mather Creek watershed.

Table 22: Percentage of the Mather Creek watershed harvested historically at different elevations.

Time / Elevation	1973-2007	2008-2014	Total	
	<10% ECA	10%-22% ECA		
H0 - H20	0%	0%	0%	7.09%
H20 - H40	0.47%	0.46%	0.93%	
H40 - H60	1.92%	4.24%	6.16%	
H60 - H80	3.85%	5.00%	8.85%	17.13%
H80 - H100	6.26%	2.02%	8.28%	
Total	12.50%	11.72%	24.22%	

At Baker Creek, ECA levels of (i) 10%, (ii) 20%, (iii) 30%, and (iv) 37% resulted in (i) 31% and 30%, (ii) 61% and 58%, (iii) 92% and 86%, and (iv) 113% and 110% increase in the means and standard deviations of sample peak flows. Forest harvesting at Baker Creek resulted in the highest treatment effects amongst the five pairs of watersheds. This was due to the high levels of logging, evenly distributed in a subdued watershed (Table 23). Such logging levels and patterns promote snowmelt synchronization. The subdued topography, low elevation, and plateau-like nature in most of Baker Creek allowed snowmelt to occur simultaneously at different locations of the watershed. The peak flows of Baker Creek can be sensitive to harvesting at any particular location given the inherent subdued topography. It was shown by Bewley et al. (2010 Figure 3 p. 471) that despite snow accumulation over time exhibiting different patterns in time at different locations, there was a uniformity in snowmelt because of the low relief and subdued topography of the watershed. The subdued topography of Baker Creek, compared to the more diverse and mountainous terrain in Mather Creek, can also reduce the amount of natural shading offered by the landscape. The inherent circularity of Baker Creek (rounded shape) adds to the sensitivity to forest harvesting. Due to drainage network geometry and streamflow aggregation (Gupta et al., 1980; Rinaldo et al., 1995), watersheds with greater basin circularity can increase the efficiency of runoff delivery to the main channel more so than in watersheds with other shapes (Ayalew and Krajewski, 2017). Baker Creek is a sensitive watershed to harvesting due to its inherent physiographic features in addition to high logging rates, all of which further exacerbate snowmelt synchronization in the watershed.

Table 23: Percentage of Baker Creek watershed harvested historically at different elevations.

Time / Elevation	1964-1994	1995-2005	2006-2009	2009-2012	Total	
	<10% ECA	10%-19% ECA	19%-29% ECA	29%-37% ECA		
H0 - H20	3.24%	2.43%	3.72%	2.02%	11.41%	34.76%
H20 - H40	3.59%	2.33%	2.73%	2.84%	11.49%	
H40 - H60	2.99%	4.24%	2.61%	2.02%	11.86%	
H60 - H80	2.68%	3.32%	1.57%	1.67%	9.24%	13.49%
H80 - H100	0.88%	1.48%	0.89%	1.00%	4.25%	
Total	13.38%	13.80%	11.52%	9.55%	48.25%	

5.1.2.3 Bowron River and Willow River

At Bowron River, the mean and standard deviation of peak flows were increased by (i) 13% and 28%, and (ii) 28% and 65%, at the 10% and 22% ECA levels, respectively. At Willow River, the mean and standard deviation of peak flows were increased by (i) 20% and 29%, and (ii) 43% and 64%, also at the 10% and 22% ECA levels, respectively. Given the same levels of peak ECA, the difference in treatment effects could be related to different physiographic features of the two large watersheds. Similar to Baker Creek, forest harvesting resulted in higher effects on the variability than the mean of peak flows at both Bowron River and Willow River, owing to the concept of snowmelt synchronization. A cross-comparison of the physiography with Baker Creek and Camp Creek can be used to physically explain the effects on the mean and variability of peak flows at Bowron River and Willow River.

Bowron River and Willow River were sensitive to forest harvesting due to both topographic features and logging locations. The topographies of the lower elevation terrain of Bowron River and Willow River watersheds are just as subdued if not more so than those found at the Baker Creek watershed. For areas below the H60 elevation contours, where the majority of logging occurred, the average slopes for Bowron River and Willow River were only 11.5% and 7.4%, respectively. For comparison, the average slope for the Baker Creek watershed was 9%

(Table 2). The plateau-like topography of the Baker Creek watershed contributed to the substantial hydrologic effects; having similar features for the Bowron River and Willow River watersheds mean that they could be affected in similar ways. Therefore, the two large watersheds could be just as sensitive to logging as the Baker Creek watershed, especially when the logging was concentrated on subdued topography, conducive to lesser amounts of shade provided by the landscape. In addition, cut blocks for both large watersheds are predominantly southwest-facing, similar to Camp Creek. South-facing aspects are the most sensitive to incoming shortwave radiative energy.

Although the Bowron River and Willow River watersheds are both sensitive to logging, they exhibit different treatment effects at the same ECA levels. As shown in Table 24 and Table 25, where historic forest harvesting is categorized by elevations, there has been more logging at Willow River than Bowron River, especially in high elevation bands. By the time both watersheds reached a 10% ECA level, the majority of harvesting in the Bowron River watershed had occurred at the lowest elevations. The same amount of forest harvesting moved up to the H20 to H60 elevations in Willow River, which further exacerbated treatment effects. The trend of high elevation logging of Willow River is the most apparent when 20.55% of the Willow River watershed was logged above H60 (Table 25), while only 12.24% was logged at above that elevation on Bowron River watershed (Table 24). Interestingly, the difference in topographic features can also explain the different treatment effects, especially the mean of the peak flows. The area composed of 20% of the highest elevation is located about 300 m higher in the Bowron River watershed than it is in the Willow River watershed. The higher elevation in the Bowron River watershed received little logging. The snowmelt in the upper 20% of the Bowron River watershed can perhaps mitigate some potential effects associated with forest harvesting.

Schnorbus and Alila (2004a) hypothesized that the upper 40% of the Redfish Creek watershed (an area with non-merchantable forests), where the timing and magnitude of snowmelt are largely unaffected by logging, can provide a substantial source of soil moisture input to the peak flows during the freshet, and mitigate the effects of logging in the lower 60% of the watershed.

Table 24: Percentage of the Bowron River watershed harvested historically at different elevations.

Time / Elevation	1955-1982	1983-1984	1985-2012	Total	
	<10% ECA	10%-17% ECA	22%-18% ECA		
H0 - H20	0%	0.29%	0.21%	0.50%	12.24%
H20 - H40	0.32%	0.75%	2.45%	3.52%	
H40 - H60	2.22%	2.66%	3.34%	8.22%	
H60 - H80	2.48%	3.41%	1.94%	7.83%	16.53%
H80 - H100	6.25%	0.26%	2.19%	8.70%	
Total	11.27%	7.37%	10.13%	28.77%	

Table 25: Percentage of the Willow River watershed harvested historically at different elevations.

Time / Elevation	1955-1979	1980 - 1995	1996-2012	Total	
	<10% ECA	10%-22% ECA	~22% ECA		
H0 - H20	0.36%	1.56%	0.71%	2.63%	20.66%
H20 - H40	1.81%	4.73%	1.26%	7.80%	
H40 - H60	4.62%	4.45%	1.16%	10.23%	
H60 - H80	4.38%	2.23%	2.28%	8.89%	14.04%
H80 - H100	0.79%	2.47%	1.89%	5.15%	
Total	11.96%	15.44%	7.3%	34.7%	

5.2 A meta-analysis using the nonstationary FP method reveals a highly sensitive peak flow regime to harvesting

The application of the nonstationary FP method reveals a highly sensitive peak flow regime to forest harvesting, albeit to different degrees in each of the five treatment watersheds. There are several aspects to such sensitivity:

(i) An increase in the magnitude and frequency of peak flows across not only small and medium (return periods < 10-yr) but also the large events (return periods > 10-yr).

(ii) In absolute terms, there was an increase in the effect on the magnitude and frequency of peak flows with an increase in event size.

(iii) At the 20% ECA level, large peak flows became 3 to 4 times more frequent in Mather Creek, but 10 to 20 times more frequent in Baker Creek. This is due to contrasting watershed physiographies and forest disturbance regimes.

(iv) There was no apparent threshold event size beyond which forest harvesting had no effect on the magnitude and frequency of peak flows.

(v) Peak flows were sensitive to even small ECA levels. For instance, at Camp Creek, although an ECA of 11% caused a 9-14% increase in the magnitude, all peak flows have approximately doubled in frequency.

(vi) Both small and large watersheds were affected by logging. Forest harvesting continues to impact peak flows as catchment size increases, as evident from Camp Creek (37 km^2) to Baker Creek (1564 km^2) and Bowron and Willow Rivers (>3000 km^2).

How plausible is such a high sensitivity? Especially when predicted by frequency distribution models (e.g., TM16 for Camp Creek) fitted to only four to five decades, ranging from 42 years (Mather Creek) to 56 years (Willow River) of post-harvesting peak flow data at

the five treatment watersheds? Conceding to these results, especially as outcomes of a new method, is even more challenging because they run counter to the prevalent wisdom. Such conventional wisdom can be summarized in two points: (i) forest harvesting may affect small and medium peak flows, but should not affect the larger floods; and (ii) the larger the peak flow event the smaller the effect on such an event (e.g., Calder et al., 2007; DeWalle, 2003). This deeply entrenched precept is found in forest hydrology textbooks (e.g., Brooks et al., 2012; Calder, 2005; Chang, 2012; Jeffrey, 1970; Lee, 1980). Although it has been admitted that this is a long-held dogma predating experimentation and research in forest hydrology (DeWalle, 2003 p. 1255; Pinchot, 1903 p. 58), it has been reinforced by decades of CP-based paired watershed study literature (e.g., Bathurst et al., 2011a, 2011b; Beschta, 1978; Beschta et al., 2000; Hess, 1984; Jones, 2000; Moore and Scott, 2005; Moore and Wondzell, 2005; Rothatcher, 1973; Thomas and Megahan, 1998; Troendle and King, 1985; Wright et al., 1990). For instance, Moore and Scott (2005, p. 340) conducted a CP-based analysis of peak flows at the same Camp Creek-Greata Creek paired watershed study site used in this thesis and concluded:

> *"At Camp Creek, harvesting appeared to increase the smaller, more frequent peak flows, with little to no effect on larger peak flows."*

Alila et al. (2009), Alila et al. (2010), Green and Alila (2012), Alila and Green (2014a,b), Kuraś et al. (2012), and Schnorbus and Alila (2013) challenged the CP-based studies on methodological grounds and argued that their outcomes are irrelevant to how forest harvesting affects peak flows of all sizes, but especially the larger peak flows. From a physical perspective, the reasoning often used to support the conjecture that forest harvesting does not affect large floods, originally conceived for rain but later adopted to snow environments (Brooks et al., 2012;

Chang, 2012; Jeffrey, 1970; Lee, 1980; NRC, 2008), is best described by Macdonald and Stednick (2003, p. 13):

> *"During the largest rain or snowmelt events the soils and vegetative canopy will have little additional storage capacity, and under these conditions much of the rainfall or snowmelt will be converted to runoff regardless of the amount or type of vegetative cover."*

First, in the snow environments, such a physical explanation is incomplete and has been shown to conceal the true effects on the larger peak flows (Alila et al., 2009; Green and Alila, 2012; Kuraś et al., 2012; Schnorbus and Alila, 2013). Canopy snow interception and soil storage capacities are not the only nor the most dominant factors in controlling peak flows. The CP-based explanation also ignores the significant role of energy and snowmelt in the generation of peak flows. Second, because it is CP-based, such a physical explanation is reductionist and deterministic. The threshold size flood event beyond which forest harvesting has no effect can only be predicted and physically explained stochastically (i.e., within the frequency distribution or FP framework) (Alila et al., 2009; Alila and Green, 2014a, 2014b; Green and Alila, 2012).

DeWalle (2003, p. 1255) pointed out how "specific attention was often not given to extreme events" in CP-based literature. This was typically blamed on the short sample sizes of measured peak flows associated with paired watershed studies (e.g., Jones and Grant, 2001). However, recent stationary FP-based studies, which used 100 years of peak flows simulated by deterministic hydrologic models in snow environments, revealed how larger peak flows can be substantially affected by forest harvesting (Kuraś et al., 2012; Schnorbus and Alila, 2004a, 2013). Collectively, these studies illustrate how harvesting can increase the mean and the variability of the peak flow around their mean. This in turn translated into an upward shift of the

post-harvest FFC and a divergence of the upper tails of pre- and post-harvest FFCs, at least within the simulated record of 100 years of peak flows. Green and Alila (2012) conducted a meta-analysis of long-term measured and model-simulated peak flows at four study sites in snow environments using the stationary FP method. They demonstrated how the threshold event, beyond which forest harvesting has no effect on peak flows, shifts to larger return periods with an increase in sample size. The "no-effect" threshold shifted from a return period of 20-yr, to 50-yr, to over 100-yr, when the sample size increases from 19, to 48, to 95 years of post-harvest peak flow data, respectively. Therefore, the effects of harvesting on the magnitude and frequency of peak flows can increase unchecked with an increase in event size when evaluated using a FP framework (Kuraś et al., 2012; Figure 5 p. 9; Schnorbus and Alila, 2004a; Figure 9 p. 10; Schnorbus and Alila, 2013; Figure 6 p. 525). Other independent FP-based studies, published in the wider hydrology literature, have also demonstrated how forest cover changes affect small and large floods in small (<100 km^2) and large (>7000 km^2) watersheds in the snow (Du et al., 2016; Figure 7 p. 225; Kuchment and Gelfan, 2002; p. 84; Schnorbus et al., 2010; Figure 29 p. 37) and rain (Crooks and Davies, 2001; Figure 6 p. 591; Svoboda, 1991; Figure 5 p. 467; Reynard et al., 2001; Figure 5 p. 356; Zhang et al., 2012; Figure 5 p. 2115) environments. Typically, these FP-based studies have not been cited by mainstream forest hydrology literature, perhaps because their FP-based outcomes do not conform to the well-established CP-based presumption of how forests do not affect large floods.

As a standalone study, my predicted effects of forest harvesting on large peak flows using nonstationary frequency distribution models with only four to five decades of data are understandably uncertain. However, considered in the context of the consistently emerging patterns from the collective outcomes of other FP-based studies (e.g., taken in a meta-analysis

context), conducted with a wider range of record lengths, the effects of forest harvesting on large peak flows predicted in this thesis should be considered likely, and not a mere consequence of sampling variability. This is especially the case when such effects could be supported by reasonably sound physical understanding and when such effects would likely be associated with significant practical consequences. This is an argument repeatedly emphasized across disciplines when faced with a lack of statistical power in scientific research (Amrhein et al., 2019; Johnson, 1999; Kirk, 1996; Klemeš, 1974; Lewis et al., 2010; Lykken, 1968).

If the nonstationary frequency pairing model predictions of changes in magnitudes and frequencies at each treatment watershed are real, then how else could the physics of the effects of forest harvesting on large peak flows be explained? If the prediction of a system's response necessitates the use of the frequency distribution framework, which is the case for the effects of forests on peak flows, its physics can only be understood within the same probabilistic framework (Green and Alila, 2012; Alila and Green, 2014a, 2014b). A large untapped body of literature, on the probabilistic understanding of the forests and flood relations, albeit in small-sized watersheds, exists outside forest hydrology, pioneered by Eagleson (1972). Berris and Harr (1987, p. 141) hinted to the forest hydrology community as to how the peak flow regimes of watersheds with milder sloped flood frequency curves should be more sensitive to forest harvesting. While such a hint was lost in the midst of decades of CP-based literature, where the dimension of frequency is rarely invoked, similar and related constructs have guided research on climate and land-use change effects on hydro-climatological extremes outside forest hydrology (e.g., Allen and Ingram, 2002 and references therein). For instance, hydro-climatological extremes have been recognized as highly sensitive to small changes in the mean and variance of their frequency distributions caused by climate or land-use changes (Katz, 1993; Katz and

Brown, 1992; Schaeffer et al., 2005; Wigley, 1985, 2009). Allen and Ingram (2002, p. 230) pointed out how "[e]ven modest increases in the magnitude of events in the tails of the distribution can have a very substantial impact on the expected return times of events of a given magnitude." In relation to the research work covered in this thesis, flood frequency curves in mountainous snow environments generally have relatively mild slopes, in comparison to their rain or rain-on-snow counterparts (van Tol, 2016 and references therein). Flood frequency curves in larger watersheds have even milder slopes than smaller watersheds in the snow environment (Beckers et al., 2002; Blöschl and Sivapalan, 1997). Hence, the sensitivity to harvesting in large watersheds is further amplified. Such high sensitivity to harvesting in large watersheds was demonstrated for the first time in the forest hydrology literature, using the nonstationary FP framework in this thesis. This means that small changes in the magnitude of larger peak flow events cause surprisingly large jumps in their return periods. However, this also translates into the frequency of these same large events being substantively affected by even modest harvest-induced increases in energy and melt rates at the stand- and watershed-scale. This distinctive stochastic or statistical physics phenomena are exacerbated when harvesting occurred within the critical zone (Camp Creek watershed), on southwest-facing slopes (Bowron River and Willow River watersheds), and in subdued topography (Baker Creek watersheds). These explanations lend further support to a highly sensitive peak flow regime, predicted by the nonstationary FP method, in both small and large watersheds across small, medium, and most importantly large peak flows.

5.2.1 A proposed conceptual model featuring the meta-analysis research outcomes

The collective outcomes have shown that the mean of the peak flow frequency distribution has increased for all five treatment watersheds, while the variability of peak flows increased in four watersheds and remained unchanged in Mather Creek. The differences in the treatment effects of the five pairs are hinting to different levels of sensitivity of the peak flows to harvesting, owing to the different physical characteristics of the watersheds. Therefore, understanding the impact of physiography and forest disturbance regime differences on hydrologic effects can provide a holistic understanding of how forest harvesting may be affecting the flood regime across scales and locations. The generalizing principles, driven by the integrated meta-study type of understanding at the stand- and watershed-levels discussed below, are summarized and featured in a physical model (Figure 34a).

Forest removal increases stand-level SWE due to the suppression of interception. Melt rates are increased by transitioning from a longwave- to shortwave-dominated snowmelt. Hence, the orientation, elevation gradient, and canopy density of the cut blocks can affect the stand-level hydrologic responses to harvesting. For instance, cut blocks located on a steep or south-facing slope can receive more snowmelt energy than their counterparts on a subdued or north-facing slope (Ellis et al., 2011). Large effects on SWE and snowmelt energy is also expected in cut blocks with high canopy density (Sicart et al., 2004) and at high elevations (Schnorbus and Alila 2013). The resulting effects at the forest stand level can increase the average melt rates at the watershed level, which in turn causes an upward shift in the mean of the peak flow frequency distribution. As a result, the largest increase in the mean of the frequency distribution should be associated with the largest increase in net radiation. Hence, watersheds with small aspect distributions, steep slope gradients, and high stand density are inherently sensitive because these

facets can maximize incoming solar radiation. Forest harvesting effects on net radiation and melt rates can integrate in space, affecting the variability of the peak flow frequency distribution as well. The variability of peak flows is mostly affected by the processes of integration, such as snowmelt synchronization and the snowmelt runoff delivery to the stream channel. Therefore, the largest increases in peak flow variability are expected in watersheds with minimal elevation range, minimal aspect distribution, and high drainage density. In the proposed physical model (Figure 34), the gradient of the sensitivity of peak flows to harvesting, discussed below, is illustrated by featuring the outcomes of my nonstationary FP analyses conducted for treatment watersheds with contrasting physiographies and forest disturbance regimes.

Baker Creek, for instance, is the most sensitive watershed to harvesting amongst the five pairs, attributed to its plateau-like subdued topography. The difference in the timing of snowmelt generating peak flows across a large range of elevations is minimized in subdued terrain, allowing snowmelt to occur simultaneously. Furthermore, the Baker Creek watershed is circular in shape and characterized by a high stream density (Figure 6 and Table 2), which introduces additional sensitivity in its response to harvesting by efficiently delivering snowmelt runoff to the stream channel. In summary, snowmelt synchronization is maximized by the inherent watershed characteristics and the evenly distributed logging within the Baker Creek watershed. The high sensitivity has led to the highest treatment effects on both the mean and variability of the frequency distribution, as illustrated by the first possible scenario of the physical model in Figure 34b. This translated into large peak flows becoming 15 to 25 times more frequent (50-yr to 3-yr and 100-yr to 4-yr) at a 37% ECA. The high sensitivity of the peak flow regime to forest harvesting due to subdued topography and high drainage density is also applicable to Bowron River and Willow River, featured by the second possible scenario in Figure 34c.

Mountainous watersheds with wide elevation ranges can be sensitive to logging, as demonstrated by Camp Creek. The high sensitivity is caused by the dominant south-facing aspect and the specific cut block locations in relation to the role of hypsometry. Schnorbus and Alila (2004a), Biggs and Whitaker (2012), and White et al. (2002) illustrated how the hypsometry of a watershed can play a significant role in the contribution of snowmelt to runoff during peak discharge in the snow environments. Biggs and Whitaker (2012), for instance, demonstrated how 60-80% of melt volume during the peak discharge was generated from a critical elevation zone making up only 22%-38% of total basin relief of their study watersheds (469-831km^2), depending on the snow accumulation and melt dynamics of the year. Such a critical zone consists of a mid-elevation band between approximately the H75 and H25 elevation contour lines, above which lies 75% and 25% of the total watershed area, respectively. The critical zone may correspond to a different range of total basin relief and may shift up or down in elevation from one watershed to another. For the Camp Creek watershed, 73% of the total harvested area was located between H80 and H20, and 66% was located above the H60 elevation contour (Figure 21 and Table 21). Hence, the location of harvesting on the south-facing slopes can further explain why the peak flow regime for Camp Creek was sensitive to forest harvesting. Contrarily, for the Mather Creek watershed (the least sensitive watershed among the five pairs), only 29% of the harvested area was located between H80 and H20.

The effects of harvest area and its distribution within different elevation bands on the peak flow regime were illustrated in a modelling study of 11 hypothetical harvesting scenarios in Redfish Creek, a 26 km^2 snow-dominated watershed with a high elevation range (700-2300 m) in southeastern BC, by Schnorbus and Alila (2004a). Significant effects on peak flows across a wide range of return periods occurred only for harvesting scenarios that incorporated cut blocks

between the H60 and H40 elevation contours. Such effects became increasingly more severe with an increasing proportion of harvest areas within this critical zone. Schnorbus and Alila (2004a) further demonstrated how the extent of the effects on peak flows were more dependent on the location than the size of the harvested area. The effect on the magnitude of peak flows among the various harvesting scenarios was found to be highly linearly correlated with the proportion of harvested area located within the critical zone (Schnorbus and Alila, 2004a; Figures 8a vs. 8b and related discussion). At the Redfish Creek watershed, harvesting scenarios with cut blocks equaling or exceeding 6.4% of the total watershed in size, located in the critical zone between the H60 and H40 elevation contour lines, caused statistically significant effects on peak flows across a wide range of return periods. The 11% ECA scenario at Camp Creek was associated with 12.2% of the total area of the watershed being harvested, made up of 2.4% below H80, 5.4% between H80 and H60, and 4.4% above H60 elevation contour (Figure 21 and Table 21). The total logging in the critical zone between H60 and H40 was 11.6% at Camp Creek, almost twice as much as the 6.4% suggested by Schnorbus and Alila (2004a). However, it was only 6.2% at Mather Creek (Table 22).

The effect on the magnitude of peak flows predicted by the nonstationary FP method at Camp Creek also was highly correlated with ECA (results not shown). This can be explained by the fact that harvesting occurred dominantly within what could be considered the mid-elevation critical zone, which contributes substantial melt during the peak discharges. The striking parallels in the way Redfish and Camp Creek peak flow regimes were highly sensitive to the location and size of harvest area within this critical zone may be explained by the fact that the two watersheds are both snow-dominated and mountainous with wide elevation ranges (Biggs and Whitaker, 2012; Schnorbus and Alila, 2004a; White et al., 2002). Therefore, logging at

Camp Creek resulted in higher effects on the mean than the variability, as shown by the third possible scenario in the physical model (Figure 34d). This translated into the large peak flows at Camp Creek becoming about three to four times more frequent (50-yr to 15-yr and 100-yr to 25-yr) at a 24% ECA level.

Certain topographic features can reduce a watershed's sensitivity to harvesting, which is supported by the outcomes at Mather Creek. Mather Creek has the largest elevation range amongst the five pairs. The upper and lower halves of the watershed have different slopes and aspect distributions, leading to different draining directions. The Mather Creek watershed has physiographic features that can lead to a difference in the timing of snowmelt throughout the watershed, minimizing snowmelt synchronization. In addition, the concentration of logging on the lower half of the Mather Creek watershed introduces earlier melt in this lower region that further de-synchronized the snowmelt between the lower and upper elevations, analogous to the fourth possible scenario of the physical model (Figure 34e). Therefore, 22% ECA resulted in the least effect on the mean and no change in peak flow variability, translating to large peak flows becoming only two to three times more frequent (50-yr to 20-yr and 100-yr to 30-yr).

Overall, the collective understanding in my proposed physical model of Figure 34 is largely consistent with the stationary FP-based outcomes from Green and Alila (2012), a meta-analysis of four snow-dominated watersheds. The findings of this thesis support the two hypotheses conjectured by Green and Alila (2012), in relation to the physical understanding of the effects of forest harvesting on the mean and variability around the mean of peak flows. Green and Alila (2012, Figure 7 p. 11) developed a physical model based on four small (<40 km^2) treatment watersheds with similar cut rates and logging locations to generalize such an understanding. My physical model made use of an additional five pairs of watersheds, ranging in

size from small (37 km^2) to large (3550 km^2), with contrasting physiographic characteristics and sensitivities to harvesting. The research outcomes from this thesis are one step forward in advancing the newly emerging frequency-based physical understanding of the forests and floods relation. The hypotheses underlying this physical model can be further corroborated or refuted by future studies in snow-dominated watersheds with different physiographic characteristics and forest disturbance regimes.

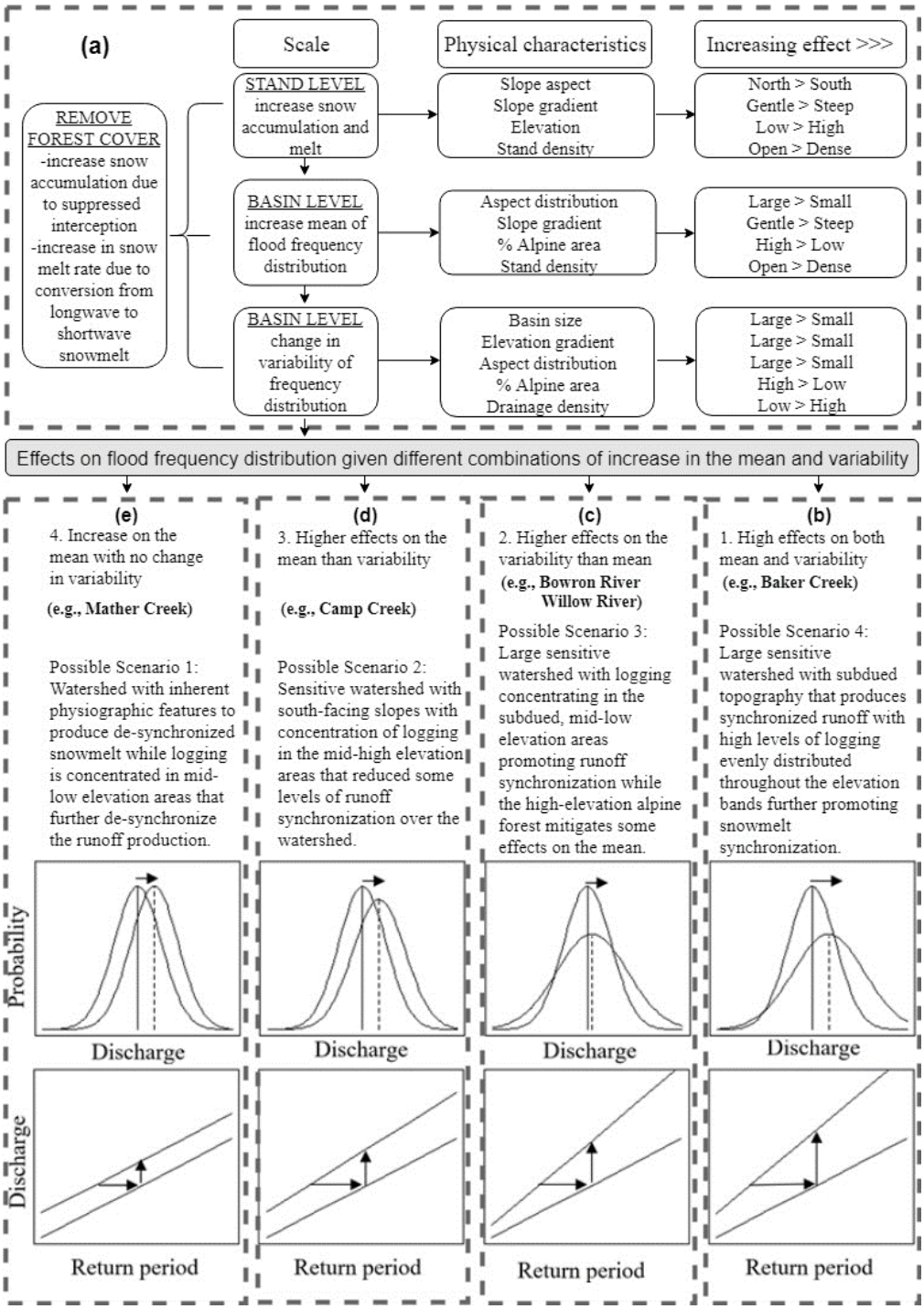

Figure 34: Conceptual model of the effects of basin characteristics on the hydrologic responses to forest harvesting at the stand- and watershed-levels (panel a). Different harvesting scenarios can lead to different effects on the frequency distributions, including high effects on both mean and variability (panel b), higher effects on the variability than mean (panel c), higher effects on the mean than variability (panel d), and an increase in the mean with no change in variability (panel e). Harvesting may also affect the form (skew or the shape parameter) of the frequency distribution, but the model only considers the effects on the mean and variability.

5.3 Performance testing and corroboration of nonstationary frequency model predictions

5.3.1 Performance testing using long-term measured peak flows

The Camp Creek-Greata Creek pair of watersheds is used in this sub-section for demonstration purposes. The long-term records of measured peak flows provide an opportunity to test the ability of the nonstationary frequency models CM11 and TM16 to reproduce the observed peak flow frequency curves for the control and treatment watersheds. The second conditional quantification technique was used for this test because it allows fixing the ECA level to specific values of interest for the Camp Creek watershed. Figure 35a shows the results of the first test of CM11, when the model was driven by the long-term average values of the climate covariates. CM11 reproduced well the frequency curve estimated by the 1971-2011 observed time series of peak flows at Greata Creek, with a slight overestimation at the upper and lower tails of the distribution.

Continuous harvesting and forest regrowth caused the ECA level at Camp Creek to be relatively stable over the last three decades (Figure 5), which is opportune for testing the performance of TM16. Figure 35b displays the results of the second test of how TM16 with ECA=24% reproduced well the frequency curve estimated by the 1981-2012 observed time series of peak flows at Camp Creek, again with slight overestimation at the upper and lower tails of the distribution.

The reliability of the estimated effects of harvesting on peak flows for any ECA level depends, in part, on how reliable TM16 is at estimating the pre-harvest peak flow frequency curve (as illustrated in Figure 35 and Table 9). The period of flow record for Camp Creek under no harvesting conditions is not long enough to provide a direct way of testing the performance of TM16 under ECA=0. Instead, the expected pre-harvest peak flow frequency curve, predicted by

the traditional pre-harvest calibration equation, was used for evaluating the performance of TM16 with ECA=0. Figure 35c shows the outcomes of how TM16 with ECA=0 reproduced reasonably well the pre-harvest (baseline or control) peak flow frequency curve, notwithstanding the uncertainty associated with the use of a calibration equation discussed in Chapter 1. The reasonable performance in Figure 35c is perhaps due to the fact that the development of the FFC under forested conditions did not extrapolate beyond the range of data used to develop the calibration equation. The largest event in the calibration occurred in 1972, with a magnitude of 3.43 m^3/s.

The nonstationary frequency model TM16 performed well in reproducing the observed peak flow frequency curves, possibly because the Camp Creek watershed has a single dominant south aspect, which is most sensitive to changes in energy and melt rates caused by harvesting. In addition, harvesting was concentrated over the mid-elevation zone, contributing to the majority of melt during the annual peak discharge (Biggs and Whitaker, 2012; Schnorbus and Alila, 2004a). Collectively, these factors contribute to SWE and temperature being strong predictors of the frequency distribution of peak flows. Furthermore, the relatively slow recovery and the fact that ECA was relatively stable at around 24% for long enough, provided a strong basis for testing model performance. Therefore, the Camp Creek-Greata Creek pair may provide a textbook case for illustrating the application of the nonstationary FP method.

Could the challenge of overfitting, commonly encountered in hydrological modelling, have contributed to this notable performance of the CM11 (Greata Creek) and TM16 (Camp Creek) models? By analogy, the nonstationary FP method introduced in this thesis could be categorized as an application of the so-called top-down hydrologic modelling (Sivapalan et al., 2003), where the hydrologic model attempts to predict the overall watershed function based on

the modeller's interpretation of the observed watershed response (peak flows in this case). The method closely resembles the derived flood frequency approach (Eagleson, 1972), recognized as a bottom-up approach by Klemeš (1983). The similarity between Eagleson's approach and the method introduced in this thesis is that both attempt to physically explain and predict peak flows using a stochastic framework. The top-down approach leads to models with only a few necessary parameters, i.e. parsimony (Barrett and Charbeneau, 1997; Perrin et al., 2003). The climate covariates have a strong physical basis, at both the forest stand and watershed levels (e.g., Sicart et al., 2004; Ellis et al., 2011; Curry and Zwiers, 2018). Therefore, efforts were made to reduce the effects of overfitting in this research.

Nonstationary frequency models have the ability to reproduce FFCs of watersheds with sizes ranging from 133 km^2 to 4780 km^2. Similar performance testing was conducted for the other pairs of watersheds, except for Willow River where continuous forest harvesting occurred throughout the record period, making it difficult to find a time period with stable ECA conditions to conduct performance testing (Figure 18). The outcomes of the testing procedures for the other control-treatment pairs of watersheds led to similar performance patterns found at the Greata Creek-Camp Creek pair. The FFCs can be found in Appendix A.

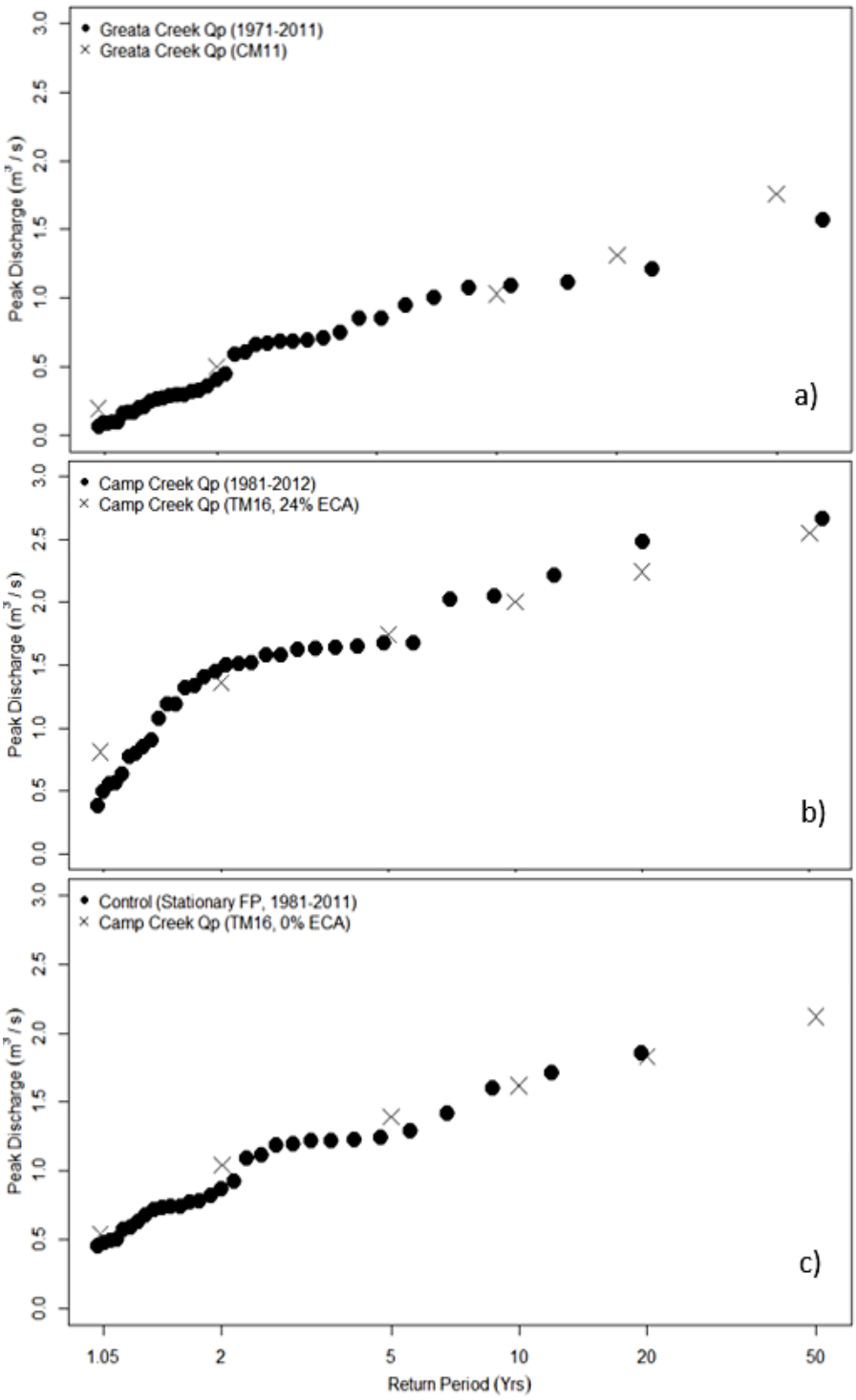

Figure 35: Performance testing of nonstationary models: a) FFC predicted by CM11 versus FFC estimated by 1971 to 2011 observed time series of peak flows at Greata Creek; b) FFC predicted by TM16 with ECA=24% versus FFC estimated by observed peak flows from 1981 to 2012; and c) FFC predicted by TM16 with ECA=0% versus FFC estimated using data from 1981 to 2011 with calibration equation from 1971 to 1976 (Camp Qp (m^3/s) = 1.22 * Greata Qp (m^3/s) + 0.38 (R^2 = 0.90)).

5.3.2 Nonstationary FP predicts rational relationships between watershed physiography, logging regime, and peak flows

The nonstationary FP revealed how forest harvesting only affected the mean of the peak flows at Mather Creek (Figure 24), while both mean and variability were affected at Baker Creek (Figure 25). The increase in the mean is also much higher at Baker Creek than Mather Creek for the same harvesting rates. As discussed in Section 5.2, these distinctive nonstationary FP predictions are consistent with how the contrasting physiographies, logging rates, and cut block locations are expected to affect the peak flow regime in the two watersheds. However, when plotting the peak flow time series, Mather Creek and Baker Creek exhibit similar patterns as shown in Figure 36a, despite the fact that the nonstationary FP analyses revealed contrasting sensitivities and treatment effects between the two watersheds. The similarities in patterns are most apparent starting in the mid-1990s, indicated by the "fan" shape, when forest harvesting started to accelerate at both treatment watersheds (Figure 36a). Hence, it is reasonable to conclude that the fan shape of the peak flows after the year 2000 is caused by forest harvesting, because both treatment watersheds exhibit similar patterns in the peak flow time series. This is especially the case because the same patterns could not be found in the peak flow time series of the respective control watersheds (Figure 36b). It is remarkable how the treatment effects predicted by the nonstationary FP models, which could have been concealed by the large temporal variability in the peak flow time series (Figure 36a), are in line with the interpretation of the physical processes related to watershed characteristics and disturbance regimes.

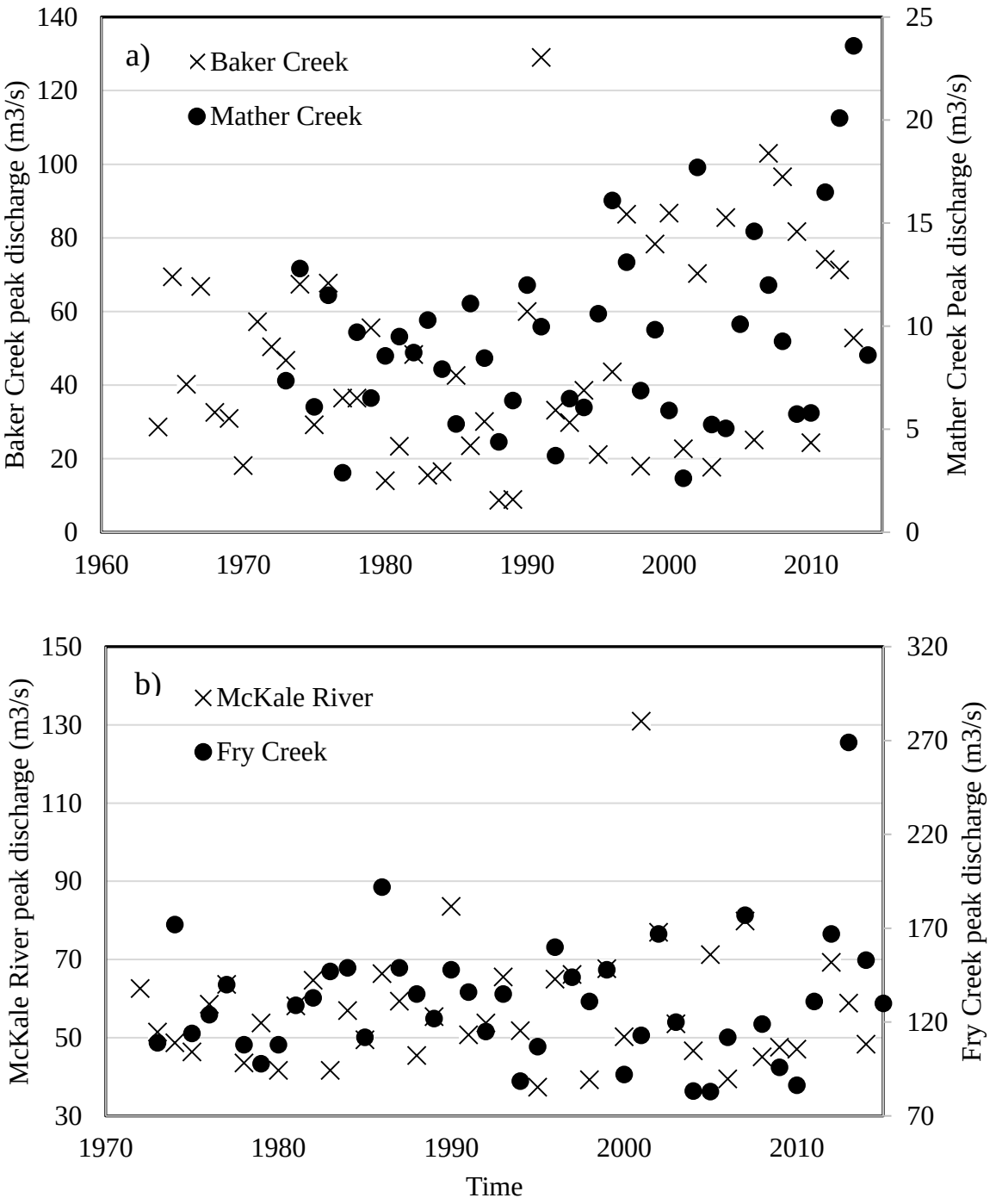

Figure 36: Peak flow time series of a) Baker Creek and Mather Creek, b) McKale River and Fry Creek.

5.3.3 Nonstationary FP predictions are identifiable in the measured time series of peak flows of Baker Creek

Remarkably, the changes in peak flow frequency caused by forest harvesting on the Baker Creek watershed can be readily identified in the peak flow time series plot (Figure 37), and are consistent with those predicted by the nonstationary FP models (Figure 25). The horizontal dashed lines in Figure 37 points to the magnitude of 50-yr and 20-yr peak flow events estimated by the nonstationary FP method (Table 15), while the vertical dashed line indicates the time at which ECA started to accelerate as a result of harvesting. Prior to 1996, the 50-yr event was exceeded once, while the 20-yr event was exceeded twice. However, these 50-yr and 20-yr events were exceeded six and ten times in 17 years post 1996, respectively. On average, this translates into the 50-yr event becoming a 3-yr event and the 20-yr event becoming a 2-yr event, as a result of the harvesting.

Despite the fact that the attribution process proposed in this thesis requires a nearby control watershed, the predicted signal by the nonstationary FP method is visually identifiable from the time series plot of Baker Creek (Figure 37). The harvesting signals on the Baker Creek peak flows are obvious even without accounting for the effects of the difference in climate of the pre- and post-1996 periods on the background variability in peak flows. This is perhaps due to the plateau-like topography that made the peak flow regime highly sensitive to the rather aggressive forest harvesting. The changes in the frequency of peak flows at Baker Creek are also consistent with those predicted by Forest Practices Board (2007) and Schnorbus et al. (2010), via the use of DHSVM and Variable Infiltration Capacity (VIC) deterministic models, respectively. These two studies simulated long-term peak flows under various forest disturbance scenarios at

the Baker Creek watershed. They subsequently analyzed the effects of forest harvesting on the peak flow regime using stationary frequency pairing.

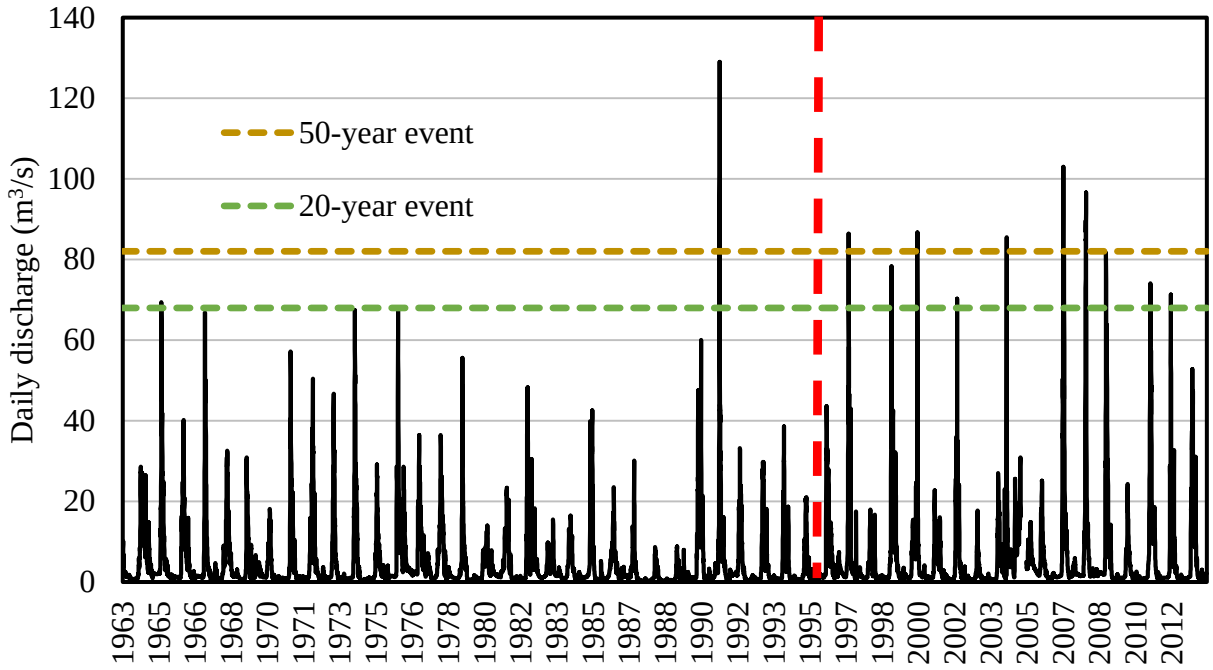

Figure 37: The historic daily discharge of Baker Creek with the horizontal dashed lines showing the magnitude of the 50-yr and 20-yr events and the vertical dashed line indicating the time where ECA started to increase as a result of logging.

5.3.4 Documented changes in channel geomorphology at Bowron River and Willow River corroborate the nonstationary FP predictions

The nonstationary FP models for Bowron River and Willow River showed large peak flows becoming 5 to 20 times more frequent as a result of forest harvesting (20-yr becomes 4-yr event and 100-yr becomes 5-yr event). The increase in these flows can affect various hydro-geomorphological processes (Poff et al., 1997), such as immobilizing sediments (Gomi and Sidle, 2003), enhancing surface erosion (Roberts and Church, 1986), and increasing landslides and debris flows (Brardinoni et al., 2003). In some watersheds, the geomorphology of channel networks may be resilient to changes in the peak flow regime. However, in other more sensitive watersheds changes to the channel network can be identified by evaluating aerial photographs before and after the disturbance. The geomorphic alterations can be potentially linked to forest harvesting induced changes in the peak flows (Imaizumi et al., 2008; Lyons and Beschta, 1983). This provides an indirect way of validating the peak flow changes predicted by the nonstationary FP models.

Beaudry and Gottesfeld (2000) showed a loss of sinuosity and an increase in the average channel width in 12 medium-sized sub-basins within Bowron River and Willow River watersheds, ranging from 20 to 120 km^2. The authors hypothesized that these changes were caused by forest harvesting. Besides the geomorphic changes to the stream channels, Bowron Watershed Committee (1997) suggested that forest harvesting at the 24% ECA level could have triggered landslide activities when the logging occurred in the mid-low elevations at Haggen Creek, a 250 km^2 sub-basin of the Bowron River watershed. Firth Hollins Resource Science Corporation (1994) speculated that about one-third of the 550 landslides identified in the Bowron River watershed could be attributed to logging activities in the mid-1980s. The historic logging

and associated hydrologic effects on the sub-basins can perhaps integrate in space to produce distinguishable geomorphic changes near the outlet of Bowron River and Willow River.

My independent evaluation of aerial photos taken by the BC Provincial Government (Appendix B) shows some obvious changes to the channel in Bowron River between 1977 and 2015, when the channel experienced an increase in width and a reduction in sinuosity (Figure 38). There were no obvious changes to the channel in the nearby control watershed McGregor River between 1964 and 2015 (Figure 39). This lends some confidence to the assumption that the geomorphic changes to Bowron River could be attributed to the increased high flows from logging activities. In addition, aerial photos taken in 1987 and 2015 show lower levels of channel widening at Willow River (Figure 40). However, the overall geomorphic changes are more substantial and, hence, more evident at Bowron River than Willow River. It is reasonable to expect smaller and less evident changes at Willow River because the channel has only experienced high levels of ECA (and associated changes in high flows) since the late 1990s whereas the ECA levels have remained high since the early 1980s at Bowron River. It is also possible that the geomorphology of Willow River is more resilient to changes in the flow regime than Bowron River. However, this remains a speculation awaiting further field-based research.

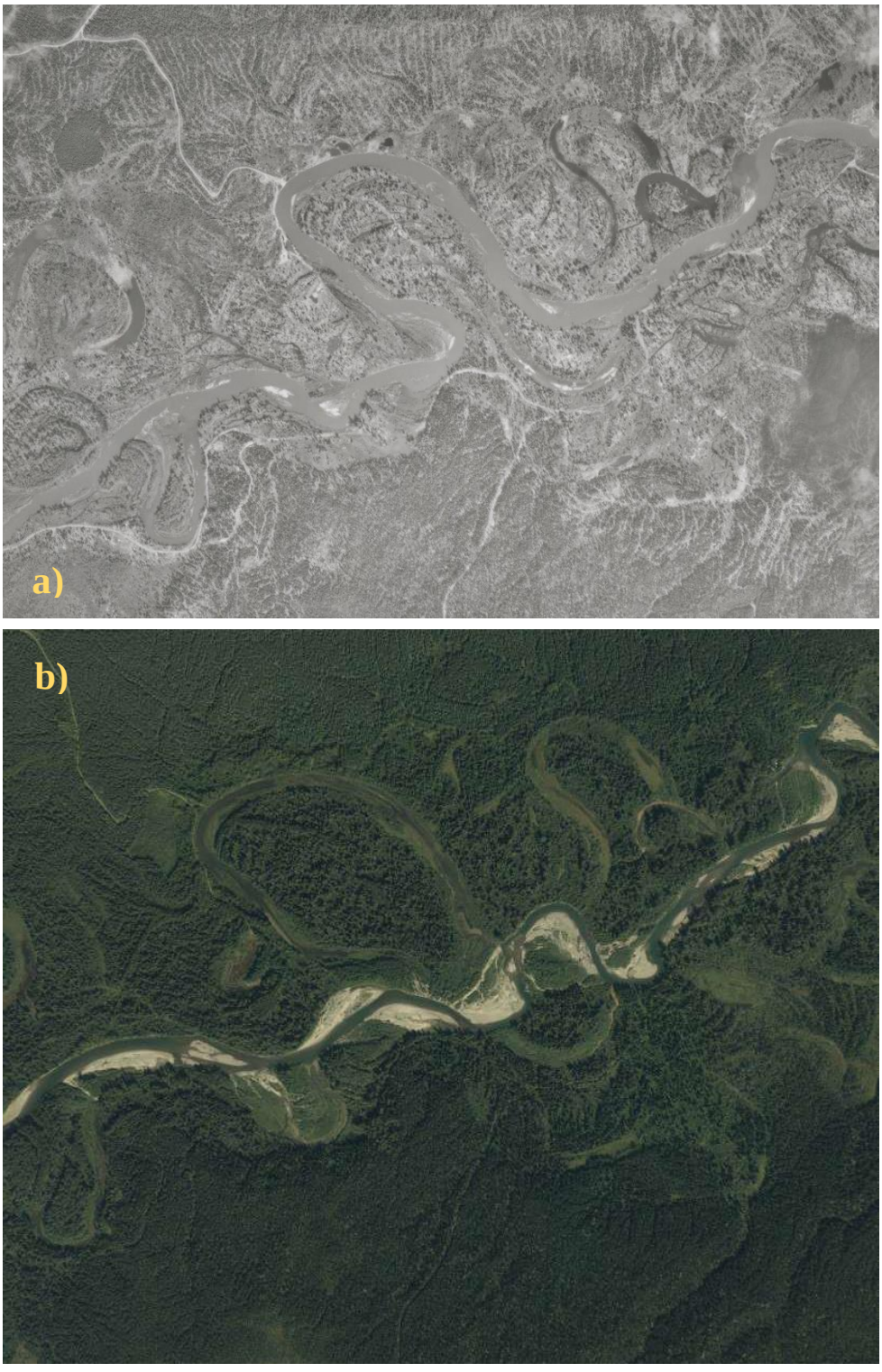

Figure 38: Aerial photos of Bowron River at 1977 (panel a) and 2015 (panel b). The corresponding roll/frame IDs are BC77004/278 and BCD15109/885.

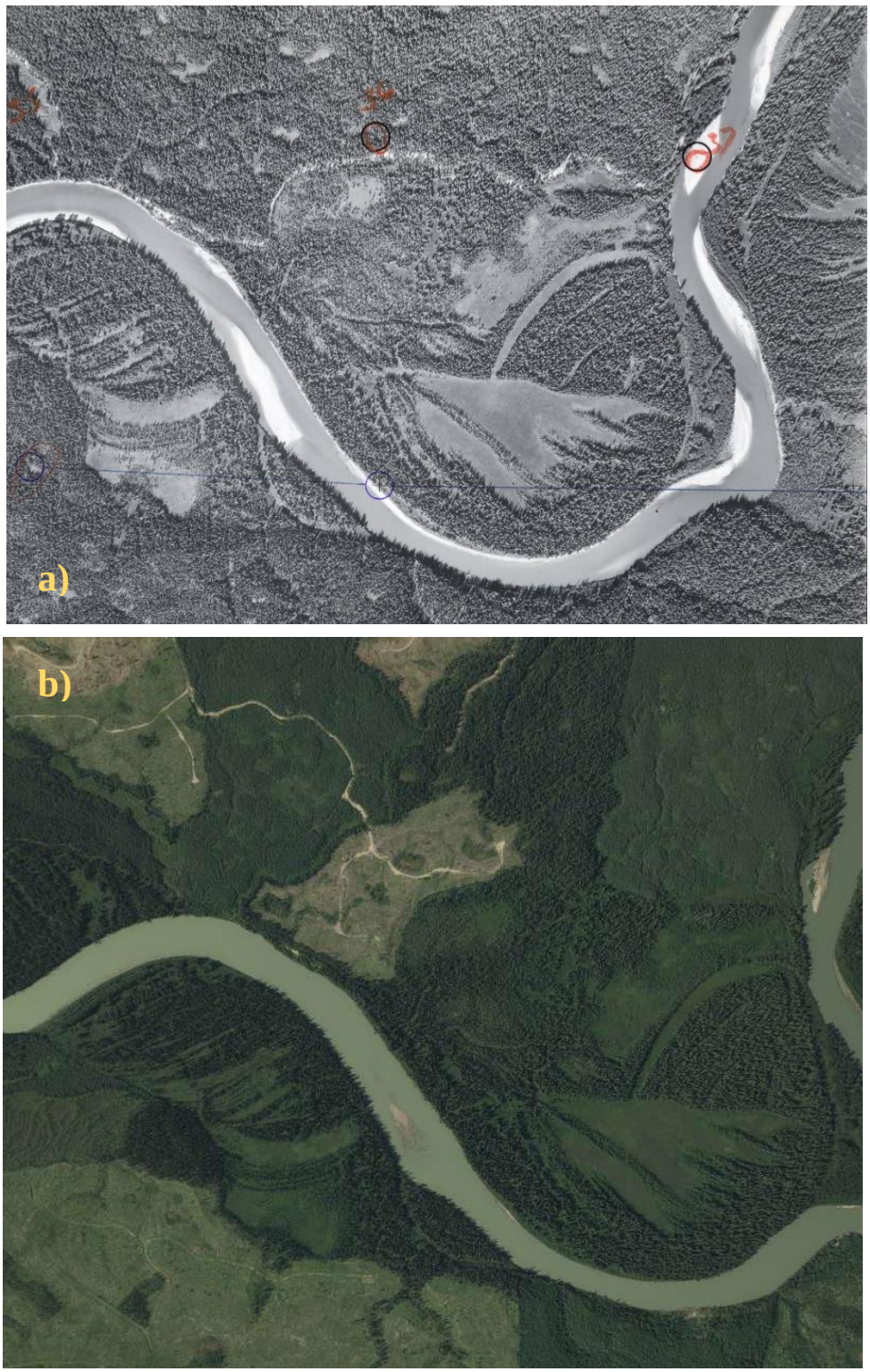

Figure 39: Aerial photos of McGregor River at 1964 (panel a) and 2015 (panel b). The corresponding roll/frame IDs are BC4284/119 and BCD15107/279.

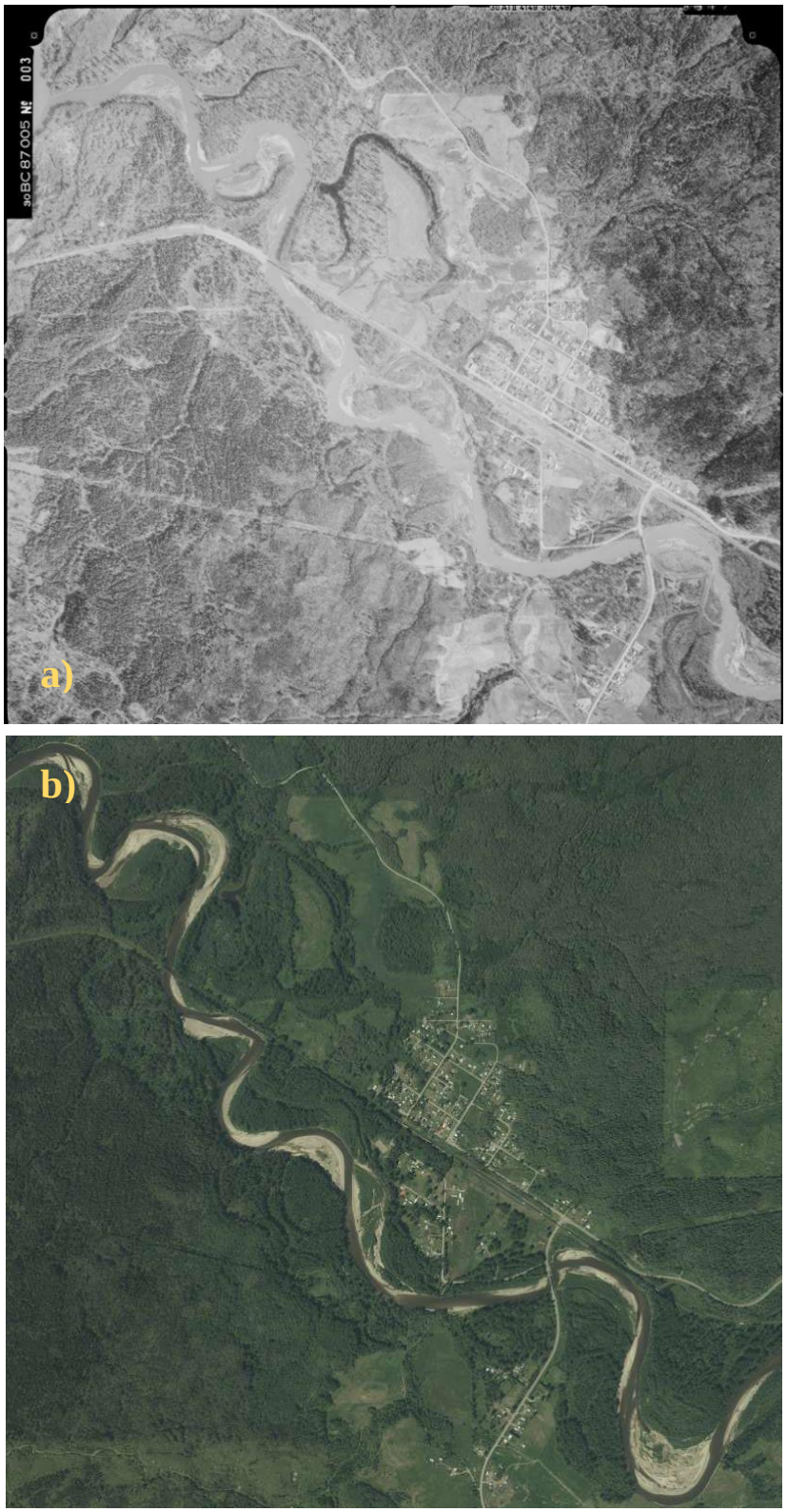

Figure 40: Aerial photos of Willow River at 1987 (panel a) and 2015 (panel b). The corresponding roll/frame IDs are BC87005/003 and BCD15109/334.

5.4 The advantages of the nonstationary FP method

5.4.1 Nonstationary FP relaxes the constraints of watershed size and proximity

It is the changing role of the control watershed under the nonstationary FP framework that allows relaxing the size and proximity constraints between control and treatment watersheds. The old CP framework is based on the pairing of the peak flow responses between the control and treatment watersheds by the same weather event (one at a time). The paired watersheds have to be neighboring and relatively small to receive the same weather input allowing a calibration equation to be developed with high enough predictive power for the peak flow response of the treatment watershed, had there been no logging during the post-treatment period (see Subsection 1.1). The new FP framework is based on pairing by equal frequency, which imposes the modelling and comparison of the pre- and post-harvest frequency distributions. These distributions can be stationary or nonstationary, due to climate variability and/or historic land-use changes. Estimations of the frequency distributions are based on the entire record of peak flows driven by the long-term climate. To account for climate variability, the nonstationary FP framework models the temporally changing frequency distributions using climate covariates in both watersheds, prior to introducing time (ECA) as a covariate in the control (treatment) watersheds. Any time trends detected in the peak flows of the treatment watershed, but not in the control watershed, can be attributed to historic forest harvesting with greater confidence. The attribution of forest harvesting to the peak flows in the treatment watershed is plausible when the peak flow frequency distribution of the control watershed is not changing in time. As a result, the new role of the control is to rule out a changing frequency distribution over time allowing for any temporal changes in the treatment watershed to be attributed to forest disturbance. This attribution process does not require the paired watersheds to be either small or in close proximity

(e.g. Prosdocimi et al., 2015). It also does not necessarily require the control and treatment watersheds to be similar in their physiographic characteristics, as long as they are influenced by the same regional climate (Cunderlik and Ouarda, 2009; Zhang et al., 2001). The physiographic features of the control and treatment watersheds are accounted for in the development of their respective flood frequency distribution models. Therefore, different physiographies do not affect the evaluation of time trends caused by time or ECA. In summary, while the weather and physiography should be as similar as possible between the paired watersheds under the old CP-based framework (Andréassian et al., 2012), these limiting constraints are relaxed under the nonstationary FP framework, due to the changing role of the control watershed.

5.4.2 Nonstationary FP can identify commonly undetectable changes in peak flows

Extreme events are highly sensitive to small, often statistically undetectable changes in mean and variability around the mean of the frequency distribution (Allen and Ingram, 2002; Porporato and Ridolfi, 1998). However, it is inherently difficult to detect changes in a hydrologic time series using traditional trend analyses (Delgado et al., 2010; Lins and Cohn, 2011; Milly et al., 2015; Reeves et al., 2007; Serinaldi and Kilsby, 2015). Detecting signals in peak flows caused by forest harvesting without a control watershed is even more challenging because the available records are typically short. Conventional trend analyses, like Man-Kendall and Spearman rho, can only correctly detect trends 50% of the time, with time trends of up to 1% in slope with 50 years of data (Yue et al., 2002). Even with a paired watershed experiment, which is designed to ‘isolate’ the effects of forest harvesting, it has been shown that forest harvesting effects on peak flows are difficult to isolate using conventional trend analyses, given the noise from natural climate variability (Burt, 1994; Burt et al., 2015). The background climate variability of peak flows can be explained using climate covariates. Under the nonstationary FP

framework, it is possible for an add-on ECA covariate to capture the remaining forest-harvesting induced signals. Therefore, the nonstationary FP can detect as small as 10% changes in the variability of peak flows (e.g., at Camp Creek).

The nonstationary FP method allows detecting signals that would have been almost impossible to detect using conventional trend analysis methods. For instance, at Baker Creek, the watershed with the highest treatment effects amongst the five pairs, the peak flow time series was not changing as a function of ECA alone (TM7, Table 13), given the large temporal variability. Therefore, the time series could have been concluded as stationary. It was only possible to detect and attribute forest harvesting signals hidden in the time series after accounting for the natural background variability of peak flows.

5.4.3 Nonstationary FP eliminates the need for a calibration equation

The role of the control watershed in the new nonstationary FP framework is different than in the CP- and stationary FP-based frameworks when evaluating the effects of harvesting on peak flows. This role eliminates the need for the calibration process and hence the associated uncertainties. In brief, the calibration equation is necessary for the CP- and stationary FP-based methods to estimate the expected peak flows, had there been no harvesting in the post-treatment period. As stated in Chapter 1, the development and use of the calibration equation is associated with several sources of uncertainty: (i) a relatively short calibration period (Bren and Lane, 2014; Kovner and Evans, 1954; Wilm, 1949); (ii) the calibration relation can change in time due to external factors (Ssegane et al., 2017); and (iii) a watershed can respond outside the range of the conditions that occurred during the calibration period (Hornbeck, 1973). The nonstationary FP method can eliminate these uncertainties altogether because of the fundamentally different

technique for quantifying the forest harvesting effects on peak flows by using snapshots of historically changing peak flow frequency distributions.

5.4.4 Nonstationary FP can improve the estimation of the effect on extreme events

Another advantage of nonstationary FP is that it can make use of a longer sample size than both the CP and stationary FP methods. Historically, the sample size has always been blamed for not being long enough to reveal much about forest harvest effects on the larger peak flows. For instance, Thomas and Megahan (1998), in a CP-based study, evaluated forest harvesting effects on peak flows based on subsets of five years of post-harvesting peak flows to meet the stationarity assumption. Green and Alila (2012), in a stationary FP-based study, evaluated forest harvesting effects at Camp Creek using 19 years of peak flows, although 45 years of data were available. Even though there are de-trending techniques that can be used to help meet the stationarity assumption, such techniques can be cumbersome and are associated with uncertainties (Fatichi et al., 2009; Koutsoyiannis, 2006; Serinaldi, 2010). The new FP method can accommodate nonstationarities inherent in the peak flows and allows the use of a much longer record. It improves the estimation and makes better inferences about the effects on extreme events. In this thesis, for instance, 45 years of peak flows were used at Camp Creek, instead of only the 19 years used by Green and Alila (2012).

5.4.5 Nonstationary FP can predict the recovery of the peak flow regime to pre-harvest conditions

The nonstationary FP method allows for understanding and predicting hydrologic effects at various stages of forest disturbance history in a watershed. This is equal to, if not more important than, quantifying the immediate effects post-harvesting. For instance, an engineer who is designing a structure with a life span of 50 years on the basis of the 100-yr event (Obeysekera and Salas, 2014), needs to accommodate how the 100-yr event will change in the next 50 years as a result of future forest management. While the stationary FP does not allow for quantifying treatment effects at various ECA levels, the nonstationary FP method does. Consequently, the nonstationary FP can have more practical implications for forest management, general ecosystem planning, and engineering designs than the stationary FP method.

For example, the continuous harvesting activities and the nature of slow forest regrowth, characteristic of its dry snow environment in the Camp Creek watershed, caused the FFC to shift upward as the ECA increased with time (Figure 20). However, in most paired watershed experiments a harvesting scenario is applied only once, then the flows are monitored for decades during forest re-establishment in the harvested areas. In this case, the FFC should shift downward as the ECA decreases with time until it returns to the pre-harvest level. Therefore, the nonstationary FP method can provide answers to the hydrologic recovery question of how long it takes for the peak flow regime to partially or fully recover to pre-harvest conditions.

5.4.6 Nonstationary FP can illuminate the unrelenting disagreements in the CP-based literature

For close to a century, the CP framework has dominated research on forest harvesting effects on peak flows. The CP-based peak flow response to forest practices has been, and continues to be, characterized as "highly variable, and for the most part unpredictable" (Hibbert (1967, p. 535), echoed by Eisenbies et al. (2007); R. D. Harr (presented paper, 1979), echoed by Hewlett (1982, p. 557); Leopold (1972), echoed by Jones (2000)). In the new era of research on this topic, guided by the FP framework, the nonstationary method is a step in the right direction. It has the potential to illuminate many misconceptions and misunderstandings in the CP-based literature (Alila et al., 2010). This will allow moving beyond the unrelenting lack of consensus on the topic of forest harvesting effects on the peak flow regime, and forests and floods in general.

Chapter 6: Conclusion

6.1 Philosophical reflections on the science of forests and floods

Scientists have been disagreeing for decades on how forests, and conversely forest harvesting practices, affect floods (e.g., Alila et al., 2009, 2010; Alila and Green, 2014a, 2014b; Anderson, 1949, 1950; Bathurst, 2014; Birkinshaw, 2014; Bradshaw et al., 2009; Burton, 1997, 1999; Harr et al., 1979; Harr, 1986; Ives, 2006; Jones and Grant, 1996; Lewis et al., 2010; Rothatcher, 1973; Thomas and Megahan, 2001; Troendle and Stednick, 1999; van Dijk et al., 2009). As previously mentioned, Eisenbies et al. (2007, p. 81) described the state of science on this topic as "enigmatic." Dunne (1998, p. 795) made the daunting declaration about the state of forest hydrological sciences in general: "*Forest hydrology has a sad history of being embroiled in controversies that never seem to get resolved…Forest hydrologists could be recruited to defend almost any side of a debate, because our confusion about the various processes and their interactions in forests and streams…has left much room for opinion and its attendant influences*." Therefore, one may ask: Why has the topic of forests and floods been singled out?

Platt (1964, p. 350) pointed out how a failure to agree for so long, on any topic in science, could be a sign of a failure to disprove, i.e. a sign of being misguided by the wrong research questions or hypotheses. The science of forests and floods is rarely questioned, perhaps because it is a politically sensitive topic (DeWalle (2003), echoed by Stednick (2008), echoed by Alila et al. (2009)). Is it not the case that asking the right question in a scientific enquiry is, at least in part, a reflection of a sound understanding of the physics of the problem being investigated (Leopold and Langbein 1963)? If the science on this topic has been misguided, an uncomfortable question must be dealt with: What if we never got the physics of forests and floods right?

Confronting this question head-on is crucial, as reliable predictions of a system's response are predicated on a sound understanding of its operation.

The CP-based way of evaluating how harvesting affects peak flows appears to have obfuscated what may now be viewed in hindsight as rather obvious. First, the flood regime of mountainous watersheds can be sensitive to even small harvesting rates when the logging is located in the mid-elevation critical zone, which contributes substantial melt volume during the peak discharge (e.g., Camp Creek watershed, 37 km^2). Second, watersheds with subdued topography are even more sensitive to logging, because of the spatial synchronization of snowmelt, regardless of the cut block location or watershed size (e.g., Baker Creek watershed, 1564 km^2). Finally, the FP-based outcomes for Camp Creek and Baker Creek showed that the larger the watershed, the bigger the treatment effects. Hence, the "no-effect" contention in large watersheds appears to have been largely misled by the CP-based, deterministic, and reductionist research hypotheses, questions, and methods.

What may not be so obvious is why it has taken this long to recognize that such a high sensitivity of peak flows to harvesting can only be revealed through the frequency-pairing framework, a method well established in the wider science literature (e.g. climatology; Wigley, 1985 and references therein). Hewlett and Helvey (1970, p. 779) pointed out how the *"more difficult question concerns the frequency"* and how this *"might seriously affect flooding and flood damage downstream. ...Complete answers to old questions, particularly when surrounded by years of controversy, are slow in coming."*

Hewlett (1982, p. 546), taking stock and looking ahead, attentively advised the forest hydrology community:

[H]ydrologists have understandably been confused by the difficulties inherent in describing the nature and frequency of floods to laymen, who are apt to have little patience with probability statements. ...But among ourselves we must drop back to rigorous language in order to discuss and trade information about land-use causes and flood effects.

These rare quotes should be interpreted as appeals from luminous hydrologists to the wider forest hydrology community to abandon the deterministic approach and adopt a probabilistic framework for understanding and predicting the effects of forest harvesting practices on floods. Klemeš (1978, p. 291) stated:

"[a] very popular misconception is to identify causality with determinism… A Causal relationship is not necessarily a deterministic one and a deterministic relationship is not necessarily causal."

However, for over a century published CP-based paired-watershed studies rarely invoked the dimension of frequency in investigating the effects of harvesting on peak flows. A decade has passed since Alila et al. (2009) first made the case that pairing must be by equal frequency, and not equal chronology, and how the latter leads to irrelevant outcomes. Follow up papers, also by Alila and co-workers, furthered the case for FP over CP. It is interesting, that historic CP-based studies with diametrically opposite outcomes from FP-based research (i.e., the "no-effect" contention in large watersheds) are still reported in the literature, as if they are scientifically defensible, or never been challenged on methodological grounds (e.g., Bathurst et al., 2018, 2011b, 2011a; Birkinshaw et al., 2011; Perry et al., 2016).

Kiang (1995) points out how misconceptions in archival science are not easily, or quickly, corrected. They need wide recognition if they are to be overcome. Platt (1964, p. 350) stated:

> *"The difficulty is that disproof is a hard doctrine. If you have a hypothesis and I have another hypothesis, evidently one of them must be eliminated. The scientist seems to have no choice but to be either soft-headed or disputatious. Perhaps this is why so many tend to resist the strong analytical approach - and why some great scientists are so disputatious."*

The only way forward is to abandon the old and adopt the new (Alila et al., 2009, 2011; Alila and Green 2014a,b), as clinging to the old CP-based methods and regurgitating their outcomes continue to unduly influence professional practice and land-use policies worldwide (e.g., Bruijnzeel, 1990; Calder, 2005; Calder et al., 2007; Eaton and Church, 2001; Eisenbies et al., 2007; FAO, 2003; FAO/CIFOR, 2005; Grant et al., 2008; Hamilton, 2008; Hewlett, 1982; MacDonald and Stednick, 2003; Perry et al., 2016; Stratford et al., 2017; Troendle et al., 2006; van Dijk et al., 2009; Winkler et al., 2010).

6.2 Summary

Merz et al. (2012, p. 1385) stated: "*The current mainstream of flood trend studies focuses on detection. The far more difficult problem of trend attribution is addressed, if at all, rather sloppily…we call for more scientific rigour in flood detection and attribution studies*." This research falls within the newly emerging field of "attribution science", that uses a combination of observations and models to tease apart the factors that contribute to extremes (Merz et al., 2012; Prosdocimi et al., 2015; Stott et al., 2004; van Oldenborgh et al., 2017). Although the main objective was to introduce a new method for detecting, attributing, and quantifying forest

harvesting effects on the peak flow regime, this thesis paves the way to a wider range of applications, not just in forest hydrology and the wider field of hydrology, but also in other geoscience fields. Taking advantage of recent developments in nonstationary extreme value theory, for the first time in forest hydrology literature, an FP-based method that allows parameters of the frequency distributions to change in time using physically-based covariates, was successfully applied to peak flows of five pairs of control and treatment watersheds in the snow environments of British Columbia, Canada.

The nonstationary FP modelling outcomes have shown various levels of effects on the mean (28% to 113%) and standard deviation (no effects to 110%) of peak flows because of forest harvesting (22% to 37% ECA levels) in watersheds ranging from 37 km^2 to 3550 km^2. Forest harvesting affects the stand-level snow hydrology, which results in more snow accumulation and higher melt rates in the cut blocks. These stand-level hydrologic effects can integrate across space to affect the peak flows generated at the watershed level. Differences in logging rates and spatial distributions of cut blocks led to different sensitivities to harvesting, all of which were linked to the varying physiographic features amongst the five treatment watersheds.

The Camp Creek watershed (37 km^2) is sensitive to forest harvesting due to the pre-dominantly south-facing aspect. The concentration of harvesting in the south-facing, mid-elevation zone suppressed snowmelt synchronization over the watershed, which in turn inhibited some of the effects on the variability of peak flows around their mean. Hence, forest harvesting resulted in greater effects on the mean than the variability of peak flows. Mather Creek (133 km^2) is not as sensitive as Camp Creek because snowmelt generation is de-synchronized by the unique topography of this watershed. The concentration of logging in the lower half of the watershed can further de-synchronize snowmelt and limit the increase in peak flow variability.

Baker Creek (1564 km^2) is the most sensitive watershed as a result of its subdued topography, high levels of harvesting, and the even distribution of harvesting within the watershed. All of these facets promote snowmelt synchronization, leading to the highest treatment effects amongst the five treatment watersheds I studied. Bowron River (3550 km^2) and Willow River (3110 km^2) are also sensitive watersheds, because of their subdued topography and southwest-slopes in the mid-low elevations, where logging was concentrated. The contrasting watershed sensitivities have led to a wide range of effects on the peak flow frequency. The 100-yr event became 3 times more frequent for the least sensitive watershed Mather Creek, while the100-yr became 25 times more frequent for the most sensitive watershed Baker Creek. The first order controls of the treatment effects, revealed by the nonstationary frequency analyses at the five pairs of watersheds, are largely consistent with those hypothesized by Green and Alila (2012) in their meta-study of stationary frequency analyses of four snow-dominated watersheds. The collective outcomes from this thesis furthered the development of a physical model to advance the understanding and prediction of the frequency-based relations between forests and floods.

The outcomes of the FP-based nonstationary analysis brought to light some compelling advantages over its stationary FP counterpart. For instance, pairing by frequency in a nonstationary framework relaxes the fundamental constraints associated with watershed size and proximity between the control and treatment watersheds. This advantage opens the doors wide for future opportunistic paired watershed studies using data outside of the experimental watershed domain. This new method can quantify the treatment effects at different stages of disturbance, as well as hydrologic recovery. Even with moderate levels of harvesting, the method can detect small changes in the peak flow time series after accounting for the natural background variability of peak flows. It allows frequency analyses to be conducted using a larger sample

size, which improves estimation and allows better inferences about the effects on extreme events. In summary, the nonstationary FP framework can move the forest hydrology literature forward and continue to shed light on the CP-based confusions, misunderstandings, and misconceptions.

6.3 Recommendations for future research

Without further FP-based research, it would be difficult to establish sustainable forest management guidelines, such as annual harvest volumes and long-term timber supply rates, that account for the inherent physical characteristics of watershed and forest harvesting and regrowth regimes. Future research, fundamental to improving the understanding of forest harvesting effects on peak flows, can focus on improving the performance of nonstationary FP models by addressing several uncertainties.

Climate data, transposed from regional snow pillows and weather stations to model the frequency distribution parameters with covariates, may not be accurately representing the meteorological conditions in the watersheds, especially for the extreme hydro-meteorological years. This is one source of uncertainty associated with the current application of nonstationary FP analysis, which can be evaluated using deterministic hydrologic models. The Distributed Hydrology Soil Vegetation Model (DHSVM) (e.g., Schnorbus and Alila, 2004a, 2013) and Variable Infiltration Capacity (VIC) models (e.g., Schnorbus et al., 2010) were used successfully in the BC snow environment to evaluate the effects of forest harvesting on hydrologic responses, in watersheds across a wide range of scales. Climate inputs such as SWE, temperature, and warming rates preceding peak flows can be obtained within the modelling domain and compared with measured values from nearby weather stations. This comparison is useful to evaluate the spatial variations of climate within large watersheds (when the climate inputs are generated at different locations). Similar evaluations between simulated and measured climate inputs, and

climate inputs and hydrologic responses were conducted by Curry and Zwiers (2018) in the Fraser River Basin of British Columbia.

Driving these hydrologic models often requires long-term synthetic weather data, which are products of numerical weather prediction models that interpolate and extrapolate in time and space. These weather predictions, similar to those generated by the hydrologic models, can be compared to climate inputs obtained from weather stations to conduct the same evaluation (of the spatial variations of climate within large watersheds). For instance, Schnorbus and Alila (2004b) provided an empirical-stochastic tool to generate hourly weather data for the DHSVM application of the Redfish Creek experiment (Schnorbus and Alila, 2004a; Whitaker et al., 2003). The Parameter Elevation Regressions on Independent Slopes Model (PRISM) (Daly et al., 2008) is another popular tool used in hydrologic modelling (e.g., Gao et al., 2017). Other commonly used models to simulate long-term weather in North America to conduct hydrologic simulations can be found in Elsner et al. (2014).

There are three additional sources of uncertainty that can be tested using deterministic hydrologic models. The FP modelling in this research assumed linear relationships between the location and scale parameters of the frequency distributions and the climate covariates. Any non-linearity, perhaps masked by the natural background variability given the relatively short sample size, was unaccounted for. At Camp Creek, for instance, a longer record of simulated peak flows from a potential DHSVM application (e.g., Schnorbus and Alila, 2004a, 2013), could reveal nonlinearities which have been difficult to discern from the 45 years of measured peak flows used in this thesis. In addition, the uncertainties associated with treatment effects predicted at various ECA levels by the nonstationary FP models (e.g., Figure 20) can be evaluated using the deterministic hydrologic models. Hypothetical harvesting scenarios can be incorporated into the

model domain to evaluate harvesting effects at different levels and/or locations (Schnorbus et al., 2010; Schnorbus and Alila, 2004a, 2013). Therefore, the historic snapshots of treatment conditions (e.g., Figure 21) can be incorporated via scenario analyses, allowing for the comparison of FFCs predicted by the deterministic hydrologic models and nonstationary FP models. Lastly, since hydrologic responses can be potentially affected by both roads and tree removal, it is difficult to disentangle their respective effects using measured flows at existing paired watershed study sites (Jones and Grant, 1996; Thomas and Megahan, 1998). In future studies, the management scenarios of vegetation removal and roads can be introduced separately in a physically-based model, hence allowing for the isolation of their respective effects (e.g., Bowling et al., 2000; Bowling and Lettenmaier, 2001; Kuraś et al., 2012; La Marche and Lettenmaier, 2001; Tague and Band, 2001). This is in line with recommendations by others who suggested how process-based studies ‘‘should be coupled with the development and validation of physically-based, distributed hydrologic models in order to forecast the effects of forest cutting and roading activities on a given watershed’’ (Thomas and Megahan, 1998, p. 3403).

In addition to improving the performance of nonstationary FP modelling, new research can be conducted to advance the probabilistic understanding of the forests and flood relations. One dimension of this new research would be to apply the same method in existing paired watersheds, and other opportunistic paired watersheds, not just in the snow environments but also in other hydro-climate regimes. In some jurisdictions, such as Northern BC, the coverage of snow pillows and weather stations is much lower and there is a lack of forest cover information. Instead of using the BC VRI database to obtain forest cover information, remote sensing technology can make use of existing satellite images to obtain historic forest cover information (Sachs et al., 1998; Staus et al., 2002). There are studies that have used historic satellite images

to predict the hydrologic responses in large, snow-dominated watersheds (e.g., Yang, 2003; Yang et al., 2009). In addition, there are other means of conducting a landscape-level survey using remote sensing technology via unmanned automated vehicles (UAV). These UAV applications are growing in popularity due to their affordability and flexibility (Koh and Wich, 2012). In addition, given the lack of weather stations, the temporal variability of peak flows in the snow environment can be explained by climate indices representing large scale atmospheric circulations, which heavily influence winter precipitation and peak flows. These climates indices are Pacific Decadal Oscillation (PDO), Pacific-North American (PNA), El Niño-Southern Oscillation (ENSO), Southern Oscillation Index (SOI), and Sea Surface Temperature (SST) (Curry and Zwiers, 2018; Kwon et al., 2008; Thorne and Woo, 2011). These climate indices are also useful when explaining the variability of hydrologic responses in other hydro-climate regimes.

There are two research approaches from outside of the forest hydrology literature that can be used to advance the current research agenda in attributing signals to forest land-use changes. For instance, fingerprinting is a method that was specifically developed to identify the sources and processes that contribute to an observed signal (Viglione et al., 2016). Fingerprinting is a commonly used technique to trace the origin of nutrients in the food web by matching the specific chemical compounds between the samples and potential sources (Larsen et al., 2013). In a similar vein, fingerprinting is used in geoscience to trace the origin of sediments by matching the physical and/or geochemical properties of sediments at various locations with those from source areas (Walling, 2013, p. 1658). The fingerprinting method has been used in the climate science literature to identify signals related to anthropogenic climate change (e.g., Hegerl et al., 1997, 1996; Hidalgo et al., 2009; Levine and Berliner, 1999). Since the harvesting impacts in

sub-basins can integrate to produce a watershed-level signal on the peak flows (Subsection 5.3), the method of fingerprinting can be applied to forest hydrology by matching the signals at the outlet of a large harvested watershed (e.g., Bowron River) with those generated in its sub-basins (e.g., Haggen Creek).

Another technique that is worth noting is constructing a multivariate distribution of peak flows based on the notion of the copula (Favre et al., 2004). The peak flow time series from a treatment watershed is inherently a multivariate frequency distribution driven by multiple factors, such as climate inputs and forest harvesting. The copula framework uses efficient algorithms to simulate joint distributions of the observed hydrologic responses based on different driving factors. Copulas have been widely used in the finance (e.g., Embrechts et al., 2002), hydrology (e.g., Long and Krzysztofowicz, 1992; Singh and Singh, 1991), and actuarial sciences (e.g., Frees and Valdez, 1998) as a tool to estimate conditional distributions. The conditional distributions produced using the copula framework are analogous to those developed under the second conditional quantification technique (see Subsection 3.4). For instance, the frequency distributions in this thesis were developed based on the conditions of an average long-term climate and specific ECA levels (e.g., flood frequency curves at different ECA levels, Figure 20). Therefore, these conditions associated with climate and land-use can perhaps be incorporated in a copula framework allowing for the quantification of forest harvesting effects on the peak flow regime.

Bibliography

Acero, F.J., García, J.A., Gallego, M.C., 2011. Peaks-over-threshold study of trends in extreme rainfall over the Iberian Peninsula. J. Clim. 24, 1089–1105. https://doi.org/10.1175/2010JCLI3627.1

Alila, Y., Beckers, J., 2001. Using numerical modelling to address hydrologic forest management issues in British Columbia. Hydrol. Process. 15, 3371–3387. https://doi.org/10.1002/hyp.1038

Alila, Y., Green, K.C., 2014a. Reply to comment by Bathurst on "A paradigm shift in understanding and quantifying the effects of forest harvesting on floods in snow environments." Water Resour. Res. 50, 2759–2764. https://doi.org/10.1002/2013WR014334

Alila, Y., Green, K.C., 2014b. Reply to comment by Birkinshaw on "A paradigm shift in understanding and quantifying the effects of forest harvesting on floods in snow environments." Water Resour. Res. 50, 2769–2774. https://doi.org/10.1002/2013WR014198

Alila, Y., Hudson, R., Kuraś, P.K., Schnorbus, M., Rasouli, K., 2010. Reply to comment by Jack Lewis et al. on "Forests and floods: A new paradigm sheds light on age-old controversies." Water Resour. Res. 46, W05802. https://doi.org/10.1029/2009WR009028

Alila, Y., Kuraś, P.K., Schnorbus, M., Hudson, R., 2009. Forests and floods: A new paradigm sheds light on age-old controversies. Water Resour. Res. 45, 1–24. https://doi.org/10.1029/2008WR007207

Allen, M.R., Ingram, W.J., 2002. Constraints on future changes in climate and the hydrologic cycle. Nature 419, 224–232. https://doi.org/10.1038/nature01092

Amrhein, V., Greenland, S., McShane, B., 2019. Scientists rise up against statistical significance. Nature 567, 305–307. https://doi.org/10.1038/d41586-019-00857-9

Anderson, H.W., 1950. Discussion of "Flood frequencies and sedimentation from forest watersheds." Trans. Am. Geophys. Union 31, 621. https://doi.org/10.1029/TR031i004p00621

Anderson, H.W., 1949. Flood frequencies and sedimentation from forest watersheds. Trans. Am. Geophys. Union 30, 567. https://doi.org/10.1029/TR030i004p00567

Andréassian, V., Lerat, J., Le Moine, N., Perrin, C., 2012. Neighbors: Nature's own hydrological models. J. Hydrol. 414, 49–58. https://doi.org/10.1016/j.jhydrol.2011.10.007

Ayalew, T.B., Krajewski, W.F., 2017. Effect of river network geometry on flood frequency: a tale of two watersheds in Iowa. J. Hydrol. Eng. 22, 06017004. https://doi.org/10.1061/(ASCE)HE.1943-5584.0001544

Barrett, M.E., Charbeneau, R.J., 1997. A parsimonious model for simulating flow in a karst aquifer. J. Hydrol. 196, 47–65. https://doi.org/10.1016/S0022-1694(96)03339-2

Bathurst, J., Birkinshaw, S., Johnson, H., Kenny, A., Napier, A., Raven, S., Robinson, J., Stroud, R., 2018. Runoff, flood peaks and proportional response in a combined nested and paired forest plantation/peat grassland catchment. J. Hydrol. 564, 916–927. https://doi.org/10.1016/J.JHYDROL.2018.07.039

Bathurst, J.C., 2014. Comment on "A paradigm shift in understanding and quantifying the effects of forest harvesting on floods in snow environments" by K. C. Green and Y. Alila. Water Resour. Res. 50, 2756–2758. https://doi.org/10.1002/2013WR013613

Bathurst, J.C., Birkinshaw, S.J., Cisneros, F., Fallas, J., Iroumé, A., Iturraspe, R., Novillo, M.G., Urciuolo, A., Alvarado, A., Coello, C., Huber, A., Miranda, M., Ramirez, M., Sarandón, R., 2011a. Forest impact on floods due to extreme rainfall and snowmelt in four Latin American environments 2: Model analysis. J. Hydrol. 400, 292–304. https://doi.org/10.1016/J.JHYDROL.2010.09.001

Bathurst, J.C., Iroumé, A., Cisneros, F., Fallas, J., Iturraspe, R., Novillo, M.G., Urciuolo, A., Bièvre, B. de, Borges, V.G., Coello, C., Cisneros, P., Gayoso, J., Miranda, M., Ramírez, M., 2011b. Forest impact on floods due to extreme rainfall and snowmelt in four Latin American environments 1: Field data analysis. J. Hydrol. 400, 289–291. https://doi.org/10.1016/j.jhydrol.2010.11.044

Beaudry, P., Nassey, J., 1994. Watershed assessment – middle reach Bowron River. Ministry of Forest, Prince George Forest Region.

Beaudry, P.G., Gottesfeld, A., 2000. Effects of forest-harvest rates on stream-channel changes in the central interior of British Columbia, in: Watershed Assessment in the Southern Interior of British Columbia. Penticton, British Columbia, Canada, pp. 151–173.

Beckers, J., Alila, Y., Mtiraoui, A., 2002. On the validity of the British Columbia Forest Practices Code guidelines for stream culvert discharge design. Can. J. For. Res. 32, 684–692. https://doi.org/10.1139/x02-010

Beguería, S., Angulo-Martínez, M., Vicente-Serrano, S.M., López-Moreno, J.I., El-Kenawy, A., 2011. Assessing trends in extreme precipitation events intensity and magnitude using non-stationary peaks-over-threshold analysis: A case study in northeast Spain from 1930 to 2006. Int. J. Climatol. 31, 2104–2114. https://doi.org/10.1002/joc.2218

Beguería, S., Vicente-Serrano, S.M., 2006. Mapping the hazard of extreme rainfall by peaks over threshold extreme value analysis and spatial regression techniques. J. Appl. Meteorol. Climatol. 45, 108–124. https://doi.org/10.1175/JAM2324.1

Bendel, R.B., Afifi, A.A., 1977. Comparison of stopping rules in forward "stepwise" regression. J. Am. Stat. Assoc. 72, 46–53. https://doi.org/10.1080/01621459.1977.10479905

Benson, M.A., 1964. Factors influencing the occurrence of floods in the Southwest. U.S. Geological Survey, Reston, Virginia, USA.

Bernier, N.B., Thompson, K.R., Ou, J., Ritchie, H., 2007. Mapping the return periods of extreme sea levels: Allowing for short sea level records, seasonality, and climate change. Glob. Planet. Change 57, 139–150. https://doi.org/10.1016/j.gloplacha.2006.11.027

Berris, S.N., Harr, R.D., 1987. Comparative snow accumulation and melt during rainfall in forested and clear-cut plots in the Western Cascades of Oregon. Water Resour. Res. 23, 135–142. https://doi.org/10.1029/WR023i001p00135

Beschta, R.L., 1978. Long-term patterns of sediment production following road construction and logging in the Oregon Coast Range. Water Resour. Res. 14, 1011–1016. https://doi.org/10.1029/WR014i006p01011

Beschta, R.L., Pyles, M.R., Skaugset, A.E., Surfleet, C.G., 2000. Peak flow responses to forest practices in the western cascades of Oregon , USA. J. Hydrol. 233, 102–120. https://doi.org/10.1016/S0022-1694(00)00231-6

Bewley, D., Alila, Y., Varhola, A., 2010. Variability of snow water equivalent and snow energetics across a large catchment subject to Mountain Pine Beetle infestation and rapid salvage logging. J. Hydrol. 388, 464–479. https://doi.org/10.1016/j.jhydrol.2010.05.031

Biggs, T.W., Whitaker, T.M., 2012. Critical elevation zones of snowmelt during peak discharges in a mountain river basin. J. Hydrol. 438–439, 52–65. https://doi.org/10.1016/j.jhydrol.2012.02.048
Birkinshaw, S.J., 2014. Comment on "A paradigm shift in understanding and quantifying the effects of forest harvesting on floods in snow environments" by K.C. Green and Y. Alila. Water Resour. Res. 50, 2765–2768. https://doi.org/10.1002/2013WR013586
Birkinshaw, S.J., Bathurst, J.C., Iroumé, A., Palacios, H., 2011. The effect of forest cover on peak flow and sediment discharge-an integrated field and modelling study in central-southern Chile. Hydrol. Process. 25, 1284–1297. https://doi.org/10.1002/hyp.7900
Bjorndal, K.A., Wetherall, J.A., Bolten, A.B., Mortimer, J.A., 1999. Twenty-six years of green turtle nesting at Tortuguero, Costa Rica: An encouraging trend. Conserv. Biol. 13, 126–134. https://doi.org/10.1046/j.1523-1739.1999.97329.x
Black, T.A., Chen, J.M., Lee, X., Sagar, R.M., 1991. Characteristics of shortwave and longwave irradiances under a Douglas-fir forest stand. Can. J. For. Res. 21, 1020–1028. https://doi.org/10.1139/x91-140
Blöschl, G., Sivapalan, M., 1997. Process controls on regional flood frequency: Coefficient of variation and basin scale, in: Water Resources Research. Blackwell Publishing Ltd, pp. 2967–2980. https://doi.org/10.1029/97WR00568
Bonell, M., Bruijnzeel, L.A., 2005. Forests, water and people in the humid tropics: Past, present and future hydrological research for integrated land and water management. Cambridge University Press, Cambridge, UK. https://doi.org/10.1017/CBO9780511535666
Borga, M., Gaume, E., Creutin, J.D., Marchi, L., 2008. Surveying flash floods: Gauging the ungauged extremes. Hydrol. Process. https://doi.org/10.1002/hyp.7111
Bowling, L.C., Lettenmaier, D.P., 2001. The effects of forest roads and harvest on catchment hydrology in a mountainous maritime environment, in: Wigmosta, M.S., Burges, S.J. (Eds.), Influence of Urban and Forest Land Use on the Hydrologic-Geomorphic Responses of Watersheds. AGU Water Science and Applications Series, 2, in press, pp. 145–164.
Bowling, L.C., Lettenmaier, D.P., 1997. Evaluation of the effects of forest roads on streamflow in Hard and Ware Creeks. Washington, Water Resour. Ser. Tech. Rep. 155, 189 pp., Univ. of Wash., Seattle.
Bowling, L.C., Storck, P., Lettenmaier, D.P., 2000. Hydrologic effects of logging in Western Washington. Water Resour. Res. 36, 3223–3240. https://doi.org/10.1029/2000WR900138
Bowron Watershed Committee, 1997. Upper Bowron River Watershed IWAP Level 1: analysis and recommendations. Prepared by P. Beaudry and R. Delong, 1996. Upper Bowron River Watershed Interior Watershed Assessment Procedure Level 1: analysis and recommendations. Ministry of Forests. Forest Resources Section. Prince George Forest Region. Internal Publication.
Bradshaw, C.J.A., Sodhi, N.S., Brook, B.W., 2009. Flooding policy makers with evidence to save forests. Ambio 38, 125–126. https://doi.org/10.1890/070193
Brardinoni, F., Hassan, M.A., Slaymaker, H.O., 2003. Complex mass wasting response of drainage basins to forest management in coastal British Columbia. Geomorphology 49, 109–124. https://doi.org/10.1016/S0169-555X(02)00166-6
Bren, L.J., Lane, P.N.J., 2014. Optimal development of calibration equations for paired catchment projects. J. Hydrol. 519, 720–731. https://doi.org/10.1016/j.jhydrol.2014.07.059
Brooks, K.N., Ffolliott, P.F., Magner, J.A., 2012. Hydrology and the Management of Watersheds, Fourth. ed. Wiley-Blackwell. https://doi.org/10.1002/9781118459751

Brown, A.E., Zhang, L., McMahon, T.A., Western, A.W., Vertessy, R.A., 2005. A review of paired catchment studies for determining changes in water yield resulting from alterations in vegetation. J. Hydrol. 310, 28–61. https://doi.org/10.1016/j.jhydrol.2004.12.010
Buishand, T.A., 1982. Some methods for testing the homogeneity of rainfall records. J. Hydrol. 58, 11–27. https://doi.org/10.1016/0022-1694(82)90066-X
Burt, T.P., 1994. Long-term study of the natural environment - perceptive science or mindless monitoring? Prog. Phys. Geogr. 18, 475–496. https://doi.org/10.1177/030913339401800401
Burt, T.P., Howden, N.J.K., McDonnell, J.J., Jones, J.A., Hancock, G.R., 2015. Seeing the climate through the trees: observing climate and forestry impacts on streamflow using a 60-year record. Hydrol. Process. 29, 473–480. https://doi.org/10.1002/hyp.10406
Burton, T.A., 1999. Reply to Discussion by C.A. Troendle and J.D. Stednick: "Effects of Basin Scale Timber Harvest on Water Yield and Peak Streamflow." J. Am. Water Resour. Assoc. 35, 183–184. https://doi.org/10.1111/J.1752-1688.1999.TB05463.X
Burton, T.A., 1997. Effects of basin-scale timber harvest on water yield and peak streamflow. J. Am. Water Resour. Assoc. 33, 1187–1196. https://doi.org/10.1111/j.1752-1688.1997.tb03545.x
Buttle, J.M., Metcalfe, R.A., 2000. Boreal forest disturbance and streamflow response, northeastern Ontario. Can. J. Fish. Aquat. Sci. 57, 5–18. https://doi.org/10.1139/cjfas-57-S2-5
Caires, S., Swail, V.R., Wang, X.L., 2006. Projection and analysis of extreme wave climate. J. Clim. 19, 5581–5605. https://doi.org/10.1175/JCLI3918.1
Calder, I.R., 2005. Blue Revolution: Integrated Land and Water Resource Management. Earthscan, London.
Calder, I.R., Smyle, J., Aylward, B., 2007. Debate over flood-proofing effects of planting forests. Nature 450, 945. https://doi.org/10.1038/450945b
Casella, G., Berger, R., 2002. Statistical Inference. Duxbury Press, Pacific Grove, CA.
Chang, M., 2012. Forest Hydrology, 3rd ed. CRC Press, Boca Raton. https://doi.org/10.1201/b13614
Chebana, F., Ouarda, T.B.M.J., Duong, T.C., 2013. Testing for multivariate trends in hydrologic frequency analysis. J. Hydrol. 486, 519–530. https://doi.org/10.1016/j.jhydrol.2013.01.007
Cheng, J.D., 1989. Streamflow changes after clear-cut logging of a pine beetle-infested watershed in southern British Columbia, Canada. Water Resour. Res. 25, 449–456. https://doi.org/10.1029/WR025i003p00449
Coles, S., 2001. An introduction to statistical modeling of extreme values, Springer Series in Statistics. Springer, London, U.K. https://doi.org/10.1007/978-1-4471-3675-0
Condon, L.E., Gangopadhyay, S., Pruitt, T., 2015. Climate change and non-stationary flood risk for the upper Truckee River basin. Hydrol. Earth Syst. Sci. 19, 159–175. https://doi.org/10.5194/hess-19-159-2015
Conlin, T., Cheyne, D., Dymond, J., 2004. Soil temperatures and suckering response of trembling aspen (Populus tremuloides Michx.) following disposal of hog on winter-logged cutblocks. For. Chron. 80, 687–693. https://doi.org/10.5558/tfc80687-6
Cooley, D., 2013. Return periods and return levels under climate change. Color. State Univ. 65, 15–37. https://doi.org/10.1007/978-94-007-4479-0
Coulson, M., Obedkoff, W., 1998. British Columbia Streamflow Inventory, in: British Columbia Streamflow Inventory.

Crooks, S., Davies, H., 2001. Assessment of land use change in the Thames catchment and its effect on the flood regime of the river. Phys. Chem. Earth, Part B Hydrol. Ocean. Atmos. 26, 583–591. https://doi.org/10.1016/S1464-1909(01)00053-3
Cunderlik, J.M., Ouarda, T.B.M.J., 2009. Trends in the timing and magnitude of floods in Canada. J. Hydrol. 375, 471–480. https://doi.org/10.1016/j.jhydrol.2009.06.050
Curry, C.L., Zwiers, F.W., 2018. Examining controls on peak annual streamflow and floods in the Fraser River Basin of British Columbia. Hydrol. Earth Syst. Sci. 22, 2285–2309. https://doi.org/10.5194/hess-22-2285-2018
Daly, C., Halbleib, M., Smith, J.I., Gibson, W.P., Doggett, M.K., Taylor, G.H., Curtis, J., Pasteris, P.P., 2008. Physiographically sensitive mapping of climatological temperature and precipitation across the conterminous United States. Int. J. Climatol. 28, 2031–2064. https://doi.org/10.1002/joc.1688
Dawson, A.B., 1989. Soils of the Price George-McLeod Lake area. Victoria, B.C.
Degaetano, A.T., 2001. Spatial grouping of United States climate stations using a hybrid clustering approach. Int. J. Climatol. 21, 791–807. https://doi.org/10.1002/joc.645
Del Castillo, J., Daoudi, J., 2009. Estimation of the generalized Pareto distribution. Stat. Probab. Lett. 79, 684–688. https://doi.org/10.1016/j.spl.2008.10.021
Delgado, J.M., Apel, H., Merz, B., 2010. Flood trends and variability in the Mekong river. Hydrol. Earth Syst. Sci. 14, 407–418. https://doi.org/10.5194/hess-14-407-2010
Déry, S.J., Hernández-Henríquez, M.A., Owens, P.N., Parkes, M.W., Petticrew, E.L., 2012. A century of hydrological variability and trends in the Fraser River Basin. Environ. Res. Lett. 7, 024019. https://doi.org/10.1088/1748-9326/7/2/024019
DeWalle, D.R., 2003. Forest hydrology revisited. Hydrol. Process. 17, 1255–1256. https://doi.org/10.1002/hyp.5115
Dolidon, N., Hofer, T., Jansky, L., Sidle, R., 2009. Watershed and forest management for landslide risk reduction, in: Landslides – Disaster Risk Reduction. Springer Berlin Heidelberg, Berlin, Heidelberg, pp. 633–649. https://doi.org/10.1007/978-3-540-69970-5_33
Du, E., Link, T.E., Wei, L., Marshall, J.D., 2016. Evaluating hydrologic effects of spatial and temporal patterns of forest canopy change using numerical modelling. Hydrol. Process. 30, 217–231. https://doi.org/10.1002/hyp.10591
Du, T., Xiong, L., Xu, C.Y., Gippel, C.J., Guo, S., Liu, P., 2015. Return period and risk analysis of nonstationary low-flow series under climate change. J. Hydrol. 527, 234–250. https://doi.org/10.1016/j.jhydrol.2015.04.041
Dung, B.X., Miyata, S., Gomi, T., 2011. Effect of forest thinning on overland flow generation on hillslopes covered by Japanese cypress. Ecohydrology 4, 367–378. https://doi.org/10.1002/eco.135
Dunne, T., 1998. Critical data requirements for prediction of erosion and sedimentation in mountain drainage basins. J. Am. Water Resour. Assoc. 34, 795–808. https://doi.org/10.1111/j.1752-1688.1998.tb01516.x
Eagleson, P.S., 1972. Dynamics of flood frequency. Water Resour. Res. 8, 878–898. https://doi.org/10.1029/WR008i004p00878
Eastoe, E.F., Tawn, J.A., 2009. Modelling non-stationary extremes with application to surface level ozone. J. R. Stat. Soc. Ser. C Appl. Stat. 58, 25–45. https://doi.org/10.1111/j.1467-9876.2008.00638.x

Eaton, B., Church, M., 2001. Hydrological effects of forest harvest in the Pacific Northwest. Riparian Decis. Tool Tech. Rep. 3, Dep. of Geogr., Univ. of B. C., Vancouver, B. C., Canada.
Eaton, B.C., Moore, R.D., 2010. Chapter 4: Regional Hydrology, in: Pike, R. (Ed.), Watershed Management: Compendium of Forest Hydrology and Geomorphology in British Columbia. Victoria: Ministry of Forests.
Eisenbies, M.H., Aust, W.M., Burger, J.A., Adams, M.B., 2007. Forest operations, extreme flooding events, and considerations for hydrologic modeling in the Appalachians—A review. For. Ecol. Manage. 242, 77–98. https://doi.org/10.1016/j.foreco.2007.01.051
El Adlouni, S., Bobée, B., Ouarda, T.B.M.J., 2008. On the tails of extreme event distributions in hydrology. J. Hydrol. 355, 16–33. https://doi.org/10.1016/j.jhydrol.2008.02.011
Ellis, C.R., Pomeroy, J.W., 2007. Estimating sub-canopy shortwave irradiance to melting snow on forested slopes. Hydrol. Process. 21, 2581–2593. https://doi.org/10.1002/hyp.6794
Ellis, C.R., Pomeroy, J.W., Essery, R.L.H., Link, T.E., 2011. Effects of needleleaf forest cover on radiation and snowmelt dynamics in the Canadian Rocky Mountains. Can. J. For. Res. 41, 608–620. https://doi.org/10.1139/X10-227
Ellis, C.R., Pomeroy, J.W., Link, T.E., 2013. Modeling increases in snowmelt yield and desynchronization resulting from forest gap-thinning treatments in a northern mountain headwater basin. Water Resour. Res. 49, 936–949. https://doi.org/10.1002/wrcr.20089
Elsner, M.M., Gangopadhyay, S., Pruitt, T., Brekke, L.D., Mizukami, N., Clark, M.P., 2014. How does the choice of distributed meteorological data affect hydrologic model calibration and streamflow simulations? J. Hydrometeorol. 15, 1384–1403. https://doi.org/10.1175/jhm-d-13-083.1
Embrechts, P., McNeil, A., Straumann, D., 2002. Correlation and dependence in risk management: Properties and pitfalls, in: Risk Management: Value at Risk and Beyond. Cambridge University Press, New York, pp. 176–223.
Fatichi, S., Barbosa, S.M., Caporali, E., Silva, M.E., 2009. Deterministic versus stochastic trends: Detection and challenges. J. Geophys. Res. Atmos. 114. https://doi.org/10.1029/2009JD011960
Favre, A.C., Adlouni, S. El, Perreault, L., Thiémonge, N., Bobée, B., 2004. Multivariate hydrological frequency analysis using copulas. Water Resour. Res. 40. https://doi.org/10.1029/2003WR002456
Ferro, C.A.T., Segers, J., 2003. Inference for clusters of extreme values. J. R. Stat. Soc. Ser. B Stat. Methodol. 65, 545–556. https://doi.org/10.1111/1467-9868.00401
Firth Hollins Resource Science Corporation, 1994. Landslide mapping upper Bowron Watershed. Watershed Restoration Programme.
Frazier, P., Page, K., 2006. The effect of river regulation on floodplain wetland inundation, Murrumbidgee River, Australia. Mar. Freshw. Res. 57, 133–141. https://doi.org/10.1071/MF05089
Frees, E.W., Valdez, E.A., 1998. Understanding relationships using copulas. North Am. Actuar. J. 2, 1–25. https://doi.org/10.1080/10920277.1998.10595667
Gado, T.A., Nguyen, V.T. Van, 2016. An at-site flood estimation method in the context of nonstationarity I. A simulation study. J. Hydrol. 535, 710–721. https://doi.org/10.1016/j.jhydrol.2015.12.063

Ganatsios, H.P., Tsioras, P.A., Pavlidis, T., 2010. Water yield changes as a result of silvicultural treatments in an oak ecosystem. For. Ecol. Manage. 260, 1367–1374. https://doi.org/10.1016/J.FORECO.2010.07.033
Gao, J., Sheshukov, A.Y., Yen, H., White, M.J., 2017. Impacts of alternative climate information on hydrologic processes with SWAT: A comparison of NCDC, PRISM and NEXRAD datasets. Catena 156, 353–364. https://doi.org/10.1016/j.catena.2017.04.010
Garvelmann, J., Pohl, S., Weiler, M., 2014. Variability of observed energy fluxes during rain-on-snow and clear sky snowmelt in a midlatitude mountain environment. J. Hydrometeorol. 15, 1220–1237. https://doi.org/10.1175/JHM-D-13-0187.1
Gilleland, E., Katz, R.W., 2016. extRemes 2.0: an extreme value analysis package in R. J. Stat. Softw. 72, 1–39. https://doi.org/10.18637/jss.v072.i08
Gomi, T., Sidle, R.C., 2003. Bed load transport in managed steep-gradient headwater streams of southeastern Alaska. Water Resour. Res. 39. https://doi.org/10.1029/2003WR002440
Grant, G.E., Lewis, S.L., Swanson, F.J., Cissel, J.H., Mcdonnell, J.J., 2008. Effects of forest practices on peak flows and consequent channel response : a state-of-science report for Western Oregon and Washington, Gen. Tech. Rep. PNW-GTR-760. Pac. Northwest Res., Stn., U.S. Dep. of Agric., Portland, Oreg.
Green, K.C., Alila, Y., 2012. A paradigm shift in understanding and quantifying the effects of forest harvesting on floods in snow environments. Water Resour. Res. 48, 1–21. https://doi.org/10.1029/2012WR012449
Gupta, V.K., Dawdy, D.R., 1995. Physical interpretations of regional variations in the scaling exponents of flood quantiles. Hydrol. Process. 9, 347–361. https://doi.org/10.1002/hyp.3360090309
Gupta, V.K., Waymire, E., Wang, C.T., 1980. A representation of an instantaneous unit hydrograph from geomorphology. Water Resour. Res. 16, 855–862. https://doi.org/10.1029/WR016i005p00855
Hamilton, L.S., 2008. Forests and water: A thematic study prepared in the framework of the Global Forest Resources Assessment 2005. FAO For. Pap., 155, U.N. Food Agric. Organ., Rome.
Harr, R.D., 1986. Effects of clearcutting on rain-on-snow runoff in Western Oregon: a bew look at old studies. Water Resour. Res. 22, 1095–1100. https://doi.org/10.1029/WR022i007p01095
Harr, R.D., 1981. Some characteristics and consequences of snowmelt during rainfall in western Oregon. J. Hydrol. 53, 277–304. https://doi.org/10.1016/0022-1694(81)90006-8
Harr, R.D., Fredriksen, R.L., Rothacher, J., 1979. Changes in streamflow following timber harvest in southwestern Oregon. Res. Pap. PNW-RP-249. Portland, OR U.S. Dep. Agric. For. Serv. Pacific Northwest Res. Stn. 22 p. 249.
Harr, R.D., Harper, W.C., Krygier, J.T., 1975. Changes in storm hydrographs after road building and clear-cutting in the Oregon Coast Range. Water Resour. Res. 11, 436–444. https://doi.org/10.1029/WR011i003p00436
Hegerl, G.C., Hasselmann, K., Cubasch, U., Mitchell, J.F.B., Roeckner, E., Voss, R., Waszkewitz, J., 1997. Multi-fingerprint detection and attribution analysis of greenhouse gas, greenhouse gas-plus-aerosol and solar forced climate change. Clim. Dyn. 13, 613–634. https://doi.org/10.1007/s003820050186
Hegerl, G.C., Von Storch, H., Hasselmann, K., Santer, B.D., Cubasch, U., Jones, P.D., 1996. Detecting greenhouse-gas-induced climate change with an optimal fingerprint method. J.

Clim. 9, 2281–2306. https://doi.org/10.1175/1520-0442(1996)009<2281:DGGICC>2.0.CO;2
Hess, S., 1984. Timber harvesting and flooding. J. Soil Water Conserv. 39, 115–117.
Hewlett, J.D., 1982. Forests and floods in the light of recent investigation, in: Canadian Hydrology Symposium: 82. Associate Committee on Hydrology, National Research Council, Ottawa, pp. 543–559.
Hewlett, J.D., Helvey, J.D., 1970. Effects of forest clear-felling on the storm hydrograph. Water Resour. Res. 6, 768–782. https://doi.org/10.1029/WR006i003p00768
Hewlett, J.D., Lull, H.W., Reinhart, K.G., 1969. In defense of experimental watersheds. Water Resour. Res. 5, 306–316. https://doi.org/10.1029/WR005i001p00306
Hibbert, A.R., 1967. Forest treatment effects on water yield. Int. Symp. For. Hydrol. Sopper, W.E. Lull, H.W. (eds). Pergamon. https://doi.org/10.1.1.545.6751
Hidalgo, H.G., Das, T., Dettinger, M.D., Cayan, D.R., Pierce, D.W., Barnett, T.P., Bala, G., Mirin, A., Wood, A.W., Bonfils, C., Santer, B.D., Nozawa, T., 2009. Detection and attribution of streamflow timing changes to climate change in the Western United States. J. Clim. 22, 3838–3855. https://doi.org/10.1175/2009JCLI2470.1
Hornbeck, J.W., 1973. The problem of extreme events in paired-watershed studies. Res. Note NE-175. Up. Darby, PA U.S. Dep. Agric. For. Serv. Northeast. For. Exp. Station. 4p. 175.
Hosking, J.R.M., Wallis, J.R., 1997. Regional frequency analysis: an approach based on L-Moments. Cambridge Univ. Press, Cambridge, U.K.
Hosking, J.R.M., Wallis, J.R., 1987. Parameter and quantile estimation for the generalized pareto distribution. Technometrics 29, 339–349. https://doi.org/10.2307/1269343
Hundecha, Y., St-Hilaire, A., Ouarda, T.B.M.J., El Adlouni, S., Gachon, P., 2008. A non-stationary extreme value analysis for the assessment of changes in extreme annual wind speed over the Gulf of St.Lawrence. J. Appl. Meteorol. Climatol. 47, 2745. https://doi.org/10.1175/2008JAMC1665.1
Imaizumi, F., Sidle, R.C., Kamei, R., 2008. Effects of forest harvesting on the occurence of landslides and debris flows in steep terrain of central Japan. Earth Surf. Process. Landforms 33, 827–840. https://doi.org/10.1002/esp.1574
Ives, J.D., 2006. Comment: Forests and floods: drowning in fiction or thriving on facts? Mt. Res. Dev. 26, 187–188. https://doi.org/10.1659/0276-4741(2006)26[187:FAFDIF]2.0.CO;2
Jain, A., Nandakumar, K., Ross, A., 2005. Score normalization in multimodal biometric systems. Pattern Recognit. 38, 2270–2285. https://doi.org/10.1016/J.PATCOG.2005.01.012
Jeffrey, W.W., 1970. Hydrology of land use, in: Gray, D.M. (Ed.), Handbook on the Principles of Hydrology. Water Inf. Cent., Port Washington, N.Y., pp. 13.1-13.57.
Jennings, M.E., Thomas, Jr., W.O., Riggs, H.C., 1994. Nationwide summary of US Geological Survey regional regression equations for estimating magnitude and frequency of floods for ungaged sites, 1993. US Geol. Surv. Water-Resources Investig. Rep. 94-4002 203pp.
Johnson, D.H., 1999. The insignificance of statistical significance testing. J. Wildl. Manage. 63, 763–772. https://doi.org/10.2307/3802789
Johnson, L.R., Page-Dumroese, D., Han, H.-S., 2007. Effects of machine traffic on the physical properties of ash-cap soils, in: Volcanic-Ash-Derived Forest Soils of the Inland Northwest: Properties and Implications for Management and Restoration. Fort Collins, CO: U.S. Department of Agriculture, Forest Service, Rocky Mountain Research Station, Coeur d'Alene, pp. 69–82.

Jones, J.A., 2000. Hydrologic processes and peak discharge response to forest removal, regrowth, and roads in 10 small experimental basins, western Cascades, Oregon. Water Resour. Res. 36, 2621–2642. https://doi.org/10.1029/2000WR900105
Jones, J.A., Grant, G.E., 2001. Comment on "Peak flow responses to clear-cutting and roads in small and large basins, Western Cascades, Oregon" by J.A. Jones and G.E. Grant. Water Resour. Res. 37, 179–180. https://doi.org/10.1029/2000WR900115
Jones, J.A., Grant, G.E., 1996. Peak flow responses to clear-cutting and roads in small and large basins, western Cascades, Oregon. Water Resour. Res. 32, 959–974. https://doi.org/10.1029/95WR03493
Jones, J.A., Post, D., 2004. Seasonal and successional streamflow response to forest cutting and regrowth in the northwest and eastern United States. Water Resour. Res. 40, W05203. https://doi.org/10.1029/2003WR002952
Kahya, E., Kalayci, S., 2004. Trend analysis of streamflow in Turkey. J. Hydrol. 289, 128–144. https://doi.org/10.1016/j.jhydrol.2003.11.006
Katz, R.W., 1993. Towards a statistical paradigm for climate change. Clim. Res. 2, 167–175. https://doi.org/10.3354/cr002167
Katz, R.W., Brown, B.G., 1992. Extreme events in a changing climate: Variability is more important than averages. Clim. Change 21, 289–302. https://doi.org/10.1007/BF00139728
Katz, R.W., Brush, G.S., Parlange, M.B., 2005. Statistics of extremes: Modeling ecological disturbances. Ecology 86, 1124–1134. https://doi.org/10.1890/04-0606
Katz, R.W., Parlange, M.B., Naveau, P., 2002. Statistics of extremes in hydrology. Adv. Water Resour. 25, 1287–1304. https://doi.org/10.1016/S0309-1708(02)00056-8
Khaliq, M.N., Ouarda, T.B.M.J., Ondo, J.-C., Gachon, P., Bobée, B., 2006. Frequency analysis of a sequence of dependent and/or non-stationary hydro-meteorological observations: A review. J. Hydrol. 329, 534–552. https://doi.org/10.1016/j.jhydrol.2006.03.004
Kiang, N.Y., 1995. How are scientific corrections made? Sci. Eng. Ethics 1, 347–356. https://doi.org/10.1007/BF02583252
King, J.G., 1989. Streamflow responses to road building and harvesting: A comparison with the equivalent clearcut area procedure. U.S. Res. Pap. INT-401, 401, 13 pp., Intermtn. Res. Stn., For. Serv., U.S. Dep. https://doi.org/10.2737/INT-RP-401
King, J.G., Tennyson, L.C., 1984. Alteration of streamflow characteristics following road construction in North Central Idaho. Water Resour. Res. 20, 1159–1163. https://doi.org/10.1029/WR020i008p01159
King, K.W., Smiley, P.C., Baker, B.J., Fausey, N.R., 2008. Validation of paired watersheds for assessing conservation practices in the Upper Big Walnut Creek watershed, Ohio. J. Soil Water Conserv. 63, 380–395. https://doi.org/10.2489/jswc.63.6.380
Kirk, R.E., 1996. Practical significance: A concept whose time has come. Educ. Psychol. Meas. 56, 746–759. https://doi.org/10.1177/0013164496056005002
Klemeš, V., 1983. Conceptualization and scale in hydrology. J. Hydrol. 65, 1–23. https://doi.org/10.1016/0022-1694(83)90208-1
Klemeš, V., 1978. Physically based stochastic hydrologic analysis. In V. Te Chow (Ed.), in: Advances in Hydroscience Vol.11. Academic Press, pp. 285–356.
Klemeš, V., 1974. Some problems in pure and applied stochastic hydrology, in: U.S. Dep. of Agric. (Ed.), Misc Publ US Dep Agric Econ Res Serv. Washington, D. C, pp. 2–15.
Koh, L.P., Wich, S.A., 2012. Dawn of drone ecology: Low-cost autonomous aerial vehicles for conservation. Trop. Conserv. Sci. https://doi.org/10.1177/194008291200500202

Koutsoyiannis, D., 2006. Nonstationarity versus scaling in hydrology. J. Hydrol. 324, 239–254. https://doi.org/10.1016/j.jhydrol.2005.09.022
Kovner, J.L., Evans, T.C., 1954. A method for determining the minimum duration of watershed experiments. Eos, Trans. Am. Geophys. Union 35, 608–612. https://doi.org/10.1029/TR035i004p00608
Kuraś, P.K., Alila, Y., Weiler, M., 2012. Forest harvesting effects on the magnitude and frequency of peak flows can increase with return period. Water Resour. Res. 48. https://doi.org/10.1029/2011WR010705
Kuraś, P.K., Weiler, M., Alila, Y., 2008. The spatiotemporal variability of runoff generation and groundwater dynamics in a snow-dominated catchment. J. Hydrol. 352, 50–66. https://doi.org/10.1016/j.jhydrol.2007.12.021
Kwon, H-H., Brown, C., Lall, U., 2008. Climate informed flood frequency analysis and prediction in Montana using hierarchical Bayesian modeling. Geophys. Res. Lett. 35, L05404. https://doi.org/10.1029/2007GL032220
Kyselý, J., Picek, J., Beranová, R., 2010. Estimating extremes in climate change simulations using the peaks-over-threshold method with a non-stationary threshold. Glob. Planet. Change 72, 55–68. https://doi.org/10.1016/j.gloplacha.2010.03.006
La Marche, J.L., Lettenmaier, D.P., 2001. Effects of forest roads on flood flows in the Deschutes River, Washington. Earth Surf. Process. Landforms 26, 115–134. https://doi.org/10.1002/1096-9837(200102)26:2<115::AID-ESP166>3.0.CO;2-O
Lane, P.N.J., Best, A.E., Hickel, K., Zhang, L., 2005. The response of flow duration curves to afforestation. J. Hydrol. 310, 253–265. https://doi.org/10.1016/j.jhydrol.2005.01.006
Langbein, W.B., 1949. Annual floods and the partial-duration flood series. Trans. Am. Geophys. Union 30, 879. https://doi.org/10.1029/TR030i006p00879
Larsen, T., Ventura, M., Andersen, N., O'Brien, D.M., Piatkowski, U., McCarthy, M.D., 2013. Tracing carbon sources through aquatic and terrestrial food webs using amino acid stable isotope fingerprinting. PLOS ONES 8, e73441. https://doi.org/10.1371/journal.pone.0073441
Le Tellier, V., Carrasco, A., Asquith, N., 2009. Attempts to determine the effects of forest cover on stream flow by direct hydrological measurements in Los Negros, Bolivia. For. Ecol. Manage. 258, 1881–1888. https://doi.org/10.1016/J.FORECO.2009.04.031
Leclerc, M., Ouarda, T.B.M.J., 2007. Non-stationary regional flood frequency analysis at ungauged sites. J. Hydrol. 343, 254–265. https://doi.org/10.1016/j.jhydrol.2007.06.021
Lee, R., 1980. Forest hydrology., Forest hydrology. Columbia University Press., New York.
Lee, T., Ouarda, T.B.M.J., 2010. Long-term prediction of precipitation and hydrologic extremes with nonstationary oscillation processes. J. Geophys. Res. Atmos. 115. https://doi.org/10.1029/2009JD012801
Leopold, L.B., 1972. Hydrologic research on instrumented watersheds. IASH Publ. 97, 135–150.
Leopold, L.B., Langbein, W.B., 1963. Association and determinacy in geomorphology, in: C. C. Albritton Jr. (Ed.), The Fabric of Geology. Freeman, Cooper & Co., Stanford, Calif, pp. 184–192.
Levine, R.A., Berliner, L.M., 1999. Statistical principles for climate change studies. J. Clim. 12, 564–574. https://doi.org/10.1175/1520-0442(1999)012<0564:SPFCCS>2.0.CO;2
Lewis, J., Reid, L.M., Thomas, R.B., 2010. Comment on "forest and floods: A new paradigm sheds light on age old controversies" by Younes Alila et al. Water Resour. Res. 46. https://doi.org/10.1029/2009WR008766

Link, T., Marks, D., 1999a. Point simulation of seasonal snow cover dynamics beneath boreal forest canopies. J. Geophys. Res. 104, 27841–27857. https://doi.org/10.1029/1998JD200121
Link, T., Marks, D., 1999b. Distributed simulation of snowcover mass- and energy-balance in the boreal forest. Hydrol. Process. 13, 2439–2452. https://doi.org/10.1002/(SICI)1099-1085(199910)13:14/15<2439::AID-HYP866>3.0.CO;2-1
Lins, H.F., Cohn, T.A., 2011. Stationarity: Wanted dead or alive? J. Am. Water Resour. Assoc. 47, 475–480. https://doi.org/10.1111/j.1752-1688.2011.00542.x
Long, D., Krzysztofowicz, R., 1992. Farlie-Gumbel-Morgenstern bivariate densities: Are they applicable in hydrology? Stoch. Hydrol. Hydraul. 6, 47–54. https://doi.org/10.1007/BF01581674
López-Moreno, J.I., Revuelto, J., Gilaberte, M., Morán-Tejeda, E., Pons, M., Jover, E., Esteban, P., García, C., Pomeroy, J.W., 2013. The effect of slope aspect on the response of snowpack to climate warming in the Pyrenees. Theor. Appl. Climatol. 117, 207–219. https://doi.org/10.1007/s00704-013-0991-0
López, J., Francés, F., 2013. Non-stationary flood frequency analysis in continental Spanish rivers, using climate and reservoir indices as external covariates. Hydrol. Earth Syst. Sci. 17. https://doi.org/10.5194/hess-17-3189-2013
Loukas, A., Vasiliades, L., Dalezios, N.R., 2000. Flood producing mechanisms identification in southern British Columbia, Canada. J. Hydrol. 227, 218–235. https://doi.org/10.1016/S0022-1694(99)00182-1
Luce, C.H., 2002. Hydrological processes and pathways affected by forest roads: what do we still need to learn? Hydrol. Process. 16, 2901–2904. https://doi.org/10.1002/hyp.5061
Luce, C.H., Wemple, B.C., 2001. Introduction to special issue on hydrologic and geomorphic effects of forest roads. Earth Surf. Process. Landforms 26, 111–113. https://doi.org/10.1002/1096-9837(200102)26:2<111::AID-ESP165>3.0.CO;2-2
Lundquist, J.D., Dettinger, M.D., Cayan, D.R., 2005. Snow-fed streamflow timing at different basin scales: Case study of the Tuolumne River above Hetch Hetchy, Yosemite, California. Water Resour. Res. 41, W07005. https://doi.org/10.1029/2004WR003933
Lykken, D.T., 1968. Statistcal significance in psychological research. Psychol. Bull. 70, 151–159. https://doi.org/10.1037/h0026141
Lyons, J.K., Beschta, R.L., 1983. Land use, floods, and channel changes: Upper Middle Fork Willamette River, Oregon (1936–1980). Water Resour. Res. 19, 463–471. https://doi.org/10.1029/WR019i002p00463
Macdonald, J.S., Beaudry, P.G., MacIsaac, E.A., Herunter, H.E., 2003. The effects of forest harvesting and best management practices on streamflow and suspended sediment concentrations during snowmelt in headwater streams in sub-boreal forests of British Columbia, Canada. Can. J. For. Res. 33, 1397–1407. https://doi.org/10.1139/x03-110
MacDonald, L.H., 2000. Evaluating and managing cumulative effects: process and constraints. Environ. Manage. 26, 299–315. https://doi.org/10.1007/s002670010088
Macdonald, L.H., Hoffman, J.A., 1995. Causes of peak flows in Northwestern Montana and Northeastern Idaho. Water Resour. Bull. 31, 79–95. https://doi.org/10.1111/j.1752-1688.1995.tb03366.x
MacDonald, L.H., Stednick, J.D., 2003. Forests and water: a state-of-the-art review for Colorado. Completion Rep., 196, 65 pp., Colo. Water Resour. Res. Inst., Fort Collins.

Marks, D., Kimball, J., Tingey, D., Link, T., 1998. The sensitivity of snowmelt processes to climate conditions and forest cover during rain-on-snow: a case study of the 1996 Pacific Northwest flood. Hydrol. Process. 12, 1569–1587. https://doi.org/10.1002/(SICI)1099-1085(199808/09)12:10/11<1569::AID-HYP682>3.0.CO;2-L

Marks, D., Link, T., Winstral, A., Garen, D., 2001. Simulating snowmelt processes during rain-on-snow over a semi-arid mountain basin. Ann. Glaciol. 32, 195–202. https://doi.org/10.3189/172756401781819751

Mazurkiewicz, A.B., Callery, D.G., McDonnell, J.J., 2008. Assessing the controls of the snow energy balance and water available for runoff in a rain-on-snow environment. J. Hydrol. 354, 1–14. https://doi.org/10.1016/j.jhydrol.2007.12.027

McDonnell, J.J., Sivapalan, M., Vaché, K., Dunn, S., Grant, G., Haggerty, R., Hinz, C., Hooper, R., Kirchner, J., Roderick, M.L., Selker, J., Weiler, M., 2007. Moving beyond heterogeneity and process complexity: A new vision for watershed hydrology. Water Resour. Res. https://doi.org/10.1029/2006WR005467

Megahan, W.F., 1972. Subsurface flow interception by a logging road in mountains of central Idaho, in: National Synposium on Watersheds in Transition. American Water Resources Association, Minneapolis, Minn., pp. 350–356.

Merz, B., Vorogushyn, S., Uhlemann, S., Delgado, J., Hundecha, Y., 2012. HESS Opinions "More efforts and scientific rigour are needed to attribute trends in flood time series." Hydrol. Earth Syst. Sci. 16, 1379–1387. https://doi.org/10.5194/hess-16-1379-2012

Miller, R.E., Colbert, S.R., Morris, L.A., 2004. Effects of heavy equipment on physical properties of soils and on long-term productivity: A review of literature and current research. Technical bulletin No. 0887. Research Triangle Park, NC: National Council for Air and Stream Improvement, Inc.

Milly, P.C.D., Betancourt, J., Falkenmark, M., Hirsch, R.M., Kundzewicz, Z.W., Lettenmaier, D.P., Stouffer, R.J., Dettinger, M.D., Krysanova, V., 2015. On critiques of "Stationarity is Dead: Whither Water Management?" Water Resour. Res. 51, 7785–7789. https://doi.org/10.1002/2015WR017408

Moore, R.D., Scott, D.F., 2005. Camp Creek revisited: Streamflow changes following salvage harvesting in a medium-sized, snowmelt dominated catchment. Can. Water Resour. J. 30, 331–344. https://doi.org/10.4296/cwrj3004331

Moore, R.D., Wondzell, S.M., 2005. Physical hydrology and the effects of forest harvesting in the pacific northwest: a review. J. Am. Water Resour. Assoc. 41, 763–784. https://doi.org/j.1752-1688.2005.tb03770.x

Musselman, K.N., Pomeroy, J.W., Link, T.E., 2015. Variability in shortwave irradiance caused by forest gaps: Measurements, modelling, and implications for snow energetics. Agric. For. Meteorol. 207, 69–82. https://doi.org/10.1016/j.agrformet.2015.03.014

Negley, T.L., Eshleman, K.N., 2006. Comparison of stormflow responses of surface-mined and forested watersheds in the Appalachian Mountains, USA. Hydrol. Process. 20, 3467–3483. https://doi.org/10.1002/hyp.6148

Neill, C.R., 2004. Guide to Bridge Hydraulics, Second Edi. ed. Thoas Telford, Heron Quay, London.

Nippgen, F., McGlynn, B.L., Emanuel, R.E., Vose, J.M., 2016. Watershed memory at the Coweeta Hydrologic Laboratory: The effect of past precipitation and storage on hydrologic response. Water Resour. Res. 52, 1673–1695. https://doi.org/10.1002/2015WR018196

NRC, 2008. Hydrologic effects of a changing forest landscape. Natonal Academies, Washington, DC.
Obeysekera, J., Salas, J.D., 2016. Frequency of recurrent extremes under nonstationarity. J. Hydrol. Eng. 21. https://doi.org/10.1061/(ASCE)HE.1943-5584.0001339.
Obeysekera, J., Salas, J.D., 2014. Quantifying the uncertainty of design floods under nonstationary conditions. J. Hydrol. Eng. 19, 1438–1446. https://doi.org/10.1061/(ASCE)HE.1943-5584.0000931
Ouarda, T.B.M.J., El Adlouni, S., 2011. Bayesian nonstationary frequency analysis of hydrological variables. J. Am. Water Resour. Assoc. 47, 496–505. https://doi.org/10.1111/j.1752-1688.2011.00544.x
Perrin, C., Michel, C., Andréassian, V., 2003. Improvement of a parsimonious model for streamflow simulation. J. Hydrol. 279, 275–289. https://doi.org/10.1016/S0022-1694(03)00225-7
Perry, G., Lundquist, J.D., Moore, R.D., 2016. Review of the potential effects of forest practices on stream flow in the Chehalis River Basin. Prepared for Washington State Department of Ecology, Chehalis Basin Strategy. University of Washington, Seattle, WA. 46 p.
Pilgrim, D.H., 1983. Some problems in transferring hydrological relationships between small and large drainage basins and between regions. J. Hydrol. 65, 49–72. https://doi.org/10.1016/0022-1694(83)90210-X
Pilon, P.J., Harvey, K.D., 1994. Consolidated Frequency Anaysis. CFA Package, Environment Canada, Atmospheric Environment Service, Ottawa, Ontario.
Pinchot, G., 1903. A primer of forestry. Washington, Gov't print. off, 1903. Web.. Retrieved from the Library of Congress, <lccn.loc.gov/04018259>.
Platt, J.R., 1964. Strong Inference. Science (80-.). 146, 347–353. https://doi.org/10.1126/science.146.3642.347
Poff, N.L., Allan, J.D., Bain, M.B., Karr, J.R., Prestegaard, K.L., Richter, B.D., Sparks, R.E., Stromberg, J.C., 1997. A paradigm for river conservation and restoration. Bioscience 47, 769–784. https://doi.org/10.2307/1313099
Pomeroy, J., Ellis, C., Rowlands, A., Essery, R., Hardy, J., Link, T., Marks, D., Sicart, J.E., 2008. Spatial variability of shortwave irradiance for snowmelt in forests. J. Hydrometeorol. 9, 1482–1490. https://doi.org/10.1175/2008JHM867.1
Pomeroy, J.W., Fang, X., Marks, D.G., 2016. The cold rain-on-snow event of June 2013 in the Canadian Rockies - characteristics and diagnosis. Hydrol. Process. 30, 2899–2914. https://doi.org/10.1002/hyp.10905
Pomeroy, J.W., Parviainen, J., Hedstrom, N., Gray, D.M., 1998. Coupled modelling of forest snow interception and sublimation. Hydrol. Process. 12, 2317–2337. https://doi.org/10.1002/(SICI)1099-1085(199812)12:15<2317::AID-HYP799>3.0.CO;2-X
Porporato, A., Ridolfi, L., 1998. Influence of weak trends on exceedance probability. Stoch. Hydrol. Hydraul. 12, 1–14. https://doi.org/10.1007/s004770050006
Price, K., Roburn, A., MacKinnon, A., 2009. Ecosystem-based management in the Great Bear Rainforest. For. Ecol. Manage. 258, 495–503. https://doi.org/10.1016/J.FORECO.2008.10.010
Prosdocimi, I., Kjeldsen, T.R., Miller, J.D., 2015. Detection and attribution of urbanization effect on flood extremes using nonstationary flood-frequency models. Water Resour. Res. 51, 4244–4262. https://doi.org/10.1002/2015WR017065

Prosdocimi, I., Kjeldsen, T.R., Svensson, C., 2014. Non-stationarity in annual and seasonal series of peak flow and precipitation in the UK. Nat. Hazards Earth Syst. Sci. 14, 1125–1144. https://doi.org/10.5194/nhess-14-1125-2014

Pujol, N., Neppel, L., Sabatier, R., 2007. Regional tests for trend detection in maximum precipitation series in the French Mediterranean region. Hydrol. Sci. J. 52, 956–973. https://doi.org/10.1623/hysj.52.5.956

R Core Team, 2016. R: A language and environment for statistical computing, R Foundation for Statistical Computing. Vienna, Austria, URL: https://www.R-project.org/.

Read, L.K., Vogel, R.M., 2015. Reliability, return periods, and risk under nonstationarity. Water Resour. Res. 51, 6381–6398. https://doi.org/10.1002/2015WR017089

Reeves, J., Chen, J., Wang, X.L., Lund, R., Lu, Q.Q., 2007. A review and comparison of changepoint detection techniques for climate data. J. Appl. Meteorol. Climatol. 46, 900–915. https://doi.org/10.1175/JAM2493.1

Renard, B., Lang, M., Bois, P., 2006. Statistical analysis of extreme events in a non-stationary context via a Bayesian framework: Case study with peak-over-threshold data. Stoch. Environ. Res. Risk Assess. 21, 97–112. https://doi.org/10.1007/s00477-006-0047-4

Restrepo, P.J., Bras, R.L., 1985. A view of maximum-likelihood estimation with large conceptual hydrologic models. Appl. Math. Comput. 17, 375–403. https://doi.org/10.1016/0096-3003(85)90042-6

Reynard, N.S., Prudhomme, C., Crooks, S.M., 2001. The flood characteristics of large U.K. rivers: potential effects of changing climate and land use. Clim. Change 48, 343–359. https://doi.org/10.1023/A:1010735726818

Reynolds, E.R.C., Leyton, L., 1967. Research data for forest policy: the purpose, methods, and progress of forest hydrology, in: 9th Forestry Conference. Commonwealth Forestry Inst., Univ. Oxford, p. 16.

Rinaldo, A., Vogel, G.K., Rigon, R., Rodriguez-Iturbe, I., 1995. Can one fauge the shape of a basin? Water Resour. Res. 31, 1119–1127. https://doi.org/10.1029/94WR03290

Roberts, R.G., Church, M., 1986. The sediment budget in severely disturbed watersheds, Queen Charlotte Ranges, British Columbia. Can. J. For. Res. 16, 1092–1106. https://doi.org/10.1139/x86-189

Rosburg, T.T., Nelson, P.A., Bledsoe, B.P., 2017. Effects of urbanization on flow duration and stream Flashiness: a case study of Puget Sound streams, Western Washington, USA. J. Am. Water Resour. Assoc. 53, 493–507. https://doi.org/10.1111/1752-1688.12511

Roth, M., Buishand, T.A., Jongbloed, G., Klein Tank, A.M.G., Van Zanten, J.H., 2012. A regional peaks-over-threshold model in a nonstationary climate. Water Resour. Res. 48, 1–12. https://doi.org/10.1029/2012WR012214

Rothatcher, J., 1973. Does harvest in west slope Douglas-fir increase peak flow in small forest streams? U.S. Dep. Agric. For. Serv. Pacific Northwest Res. Station. PNW-163, 1.

Sachs, D.L., Sollins, P., Cohen, W.B., 1998. Detecting landscape changes in the interior of British Columbia from 1975 to 1992 using satellite imagery. Can. J. For. Res. 28, 23–36. https://doi.org/10.1139/x97-186

Salas, J.D., Obeysekera, J., 2014. Revisiting the concepts of return period and risk for nonstationary hydrologic extreme events. J. Hydrol. Eng. 19, 554–568. https://doi.org/10.1061/(ASCE)HE.1943-5584.0000820

Salas, J.D., Rajagopalan, B., Saito, L., Brown, C., 2012. Special section on climate change and water resources: climate nonstationarity and water resources management. J. Water Resour. Plan. Manag. 138, 385–388. https://doi.org/10.1061/(ASCE)WR.1943-5452.0000279
Schaeffer, M., Selten, F.M., Opsteegh, J.D., 2005. Shifts of means are not a proxy for changes in extreme winter temperatures in climate projections. Clim. Dyn. 25, 51–63. https://doi.org/10.1007/s00382-004-0495-9
Schnorbus, M., Alila, Y., 2013. Peak flow regime changes following forest harvesting in a snow-dominated basin: Effects of harvest area, elevation, and channel connectivity. Water Resour. Res. 49, 517–535. https://doi.org/10.1029/2012WR011901
Schnorbus, M., Alila, Y., 2004a. Forest harvesting impacts on the peak flow regime in the Columbia Mountains of southeastern British Columbia: An investigation using long-term numerical modeling. Water Resour. Res. 40, W05205. https://doi.org/10.1029/2003WR002918
Schnorbus, M., Alila, Y., 2004b. Generation of an hourly meteorological time series for an alpine basin in British Columbia for use in numerical hydrologic modeling. J. Hydrometeorol. 5, 862–882. https://doi.org/10.1175/1525-7541(2004)005<0862:GOAHMT>2.0.CO;2
Schnorbus, M., Bennett, K., Werner, A., 2010. Quantifying the water resource impacts of mountain pine beetle and associated salvage harvest operations across a range of watershed scales: Hydrologic modelling of the Fraser River Basin. (Information Report BC-X-423), Natural Resources Canada, Canadian Forestry Service, Pacific Forestry Centre, Victoria, BC.
Schultz, C., 2012. Model investigation overthrows assumptions of watershed research. Eos, Trans. Am. Geophys. Union 93, 150–151. https://doi.org/10.1029/2012EO140026
Schulze, R., 2000. Transcending scales of space and time in impact studies of climate and climate change on agrohydrological responses. Agric. Ecosyst. Environ. 82, 185–212. https://doi.org/10.1016/S0167-8809(00)00226-7
Searcy, J.K., Hardison, C.H., 1960. Double Mass Curves. Manual of hydrology: Part 1. General Surface Water Techniques. US Geol. Surv. Watter-Supply Pap. 1541-B.
Serengil, Y., Gökbulak, F., Özhan, S., Hızal, A., Şengönül, K., Nihat Balcı, A., Özyuvacı, N., 2007. Hydrological impacts of a slight thinning treatment in a deciduous forest ecosystem in Turkey. J. Hydrol. 333, 569–577. https://doi.org/10.1016/J.JHYDROL.2006.10.017
Serinaldi, F., 2010. Use and misuse of some Hurst parameter estimators applied to stationary and non-stationary financial time series. Phys. A Stat. Mech. its Appl. 389, 2770–2781. https://doi.org/10.1016/j.physa.2010.02.044
Serinaldi, F., Kilsby, C.G., 2015. Stationarity is undead: Uncertainty dominates the distribution of extremes. Adv. Water Resour. 77, 17–36. https://doi.org/10.1016/j.advwatres.2014.12.013
Seyednasrollah, B., Kumar, M., 2013. Effects of tree morphometry on net snow cover radiation on forest floor for varying vegetation densities. J. Geophys. Res. Atmos. 118, 12,508-12,521. https://doi.org/10.1002/2012JD019378
Shrestha, R.R., Cannon, A.J., Schnorbus, M.A., Zwiers, F.W., 2017. Projecting future nonstationary extreme streamflow for the Fraser River, Canada. Clim. Change 145, 289–303. https://doi.org/10.1007/s10584-017-2098-6
Sicart, J.E., Essery, R.L.H., Pomeroy, J.W., Hardy, J., Link, T., Marks, D., 2004. A sensitivity study of daytime net radiation during snowmelt to forest canopy and atmospheric

conditions. J. Hydrometeorol. 5, 774–784. https://doi.org/10.1175/1525-7541(2004)005<0774:ASSODN>2.0.CO;2
Silva, A.T., Naghettini, M., Portela, M.M., 2016. On some aspects of peaks-over-threshold modeling of floods under nonstationarity using climate covariates. Stoch. Environ. Res. Risk Assess. 30, 207–224. https://doi.org/10.1007/s00477-015-1072-y
Singh, K., Singh, V.P., 1991. Derivation of bivariate probability density functions with exponential marginals. Stoch. Hydrol. Hydraul. 5, 55–68. https://doi.org/10.1007/BF01544178
Siriwardena, L., Finlayson, B.L., McMahon, T.A., 2006. The impact of land use change on catchment hydrology in large catchments: The Comet River, Central Queensland, Australia. J. Hydrol. 326, 199–214. https://doi.org/10.1016/j.jhydrol.2005.10.030
Sivapalan, M., 2003. Process complexity at hillslope scale, process simplicity at the watershed scale: is there a connection? Hydrol. Process. 17, 1037–1041. https://doi.org/10.1002/hyp.5109
Sivapalan, M., Blöschl, G., Zhang, L., Vertessy, R., 2003. Downward approach to hydrological prediction. Hydrol. Process. 17, 2101–2111. https://doi.org/10.1002/hyp.1425
Slivitzsky, M.S., Hendler, M., 1964. Watershed research as a basis for water resources development, in: Fourth Canadian Hydrol. Symp. Natl. Res. Council, 10 PP., Mime.
Ssegane, H., Amatya, D.M., Muwamba, A., Chescheir, G.M., Appelboom, T., Tollner, E.W., Nettles, J.E., Youssef, M.A., Birgand, F., Skaggs, R.W., 2017. Calibration of paired watersheds: Utility of moving sums in presence of externalities. Hydrol. Process. 31, 3458–3471. https://doi.org/10.1002/hyp.11248
Staus, N.L., Strittholt, J.R., Dellasala, D.A., Robinson, R., 2002. Rate and pattern of forest disturbance in the Klamath-Siskiyou ecoregion, USA between 1972 and 1992. Landsc. Ecol. 17, 455–470. https://doi.org/10.1023/A:1021274701133
Stednick, J.D., 2008. Research opportunities in hydrology and biology in future watershed studies, in: J. D. Stednick (Ed.), Hydrological and Biological Responses to Forest Practices. Springer New York, New York, NY, pp. 307–314. https://doi.org/10.1007/978-0-387-69036-0_17
Stephan, K., Kavanagh, K.L., Koyama, A., 2012. Effects of spring prescribed burning and wildfires on watershed nitrogen dynamics of central Idaho headwater areas. For. Ecol. Manage. 263, 240–252. https://doi.org/10.1016/J.FORECO.2011.09.013
Stott, P.A., Stone, D.A., Allen, M.R., 2004. Human contribution to the European heatwave of 2003. Nature 432, 610–613. https://doi.org/10.1038/nature03089
Stratford, C., Miller, J., House, A., Old, G., Acreman, M., Duenas-Lopez, M.A., Nisbet, T., Burgess-Gamble, L., Chappell, N., Clarke, S., Leeson, L., Monbiot, G., Paterson, J., Robinson, M., Rogers, M., Tickner, D., 2017. Do trees in UK-relevant river catchments influence fluvial flood peaks?: a systematic review. NERC/Centre for Ecology & Hydrology, 46pp. (CEH Project no. NEC06063), Wallingford, UK.
Strupczewski, W.G., Singh, V.P., Feluch, W., 2001. Non-stationary approach to at-site flood frequency modelling I. Maximum likelihood estimation. J. Hydrol. 248, 123–142. https://doi.org/10.1016/S0022-1694(01)00397-3
Sugahara, S., da Rocha, R.P., Silveira, R., 2009. Non-stationary frequency analysis of extreme daily rainfall in Sao Paulo, Brazil. Int. J. Climatol. 29, 1339–1349. https://doi.org/10.1002/joc.1760

Sun, X., Thyer, M., Renard, B., Lang, M., 2014. A general regional frequency analysis framework for quantifying local-scale climate effects: A case study of ENSO effects on Southeast Queensland rainfall. J. Hydrol. 512, 53–68. https://doi.org/10.1016/j.jhydrol.2014.02.025

Svoboda, A., 1991. Changes in flood regime by use of the modified curve number method. Hydrol. Sci. J. 36, 461–470. https://doi.org/10.1080/02626669109492531

Swank, W.T., Swift, L.W., Douglass, J.E., 1988. Streamflow changes associated with forest cutting, species conversions, and natural disturbances. For. Hydrol. Ecol. Coweeta 66, 297–312. https://doi.org/10.1007/978-1-4612-3732-7_22

Swindel, B.F., Douglass, J.E., 1984. Describing and testing nonlinear treatment effects in paired watershed experiments. For. Sci. 30, 305–313. https://doi.org/10.1093/forestscience/30.2.305

Tague, C., Band, L., 2001. Simulating the impact of road construction and forest harvesting on hydrologic response. Earth Surf. Process. Landforms 26, 135–151. https://doi.org/10.1002/1096-9837(200102)26:2<135::AID-ESP167>3.3.CO;2-A

Talbot, J., Plamondon, A.P., 2002. The diminution of snowmelt rate with forest regrowth as an index of peak flow hydrologic recovery, Montmorency Forest, Quebec, in: Proceedings of the 59th Eastern Snow Conference. Stowe, Vermont USA, pp. 85–91.

Thiombiano, A.N., El Adlouni, S., St-Hilaire, A., Ouarda, T.B.M.., El-Jabi, N., 2017. Nonstationary frequency analysis of extreme daily precipitation amounts in Southeastern Canada using a peaks-over-threshold approach. Theor. Appl. Climatol. 129, 413–426. https://doi.org/10.1007/s00704-016-1789-7

Thomas, B.E., Lindskov, K.L., 1983. Methods for estimating peak discharge and flood boundaries of streams in Utah, USGS Water Resources Investigations Report 83-4129. https://doi.org/10.3133/wri834129

Thomas, R.B., 1990. Problems in determining the return of a watershed to pretreatment conditions: techniques applied to a study at Caspar Creek, California. Water Resour. Res. 26, 2079–2087. https://doi.org/10.1029/WR026i009p02079

Thomas, R.B., Megahan, W.F., 2001. Reply to comment on '"Peak flow responses to clear-cutting and roads in small and large basins, western Cascades, Oregon."' Water Resour. Res. 37, 181–183. https://doi.org/10.1029/2000WR900277

Thomas, R.B., Megahan, W.F., 1998. Peak flow responses to clear-cutting and roads in small and large basins, western Cascades, Oregon: A second opinion. Water Resour. Res. 34, 3393–3403. https://doi.org/10.1029/98WR02500

Thorne, R., Woo, M.K., 2011. Streamflow response to climatic variability in a complex mountainous environment: Fraser River Basin, British Columbia, Canada. Hydrol. Process. 25, 3076–3085. https://doi.org/10.1002/hyp.8225

Thyer, M., Beckers, J., Spittlehouse, D.L., Alila, Y., Winkler, R.D., 2004. Diagnosing a distributed hydrologic model for two high-elevation forested catchments based on detailed stand- and basin-scale data. Water Resour. Res. 40, W01103. https://doi.org/10.1029/2003WR002414

Tramblay, Y., Neppel, L., Carreau, J., Najib, K., 2013. Non-stationary frequency analysis of heavy rainfall events in southern France. Hydrol. Sci. J. 58, 280–294. https://doi.org/10.1080/02626667.2012.754988

Treacy, S., 2012. Deforestation in snowy regions causes more floods. Am. Geophys. Union. https://doi.org/news.agu.org/press-release/deforestation-in-snowy-regions-causes-more-floods/
Troendle, C.A., King, R.M., 1987. The effect of partial and clearcutting on streamflow at Deadhorse Creek, Colorado. J. Hydrol. 90, 145–157. https://doi.org/10.1016/0022-1694(87)90177-6
Troendle, C.A., King, R.M., 1985. The Effect of Timber Harvest on the Fool Creek Watershed, 30 Years Later. Water Resour. Res. 21, 1915–1922. https://doi.org/0.1029/WR021i012p01915
Troendle, C.A., Macdonald, L.H., Luce, C.H., 2006. Fuels management and water yield, in Cumulative Watershed Effects of Fuels Management: A Western Synthesis. Gen. Tech. report, Rocky Mt. Res. Stn., U.S. Dep. Agric., Fort Collins, Colo.
Troendle, C.A., Olsen, W.A., 1994. Potential effects of timber harvest and water management on streamflow dynamics and sediment transport. Sustain. Ecol. Syst. Implement. an Ecol. Approach to L. Manag. Gen. Tech. Rep., RM-247 34-41 ,For. Serv., U.S. Dep. of Agric., Flagstaff,.
Troendle, C.A., Stednick, J.D., 1999. Discussion: "Effects of basin scale timber harvest on water yield and peak streamflow" by Timothy A. Burton. J. Am. Water Resour. Assoc. 35, 1187–1196. https://doi.org/10.1111/j.1752-1688.1999.tb05462.x
Troendle, C.A., Wilcox, M.S., Bevenger, G.S., Porth, L.S., 2001. The Coon Creek water yield augmentation project: implementation of timber harvesting technology to increase streamflow. For. Ecol. Manage. 143, 179–187. https://doi.org/10.1016/S0378-1127(00)00516-8
U S Army Corps of Engineers, 1956. Snow Hydrology. USACE Publ.
Valdal, E.J., Quinn, M.S., 2011. Spatial analysis of forestry related disturbance on Westslope Cutthroat Trout (Oncorhynchus clarkii lewisi): implications for policy and management. Appl. Spat. Anal. Policy 4, 95–111. https://doi.org/10.1007/s12061-009-9045-5
van Dijk, A.I.J.M., van Noordwijk, M., Calder, I.R., Bruijnzeel, L.A., Schellekens, J., Chappell, N., 2009. Forest-flood relation still tenuous - comment on 'Global evidence that deforestation amplifies flood risk and severity in the developing world' by C.J.A. Bradshaw, N.S. Sodi, K. S.-H. Peh and B.W. Brook. Glob. Chang. Biol. 15, 110–115. https://doi.org/10.1111/j.1365-2486.2008.01708.x
Van Haveren, B.P., 1988. A reevaluation of the Wagon Wheel Gap forest watershed experiment. For. Sci. 34, 208–214. https://doi.org/10.1093/forestscience/34.1.208
van Oldenborgh, G.J., van der Wiel, K., Sebastian, A., Singh, R., Arrighi, J., Otto, F., Haustein, K., Li, S., Vecchi, G., Cullen, H., 2017. Attribution of extreme rainfall from Hurricane Harvey, August 2017. Environ. Res. Lett. 13. https://doi.org/10.1088/1748-9326/aa9ef2
van Tol, S., 2016. Hydrology and scaling relationships of snowy mountain rivers. Master of Philosophy thesis, School of Earth and Environmental Sciences, University of Wollongong.
Varhola, A., Coops, N.C., Bater, C.W., Teti, P., Boon, S., Weiler, M., 2010a. The influence of ground- and lidar-derived forest structure metrics on snow accumulation and ablation in disturbed forests. Can. J. For. Res. 40, 812–821. https://doi.org/10.1139/X10-008
Varhola, A., Coops, N.C., Weiler, M., Moore, R.D., 2010b. Forest canopy effects on snow accumulation and ablation : An integrative review of empirical results. Jounral Hydrol. 392, 219–233. https://doi.org/10.1016/j.jhydrol.2010.08.009

Viglione, A., Merz, B., Viet Dung, N., Parajka, J., Nester, T., Blöschl, G., 2016. Attribution of regional flood changes based on scaling fingerprints. Water Resour. Res. 52, 5322–5340. https://doi.org/10.1002/2016WR019036

Villarini, G., Serinaldi, F., Smith, J.A., Krajewski, W.F., 2009a. On the stationarity of annual flood peaks in the continental United States during the 20th century. Water Resour. Res. 45, W08417. https://doi.org/10.1029/2008WR007645

Villarini, G., Smith, J.A., Napolitano, F., 2010. Nonstationary modeling of a long record of rainfall and temperature over Rome. Adv. Water Resour. 33, 1256–1267. https://doi.org/10.1016/j.advwatres.2010.03.013

Villarini, G., Smith, J.A., Serinaldi, F., Bales, J., Bates, P.D., Krajewski, W.F., 2009b. Flood frequency analysis for nonstationary annual peak records in an urban drainage basin. Adv. Water Resour. 32, 1255–1266. https://doi.org/10.1016/j.advwatres.2009.05.003

Villarini, G., Smith, J.A., Serinaldi, F., Ntelekos, A.A., Schwarz, U., 2012. Analyses of extreme flooding in Austria over the period 1951-2006. Int. J. Climatol. 32, 1178–1192. https://doi.org/10.1002/joc.2331

Vogel, A.L., Lopes, V.L., 2010. Evaluating watershed experiments through recursive residual analysis. J. Irrig. Drain. Eng. 136, 348–353. https://doi.org/10.1061/(ASCE)IR.1943-4774.0000203

Vogel, R.M., Fennessey, N.M., 1994. Flow-duration curves. I: new interpretation and confidence intervals. J. Water Resour. Plan. Manag. 120, 485–504. https://doi.org/10.1061/(ASCE)0733-9496(1994)120:4(485)

Vogel, R.M., Fennessey, N.M., 1993. L moment diagrams should replace product moment diagrams. Water Resour. Res. 29, 1745–1752. https://doi.org/10.1029/93WR00341

Walling, D.E., 2013. The evolution of sediment source fingerprinting investigations in fluvial systems. J. Soils Sediments 13, 1658–1675. https://doi.org/10.1007/s11368-013-0767-2

Waltemeyer, S.D., 1986. Techniques for estimating flood-flow frequency for unregulated streams in New Mexico, USGS Water Resources Investigations Report 86-4104. https://doi.org/10.3133/wri864104

Wang, Y., 2000. Development of methods for regional flood estimates in the province of British Columbia , Canada. Ph.D thesis, Department of Forestry, University of British Columbia.

Watt, W.E., 1989. Hydrology of floods in Canada - a guide to planning and design. National Research Council of Canada, Associate Committee on Hydrology, Ottawa, Canada.

Wemple, B.C., Jones, J.A., 2003. Runoff production on forest roads in a steep , mountain catchment. Water Resour. Res. 39, 1–17. https://doi.org/10.1029/2002WR001744

Wheater, H., Evans, E., 2009. Land use, water management and future flood risk. Land Use Policy 26, S251–S264. https://doi.org/10.1016/j.landusepol.2009.08.019

Whipkey, R.Z., 1965. Subsurface stormflow from forested slopes. Hydrol. Sci. J. 10, 74–85. https://doi.org/10.1080/02626666509493392

Whitaker, A., Alila, Y., Beckers, J., Toews, D., 2003. Application of the Distributed Hydrology Soil Vegetation Model to Redfish Creek, British Columbia: model evaluation using internal catchment data. Hydrol. Process. 17, 199–224. https://doi.org/10.1002/hyp.1119

White, A.B., Gottas, D.J., Strem, E.T., Ralph, F.M., Neiman, P.J., 2002. An automated brightband height detection algorithm for use with Doppler radar spectral moments. J. Atmos. Ocean. Technol. 19, 687–697. https://doi.org/10.1175/1520-0426(2002)019<0687:AABHDA>2.0.CO;2

Wigbout, M., 1973. Limitations in the use of double-mass curves. J. Hydrol. 12, 132–138.

Wigley, T.M.L., 2009. The effect of changing climate on the frequency of absolute extreme events. Clim. Change 97, 67–76. https://doi.org/10.1007/s10584-009-9654-7
Wigley, T.M.L., 1985. Climatology - impact of extreme events. Nature 316, 106–107. https://doi.org/10.1038/316106a0
Wigmosta, M.S., Vail, L.W., Lettenmaier, D.P., 1994. A distributed hydrology-vegetation model for complex terrain. Water Resour. Res. 30, 1665–1679. https://doi.org/10.1029/94WR00436
Williams, C.J., McNamara, J.P., Chandler, D.G., 2009. Controls on the temporal and spatial variability of soil moisture in a mountainous landscape: The signature of snow and complex terrain. Hydrol. Earth Syst. Sci. 13, 1325–1336. https://doi.org/10.5194/hess-13-1325-2009
Wilm, H.G., 1949. How long should experimental watersheds be calibrated? Trans. Am. Geophys. Union 30, 272. https://doi.org/10.1029/TR030i002p00272
Winkler, R.D., Boon, S., 2015. Revised snow recovery estimates for pine-dominated forests in interior British Columbia. BC Ext. Note 116.
Winkler, R.D., Moore, R.D., Redding, T.E., Spittlehouse, D., Smerdon, B., Carlyle-Moses, D., 2010. The effects of forest disturbance on hydrologic processes and watershed response, in: Pike et al., R.G. (Ed.), Compendium of Forest Hydrology and Geomorphology in British Columbia. B. C. Minist. of For. and Range Res. Branch, Victoria, B. C., Canada, pp. 179–212.
Wright, K.A., Sendek, K.H., Rice, R.M., Thomas, R.B., 1990. Logging effects on streamflow: Storm runoff at Caspar Creek in northwestern California. Water Resour. Res. 26, 1657–1667. https://doi.org/10.1029/WR026i007p01657
Yan, L., Xiong, L., Liu, D., Hu, T., Xu, C.Y., 2017. Frequency analysis of nonstationary annual maximum flood series using the time-varying two-component mixture distributions. Hydrol. Process. 31, 69–89. https://doi.org/10.1002/hyp.10965
Yang, D., 2003. Streamflow response to seasonal snow cover extent changes in large Siberian watersheds. J. Geophys. Res. 108, 4578. https://doi.org/10.1029/2002JD003149
Yang, D., Zhao, Y., Armstrong, R., Robinson, D., 2009. Yukon River streamflow response to seasonal snow cover changes. Hydrol. Process. 23, 109–121. https://doi.org/10.1002/hyp.7216
Yihdego, Y., Webb, J., 2013. An empirical water budget model as a tool to identify the impact of land-use change in stream flow in Southeastern Australia. Water Resour. Manag. 27, 4941–4958. https://doi.org/10.1007/s11269-013-0449-2
Yoccoz, N.G., 1991. Use, overuse and misuse of significance tests in evolutionary biology and ecology. Bull. Ecol. Soc. Am. 72, 106–111. https://doi.org/10.2307/20167258
Yue, S., Pilon, P., Cavadias, G., 2002. Power of the Mann–Kendall and Spearman's rho tests for detecting monotonic trends in hydrological series. J. Hydrol. 259, 254–271. https://doi.org/10.1016/S0022-1694(01)00594-7
Yue, S., Wang, C.Y., 2004. Determination of regional probability distributions of Canadian flood flows using L-moments. J. Hydrol. (New Zealand) 43, 59–73.
Zegre, N.P., Miller, A.J., Maxwell, A., Lamont, S.J., 2014. Multiscale analysis of hydrology in a mountaintop mine-impacted watershed. JAWRA J. Am. Water Resour. Assoc. 50, 1257–1272. https://doi.org/10.1111/jawr.12184

Zhang, L., Zhao, F.F., Brown, A.E., 2012. Predicting effects of plantation expansion on streamflow regime for catchments in Australia. Hydrol. Earth Syst. Sci. 16, 2109–2121. https://doi.org/10.5194/hess-16-2109-2012

Zhang, M., Wei, X., 2014. Contrasted hydrological responses to forest harvesting in two large neighbouring watersheds in snow hydrology dominant environment: Implications for forest management and future forest hydrology studies. Hydrol. Process. 28, 6183–6195. https://doi.org/10.1002/hyp.10107

Zhang, M., Wei, X., Li, Q., 2016. A quantitative assessment on the response of flow regimes to cumulative forest disturbances in large snow-dominated watersheds in the interior of British Columbia, Canada. Ecohydrology 9, 843–859. https://doi.org/10.1002/eco.1687

Zhang, Q., Gu, X., Singh, V.P., Xiao, M., Xu, C.Y., 2015. Flood frequency under the influence of trends in the Pearl River basin, China: Changing patterns, causes and implications. Hydrol. Process. 29, 1406–1417. https://doi.org/10.1002/hyp.10278

Zhang, X., David Harvey, K., Hogg, W.D., Yuzyk, T.R., 2001. Trends in Canadian streamflow. Water Resour. Res. 37, 987–998. https://doi.org/10.1029/2000WR900357

Appendices

Appendix A: Performance test of nonstationary models

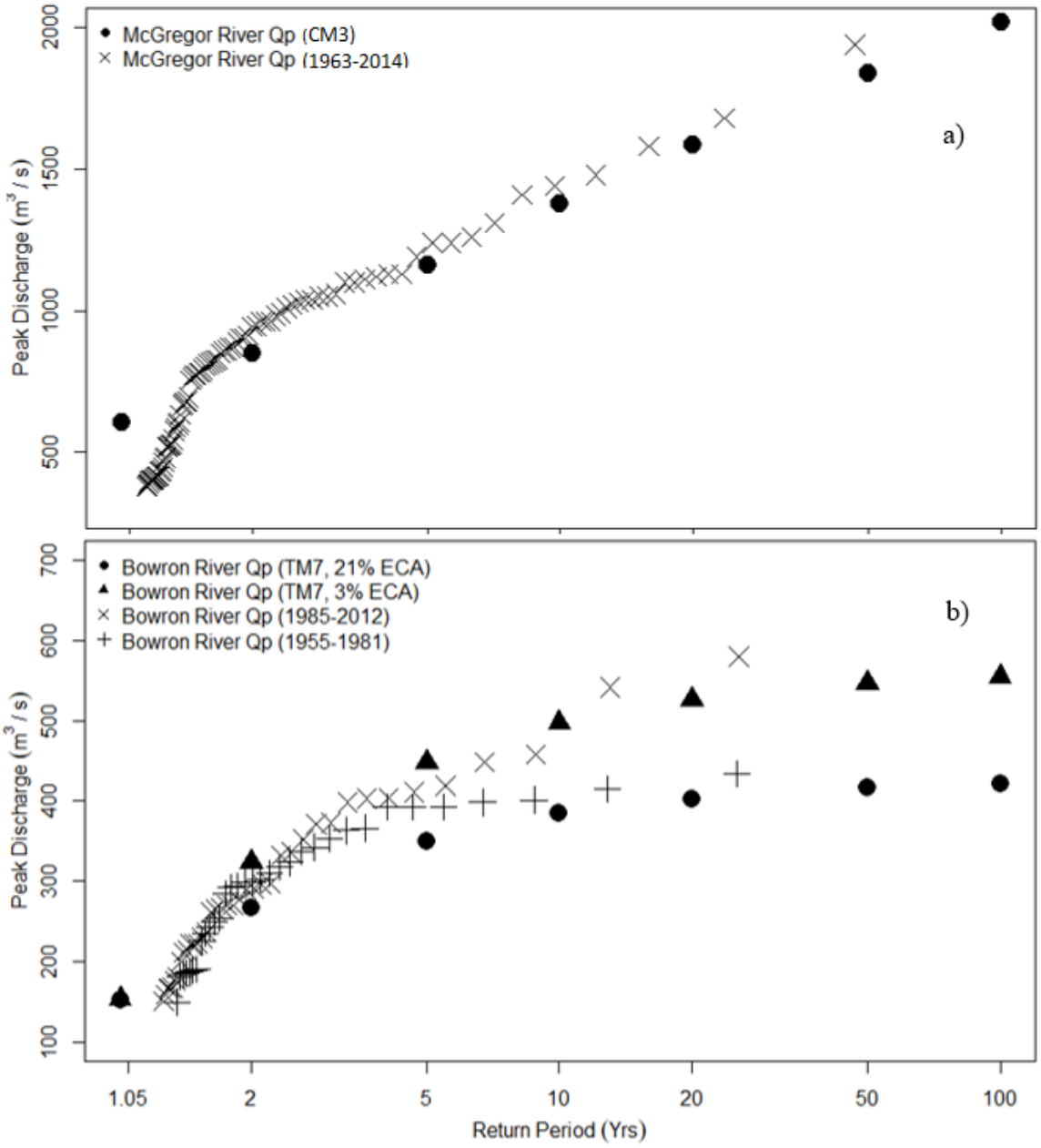

Figure A1: Performance testing of nonstationary models: (a) FFC predicted by CM2 versus FFC estimated by 1963 to 2014 observed time series of peak flow at McGregor River; (b) FFC predicted by TM7 with ECA = 3% and 21% versus FFC estimated on observed peak flows from 1955 to 1981, and 1985 to 2012, representing 3% and 23% ECA conditions, respectively.

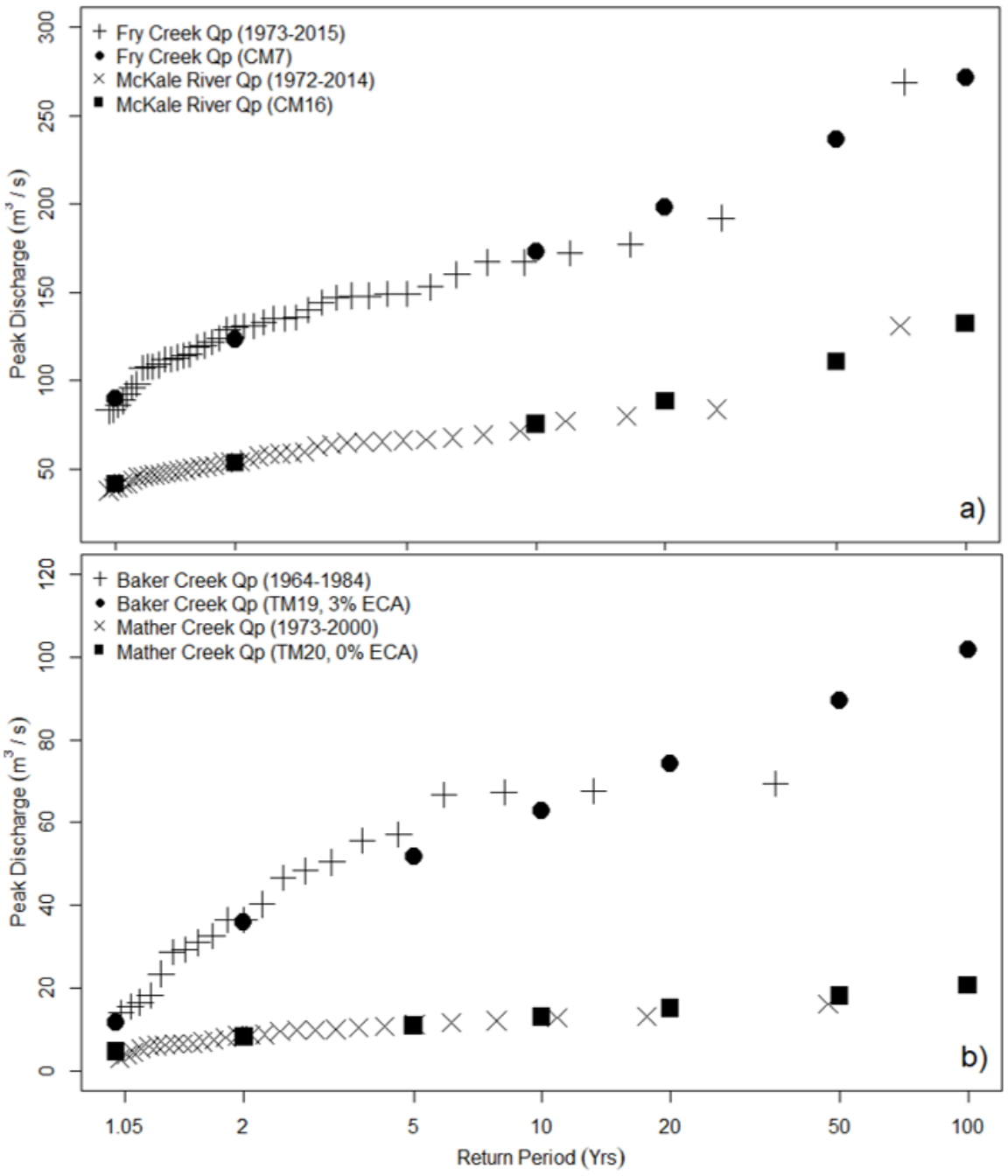

Figure A2: Performance testing of nonstationary models: (a) FFC predicted by CM7 (CM16) versus FFC estimated by 1973 to 2015 (1972 to 2014) observed time series of peak flow at Fry Creek (McKale River); (b) FFC predicted by TM19 (TM20) with ECA = 3% (0%) versus FFC estimated on observed peak flows from 1964 to 1984 (1973 to 2000), representing 3% (0%) ECA conditions pf peak flows at Baker Creek (Mather Creek).